Innate immune responses of lumpfish (Cyclopterus lumpus)

Transcriptome analysis and characterization of pro-inflammatory cytokines

Håvard Øritsland Eggestøl

Thesis for the degree of Philosophiae Doctor (PhD)
University of Bergen, Norway
2020

UNIVERSITY OF BERGEN

Innate immune responses of lumpfish (Cyclopterus lumpus)

Transcriptome analysis and characterization of pro-inflammatory cytokines

Håvard Øritsland Eggestøl

Thesis for the degree of Philosophiae Doctor (PhD)
at the University of Bergen

Date of defense: 05.03.2020

Year: 2020

Title: Innate immune responses of lumpfish (Cyclopterus lumpus)

Name: Håvard Øritsland Eggestøl

Print: Skipnes Kommunikasjon / University of Bergen

Scientific environment

The present work was carried out at the Fish Immunology group, a part of the Fish Health discipline group at the Department of Biological Sciences, University of Bergen, Norway in the period 2015 to 2019. This project was co-funded by the Norwegian Research Council (Project number: 244148) and University of Bergen.

Acknowledgements

First and foremost, I would like to thank my supervisor associate professor Gyri Teien Haugland. Her knowledge and guidance throughout this process has been instrumental in the completion of my task, and I am very grateful to her. Especially, I would like to express my sincere gratitude to Harald Sæbø Lunde (MSc.). His technical and scientific contributions, and the co-unravelling of computational enigmas has been invaluable. Further, I'm grateful for his friendship and tolerance of all my bad jokes. Together with associate professor Gyri Haugland he has played a pivotal role in the compilation of the articles included in this doctoral dissertation.

A profound thank you is also due to Professor Heidrun Wergeland for her wise council and encouragement. Her academic experience has provided a solid foundation from which I have been able to gain support during particularly challenging work.

Thank you to all my colleagues in the fish immunology group at the department of biological science at UiB, for your friendship and for a great work environment over the past 7 years. And further I owe a thank you to my collaboration partners in both the LumpfISH-project and in the preparation of the manuscripts.

Many thanks and appreciation to my parents, siblings and extended family for their love, patience and support throughout the years. Thank you as well to my friends for their advice, encouragement, kind words and the joyful distraction/adventures over the years.

A special thank you to my best friend of many years Anders Parmann, for being there when I needed it most. Thank you. And finally, a very huge thank you to my girlfriend Sophie Mallinson for being the very best person I could have hoped for. Through filling my heart and thoughts with dreams, words and your loving nature, you have created a deep and sound foundation that has been fundamental to my work, well-being and life quality during this academic hardship.

Abstract

In recent years, lumpfish and different species of wrasse are used as cleaner fish for removal of sea lice from farmed Atlantic salmon in Europe and Canada. The production of lumpfish is successful, but there are challenges with high mortality due to bacterial infections. In-depth knowledge of the immune system in lumpfish, particularly immune responses upon bacterial infections and identification of immune genes, will make an important basis for development of immune-prophylactic measures to this species. Prior to this study, there were no available sequences of lumpfish immune genes in public databases.

To obtain sequence information from lumpfish, RNA sequencing of head kidney leukocytes (HKLs) exposed to *Vibrio anguillarum* O1, followed by *de novo* transcriptome assembly, was performed. The transcriptome encompassed 221659 trinity genes, 9033 differentially expressed genes (DEG) at 6 hours post exposure (hpe) and 15225 DEG at 24 hpe. The DEG analysis of the lumpfish transcriptome clearly showed that the alternative pathway of the complement cascade is one of the chief mechanisms in the *V. anguillarum* response in lumpfish HKLs. Furthermore, the DEG analysis also clearly showed that the TLR signaling through the canonical NF-κB pathway was the major pathway in the adaptation of the innate immune response. Further, a wider MAPK pathway regulation was observed, involving all the sub pathways, however, at much less potent regulation levels compared with NF-κB. Globally, the DEG analysis displayed a picture of a pro-inflammatory reaction, initiated by the soluble Toll-like receptor 5 (TLR5S) and the alternative complement pathway, and resulting in high up-regulation of the cytokines interleukin (IL)-1β, IL-6, CXCL8 (also known as IL-8) and tumor necrosis factor (TNF)-α.

Further characterization of the lumpfish IL-1 family, both ligands, receptors (IL-1R) and IL-1 signaling pathways were performed. Full-length sequences of the ligands IL-1β, IL-18, and the fish-specific IL-1 family members nIL-1F and IL-1Fm2, the receptors IL-1R1, IL-1R2,

IL-1R4 (ST2/IL-33 receptor/IL-1RL), IL-1R5 (IL-18R1) and partial sequences of DIGIRR and IL-1R3 (IL-RAcP) were identified. *In vitro* stimulation of lumpfish leukocytes with a selection of PAMPs, showed that lumpfish IL-1β and nIL-1F were upregulated most potently by flagellin. The phylogenetic analysis of the IL-1 family ligands showed that IL-1β, nIL-1F1 and IL-1Fm2 are more like each other than to IL-18. Furthermore, sequences from lobe-finned fish and shark were clustered within the nIL-1F clade, suggesting that nIL-1F, together with IL-1β are ancestral genes. This is the first report describing the occurrence of nIL-1F in non-teleost species.

Characterization of lumpfish TNF-α revealed that it contained the hallmark properties of TNF-family at nucleotide and peptide levels. The phylogenetic analysis of teleost TNF-α clarified the evolutionary history of this gene within Teleostei. Basally in Teleostei the gene is duplicated. One gene retains the structure, while the other gene loses the amino acids at the C-terminus end of the transmembrane domain. This loss has been suggested to cause an impaired secretion of the molecule. Interestingly, all sequences within Ostariophysi were of this second type with questioned secretabillity. Further, duplication of the TNF-α genes have occurred in Salmonidae and Cyprininae. Although characterization of lumpfish IL-6 revealed a classic gene arrangement, two isoforms were predicted - one classic isoform (IL-6i1) and one isoform containing an alternatively retained intron (IL-6i2). The predicted peptide sequence of the IL-6i2 contained a signal peptide first revealed after proteolytic cleavage. Caspase 1 was predicted to cleave in this region. It is therefore hypothesized that lumpfish IL-6 kinetics may be dependent on caspase 1 processing. In the normal tissues and unstimulated leukocytes, the levels of TNF-α transcripts were higher than IL-6 transcripts, except for eye and brain where the transcript levels of IL-6 were unexpectedly high. Both genes displayed a similar induction pattern to PAMP stimulation *in vitro* and both were most potently stimulated by flagellin. IL-6 was more potently stimulated that TNF-α.

In conclusion, the lumpfish innate immune responses are potent and consist of most of the molecules for a modern teleost. The alternative complement pathway and TLR signaling pathway are fundamental to the *in vitro* response to *V. anguillarum* O1 in lumpfish leukocytes. The identification and characterization of the major pro-inflammatory cytokines and design of qPCR assays in lumpfish provides a valuable tool to measure innate immune responses in lumpfish e.g. upon immune modulation, such as vaccination, microbial diseases or physiological trials.

Table of contents

Abbreviations

AB	Antibody
AD	Acidic activation domain
BCR	B cell receptor
BIR	Baculovirus inhibitor of apoptosis protein repeat
BLAST	Basic local alignment search tool
CARD	Caspase-activated and recruitment domain
CFH	Complement factor H
CLC	Charcot-Leyden crystal
CNTF	Ciliary neurotrophic factor
CpG	Cytosine phosphodiester guanine
CT	Cardiotropin
DAMP	Danger associated molecular patterns
DC	Dendritic cell
DEG	Differentially expressed genes
e.g.	For example
EBD	Effector binding domain
G-	Gram negative
G+	Gram positive
GITRL	Glucocorticoid-induced TNA receptor-related protein ligand
GO	Gene ontology
HKL	Head kidney leukocytes
HPE	Hours post exposure
HUGO	Human genome organization
iE-DA	γ-D-glutamyl-meso-diaminopimelic acid
IL	Interleukin
IFN	Interferon
IPAF	Ice Protease Activating Factor
IUCN	International Union for Conservation of Nature
JNK	c-Jun N-terminal kinase
KO	Knockout
LCA	Least common ancestor
LIF	Leukemia inhibitory factor
LPS	Lipopolysaccharide
LRR	Leucine rich repeat
LTA	Lipoteichoic acid
MAC	Membrane attack complex

MALT	Mucosa-associated lymphoid tissue
MAPK	Mitogen-activated protein kinase
MASP	MBL associated serine proteases
MBL	Mannose binding lectin
MDP	Muramyl dipeptides
MYA	Million years ago
NACHT	Central nucleotide oligomerization
NALT	Nasal associated lymphoid tissue
NCC	Nonspecific cytotoxic cells
NF-κB	Nuclear factor-κB
NK	Natural killer
NLR	NOD like receptor
NOD	Nucleotide oligomerization domain
OSM	Oncostatin M
PAMP	Pathogen associated molecular pattern
PGLYRP	PGN recognition protein
PGN	Peptidoglycan
PHA	Phytohemagglutinin
Poly (I:C)	Polyinosinic:polycytidylic acid
PRM	Pathogen recognition molecule
PRR	Pathogen recognition receptor
PYD	Pyrin domain
RANKL	Receptor activator of nuclear factor kappa-B ligand
SARM	Sterile α- and armadillo-motif-containing protein
TAMP	Tumor associated molecular pattern
TCR	T cell receptor
TGF	Transforming growth factor
TICAM	TIR-domain containing adaptor molecule
TIRAP	TIR adaptor protein
TLR	Toll-like receptor
TS	Teleost specific
WGD	Whole genome duplication

List of papers

Paper I

Eggestøl, H.Ø., Lunde, H.S., Rønneseth, A., Fredman, D., Petersen, K., Mishra, C.K., Furmanek, T., Colquhoun, D.J., Wergeland, H.I., Haugland, G.T., 2018. Transcriptome-wide mapping of signaling pathways and early immune responses in lumpfish leukocytes upon in vitro bacterial exposure. Sci Rep. 8, 5261. https://doi.org/10.1038/s41598-018-23667-x

Paper II

Eggestøl, H.Ø., Lunde, H.S., Haugland, G.T., 2020. The pro-inflammatory cytokines TNF-α and IL-6 in lumpfish (*Cyclopterus lumpus* L.) -identification, molecular characterization, phylogeny and gene expression analyses. Dev Comp Immunol. 105, 103608.

Paper III

Eggestøl, H.Ø., Lunde, H.S., Knutsen, T.M., Haugland, G.T., 2020. Interleukin-1 ligands and receptors in lumpfish (*Cyclopterus lumpus* L.): molecular characterization, phylogeny, gene expression and transcriptome analyses, Front. Immunol. Revised manuscript has been submitted.

Introduction

Lumpfish utilization and major infectious diseases

Reported lumpfish (*Cyclopterus lumpus*) farming started in 2012. This makes it a novel species in aquaculture, although it has been caught in wild fisheries for a long time and valued for its roe – a sought after commodity in the making of caviar. However, roe is not the reason why lumpfish fish farmers started rearing lumpfish. Fish farmers started to rear lumpfish due to its ability to control salmon louse (*Lepeophtheirus salmonis*) levels in the salmon net pens. Along with lumpfish, several species of wrasse (Labridae) have shown adequate capability of controlling the salmon louse levels (Powell et al., 2018). The supply of wrasse has mostly been from the wild fisheries, while the aquaculture has supplied most of the lumpfish. The supply of wrasse has only increased modestly, while lumpfish production has grown exponentially. The average price for lumpfish has continued to increase and in 2018 it reached approximately 21 NOK/fish of deployment size.

The production of lumpfish relies on the capture of wild brood stock, and raising the offspring in captivity (Powell et al., 2018). This practice may pose a strain on natural populations, and the species is classified as near threatened by the International Union for Conservation of Nature (IUCN). There are growing concerns that over-exploitation of wild stocks and translocation of hatchery-reared lumpfish may compromise the genetic diversity of native populations. These concerns were strengthened by a recent study showing that some lumpfish populations are very small and have low genetic introgression (Whittaker et al., 2018). The effective population sizes of North East Atlantic (Iceland, Faroe Island and Norway) populations were found to be consistently low, and susceptible to these concerns.

The production of lumpfish is successful and the number of deployed lumpfish in salmon cages in Norway in 2018 was 30 million fish (Norwegian Directory of Fisheries). However, high mortality among farmed lumpfish has been reported, both during production, during

transportation and in net pens. Lumpfish suffer from diseases in the same manner as all other organisms, and high mortality caused by bacterial diseases has been observed. In recent years, viral diseases have also been reported (Table 1). In addition, some of the incidents were related to sub-optimal handling and conditions in the net pens, such as; low oxygen levels during transportation, lack of equipment suitable for lumpfish and lack of feed in the net pens. However, mortalities caused by bacterial infections have caused the major disease outbreaks in lumpfish. In particular, three bacteria have been highly problematic: *V. anguillarum*, atypical *Aeromonas salmonicida* and *Pasteurella* sp., and are still a major problem (Walde et al., 2019), Table 1.

V. anguillarum, also known as *Listonella anguillarum*, is a Gram-negative (G-) comma shaped rod bacterium. It is polarly flagellated, non-spore forming, halophilic, facultatively anaerobic and the causative agent of vibriosis, a deadly hemorrhagic septicemic disease affecting various marine and limnological organisms including vertebrates, mollusks and crustaceans (Bergman, 1909; Farmer et al., 2015; Frans et al., 2011). It causes high morbidity and mortality rates in aquaculture and larviculture worldwide, thereby causing severe economic losses (Frans et al., 2011). In lumpfish, *V. anguillarum* is suspected to cause a classic vibriosis characterized by lesions, enlarged anus, pale gills, ascites and inflamed gut (Gulla, 2016). The classic vibriosis in lumpfish is to a large extent under control, as successful vaccines have been developed and deployed. However, lumpfish are still vulnerable to *Vibrio* infections in early life stages and before the vaccine gives protection. Also, a marketing license is needed as the vaccine is today distributed under an exemption from the Norwegian law.

A. salmonicida was first described in Emmerich and Webel (1894) as the bacteria of trout disease. The disease was a major threat in salmon farming until effective oil-adjuvanted vaccines were developed (Midtlyng, 1996). Clinical outbreaks in salmon are seldom observed today. There are several recognized subspecies of *A. salmonicida*, but many

laboratories are satisfied with only distinguishing between typical and atypical *A. salmonicida*. Strains belonging to the subspecies *salmonicida* are denoted as typical while others are denoted as atypical, leaving the atypical *A. salmonicida* taxonomically more diverse than the typical (Wiklund and Dalsgaard, 1998). Gulla et al., (2016) created a rapid and inexpensive method for distinguishing between the different *A. salmonicida* subspecies by typing its vapA gene, a gene encoding the A-layer protein. Typical isolates are often related to disease in salmonids (furunculosis), atypical isolates are most commonly recovered from non-salmonid fish (disease often termed atypical furunculosis) (Gulla, 2017). Macroscopically dark skin, skin lesions, hemorrhages, hemorrhaged swollen anus and multiple white nodules in kidney was observed in intraperitoneal and cohabitation *A. salmonicida* infected lumpfish (Rønneseth et al., 2017).

Disease caused by *Pasteurella* sp., known as pasteurellosis, in farmed lumpfish has steadily increased during the years of production and is today one of the most prevalent bacterial disease agents in Norwegian lumpfish aquaculture. Although the bacterium has not yet been described to the genus level, phylogenetic analysis revealed a close relation to *Pasteurella* sp. from Atlantic salmon in Norway (Alarcon et al., 2016a). Macroscopically affected fish show skin lesions, especially around the eyes, hemorrhages of internal organs, gill, fins and granulomas. Histopathological observations include; multifocal bacterial microcolonies in skin, gills and internal organs (Alarcon et al., 2016a; Ellul et al., 2019 b). It can resemble the histopathology of *A. salmonicida* (Scholz et al., 2018). The *Pasteurella* sp. can cause extreme mortalities (up to 100%), and antibiotic treatment does not completely treat the population, as subclinical carriers post treatment is common and outbreaks can reemerge after stress-events. It has been speculated that *Pasteurella* sp. is a facultative intracellular bacterium, possibly explaining the lack of efficiency in antibiotic treatments (Ellul et al., 2019 b). The currently available commercial vaccines to lumpfish do not contain *Pasteurella* sp., and if it has a facultative intracellular lifestyle, it will be very difficult to develop efficient vaccines. Vaccine trials have been conducted – although

the mortality kinetics of challenge trials were affected by the vaccines, the end mortality was not. It is suggested that this is either an effect of the vaccine-preparation or due to the possible intracellular nature of *Pasteurella* sp. (Ellul et al., 2019 a). These properties make *Pasteurella* sp. a serious threat against aquaculture applications of lumpfish.

In the most recent years, *Pseudomonas anguilliseptica* has proven to be an elusive agent and is considered an emerging pathogen. None of the current disease combating measurements have hindered the spread of *P. anguilliseptica*, as outbreaks of this pathogen is strongly correlated to the production of lumpfish ($r^2 = 0.9932$, Fig. 1) – as more lumpfish are sold, more outbreaks caused by *P. anguilliseptica* are observed. When using the parameter "sold lumpfish" as proxy for number of lumpfish in Norwegian fish farming, these data entail that *P. anguilliseptica* is a proficient pathogen at exploiting the production and utilization conditions in Norway. In order to gain control of this disease,

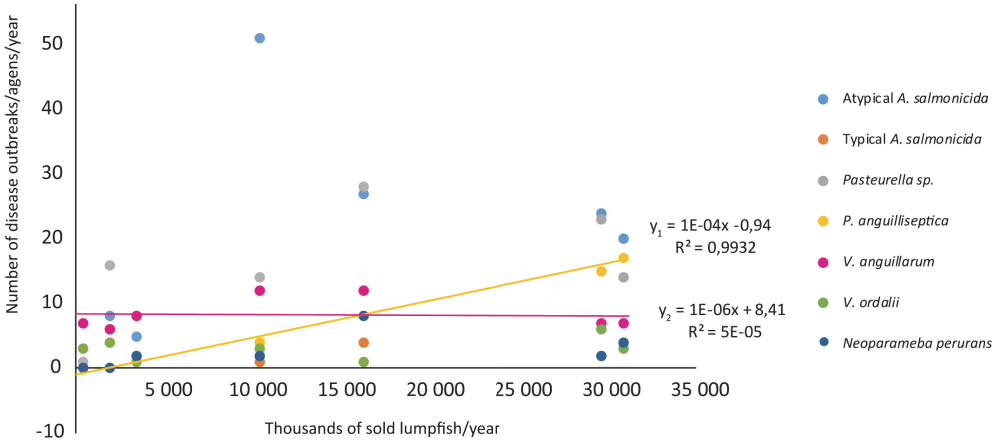

Figure 1. Scatterplot of number of Norwegian lumpfish localities with disease outbreaks in plotted against yearly production of lumpfish. y_1 = the linearly relationship between *P. anguilliseptica* outbreaks and amount of sold lumpfish. Illustrated by the yellow trend line. y_2 = the linearly relationship between *V. anguillarum* outbreaks and amount of produced lumpfish. Illustrated by the pink trend line. R^2 reflects the Pearson correlation effect of the respective y_x. The data presented here is a compilation of data from the Fish Health report 2018, Table 10.1, of the Norwegian Veterinary Institute and the sales report 2012-2018 of sold cleaner fish from the Norwegian directorate of Fisheries.

development of either new farming routines or veterinary practices, such as vaccines and antibiotic treatment, must occur. *P. anguilliseptica* vaccines for other species exist today (Jang et al., 2014) and could possibly be adjusted to lumpfish and included in polyvalent vaccines. Although *P. anguilliseptica* infections are not associated with high mortalities, its increasing prevalence should be taken seriously, especially considering the possibility for development of antibiotic resistance which can be transferred to more bacteria.

Table 1. Diversity of pathogens isolated from diseased lumpfish.

Koch's postulate has not been fulfilled for all microbes in this list.

Pathogen	Disease	Type of pathogen	Description in lumpfish
Aeromonas salmonicida	Furunculosis	Bacteria (G-)	(Gulla et al., 2016)
Moritella viscosa	Winter ulcer disease	Bacteria (G-)	(Scholz et al., 2018)
Pasteurella sp.	Pasteurellosis	Bacteria (G-)	(Alarcon et al., 2016a)
Piscirickettsia salmonis	Piscirickettsiosis	Bacteria (G-)	(Marcos-Lopez et al., 2017)
Pseudomonas anguilliseptica	Red spot disease	Bacteria (G-)	(Scholz et al., 2018)
Tenacibaculum maritimum	Tenacibaculosis	Bacteria (G-)	(Småge et al., 2016)
Vibrio anguillarum	Vibriosis	Bacteria (G-)	(Marcos-Lopez et al., 2013)
Vibrio spp.	Atypical vibriosis	Bacteria (G-)	(Walde et al., 2019)
Exophiala angulospora		Fungi	(Scholz et al., 2018)
Exophiala psychrophila		Fungi	(Scholz et al., 2018)
Nucleospora cyclopteri		Fungi	(Alarcon et al., 2016b)
Tetramicra brevifilum		Fungi	(Scholz et al., 2017)
Anisakis simplex		Metazoa	(Johansen et al., 2016)
Caligus elongatus		Metazoa	(Johansen et al., 2016)
Gyrodactylus cyclopteri		Metazoa	(Johansen et al., 2016)
Hysterothylacium aduncum		Metazoa	(Johansen et al., 2016)
Ichthyophonus hoferi -like		Metazoa	(Bornø & Linaker 2014)
Kudoa islandica	Soft flesh disease	Metazoa	(Kristmundsson & Freeman 2014)
Myxobolus albi		Metazoa	(Cavin et al., 2012)
Neoparamoeba perurans	Amoebic gill disease	Protozoa	(Haugland et al., 2017)
Trichodina spp.		Protozoa	(Johansen et al., 2016)
Lumpfish flavivirus		Virus	(Skoge et al., 2018)
New ranavirus		Virus	(Scholz et al., 2018)
Viral hemorrhagic septicemia virus	VHS	Virus	(Guethmundsdottir et al., 2019)

The innate immune system of teleosts

The immune system is divided into the innate (non-specific) and the acquired (specific) immune system. However, growing evidence reveal interplay and functional overlap between these sections. Despite this, it is a valuable distinction. Chiefly, the potency of the innate immune system is dependent on genetic inheritance, while the potency of the adaptive immune system is dependent on the individual microbial exposure history. In addition, the innate immune system is more structurally and functionally diverse while the adaptive immune system is a highly specialized system that has honed a few effector mechanisms with highly specific initiators - the T-cell receptor (TCR) and B-cell receptor (BCR). Furthermore, the innate immune system is considered a rapid response system while the adaptive immune system is considered a slow, but heavy hitting, defense system.

The immune response to a new pathogen occurs in three phases. The first phase includes the anatomical barriers and some immediately acting humoral factors. In the second phase of the response, innate immune cells sense the presence of the pathogen. This activates the innate immune cells, which initiate several different effector mechanisms. If these responses are not enough to handle the infection, mechanisms will be engaged to induce the third phase of the immune response, which leads to the expansion of antigen-specific- and memory lymphocytes.

The first phase of the immune response.

Pathogens are nearly as diverse as the tree of life; representatives within all kingdoms of life infect other representatives. When we phylogenetically limit the host to a phylum, for instance Vertebrata, the diversity is smaller, but still striking. Five groups of Vertebrate-infecting pathogens can be characterized: viruses, Bacteria, Fungi, Protozoa and Metazoa. The three former groups are often described as microbial organisms, or microbes for short, while the latter two groups are often described as parasites. These groups are

biochemically different from each other, they have different habitats and life cycles. In order to control these pathogens, the hosts have a wide range of innate and adaptive immune mechanisms. Table 1 contains a list of the lumpfish pathogens highlighting the diversity.

Pathogens can infect all body compartments. Two compartments can be defined: the extracellular and the intracellular. The extracellular compartments are separated into epithelial and interstitial spaces, while the intracellular compartments are separated into cytoplasmic and vesicular spaces. Most bacterial pathogens live and replicate in extracellular space causing extracellular infections and inflammation (see section "Inflammation"), and they are susceptible to engulfment by phagocytic cells. The phagocytic cells have receptors that can recognize the pathogen directly, but also receptors for opsonins, which are components that cover the pathogens and make it more vulnerable for phagocytosis, such as lectins and complement factors (Zhang and Wang, 2014) . In addition to phagocytic receptors, phagocytic cells have signaling PRRs, which upon binding with their respective ligands, initiate intracellular signaling cascades leading to an increased cytokine production.

Surface tissues

A tough skin, with an outer layer of keratinized dead cells, hair and fatty acids, characterizes the external surface of mammals. This provides a completely different ecological niche than the fish skin. The fish skin lacks a mechanical barrier provided by the dead cells. Further, mucus covers the teleost skin, and fish have scales instead of hair. Lumpfish also have hypodermic protrusions that break the epidermis and are covered only by mucus. Haugland et al., (2018) theorized that these protrusions might act as important gateways for pathogens if the mucus layer gets disturbed. Mucus covers all the epithelial surfaces of teleosts, and it has been of high interest in fish health research the later years. In addition to possessing local adaptive immune reactions, reviewed in Salinas (2015),

mucous tissues possess a myriad of different innate immune components and provide physical barriers. All mucosal surfaces of teleosts are in an intimate relation with the microbiota of the surrounding water, and the microbial load on the surfaces of the fish can be very high. Here follows an anatomical description of the differing surface tissues, including specialized immune adaptations for each organ.

Stratified squamous epithelium lines the mouth cavity, gill arches and esophagus, containing numerous mucus cells and taste buds. The mucus ensures easy passage of feed and protects the epithelium. The gills are in the gill cavity, the area between the gill arch and the operculum (gill lid). Two gill filaments are attached to one gill arch, both filaments are referred to as holobranch, while one of the two are referred to as hemibranch. The hemibranch is composed by stacked primary lamellae, protruding from the lateral-posterior side of each gill arch. On each primary lamellae, thin-walled tissue leaves – or secondary lamella – are stacked tight and is the site of gas exchange. Simple squamous epithelium lines the surface, it is supported by pillar cells (specialized endothelial cells) which form the capillary veins. This ensures an efficient respiratory organ by an extremely close distance between the blood and the oxygen rich water (0.5 – 4 µm in healthy individuals). Active species have larger and more numerous secondary lamellae, and more sedate species have smaller and less numerous secondary lamellae (Kryvi and Totland, 1997). In salmonids an inter-branchial lymphoid tissue has been characterized (Haugarvoll et al., 2008). It has been described as “intraepithelial cell accumulations on the caudal edge of the inter-branchial septum at the base of the gill filaments”, and “a distinct structure consisting of T cells embedded in a meshwork of epithelial cells” (Aas et al., 2014; Haugarvoll et al., 2008). This salmonid inter-branchial lymphoid tissue is the only evidence in teleosts of an organized mucosa-associated lymphoid tissue (MALT).

Recently, the nasal cavity has sparked an increased interest among fish immunologists. The detection by Tacchi et al., (2014) of a nasal associated lymphoid tissue (NALT) in

rainbow trout has been important in driving this interest. Teleosts possess two nasal cavities, both placed in between their two respective nasal openings and ends. Water flows in through the anterior opening, passes through the olfactory rosette and leaves the fish through the posterior opening. Movement of the fish is usually the cause of the water flow. A central bar of connective tissue with olfactory epithelium folds protruding from it, composes the olfactory rosette. The sensory cells of the olfactory epithelium are classical bipolar neurons – being a short dendrite ending in the surface of the epithelium with a limited number of cilia. The combined neurites of all the sensory cells encompasses the *nervus olfactorius*, and is directly coupled two *lobus olfactorius*, usually situated directly in front of *telencephalon* (Kryvi and Totland, 1997). This short distance between the water and brain is an ecological niche some microbes might exploit, as the brain's immune defense lack pro-inflammatory properties. Besides the olfactory sensory cells, the olfactory epithelium consists of support-, basal-, myeloid- and lymphoid cells (Kryvi and Totland, 1997; Tacchi et al., 2014). The lymphoid cells are also scattered throughout the *lamina propria*, and compromises the diffuse nasal associated lymphoid tissue. In rainbow trout NALT, IgT^+ B-cells contribute 50-60% of the total B-cells, resembling the population distribution of gut. IgT^+ B-cells in the nasal cavity are primarily found in the epithelial tissue while in gut IgT^+ B-cells tend to be localized in the *lamina propria*. Further, in rainbow trout mucosal Ig's coat two thirds of the microbial community colonizing the nasal cavity and 50% of the microbial community are double coated while IgT and IgM, coated with 25% each (Tacchi et al., 2014).

The digestion canal starts at the mouth and continues through the fish until its rectum. Conceptually, the digestion canal is organized in a constant fashion:1, the lumen is lined by an epithelial mucosa-layer, 2, it is supported by a sub-mucosa layer, mainly consisting of loose connective tissue known as *lamina propria*, 3, this is separated by a cell-less band of collagen, known as *stratum compactum*, and 4, it is enclosed in a layer of circular muscle followed by a layer of longitudinal muscle. This muscle layer is known as *muscularis*

externa, and is sheathed by a layer of peritoneum, known as serosa. The muscle layer ensures the passage of food by peristaltic movements. Based on distinct morphological and histological properties, the division of the digestion canal in teleosts is mouth, esophagus, stomach, gut and hindgut. The entire digestion canal is lined by varying mucous tissues, some of them are primarily important as a first-line defense of the immune system, while other also contain lymphocytes. The immunology of the digestion canal is interesting from the applied sciences regarding immune prophylaxis and production, as inflammation of the digestion canal can significantly affect growth rate and so forth. Further, the digestion canal is an important route of infection of many pathogens.

Several sphincters line the entrance of the esophagus. The esophagus mucosa layer consists of several layers of cylinder cells covered by mucus cells, lining the lumen a simple squamous cell layer. Secreted mucus on the surface of the epithelium is continually produced by the numerous mucus cells. The esophagus epithelium has several folds in both cross-sectional and longitudinal direction and beneath the *lamina propria* there are muscles, yielding a noticeable flexible tube able to move large pieces of food down to the stomach.

Some teleost species lack a stomach, and the esophagus leads the food directly into to the gut. Cleaner fish from the family Labridae is among them (Lie et al., 2018). The transition between the esophagus and stomach is not macroscopically clear, but histologically there is a defined division. The composition of stomach wall is like the gut as the mucosa layer is a folded simple cylinder epithelium supported by submucosa. Numerous granulocytes surround the stratum compactum. In addition to this general organization of the stomach and gut, they have some defining features. Tight folds line the stomach epithelium creating a microenvironment called the crypt. Chief cells line the crypt and produce the hydrochloric acid and pepsin, responsible for the bulk digestion. From humans, the pH in the stomach can reach extremely low levels, ranging from pH 1-2. A mucus layer

containing high concentrations of bicarbonate and potassium protects the chief cells, also providing a difficult pH barrier for pathogens to pass (Ross and Pawlina, 2011). The proximal region of the stomach contains a thinner muscle layer than the distal region. At the end of the distal region an area called pylorus is defined by the increased circular muscle layer, giving rise to a sphincter muscle that separates the stomach and the gut (Kryvi and Totland, 1997).

Further digestion is continued in the gut. Immediately downstream of the pylorus, the gall and pancreas ducts deposit its contents into the gut. Consequently, the pH is increased, and, fat emulsifiers, waste from blood and digestive enzymes is deposited in the gut. Distally of these ducts, pyloric caeca are often found. These are dendrite-like gut-protrusions that can be numerus, reaching hundreds in some cod species. Principally the histology of these are like the rest of the gut, although the walls are thicker. The histology of the gut resembles the histology of the stomach, with some notable exceptions. The simple cylinder epithelium has several adaptations increasing the surface tissue: cross-sectional folds, mucosa villi and epithelial microvilli. The cross-sectional folds can surpass half the circumference of the gut. Upon these folds the mucosa villi protrudes and apically on the epithelial cells the microvilli is located. Further, the epithelium contains secretory endocrine cells and intra-epithelial leukocytes with significant cytotoxic activity (Kryvi and Totland, 1997; McMillan and Secombes, 1997). However, most of the leukocytes are present in the submucosa.

Body fluids

Immunologically there are three body fluids of major importance: mucus, interstitial fluid and vascular fluid. Mucus is an extra-cellular matrix rich in glycoproteins yielding a highly viscous fluid covering all surface tissues of teleosts. In addition to all the immune components (e.g. antibodies, antimicrobial peptides) in mucus, it has important functions as it harbors commensal microbiota and is being continuously shed, thereby making it

hard for pathogens to establish a site of infection. The interstitial fluid is the fluid filling all the gaps between the cells in organs and tissues. This fluid is rich in several immune components, and sentinel cells of the innate immune system, such as macrophages and dendritic cells that continuously wade through it hunting for potential pathogenic components. The vascular fluids, blood and lymphatic fluids, are extremely important for protection, as the immune system is distributed throughout the entire body, and not localized to one specific organ. During inflammation, immune cells and immune components (e.g. humoral factors such as acute phase proteins and pro-inflammatory cytokines) must be recruited to a site of infection within short time and the vascular systems are the highways of the immune system.

The presence of a lymphatic system in teleosts has been questioned. However, recent studies have shown that zebrafish possess a secondary vascular system that shares many of the morphological, molecular and functional characteristics of lymphatic systems in other vertebrates (Jung et al., 2017, and references within). Whether this represents a true lymphatic system, as seen in higher vertebrates, or an evolutionary prototype remains to be unveiled.

Humoral components

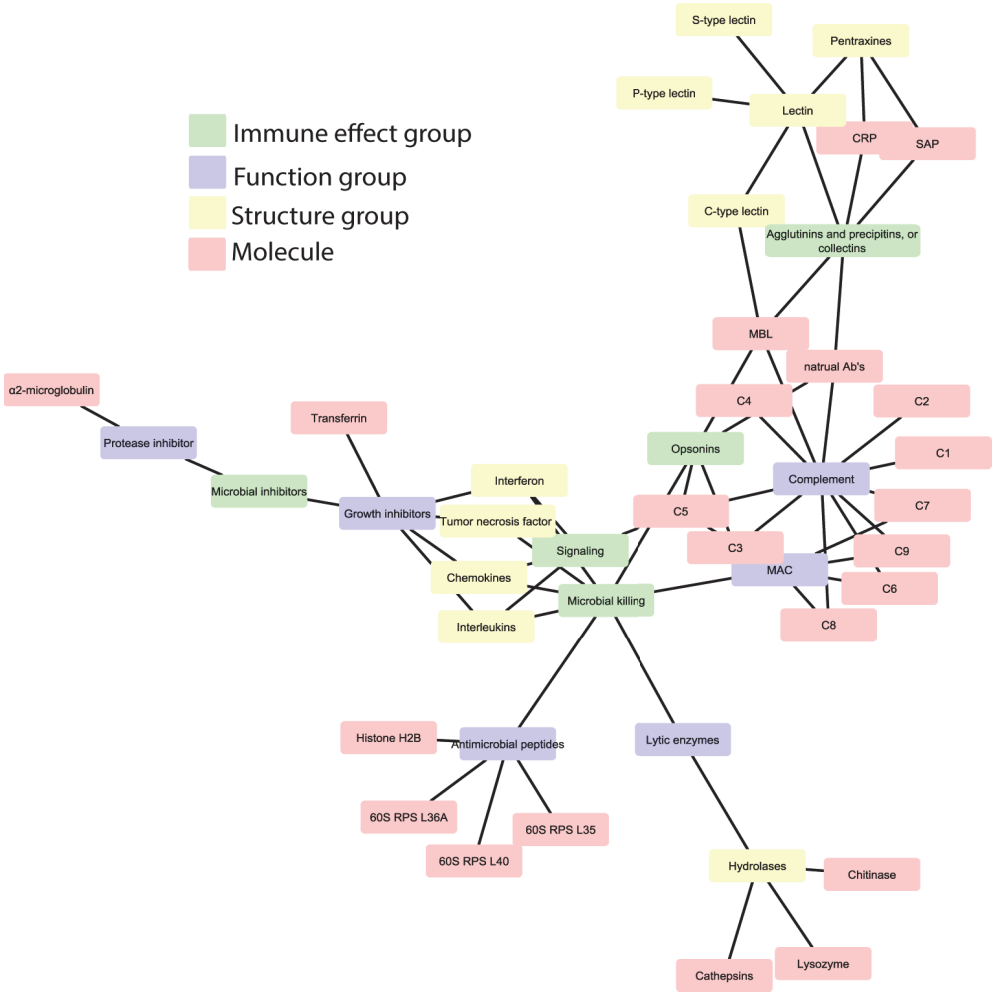

Figure 2. A non-exhaustive network overview of humoral components and related terms in the teleost innate immune system.

The humoral components of the innate immune system are numerous and diverse, and it is beyond the scope of this introduction to give an exhaustive description of it. Several reviews cover this topic (Magnadottir, 2006; Whyte, 2007; Zhu et al., 2013). The humoral components (Fig. 2) have several immune effects, such as microbial inhibition, microbial

killing, signaling, opsonization or precipitation of microbes. In the current study, we have focused on early immune responses, and thus the complement system, the PRRs and the cytokines in the humoral innate immune system are described in the following sections.

Complement system

The complement system is an essential part of the innate immune system, constituting a link between innate and adaptive and it compromises of more than 35 different soluble and membrane-bound proteins. Most complement components have been identified in teleosts (Zhang and Cui, 2014), including lumpfish (Eggestøl et al., 2018 and Haugland et al., 2018). The complement factors are synthesized as inactive precursor molecules, activated by different stimuli. These stimuli define the three different activation pathways (reviewed in Walport 2001, and references within). Activation of the classical pathway, which was the first pathway to be described, occurs through binding of an antigen by an antibody (Ab) leading to a conformational change of the Ab and the subsequent binding of C1s, -r and -q. In turn, this complex called the C1qrs complex, leads to splitting of C4 and C2 into C4a, C4b, C2a and C2b. C4b and C2b dimerize forming C4bC2b or C3 convertase, which in turn splits C3 into C3a and C3b. C3b in turn complex with C3 convertase and forms the C5 convertase. All activation pathways converge on C5 convertase, which splits C5 into the chemokine C5a and C5b. C5b activates a cascade of proteins, C6-C9, which results in a pore-forming membrane attack complex (MAC). The MAC lyse the pathogen as it permeates the membrane, causing the cytoplasm to leak out of the attacked pathogen.

Activation of the lectin pathway occurs through the binding of lectin. Ficolins and mannose binding lectin (MBL) can bind lectins, mainly mannose and N-acetylglucosamine, and activates MBL associated serine proteases (MASP). In turn the MASPs acts as the C1 complex and splits C4 and C2 in a similar manner, resulting in the processing of C5 with subsequent lysis of the pathogen.

In the alternative pathway C3 spontaneously hydrolyses in the body fluids, and binds all membranes. Membrane bound C3b binds to factor B and forms C3bBb a C3 convertase, which in turn binds another C3b forming C3bBbC3b. This complex is stabilized by properdin and functions as a C5 convertase, which causes the MAC to form. However, this pathway as described does not separate between host and pathogen cells, potentially leading to detrimental conditions for the host. In order to separate between self and non-self, host cells express a C3b receptor that binds and inhibits the C3 convertase activity, thereby stopping the complement cascade on host-cells. In teleosts the alternative pathway's components have been measured several titers higher than in mammals, likely reflecting an increased dependence on the alternative pathway (Sunyer and Tort, 1995).

Inflammation

Inflammation is a complex biological response of body tissues to harmful stimuli - microbes, irritants or damaged cells. It is a protective response that involves leukocytes, fibroblasts, vascular vessels and soluble molecules (Murphy and Weaver, 2012). In a molecular perspective, the response starts by innate immune cells detecting a pathogen-/damage associated molecular pattern (PAMP/DAMP). This leads to a transduction of intracellular signals, which ultimately leads to the production and secretion of effector molecules and a changed phenotype (see references in section "Bacteria induced PRR mediated signaling"). Typically, this will be performed by macrophages, which are sentinel cells continuously sensing its environment, but also by dendritic cells (Murphy and Weaver, 2012). The effector molecules include the pro-inflammatory cytokines IL-1β, IL-6 and TNF-α (see references in section "Pro-inflammatory cytokines"). This will initiate an immunological cascade reaction leading to granulocyte- and macrophage-infiltration, in particular neutrophils will be recruited, and vasodilation of the neighboring blood vessels (reviewed in Ryan and Majno 1977). In the late phases encapsulation by fibroblasts will occur, separating the affected tissue from healthy tissue. Also, dendritic cells migrate to the lymph node where it presents antigens to naïve T-cells. Fish do not have functionally

homologous lymph nodes as mammals, but head kidney and spleen are secondary lymphoid organs in fish where antigen presentation takes place (Haugland et al., 2018).

Phagocytosis

Phagocytosis is the process by which cells engulf large, solid particles (>1 µm) and form internal vesicles called phagosomes. It is a defensive reaction against infection and invasion of the body by foreign substances. Moreover, it is crucial to maintaining the homeostasis in the body, as it removes cell debris and apoptotic cells. Phagocytosis is therefore considered a critical process of the innate immune system (Esteban et al., 2015). In vertebrates, professional phagocytic cells are monocytes, macrophages and granulocytic cells, mainly neutrophils. Furthermore, B-cells in fish and amphibians, and the mammalian B1 cells, are professional phagocytic cells with the ability to kill internalized bacteria (Li et al., 2006; Rønneseth et al., 2015; Øverland et al., 2010). Also, thrombocytes have this ability in teleosts (Esteban et al., 2015).

The phagocytic activity of lumpfish leukocytes is very high, as characterized by Haugland et al., (2012a). Leukocytes from head kidney, peripheral blood and spleen displayed very high phagocytic and respiratory burst activity, verifying a potent oxygen-dependent killing mechanism. The phagocytic leukocytes were morphologically heterogeneous (Rønneseth et al., 2015). Except for anti-IgM antibody (detecting B-cells), lack of available antibodies made it impossible to identify the phagocytes further. Interestingly, a subset of small leukocytes with extremely high phagocytic capacity were identified (Rønneseth et al., 2015), like observations in salmon (Haugland et al., 2012b).

Cells of the innate immune system

The hematopoiesis of the cells (leukocytes) in the immune system are divided into two main lineages: the myeloid and lymphoid. Chiefly, the innate immune cells are of the myeloid cell lineage, while the adaptive immune cells are of the lymphoid lineage. However, there are some notable exception to this claim: natural killer (NK) cells in

mammals (or nonspecific cytotoxic cells (NCC), in teleosts) and plasmacytoid dendritic cells (Manz, 2018). The other innate immune cells of teleosts include monocytes, macrophages and granulocytes (Castro and Tafalla, 2015, references within and Haugland et al., 2014). The lumpfish leukocytes were morphologically (see Fig. 3) and cytochemically characterized (Haugland et al., 2012a). Furthermore, they were stained by anti-IgM antibody labelling B-cells (Rønneseth et al., 2015).

All the main subtypes of leukocytes were identified such as lymphocytes, monocytes/macrophages, neutrophils and dendritic-like cells. Monocytes circulate in the blood and differentiate into macrophages when they migrate into tissue. During inflammation, macrophages are the first cells to encounter invading pathogens, and engulf and degrade them. A range of phagocytic receptors such as glucan receptors, receptors for complement factors and Fc receptors mediate this process (Zhang and Wang, 2014). Phagocytosis has been reported to be most active within macrophages among teleost leukocytes (Esteban et al., 2015).

Three different types of granulocytes have been identified in fish: neutrophils, eosinophils and basophils. Mammalian neutrophils are crucial in the anti-microbial defense, as they kill, degrade and initiate an inflammatory response upon microbial exposure. However, morphological heterogeneity and a lack of cell-specific surface markers makes it difficult to postulate generalized claims regarding the function of teleost granulocytes (Esteban et al., 2015). Mammalian neutrophils control the microbial environment through phagocytosis and secretion of antimicrobials, like macrophages. In addition, neutrophils can produce neutrophil extracellular traps - fiber networks primarily composed by DNA that bind pathogens. It is believed that neutrophil extracellular traps limit the inherent damage to the host-cells, which occurs because of anti-microbial activity of neutrophils (Brinkmann et al., 2004).

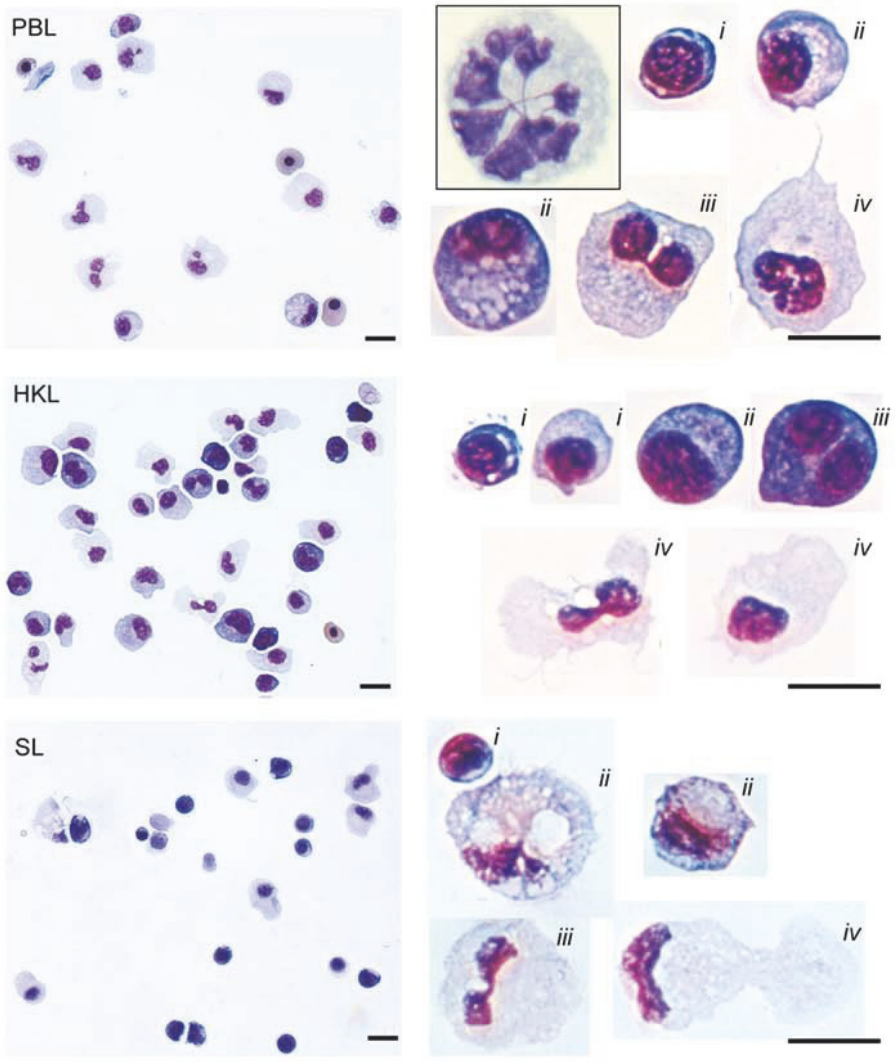

Figure 3. Morphological characterization of lumpfish leucocytes isolated from peripheral blood (PBL), head kidney (HKL) and spleen (SL). The overview photos in the left panels and the representative single cells were captured at 400 and 630 times magnification, respectively. *i* = lymphocytes, *ii* = monocytes/macrophages, *iii* = polymorphonuclear cells and *iv* = dendritic-like cells. The inset at top left of the right panel show a polymorphonuclear neutrophil isolated from Atlantic salmon for comparison. From Haugland et al. (2012a).

DCs are crucial in the mammalian immunology paradigm. Being both important cells of the innate immune system as phagocytic cells and highly potent antigen presenting cells bridging the innate and adaptive immune systems. Upon exposure to antigens, DCs engulf, degrade and present the antigens on its surface, migrates to lymphoid tissues where it activates and stimulate lymphocytes to elicit a highly specialized immune response. In zebrafish, a cell population with DC-like morphology and high affinity for peanut agglutinin was capable to phagocytose bacteria and activate T-cells in an antigen-dependent manner (Lugo-Villarino et al., 2010). Mammalian protocols for generation of DCs have been adapted to obtain cultures of highly mobile, non-adherent rainbow trout cells with irregular membrane processes and expressed surface major histocompatibility complex (MHC) class II (Bassity and Clark, 2012). The dendritic like cells in rainbow trout had tree-like morphology, expressed DC markers, were able to phagocytose small particles, were activated by TLR-ligands and migrated *in vivo*, all hallmark properties of mammalian DCs. Further, small mononuclear blood cells in Atlantic salmon expressed CD83 and MHC class II, but not IgM, CD3, CD8 and TCRα, showed intense phosphatase staining, a lack of respiratory burst, a lack of myeloperoxidase activity and acid phosphatase's sensitivity to tartrate. The morphologies were variable, and able to change upon stimulation with mitogens obtaining branching protrusions like DCs (Haugland et al., 2012b).

In addition to studies reporting the presence of DCs in immune organs and blood, DC subsets have been identified in teleost skin and gills (Granja et al., 2015; Soleto et al., 2018). The identification of DCs in fish suggest that specialized antigen presenting cells evolved in concert with the emergence of adaptive immunity (Esteban et al., 2015).

Cell-mediated cytotoxicity occurs because of altered, tumor, virus-infected or foreign cells. Mammalian NK cells do not need to be activated such as T-cells and B-cells and carry out its function as a part on the innate immune system. NK cells are large and granular cells and kill target cells by a three-step process: 1, recognition of target cell, 2, target cell

contact and formation of immunological synapse, and 3, NK cell-induced targeted cell death (Abel et al., 2018). NCC are recognized as the teleost equivalent to mammalian NK-cells (Evans and Jaso-Friedmann, 1992). They are large granular lymphoid cells without TCR or BCR that have a cytotoxic activity that is independent of prior exposure history.

Recently, a new group of innate immune cells have been recognized - the innate-like lymphocytes, including among others the NK cells (reviewed in Spits and Cupedo 2012). Evidence suggests that conventional fish lymphocytes could have developmental, morphological and functional features in common with innate-like lymphocytes of mammals. Therefore, fish lymphocytes could be of valuable comparative interest in the study of human diseases involving innate-like lymphocytes (reviewed in Scapigliati et. al 2018)

Germline encoded pathogen recognition

In addition to phagocytosis, non-self-stimuli initiate intracellular signaling pathways ensuring that the immune response is tailored to the invading pathogen. Pathogens have signature molecules, PAMPs, revealing them as intruders for the immune system. In addition to be specific for a group of pathogens and not found within the host, PAMPs are conservative and repetitive. By the requirement of conservative, it is referred to the lack of evolutionary divergence potential and by repetitive it is referred to the monomeric nature - PAMPs occurs as molecular units that is compiled together as polymer. PAMPs can be divided into subgroups based on their chemical properties. Bacterial PAMPs will be discussed in further detail in the following sections.

So-called pathogen recognition receptors (PRRs) and pathogen recognition molecules (PRMs), expressed by the host, recognize the PAMPs. PRMs can have direct killing action on the bacteria such as antimicrobial peptides, or they initiate an extracellular cascade reaction leading to an immune reaction, such as the complement system. PRRs on the other hand initiate an intracellular signaling cascade leading to a changed phenotype of

the cell including an increased secretion of immune-orchestrating cytokines. PRRs includes Toll-like receptors (TLRs).

PAMPs

The flagellum, the whip-like appendage enabling bacterial motility, is constructed of repetitive units of the peptide monomer flagellin. Earlier, flagellin was primarily viewed as a virulence factor, but is now considered a potent immune activator. Due to this potency it is recognized as an important vaccine adjuvant and immune stimulator (Tafalla et al., 2013). Flagellin is recognized by the TLR5 (Hajam et al., 2017).

Lipopolysaccharide (LPS) is a highly acylated saccharolipid located at the outer membrane of G- bacteria. It functions as a barrier preventing the passive diffusion of hydrophobic solutes into the cell, such as antibiotics and detergents, and it is considered an essential component for outer membrane biogenesis and cell viability (Zhang et al., 2013a). Although LPS is a highly potent stimulator of the mammalian immune system, its role as a PAMP in teleosts is convoluted. It is firmly proven that teleosts respond to LPS exposure, although generally considered not as potent as mammals, and the mechanism of detection in teleosts is disputed. Interestingly, LPS have been proven to be recognized by cytosolic NLRs in the teleost *Miichthys miiuy* (Bi et al., 2018). In mammals, a cascade of molecules leading to the activation of TLR4 detects LPS (reviewed by Kuzmich et al., (2017)).

Unmethylated cytosine phosphodiester guanine (CpG) are CG repeats of bacterial DNA without methylation and are considered PAMPs due to their abundance in microbial genomes and low abundance in vertebrate genomes. Methylation of DNA is a process by which methyl groups are added to the DNA. This may change the activity of a DNA segment and it is considered as an important mechanism of gene regulation. In *Escherichia coli* only 0.75% of the cytosines are methylated, compared with 74.2 % and 80.3% in mice and zebrafish, respectively (Feng et al., 2010; Marinus and Løbner-Olesen, 2014). TLR9 is

the receptor for CpG in mammals expressed in the late endosome/lysosome as a transmembrane receptor. After ligand binding, a complex cascade is initiated, resulting in production of pro-inflammatory cytokines (e.g. IL-12) or type I interferon (IFN) production (Minton, 2018; Bode et al., 2011).

The bacterial cell wall is composed of several different components, among them is peptidoglycan (PGN). Although PGN is one of the most prominent components and present in most bacteria, it is particularly numerous in Gram-positive (G+) bacteria. The structure of PGN generally consists of a sugar backbone with differing crosslinking modifications. It consists of repeating disaccharides of N-acetylmuramic acid and N-acetylglucosamine joined by β(1-4) linkages. The length of the sugar backbone varies. In the G+ genus Bacillus the length varies from 50-250 disaccharides, while in G- bacteria it is 20-40 disaccharides (Vollmer et al., 2008). Each N-acetylmuramic acid is bound to oligopeptides, which themselves bind to other oligopeptides bound to other N-acetylmuramic acid units. This creates a three-dimensional mesh-like structure. In mammals, PGN is recognized by PRMs, such as the soluble PGN recognition proteins (PGLYRPs) and by PRRs, such as nucleotide-binding oligomerization domain (NOD)-like receptors (NLR) 1 and 2 and probably TLR 2 (Wolf and Underhill, 2018). PGLYPRs are identified in zebrafish, and have bactericidal activity (Li et al., 2007).

Another component of the bacterial cell wall is the lipoteichoic acid (LTA) – a polymer present in G+ bacteria. LTA is important for growth and physiology of bacterial cells, and modification of the backbone can provide protection against cationic antimicrobial peptides. However, the exact function of the LTA is unknown (Percy and Grundling, 2014). LTA is defined as an aditol-phosphate-containing polymer that is linked via a lipid anchor in the outer cell membrane in G+ bacteria, although efforts have been made to include more complex glycosyl-phosphate-containing polymers in the definition (Reid et al.,

2012). In mammals, LTA is recognized by TLR2 and TLR2/6 heterodimer (Jang et al., 2015; Mogensen, 2009).

PRRs

While recognition of pathogens by PRMs and antibodies leads to increased phagocytosis and lysis, the PRRs tailors an immune response that is specific to the type of invading pathogen. The major families of PRRs are TLRs, NLRs, retinoic acid-inducible gene-I-like receptor (RLR), c-type lectin receptors (CLR) and absent in melanoma (AIM)-like receptor (ALR). The former two are known to contain members that are specific for extracellular bacteria and will be the focus of this discussion, where TLRs are membrane bound receptors on cell or endosomal membranes and NLRs are cytosolic receptors. In addition to the aforementioned PAMPs, many PRRs also respond to DAMPs. In general, these compounds are present inside healthy cells; however, following necrosis they leak into the interstitial space and elicits an immune response. Moreover, in mammals, some PRRs bind tumor associated molecular patterns (TAMPs) (Murphy and Weaver, 2012).

TLRs

TLRs were the first of the PRRs to be described and they are the best characterized innate immune receptors. Zhang et al., (2014) summarized the teleosts TLR types, and concluded that by 2014 twenty types of TLRs had been characterized in teleosts (TLR 1, 2, 3, 4, 5M, 5S, 7, 8, 9, 13, 14, 18, 19, 20, 21, 22, 23, 24, 25 and 26). Later Solbakken et al., (2016) showed that cod have a severely expanded TLR repertoire, and firmly determined that teleosts have a more complex TLR repertoire than mammals (13 in mice and 10 in humans), see Table 2 for an overview of full length TLRs identified in teleosts. In **paper I**, the following TLRs were identified in lumpfish: TLR1, 2, 3, 5S, 5M, 7, 8, 9, 13, 14, 21, 22 and 28. Compared to mammals, homofunctional TLRs include TLR1, 2, 3, 5, 7, 8 and 9. Although teleost TLR4s are structurally homologues to mammalian TLR4s, the ligand

specificity is different they are heterofunctional as they do not respond to LPS (Nie et al., 2018).

All TLRs are type I transmembrane proteins that contain three parts: an extracellular N-terminus with leucine-rich repeat (LRR) domain, a transmembrane domain and an intracellular toll/IL-1 receptor (TIR) domain. The specificity of the TLRs is determined by variation in sequence, number of LRR domains and overall globular structure. Many TLRs homo- or heterodimerize, increasing the number of ligands. TLR-ligand binding initiate signaling through the TIR domain and followed by intracellular signaling. These pathways, which are highly conserved, are the NF-κB and MAPK pathways (Takeuchi and Akira, 2010). The TLRs recognizing bacterial ligands in teleosts are TLR1, 2, 4, 5, 9, 14, 18, 21, 22, 25, 28, among these TLR5S, 18-20 and 22-28 are teleost specific compared with mammals (Pietretti and Wiegertjes, 2014; Wang et al., 2016b; Zhang et al., 2014).

Table 2. Overview of the full length TLRs.

Specie	TLR1	TLR2	TLR3	TLR4	TLR5	TLR6	TLR7	TLR8	TLR9	TLR10	TLR13	TLR14	TLR15	TLR18	TLR21	TLR22	TLR23	TLR25	TLR26	TLR27	TLR28
Homo sapiens	x	x	x	x	x	x	x	x	x	x											
Gallus gallus	x	x	x	x	x	x	x						x		x						
Anolis carolinensis	x	x	x	x	x	?	x				x	x	?		x		x				
Xenopus tropicalis	x	x	x		x	x	x	x	x		x	x			x		x		x		
Gadus morhua			x				x	x	x			x			x	x	x	x			
Cyclopterus lumpus	x	x	x		x	?	x	x	x		x	x			x	x					x
Oreochromis niloticus	F	x	x		x	?	x	x	x			x		x	x	x	x	x			
Poecilia formosa	x	x	x		x	?	x	x	x			x		x	x	x	x				
Takifugu rubripes	x	x	x		x	?	x	x	x			x		x	x	x	x				
Tetraodon nigroviridis	x	x	x		x	?	x	x	x			x			x	x	x				
Xiphophorus maculatus	x	x	x		x	?	x	x	x			x		x	x	x	x				
Astyanax mexicanus	x	x	x		x		x	x	x			x		x	x		x		x		
Lepisosteus oculatus	x	x	x		x	?	x	x	x			x		x			x	x		x	
Gasterosteus aculeatus	x	x	x		x	?	x	x	x			x		x	x	x					
Oryzias latipes	x	x	x		x	?	x	x	x			x		x	x	x		x			
Danio rerio	x	x	x	x*	x		x	x	x			x		x	x				x		
Latimeria chalumnae	x	x	x		x	?	x	x	x		x	x		x	x					x	
Petromyzon marinus	x		x			?	x					x			x			x			

Modified from Solbakken et al., (2016) Table 2. It has been supplemented with identified lumpfish TLRs in Eggestøl et al., (2018) and TLRs identified in Wang et al., (2015a) and Wang et al., (2016b). ? refers to a questionable identification, and * refers to a heterofunctional gene.

The vertebrate TLRs are divided into six subfamilies: TLR1-, 3-, 4-, 5-, 7-, and 11 subfamily (Palti, 2011). As the TLR3 subfamily members do not recognize bacterial ligands, they will not be further discussed.

The TLR1-family includes TLR1, TLR2, TLR6, TLR10, TLR14/18, TLR25, TLR28 and TLR28. TLR1 is important in the teleost bacterial defense, as it has been upregulated in several species upon bacteria or ligands exposure of them; large yellow croaker, miiuy croaker, zebrafish, orange spotted grouper and pufferfish (Meijer et al., 2004; Wang et al., 2013; Wang et al., 2016c; Wei et al., 2011; Wu et al., 2008). Moreover, TLR1 was also upregulated by poly (I:C) in orange spotted grouper and slightly downregulated in large yellow croaker (Wei et al., 2011). Further, in rainbow trout head kidney leukocyte (HKL), TLR1 expression was either not regulated or slightly downregulated by diacylated or triacylated lipopeptide, flagellin, poly (I:C), loxoribine and R848 (Palti et al., 2010). These data suggest that the ligand specificity of teleost TLR1 is more complex than its mammalian counterpart and is dependent on the specific evolutionary history of the studied specie.

In mammals, TLR2 heterodimerizes with TLR1 or TLR6 and form M-shaped structures which bind ligands in the internal pockets formed by the heterodimers. The heterodimers recognize lipopeptides, both diacylated and triacylated, of various origin and the characteristic G+ components LTA and PGN (Takeuchi and Akira, 2010). To date, TLR 6 has not been identified in teleosts (Nie et al., 2018). In teleosts, the reported TLR2 ligands are PGN, LTA and lipopeptides (Basu et al., 2012; Quiniou et al., 2013; Ribeiro et al., 2010; Samanta et al., 2012). A novel teleost specific TLR, TLR28, was reported to have high homology with TLR2 (Wang et al., 2016b). Similarity between TLR28 and TLR2 was also observed in lumpfish (Eggestøl et al., 2018). In miiuy croaker, TLR28 was highly expressed in liver, and its expression was upregulated by stimulation with *V. anguillarum*, *Staphylococcus aureus*, LPS and poly(I:C).

The mammalian ligand specificity of TLR4 has been a source of many enigmas in teleosts. In mammals, LPS is an important endotoxin (Takeuchi and Akira, 2010). However, teleosts are resistant to the toxic effects of LPS (Novoa et al., 2009; Sepulcre et al., 2009). Moreover, mammalian TLR4 is well established as an LPS receptor, forming a complex with LY96 (also known as MD-2) and CD14. Recognition of LPS and downstream signaling has proven elusive in teleosts. Teleost TLR4 responds to bacteria (Su et al., 2009; Zhang et al., 2013b), and in Indian major carp mrigal TLR4 expression was reported to be upregulated by LPS in all examined tissues 4h after treatment (Basu et al., 2013). However, this work is controversial and it is the only work to report LPS responsiveness of a teleost TLR4. The authors implemented an improper statistical inference (students T-test), and novel tissue-profiles were reported. Interestingly, some works report in addition to bacterial responsiveness, a possible function of TLR4 in viral recognition (Huang et al., 2012; Su et al., 2009). This heterofunctionality of teleost TLR4 is not surprising considering the comprehensive phylogenetic and syntenic analysis by Sullivan et al., (2009). They showed that the zebrafish TLR4s are of paralogues decent to the least common ancestor (LCA) of the mammalian TLR4. Further, they showed that zebrafish TLR4 does not transduce the LPS-signal, most likely due to its inability to complex with the other extracellular LPS recognizing host-proteins, rather than an incapability to signal through its TIR domain. Interestingly, teleost TLR4 is only identified within the order Cypriniformes.

The ligand of TLR5 is flagellin; this is well established within Mammalia and generally accepted within Teleostei (Nie et al., 2018; Pietretti and Wiegertjes, 2014). TLR5 is present in teleosts as both a membrane bound (TLR5M) and as a soluble (TLR5S) protein encoded by two separate genes. TLR5S was first reported in rainbow trout (Tsujita et al., 2004) and later identified in most examined teleosts (Table 2) (Zhang et al., 2014). TLR5M is similar to the mammalian TLR5, containing the typical LRR, transmembrane and TIR domains, while TLR5S only possess the LRR domains (Bai et al., 2017). The expression profiles of TLR5M and TLR5S in fish are different. Both are upregulated by bacteria, but the

expression of TLR5M was followed and facilitated by TLR5S in a positive feedback fashion (Tsujita et al., 2004). In most studies, TLR5S is more upregulated than TLR5M (Eggestøl et al., 2018 and references within). Exactly how TLR5S initiate downstream signaling is unknown, although a hypothetical mechanism has been postulated: TLR5S binds circulating flagellin and transports it to TLR5M, thereby amplifying the flagellin danger signal analogues to the mammalian TLR4 LPS mechanism (Rebl et al., 2010). Activated TLR5 directly regulate the expression of innate immune genes, such as TNF-α, IL-1β and CXCL-8, in grass carp (Xu et al., 2016b).

The TLR7 subfamily members, TLR7, -8 and -9, do not recognize microbial surface components, neither outer nor inner membrane, but they do detect nucleic acids of bacterial or viral origin (Sasai and Yamamoto, 2013). In mammals, TLR9 is activated by unmethylated CpG motifs, however it requires translocation from the endoplasmic reticulum through the Golgi apparatus to the endo/phago-lysosomes which contain the foreign DNA – a likely safeguard against activation by self-DNA (Barton et al., 2006; Leifer et al., 2004). TLR9 detects CpG oligodeoxynucleotides (ODNs) in teleosts, which is also detected by TLR21 in teleosts (Li et al., 2017b; Nie et al., 2018).

Teleost TLR13, belonging to the TLR11 family, was first identified in miiuy croaker where it was highly expressed in immune relevant organs, and recently in orange spotted grouper, TLR13 recognized bacterial RNA (Liang et al., 2018; Wang et al., 2016a). This ligand specificity is in congruence with that of mice (Li and Chen, 2012; Oldenburg et al., 2012). Other TLRs have been identified and characterized, they either recognize viral or eukaryotic PAMPs, or their ligands have not yet been identified (Nie et al., 2018).

NLR

NLRs consist typically of three domains, a C-terminal region, made up of a variable number of leucine-rich repeats (LRRs), a central nucleotide oligomerization (NACHT) domain and an N-terminal effector binding domain (EBD). The C-terminal regions recognizes the ligand

and the N-terminal EBD interacts with adaptor molecules and downstream effector proteins. The nomenclature of NLRs was unified by the HUGO nomenclature committee (Ting et al., 2008). This system divides NLRs with differing EBDs into five subfamilies – NLR-A containing acidic activation domain (AD), NLR-B containing baculovirus inhibitor of apoptosis protein repeat (BIR), NLR-C containing caspase-activation and recruitment domain (CARD), NLR-P containing pyrin domain (PYD) and NLR-X, containing other domains than the previously mentioned (Ting et al., 2008). Another nomenclature also exist, phylogenetic analyses of the central NACHT domain reveals three subfamilies: the NODs, the NLRPs (also known as NALPs) and Ice Protease Activating Factor (IPAFs) (Schroder and Tschopp, 2010).

Homologues of mammalian NLRs have been reported in many different teleost species. The high degree of homology suggests that they play a similar role in the defense against harmful pathogens, reviewed in Zhang et al., (2018). In teleosts, members of the subfamilies NLR-A, -B and –C have been identified. The nomenclature of teleost NOD1-5 varies between species due to structural differences. In zebrafish, NOD1-5 belong to the NLR-A subfamily and are referred to as NLR-A1 to -5 (Laing et al., 2008). While in channel catfish NOD1-5 are referred to as NOD1, NOD2, NLRC3, NLRC5 and NLRX1, respectively, in congruence with the nomenclature of the HUGO committee (Sha et al., 2009).

Among mammalian NLRs, NOD1 and NOD2 recognize ligands produced during synthesis or degradation of PGN. Respectively, they recognize MDP and γ-D-glutamyl-meso-diaminopimelic acid (iE-DAP) (Uehara et al., 2005). In recent years, there has been increased focus on NLRs in fish, yet only a few ligands have been identified. In goldfish NOD1 recognizes LPS, Poly(I:C) and PGN, NOD2 recognizes LPS, Poly(I:C), MDP and PGN and NLR-X1 recognizes LPS, MDP and PGN (Xie et al., 2013). In zebrafish NOD2 recognizes MDP (Zou et al., 2016). In Asian seabass, NLR-C3 responds to LPS, poly(I:C) and PGN (Paria et al., 2016). In addition to the above mentioned NLRs, which are conserved in

vertebrates, fish have a subfamily of NLRs called NLR-C (Laing et al., 2008). Interestingly, in Japanese pufferfish, NLR-C9, 10 and 12 are suggested to be involved in LPS recognition (Biswas et al., 2016), confirming that the mechanisms for LPS recognition and signaling is different in mammals and fish. These preliminary studies suggest that teleost NLRs tend to be more promiscuous, regarding their ligand specificity compared to mammalian NLRs.

Bacteria induced PRR mediated signaling

For the immune system to move beyond the first phase of the immune response, a phenotypic change of the innate cells must occur. The critical step for initiation of the cascade reaction that leads to this is the recognition of a PAMP by a PRR and the subsequent phosphorylation and/or spatial change of the intracellular domain allowing the binding of adaptor proteins. There exists several different intracellular signaling pathways, but the NF-κB and the MAPK pathways are the most important in innate immunology. In addition to being activated by PAMPs the signaling pathways can be activated by cytokines, hormones and other stress signals. An infection elicits several stress signals which occur in the same spatial-temporal space. The corresponding immune response is therefore composed by several different signaling pathways with varying degree of cross-talking. It is therefore important to remember that, for instance a LPS and a flagellin exposure, they are not isolated events. In an analogous manner to the brain, the signal-mediating pathways are cross-talking and integrates the information signals, rendering the immune cell capable of advanced decisions. It is this combined concert between different signal mediating mechanisms that enables the innate immune system to tailor an immune response to a specific pathogen.

Adaptor molecules

The downstream adaptor molecules of TLRs and NLR varies. The TLR signaling is dependent on TIR-TIR interaction between the TLR and its corresponding adaptor protein. The adaptor proteins containing TIR domains are MYD88 (myeloid differentiation primary-

response gene 88), TIRAP (TIR adaptor protein), TICAM (TIR domain-containing adaptor molecule) and SARM (sterile α- and armadillo-motif-containing protein) (O'Neill and Bowie, 2007). Almost all the TIR domain-containing adaptors reported in mammals appear to be conserved in teleosts (Takano et al., 2010). The signaling NLR adaptor protein are receptor-interacting serine/threonine-protein kinase 2 (RIP2).

MYD88 is a universal adaptor molecule, present in most TLR signaling pathways (except for TLR3), and activates the NFκB signaling pathway and expression of pro-inflammatory cytokines (Kawai and Akira, 2007). MYD88 is an important TLR signaling molecule in teleosts (Rebl et al., 2010). An artificial lack of MYD88 (knockout, KO) allowed bacteria to proliferate 100-1000 folds within 6 days, compared to MYD88 expressing zebrafish embryos. The MYD88-KO embryos were not able to clear or control the infections (Van Der Sar et al., 2006). Although MYD88 gene expression in Japanese flounder PBL was induced by PAMP stimulation, LPS and poly (I:C), the MYD88 gene expression of rainbow trout HKLs was not induced by the PAMPs poly (I:C), flagellin and R848 which mimic single-stranded RNA (Purcell et al., 2006; Takano et al., 2006). MYD88 has been identified in

Figure 4 (next page). Bacteria induced PRR intracellular signaling. The recognition of a PAMP by its PRR, activates the PRR in a manner allowing for the docking of the relevant adaptor proteins. Conceptually there are three different mechanisms for bacteria induced PRR mediated signaling: the TLR MYD88-dependent, the TLR MYD88-independent and the NLR signaling pathway. All feed into the NFκB and MAPK pathways through the TAK1/TAB complex, also the TLR MYD-88 independent feed into the pathway leading to the transcription factor IRF3. MAPK and NFκB also act as transcription factor when they are present in the nucleus. When they are present in the nucleus, they recruit RNA polymerase and eventual coactivator molecules, and start or increase the transcription of pro-inflammatory cytokines and other molecules involved in the inflammation reaction, such as phagocytosis. This figure is based upon descriptions of the illustrated pathways in the litterature (Kawasaki and Kawai, 2014; Mitchell et al., 2016; Seger and Krebs, 1995). Disagreement between teleost and mammalian systems is highlighted by bold yellow text (for references see section "Adaptor molecules"). Teleost specific ligands are not shown as the literature is highly limited regarding their adaptor molecules.

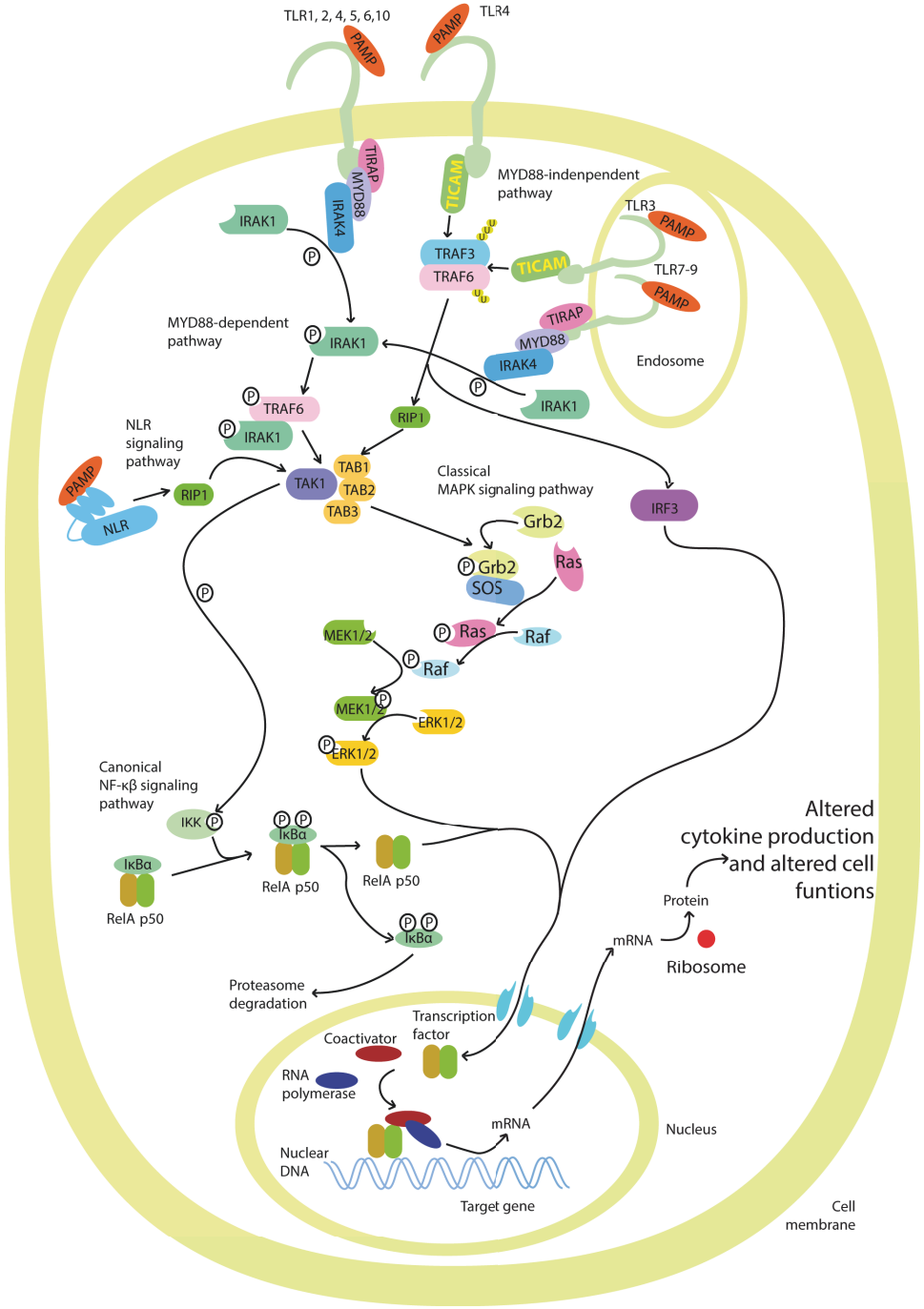
TLR1, 2, 4, 5, 6,10
PAMP
TLR4
PAMP
TIRAP
MYD88
IRAK4
TICAM
MYD88-indenpendent
pathway
IRAK1
TRAF3
TRAF6
TICAM
TLR3
PAMP
TLR7-9
PAMP
TIRAP
MYD88
IRAK4
Endosome
MYD88-dependent
pathway
IRAK1
IRAK1
TRAF6
IRAK1
RIP1
NLR
signaling
pathway
PAMP
NLR
RIP1
TAK1
TAB1
TAB2
TAB3
Classical
MAPK signaling pathway
IRF3
Grb2
Grb2
SOS
Ras
Ras
Raf
MEK1/2
Raf
MEK1/2
ERK1/2
ERK1/2
Canonical
NF-κβ signaling
pathway
IKK
IκBα
RelA p50
IκBα
RelA p50
RelA p50
IκBα
Proteasome
degradation
Altered
cytokine production
and altered cell
funtions
Protein
mRNA
Ribosome
Transcription
factor
Coactivator
RNA
polymerase
mRNA
Nucleus
Nuclear
DNA
Target gene
Cell
membrane

members across the whole teleost evolutionary tree, including cyprinids, salmonids and perciforms (Meijer et al., 2004; Purcell et al., 2006; Skjæveland et al., 2009).

Mammalian TIRAP (also known as MYD88 adaptor-like protein, MAL, or Toll/IL-1 associated protein) mediates the activation of the MYD88-dependent pathway downstream of TLR2 and -4 (Kawai and Akira, 2007). In miiuy croaker TIRAP was suggested to be involved in TLR1 mediated LPS signaling (Xu et al., 2016a). Besides the teleost miiuy croaker, TIRAP has been identified in pufferfish and zebrafish. In zebrafish TIRAP was significantly induced by *Mycobacterium marinum* intraperitoneal challenge (Meijer et al., 2004)

Mammalian TICAM 1 and 2 are paralogs of a LCA that is not duplicated in the teleost lineage. The teleost TICAM is of equal distance to both mammalian TICAM (Stein et al., 2007; Sullivan et al., 2007). Mammalian TICAM1 substitutes MYD88 in the MYD88-independent pathways of TLR3 and -4, resulting in the activation of NF-κB and IRF3. In the MYD88-independent pathway NF-κB is activated via the TRAF6 and/or RIP1 pathways, and IRF3 is activated by TBK1 (TANK-binding kinase 1). Mammalian TRAF3 links TICAM1 and TBK1, resulting in the production of type I IFN (Kumar et al., 2009). Teleost TICAM is involved in the TLR3- and -22 NF-κB inducing signaling (Fan et al., 2008; Matsuo et al., 2008; Oshiumi et al., 2008). Interestingly, although teleost TICAM does not activate IRF3, it associates with TBK1 and is involved in the production of IFNs. Further, the teleost MYD88-independent pathway activates NF-κB independent of TRAF6. The MYD88-independent pathway in zebrafish is shown to involve the RIP1 pathway (Sullivan et al., 2007). It is suggested that teleost IFN production through TICAM is different from the mammalian system (Rebl et al., 2010; Takano et al., 2010).

SARM inhibits TRIF-dependent pathway in humans, and murine SARM regulates TRIF activity (Kawai and Akira, 2007; Kenny and O'Neill, 2008). SARM have been identified in pufferfish and zebrafish (Meijer et al., 2004; Stein et al., 2007).

In lumpfish, full-length sequences of MYD88, TICAM1 and TIRAP were identified. In addition, two partial sequences of SARM were identified. TIRAP 2 was not identified in lumpfish, similarly to other fish species (Eggestøl et al., 2019).

Mammalian RIP2 mediates the NLR activation of both the NF-κB and the MAPK signaling pathways upon activation of NOD1 and -2 (Chin et al., 2002; Inohara et al., 2000; Kobayashi et al., 2002). Besides signaling transduction activating the NF-κB and the MAPK signaling pathways, mammalian RIP2 also participates in inflammasome-associated pathways (Sarkar et al., 2006). Furthermore, mammalian RIP2 has been demonstrated to be instrumental in the defense against the bacteria *Listeria monocytogens* and *Acinetobacter baumannii*, along with its upstream receptors, the NLRs, NOD1 and -2 (Bist et al., 2014; Kim et al., 2008; Park et al., 2007). Among teleosts, RIP2 has been identified in perciforms, cyprinids and salmonids fish (Jang et al., 2016; Liu et al., 2018; Stein et al., 2007; Xie and Belosevic, 2015). Teleost RIP2 gene expression has been demonstrated to be responsive to PAMPs, live and dead taxonomically different bacteria (Liu et al., 2018; Xie and Belosevic, 2015). Further, different studies in fish have shown that RIP2 activate the NF-κB signaling pathway and regulated the production of pro-inflammatory cytokines such as IL-1β and TNF-α (Jang et al., 2016; Liu et al., 2018; Xie and Belosevic, 2015).

Pro-inflammatory cytokines

Cytokines are signaling molecules secreted by cells in the immune system and they regulate immunity, inflammation and hematopoiesis. Cytokines and their receptors have an extremely high affinity for each other – even picomolar concentrations of cytokines can have a biological effect. The cytokines can have either an autocrine effect by binding to a receptor of the same cell that secreted it, a paracrine effect by binding to receptors on a target cell in close proximity to the producer cell, or an endocrine effect binding to distant target cells in different organs. Their biological effect is often described with a controlled vocabulary: pleiotropic – one cytokine with many functions, redundant – several different cytokines can mediate the same or similar functions, synergistic – two cytokines with a combined effect bigger than the additive effect by them self and antagonistic – the effect of one cytokine offset or inhibits the effect of another cytokine.

Several classification systems for cytokines exist, as for many other immune molecules. Here I classify them based on structure, since receptor-recognition is primarily dependent on the structure of the ligands. This discussion is further restricted to cytokines with pro-inflammatory properties upon bacterial exposure.

Cytokines belonging to all structural families; β-trefoil, B-jellyroll, cysteine-knot, type I α helical, type II helical and open face β sandwich, have been identified in teleosts (Zou and Secombes, 2016). Although, orthologs to several mammalian cytokines are not yet successfully identified in fish, many cytokines have been duplicated in teleosts and a plethora of cytokine paralogs exist – yielding a complexity of the teleost cytokine system, at least, on par with that of its mammalian counterpart. Despite descriptions of many different cytokines, the studies are limited to a selected number of species, usually commercially farmed species. Moreover, protein expression and functional studies are rarely the basis of the descriptions. Most descriptions are based on transcript expression studies (Zou and Secombes, 2016).

β-Trefoil cytokines

The mammalian family of β-trefoil cytokines include 11 members – interleukin (IL) 1 family 1-11 (IL-1F1-11) (Sims et al., 2001). Of these, only IL-1F2 (IL-1β) and IL-1F4 (IL-18) have been described in teleosts. Extensive genomic analysis supports the claim that teleosts do not contain other β-trefoil orthologues (Zou and Secombes, 2016). However, two β-trefoil cytokines, named novel IL 1 Family member (nIL-1F) and IL 1 Family member 2 (IL-1Fm2), have been identified in teleosts, expanding the teleost β-trefoil family to four members (Angosto et al., 2014; Wang et al., 2009, Taechavasonyoo et al., 2013). Originally, Wang et al., (2009) characterized the nIL-1F gene to be a teleost specific gene, however in **paper III**, we identify three non-teleost specific nIL-1F genes belonging to members of Sarcopterygii, Chondrichthyes and Holostei. Therefore, we postulate that nIL-1F is an ancient gene (at least 430 million years ago (mya)) that is lost in the tetrapod lineage. Interestingly the nIL-1F otomorph clade is evolutionary more distant than the formerly mentioned members, indicating a drastically different evolutionary fate for otomorph nIL-1F than the typical fish nIL-1F gene. In the literature, identification of the IL-1Fm2 gene has only occurred in the order of Perciformes (Angosto et al., 2014). This is in line with our results from the phylogenetic analysis in **paper III**, although IL-1Fm2 sequences were also found in Synbranchiformes and Anabantiformes (**paper III**), suggesting that IL-1Fm2 is present in the whole Neoteleostei clade.

The β-trefoil cytokines bind to the IL-1 receptors (IL-1R1-10, see Borachi et al., 2018), all sharing a similar secondary structure: one to three immunoglobulin domains, the membrane bound receptors contain a transmembrane domain and a TIR. Many receptors also contain a signal peptide. So far, no soluble IL-1 receptor has been identified in teleosts (Zou and Secombes, 2016). Conceptually, the ligand binding activity of IL-1Rs can have three different fates: i) pro-inflammatory – phenotypic change of the cell enabling or increasing an inflammatory reaction, ii) anti-inflammatory – phenotypic change of the cell disabling or decreasing an inflammatory reaction, or iii) no effect– no signal is transduced,

thereby reducing the effective concentration of the cytokine, any phenotypic change induced by the cytokine is reduced. In the latter fate the receptor is often referred to as a decoy receptor. All IL-1Rs heterodimerize prior to interaction with their ligands (see Fig. 5). Following ligand binding, the intracellular TIR domains interact with adaptor proteins such as MYD88 or Toll interacting protein, resulting in phosphorylation of the IL-1R associated kinases (IRAKs). In turn, they interact with the TNF receptor associated factor (TRAF) 6, thereby activating NF-κB, which is a potent transcription factor of pro-inflammatory genes (Fig .4). Most of these molecules are identified in teleosts except for TICAM 2 (also known as TRAM), IRAK2, and thus far, TRAF 1 is only described in zebrafish. As shown in **paper I and III**, most components involved in signaling were conserved in lumpfish (Eggestøl et al., 2019; Eggestøl et al., 2018).

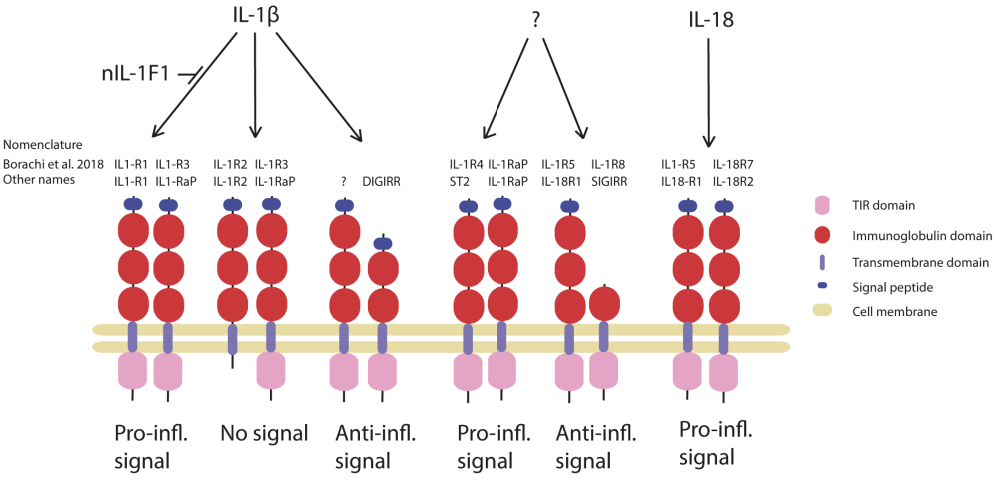

Figure 5. Interaction of teleost β-trefoil cytokines and their receptors, represented with their schematic structure

Interleukin 1β (IL-1β)

Although IL-1β is a pleiotropic cytokine with a wide range of effects, it is chiefly known as one of the main pro-inflammatory cytokines. In teleosts, IL-1β is mainly secreted from macrophages and acidophilic granulocytes (Angosto et al., 2012; Chaves-Pozo et al., 2004). In mammals, a wider range of cells have been proven to produce IL-1β, including monocytes, macrophages, dendritic cells, B-cells and NK-cells (Veerdonk and Netea, 2013). It is known that other cells are also capable of secreting IL-1β, such as endothelial cells and fibroblasts, the latter being confirmed in the perciform gilthead seabream (Murphy and Weaver, 2012; Pelegrin et al., 2004). Recombinant IL-1β has been administered to fish in order to study the local and transient effects of it (reviewed in Secombes et al., (2016)). The role as a chemoattractant was confirmed by an experiment in head kidney leukocytes, where the cells migrated in the direction of a recombinant IL-1β gradient (Peddie et al., 2001). Intraperitoneal administration in trout has shown to increase phagocyte migration into the peritoneal cavity, as well as their phagocytic and lysozyme activity (Hong et al., 2003). Intestinal administration induced severe gut inflammation and TNF-α expression in grass carp (Bo et al., 2015). Further observation of local effects of IL-1β was supplied by Taechavasonyoo et al., (2013) – they observed elevated levels of TNF-α and IL-1β gene expression in Japanese flounder muscle tissue after injection with an IL-1β expressing plasmid. Teleost IL-1β has also been linked to IL-17 family members in several studies, and it has shown to be important for antibacterial defense (Kono et al., 2011; Wang et al., 2015b; Wang et al., 2010; Wang et al., 2014). In **paper I**, we also observed a potent co-expression of IL-17 and IL-1β (Eggestøl et al., 2018). Moreover, teleost IL-1β has demonstrated its potency to stimulate antibody production, and it has been suggested that it could be used in a vaccine adjuvant (Taechavasonyoo et al., 2013; Yin and Kwang, 2000).

The mechanism of IL-1β secretion in teleosts has been a topic of debate for nearly two decades. In mammals, IL-1β is produced as an inactive cytoplasmic precursor that needs

to be proteolytic cleaved, mainly by caspase 1 to generate the active form (Thornberry et al., 1992). Caspases are known to be highly specific proteases, and caspase 1 requires the conserved amino acid sequence [F, W, Y or L], X, [H, A or T], D to successfully cleave (Earnshaw et al., 1999). However, studies have shown that several peptides with this tetramer are not cleaved by caspase 1, indicating that the tertiary structure the substrate is also important (Thornberry and Lazebnik, 1998). However, later works note that caspase 1 is a "promiscuous enzyme" with over 120 substrates and is far from an IL-1 specific peptidase (Denes et al., 2012). Conversion of an inactive pro-IL-1β to an active cytokine in fish is still debated as teleost IL-1β sequences lack caspase 1 cut site. Besides caspase 1, in mammals, elastase and cathepsin G are also able to process IL-1β in the relevant region.

In common carp, it was shown, using an IL-1β specific monoclonal antibody, that phytohemagglutinin (PHA) activated leukocytes secreted a shortened 15 kDa IL-1β compared to the theoretical non-cleaved IL-1β peptide (Mathew et al., 2002). A shortened 24 kDa IL-1β was also secreted in the culture medium of the rainbow trout monocyte/macrophage RTS11 cell line (Hong et al., 2004). In zebrafish primary leukocytes, two different mature IL-1β peptides, 22 and 18 kDa, were cleaved by two different caspases, A and B, upon infection by *Francisella noatunensis* (Vojtech et al., 2012), thus, it has been suggested that cleavage at different sites is possibly dependent on the immunological microenvironment (Zou and Secombes, 2016). Further, in seabass IL-1β has shown to be cut by a recombinant caspase 1, directly demonstrating teleost IL-1β processing by caspase 1 (Reis et al., 2012). However, the cut site was located within the first β-sheet of the mature peptide thereby questioning whether the tertiary structure of the caspase 1 processed IL-1β is altered in a manner leading it to lose its biological activity after cleavage.

Interleukin 18 (IL-18)

Initially IL-18 was found to induce IFNγ production and promote Th1 immunity in vertebrates but is known to also be involved in regulating inflammation in mucosal tissues (Dinarello, 1999; Okamura et al., 1998). Analogues to IL-1β, IL-18 is also synthesized as a pro-peptide and require proteolytic cleavage by caspase 1 post PAMP or DAMP stimulation, to become biological active. The analogy between IL-1β and IL-18 also regards their receptors, as IL-18 binds to heterodimeric receptor consisting of IL-18R1 and 2 (Fig. 5), and a soluble protein, termed IL-18 binding protein (IL-18BP), is able block this binding (Zou and Secombes, 2016) similarly as IL-1Ra for IL-1β.

Description of IL-18 in Teleostei is still in its infancy, and IL-18 has only been reported from a limited number of species: rainbow trout, turbot, seabream, pufferfish and lumpfish (Huising et al., 2004; Pereiro et al., 2012; Perez-Cordon et al., 2014; Zou et al., 2004; **paper III**). In rainbow trout, it was demonstrated a constitutive expression of IL-18 throughout all tested tissues. Also, in HKLs and RTS-11 cells expression of IL-18 was shown not to be regulated by LPS, poly (I:C) nor recombinant IL-1β, however in RTG2-cells – a fibroblast-like cell line – expression was downregulated by LPS and recombinant IL-1β. Interestingly, rainbow trout was also demonstrated to express an alternatively spliced IL-18. It contained a 17 amino acid deletion in the precursor region and expressed constitutively at a much lower level than the authentic form. However, the alternatively spliced variant expression was upregulated by LPS and poly (I:C), suggesting that IL-18 may also be dependent on proteolytic cleavage for mediating a biologically active cytokine (Zou et al., 2004). It should be noted that these claims were not supported by statistical inference.

Other IL-1 members within teleosts: nIL-1F & IL-1Fm2

In addition to IL-1β and IL-18, two other IL-1 members have been identified within Teleostei – nIL1F (also coined nIL-1Fm by Zou and Secombes (2016)) and IL1Fm2. These

fish specific members of the IL-1 family were first described by Wang et al., (2009) and Angosto et al., (2014), respectively.

Constitutive expression of nIL-1F, with high levels in immune organs, has been reported from both grass carp and rainbow trout (Wang et al., 2009; Yao et al., 2015). A caspase cut site has been identified in nIL-1F together with thrombin cut sites in grass carp, pufferfish, zebrafish, rainbow trout (Wang et al., 2009; Yao et al., 2015) and lumpfish (**paper III**). It has been suggested that nIL1F is an IL-1 receptor antagonist, like IL-1Ra (Wang et al., 2009). A study in grass carp confirmed that nIL-1F has antagonistic effect (Yao et al., 2015). Yao et al., (2015) showed that recombinant nIL-1F1 has a high affinity for IL-1R1 and that nIL-1F1 inhibits the binding of IL-1β to IL1-R1 at the lowest tested amount. In the same work, nIL-1F1 was identified in pufferfish and zebrafish. Further, an evolutionary hypothesis was postulated regarding the ancestral origins of nIL-1F1 and its functional homolog in mammals, IL-1Ra: nIL1-F1 and IL1-Ra are not orthologous due to low sequence similarity (Ogryzko et al., 2014; Wang et al., 2009; Yao et al., 2015). This was supported by low amino acid homology.

IL-1Fm2 has been reported to be constitutively expressed in seabream with the highest registered levels in thymus, liver, gill, brain and gut (Angosto et al., 2014). Under bacterial infection, the level of IL-1Fm2 increased in several organs, particularly in head kidney, spleen, blood and peritoneal exudate. PAMP stimulation of seabream macrophages and acidophilic granulocytes caused a weak to moderate induction of IL-1Fm2 expression (maximum 12-fold) (Angosto et al., 2014). This contrasts the measurement of IL-1β transcripts in the same samples, where extreme induction was observed (Sepulcre et al., 2007). The same pattern was observed in lumpfish leukocytes upon stimulation with various PAMPs (**paper III**). In seabream, recombinant IL-1Fm2 synergistically induced the expression of IL-1β, TNF-α, IL-8 and IL-10 when combined with different PAMPs, suggesting its involvement in innate immunity. No caspase 1 cut site has been identified

in lumpfish IL-1Fm2 (**paper III**). Although IL-1Fm2 in sea bass was processed prior to its release from macrophages, pan-caspases or caspase 1 inhibitors did not affect this (Angosto et al., 2014).

B-Jellyroll cytokines

The jellyroll cytokine family, also referred to as the tumor necrosis factor superfamily (TNFSF), is a large family that encompasses 19 ligands and 29 receptors in humans (Aggarwal, 2003). The three major mammalian members are; TNF-α, lymphotoxin (LT) –α (previously referred to as TNF-β) and LT-β. The lymphotoxin members are sarcopterygian specific members, while teleosts possess TNF-α and an ancient TNF-α paralog known as TNF-N. To this date TNF-N has only been identified in teleosts, however based on sequence similarity it is inferred to predate Actinopterygii and Sarcopterygii (approx. 420 mya) (Fig. 6) indicating its presence in non-teleost fish. The TNF gene is an extremely old gene predating Deuterostomia (approx. 550 mya), as TNF and its related genes have been identified in mollusks, planarians and arthropods (Hu et al., 2019; Li et al., 2017a; Qu et al., 2017). Vertebrate TNF-α evolution is complex, with numerous paralogs. In fish we count eight paralogs (including TNF-α and the lymphotoxins).

It is known from mammals that most TNF-ligands show a typical homotrimeric structure and exert their bioactivities as regulators of the immune system. TNF-α (also known as TNF) is a major activator of the pro-inflammatory responses. It is expressed as a membrane bound ligand, and upon cleavage by ADAM17 (also known as TACE), it is separated from its transmembrane domain, and is thereby secreted as a soluble ligand (Baeyens et al., 1999). Both secreted and membrane bound TNF-α bind both TNF-α receptors, TNFR1 and TNFR2. The TNFR1 is expressed in virtually all tissues, while TNFR2 is chiefly expressed by immune, endothelial and neuronal cells. Both receptors activate intracellular signaling pathways, although with different terminal outcomes. TNFR1 mediates anti-apoptotic, apoptotic and other death-inducing signals, while TNFR2

mediates mainly cell proliferation and anti-apoptotic signals (Neumann et al., 2013). In teleosts TNF-α has been identified and characterized in a range of fish (Table 3).

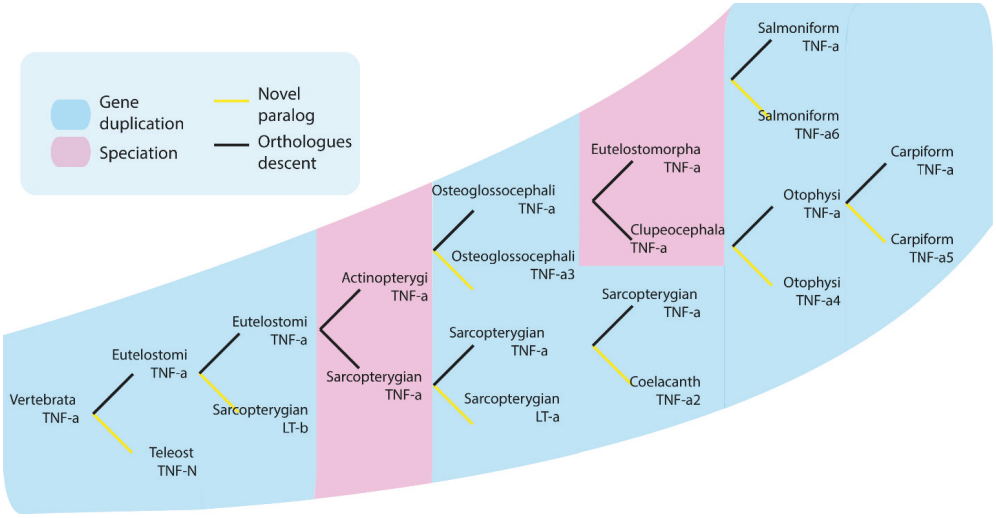

Figure 6. **Evolution of vertebrate TNF-α gene, displaying paralogues branching in fishes**. This figure is based upon a PhyloWiew search in Genomicus with ENSLBEG00000012547 (TNF-α in ballan wrasse) as reference gene. The endpoint in this overview is the earliest common clade from the last gene duplication event, i.e. lumpfish TNF-α is represented by Eutelostomorpha and human TNF-α is represented by Sarcopterygii TNF-α. Evolutionary events driving the evolutionary history is color-coded.

Table 3. Teleost TNF-α genes

Specie	Latin specie name	Reference
Zebrafish	*Danio rerio*	(Bobe and Goetz, 2001; Eimon et al., 2006)
Brook trout	*Salvelinus fontinalis*	(Bobe and Goetz, 2001)
Red seabream	*Pagrus major*	(Cai et al., 2003)
Lumpfish	*Cyclopterus lumpus*	(Eggestøl et al., 2020)
Gilthead seabream	*Sparus aurata*	(Garcia-Castillo et al., 2002)
Goldfish	*Carassius auratus*	(Grayfer et al., 2008)
Japanese flounder	*Paralichthys olivaceus*	(Hirono et al., 2000)
Rainbow trout	*Oncorhynchus mykiss*	(Hong et al., 2013; Laing et al., 2001; Zou et al., 2003a; Zou et al., 2002)
Pacific blue fin tuna	*Thunnus orientalis*	(Kadowaki et al., 2009)
Rock bream	*Oplegnathus fasciatus*	(Kim et al., 2009)
Atlantic bluefin tuna	*Thunnus thynnus*	(Lepen Pleic et al., 2014)
Ayu	*Plecoglossus altivelis*	(Lu et al., 2015)
Turbot	*Scophthalmus maximus*	(Ordas et al., 2007)
Nile tilapia	*Oreochromis niloticus*	(Praveen et al., 2006)
Common carp	*Cyprinus carpio*	(Saeij et al., 2003; Savan and Sakai, 2004)
Grass carp	*Ctenopharyngodon idella*	(Zhang et al., 2012)
Channel catfish	*Ictalurus punctatus*	(Zou et al., 2003b)

TNF-α is constitutively expressed in most examined teleost tissue, however, the plethora of teleost TNF-α paralogs are seldom sufficiently addressed, making it difficult to generalize as there is no established teleost nomenclature encompassing all the paralogs. Kadowaki et al., (2009) made the distinction between type I and II TNF-α in Pacific blue fin tuna, sharing only 43% amino acid similarity. Type I phylogenetically placed itself within the perciform TNF-α clade, while type II was placed as a separate clade. In blue fin tuna, type I TNF-α, but not type II, was not able to respond on a selection of PAMPs (Kadowaki et al., 2009). Both TNF-α were able to increase the phagocytic activity of PBLs as recombinant proteins. Type I TNF-α was expressed at consistent level throughout the examined tissues, while type II TNF-α was expressed significantly higher in spleen and blood. Such differences between type I and II has also been made in Atlantic blue fin tuna and rainbow trout (Hong et al., 2013; Lepen Pleic et al., 2014). The characterized type II TNF-α paralog is represented in Figure 6 as Osteoglossocephalai TNF-a3. However, confusingly, Hong et al., (2013) also identified a third paralog, which they named TNF-α2, while the previously coined type II TNF-α gene in tuna was named TNF-α3 in rainbow trout. The TNF-α2 gene is a type I TNF-α gene and is represented in Figure 6 as salmoniform TNF-α6.

Hong et al., (2013) reported a similar tissue-distribution as Kadowaki et al., (2009): type I TNF-α genes were higher expressed than type II TNF-α genes and type II TNF-α was most highly expressed in immune related organs. The reader should note that these trends were not supported by statistical inference. Further Hong et al., (2013) reported that all paralogs were highly responsive to PAMP and DAMP signals and that they displayed differing kinetics in head kidney cells stimulated with PHA – TNF-α1 (type I) late moderate response, TNF-α2 (type I) sustained moderate response and TNF-α3 (type II) early highly potent response. Interestingly, Hong et al., (2013) showed that type II TNF-α contained a truncated transmembrane stalk, possibly leading to a spatially unavailable TACE site. It was further speculated that this would lead type II TNF-α to be primarily responsible for

the transmembrane-bound functions, while type I TNF-α would primarily be responsible for the functions mediated by soluble TNF-α. Interestingly, in **paper II** we revealed that all TNF-α sequences within Ostariophysi are exclusively type II TNF-α, implying that Ostariophysian species may have an impaired or an alternative excretion mechanism. Conversely if the excretion mechanism is impaired, the zebrafish TNF-α literature might be reinterpreted and the use of zebrafish as a model for mammalian immunological, cancer and necrosis/apoptosis phenomena might be re-evaluated.

Recombinant teleost TNF-α has displayed pro-inflammatory properties in several independent studies, causing upregulation of IL-1β in all examined species, induction of IL-8, IL-17C and COX-2 genes in rainbow trout, elevated phagocytic activity in rock bream HKLs (Kim et al., 2009; Li and Zhang, 2016; Zhang et al., 2012; Zou et al., 2003a). Further evidence of enhanced phagocytic activity of teleost TNF-α has been supplied by Garcia-Castillo et al., (2002), Zou et al., (2003a) and Grayfer et al., (2008). In zebrafish, excess of TNF-α increased the microbicidal activity of macrophages through increased production of reactive oxygen species, upon infection with *Mycobacterium*, demonstrating an immune stimulatory effect. However, prolonged excess on TNF-α induced necroptosis of the macrophages (Roca and Ramakrishnan, 2013), indicating that tight regulation of TNF-α in fish, as in mammals, is crucial. In common carp, TNF-α treated endothelial cell supernatant promoted respiratory burst (Forlenza et al., 2009). In addition, the same supernatant promoted leukocyte migration. The link between TNF-α and leukocyte migration has also been unveiled in rainbow trout macrophages and seabass granulocytes (Garcia-Castillo et al., 2002; Zou et al., 2003a). Furthermore, it has been reported in ayu-fish that blocking of TACE-activity is linked to reduced respiratory burst (Lu et al., 2015)

The teleost TNF-N gene share homology with the mammalian CD30L and Glucocorticoid-induced TNA receptor-related protein ligand (GITRL), both genes being primarily related to lymphocytes (Glenney and Wiens, 2007). In rainbow trout two TNF-N paralogs, termed

LT-β 1 and 2, have been characterized. The former paralog was highly expressed in unstimulated HKLs, while the latter was only expressed in gill. Neither were expressed in macrophage (RTS-11) or fibroblast (RTG-2) cell lines. In HKLs expression of both paralogs increased by stimulation with PHA or LPS (Kono et al., 2006). These data are concurrent with the notion of TNF-N being primarily a lymphocyte-expressed gene. However, in zebrafish HKLs, TNF-N is only weakly induced by LPS in HKLs (Kinoshita et al., 2014). The normal tissue expression of TNF-N in zebrafish are disputed: Kinoshita et al., (2014) reported primarily expression in intestine, liver and gill, while Savan et al., (2005) reported only TNF-N expression in head kidney. In fugu TNF-N has been reported to be constitutively expressed in normal tissues (Savan et al., 2005). Description of other teleost TNFSF members has been reviewed in Biswas et al., (2015) and Glenney and Wiens (2007).

Cysteine knot cytokines

The overall structure of the cysteine knot cytokines can be described as a disulfide rich, all-beta core domain secondary structure. Particularly, of immunological importance, are members of the IL-17 family and transforming growth factor (TGF)-β. The cysteine knot structure is conserved through evolution as it is also found in invertebrates, and is an ancient family that predates Deuterostomia (approx. 550 mya) (Parthier et al., 2014). In mammals, cysteine knot cytokines are small, less than 200 amino acids, and are biologically active as covalently linked homodimers, having a molecular weight of about 40 kilo Dalton (kDa), except for IL17B which are a non-covalently linked homodimer (Meager and Wadhwa, 2013). Two clear mammalian homologs are found in teleosts, IL-17B and D. Furthermore, the isoforms IL17A/F1-3, IL-17N and IL-17C have been identified in teleosts (reviewed in Kono et al., 2011 and Secombes et al., 2016 and later works include: Costa et al., 2012; Ding et al., 2016; Du et al., 2015; Wang et al., 2015b; Wang et al., 2014; Yang et al., 2016). Although these cytokines have pro-inflammatory potential, the responses they elicit are not comparable in potency to that of TNF-α, IL-1β and many PAMPs, and their biological activity is linked to T-cells (Meager and Wadhwa, 2013). TGF

possess some immunosuppressive functions in addition to drive the Th17 differentiation in fish (Zou and Secombes, 2016). As neither the IL-17 nor TGF cytokine family encompasses major pro-inflammatory cytokines, further description of them is beyond the scope of this thesis.

Type I α helical cytokines

Most ILs and colony stimulating factors belong to the type I α helical cytokine family. ILs are divided into the; IL-2 subfamily, IL-6 subfamily and IL-12 subfamily. They signal via the type I cytokine receptor family. Of the IL-2 subfamily all molecules except IL-9 have been identified in fish, which include: IL-2, IL-4, IL-7, IL-15, and IL-21. All of them are implicated in T-cell memory or the molecules secreted by Th subsets upon stimulation (Secombes et al., 2011; Zou and Secombes, 2016).

The IL-6 subfamily in teleosts contains four members; IL-6, IL-11, CNTF (Ciliary neurotrophic factor) like and M17 (Fujiki et al., 2003; Huising et al., 2005; Wang and Secombes, 2009). The mammalian IL-6 subfamily member IL-31 is to date not identified in teleosts. Phylogenetic analysis suggests that the CNTF-like genes are orthologues to the LCA of CNTF/CLC (Charcot-Leyden crystals)/CT (cardiotropin) 1 & -2 genes in mammals and the M17 genes are orthologues to the LCA of LIF (leukemia inhibitory factor) and OSM (oncostatin M) genes in mammals (Wang and Secombes, 2009). Paralogs of teleost IL-6 subfamily members have been reported for IL-11 (Huising et al., 2005; Santos et al., 2008). There are no studies of teleost recombinant IL-11 or CNTF-like to date (Zou and Secombes, 2016). However, gene expression analysis suggests IL-11 are involved in responses against pathogenic virus, bacteria and parasite. CNTF-like expression is only weakly reduced by LPS and poly(I:C) and the pro-inflammatory cytokine IL-1β (Wang and Secombes, 2009; Wu et al., 2019). Furthermore, CNTF-like gene expression was weakly induced by *Yersinia ruckeri in vitro* in rainbow trout, however, the non-pathogen dependent effect of the trial was much larger than the pathogen dependent effect (Wang and Secombes, 2009).

Initially, IL-6 was shown to be critical to the activation and proliferation of T- and B-cells. Further, it was demonstrated that IL-6 was critical to acute phase immune responses and it was produced by monocytes and macrophages after LPS activation through TLRs. Other mammalian cells that also produce IL-6 include fibroblasts, keratinocytes and endothelial cells after stimulation with IL-1 molecules (Tanaka et al., 2014). Mammalian IL-6 are also known to increase its plasma concentration by a factor of 1 million, comparing normal with septic individuals. These extremes are associated with high mortality (Jordan et al., 2018).

The involvement of teleost IL-6 in antibody production has been reported from several species such as orange spotted grouper, Nile tilapia and Japanese pufferfish (Chen et al., 2012; Kaneda et al., 2012; Wei et al., 2018). Several studies have also reported the upregulation of IL-6 gene expression after bacterial exposure; S*treptococcus agalactiae* in *in vitro* Nile tilapia, *Edwardsiella tarda* in *in vivo* olive founder and *V. anguillarum* in *in vivo* study of gilthead seabream (Castellana et al., 2008; Nam et al., 2007; Wei et al., 2018). Further, IL-6 gene expression is affected by exposure to several PAMPs in teleosts; LPS, bacterial DNA, PGN, imiquimod and poly (I:C) (Bird et al., 2005; Castellana et al., 2008; Chen et al., 2012; Varela et al., 2012; Wei et al., 2018; Øvergard et al., 2012). Rainbow trout IL-6 gene expression is also induced by IL-1β (Costa et al., 2011). Recombinant rainbow trout IL-6 displayed typical features of mammalian IL-6, such as rapid induction of Signal transducer and activator of transcription 3 (STAT3) phosphorylation and expression of suppressor of cytokine signaling (SOCS) 1 to -3, cytokine-inducible SH2-containing protein (CISH) and interferon regulatory factor 1 (IRF-1). Interestingly, recombinant rainbow trout IL-6 displayed novel features not seen previously for IL-6: IL-6 produced during inflammation may promote macrophage proliferation locally, IL-6 induced the expression of an antimicrobial peptide (cathelicidin-2). Furthermore, IL-6 reduced the expression of IL-1β and TNF-α, indicating a role in regulation of inflammation, and IL-6 induced the expression of hepcidin in macrophage (Costa et al., 2011). Hepcidin

is an antimicrobial peptide that regulates iron homeostasis and is only expressed in hepatocytes in mammals (Lou et al., 2005; Nemeth et al., 2004).

Teleost diversity

As the previous sections have showed, there are considerable variations in the components and mechanisms of the teleost immune system. Some immune genes, such as TNF-α, have a complicated evolutionary history and basic understanding of teleost tree of life will make it less convoluted. Further, knowledge of their evolutionary histories are essential to understand their function. Also, phylogenetic analyses are important parts of the description of the molecules in this thesis. Therefore, a short section on the teleost diversity has been included.

Teleostei are a highly diverse group of animals containing approximately 50 % the diversity within Vertebrata. Teleostei, also known as true bone fish, are separated at the base from the living clades Sarcopterygii and Chondrichthyes and the fossil clade Placodermi. Teleosts occupy a great variety of different aquatic environments worldwide, from deep ocean trenches to high mountain streams, and many thrive in extreme habitats; subzero, hypersaline, hypoxic and acidic conditions (Helfman et al., 2009). Knowledge of their phylogeny has significantly advanced the last years, mainly due to the advent of novel comprehensive molecular methods applied to teleosts in conjuncture with ever increasing databases and –mining techniques that have enabled researchers to study multi-locus evolution. Although the molecular phylogeny encompasses more and more loci and species, the genome-scale studies are associated with some major challenges and a crisp-clear phylogeny is not yet resolved. In particular, the challenges of paralogy and a lack of high-quality genomes and transcriptomes relative to the number of species is problematic in teleost phylogeny. The particular areas of contention involve the branching order at the base of teleosts, the relationship among the otophysan orders, the sister group to the neoteleosts, the sister group to the acanthopterygians and the relationship among

atherinomorph orders. Although these contentions remain enigmas, most of the evolutionary backbone is known in teleost. See Figure 7 for the contemporary consensus of teleost phylogeny. Lumpfish is placed within the order Perciformes and the family Cyclopteridae (Betancur et al., 2013; Hughes et al., 2018).

The challenge of paralogy is the difficulty of inferring phylogenetic descendants based on sequence similarity, when the gene of interest has been duplicated. The assumption allowing phylogenetic inference based on sequence similarity, is that closely related species have sequences that are highly similar, while the sequences of species that are distantly related are proportionally less similar. This is often a good approach, but it has some fundamental challenges, e.g. with paralogy. When a gene is duplicated its daughter genes, the paralogs, can meet three different fates. I, one of them is retained while the other is removed from the DNA – called non-functionalization- II, both paralogs are retained and the functions of the orthologue are split between the two paralogs – called sub-functionalization - and III, both paralogs are retained, one of them retains the original functions while the other adapts new functions – called neo-functionalization. Despite the final fate of the paralogs, if both paralogs exist and they have similar functions, they will experience an increased mutation rate. This is because when one paralog get a deleterious mutation the other paralog will still produce a functional gene product and the fitness of the individual containing the deleterious mutation may not be affected. However, over time, one of three fates will manifest itself and the period of increased mutation rate will come to a halt. This increased mutation rate period causes the relation between specie and sequence relatedness to become non-linear and the interpretation is therefore much more difficult or impossible. Moreover, if genes meet fate II or III, at least one of the paralogs will get new set of exclusion rules, causing a change in rate of

Figure 7 (next page). Fossil calibrated phylogeny of 300 actinopterygians (blue and red) and three sarcopterygians (green) with divergence date estimates. The percomorph radiation is highlighted in red. Contentions is represented with yellow ovals, with alternative topology in box. From Hughes *et al.,* (2018).

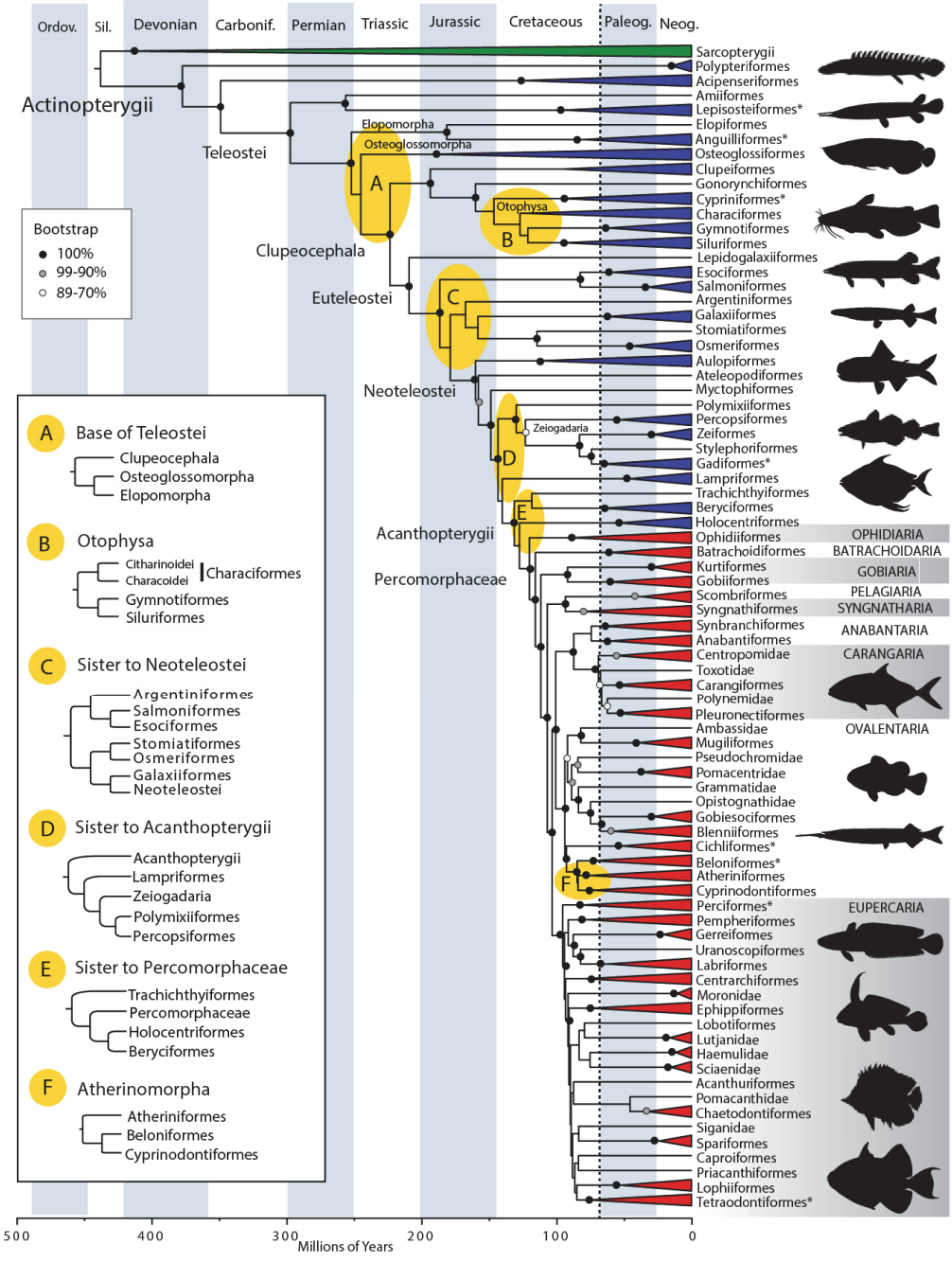
Ordov.
Sil.
Devonian
Carbonif.
Permian
Triassic
Jurassic
Cretaceous
Paleog.
Neog.
Actinopterygii
Teleostei
Elopomorpha
Osteoglossomorpha
Clupeocephala
Euteleostei
Neoteleostei
Acanthopterygii
Percomorphaceae
Otophysa
Zeiogadaria
A
B
C
D
E
F
Bootstrap
100%
99-90%
89-70%
Sarcopterygii
Polypteriformes
Acipenseriformes
Amiiformes
Lepisosteiformes*
Elopiformes
Anguilliformes*
Osteoglossiformes
Clupeiformes
Gonorynchiformes
Cypriniformes*
Characiformes
Gymnotiformes
Siluriformes
Lepidogalaxiiformes
Esociformes
Salmoniformes
Argentiniformes
Galaxiiformes
Stomiatiformes
Osmeriformes
Aulopiformes
Ateleopodiformes
Myctophiformes
Polymixiiformes
Percopsiformes
Zeiformes
Stylephoriformes
Gadiformes*
Lampriformes
Trachichthyiformes
Beryciformes
Holocentriformes
Ophidiiformes
Batrachoidiformes
Kurtiformes
Gobiiformes
Scombriformes
Syngnathiformes
Synbranchiformes
Anabantiformes
Centropomidae
Toxotidae
Carangiformes
Polynemidae
Pleuronectiformes
Ambassidae
Mugiliformes
Pseudochromidae
Pomacentridae
Grammatidae
Opistognathidae
Gobiesociformes
Blenniiformes
Cichliformes*
Beloniformes*
Atheriniformes
Cyprinodontiformes
Perciformes*
Pempheriformes
Gerreiformes
Uranoscopiformes
Labriformes
Centrarchiformes
Moronidae
Ephippiformes
Lobotiformes
Lutjanidae
Haemulidae
Sciaenidae
Acanthuriformes
Pomacanthidae
Chaetodontiformes
Siganidae
Spariformes
Caproiformes
Priacanthiformes
Lophiiformes
Tetraodontiformes*
OPHIDIARIA
BATRACHOIDARIA
GOBIARIA
PELAGIARIA
SYNGNATHARIA
ANABANTARIA
CARANGARIA
OVALENTARIA
EUPERCARIA
A Base of Teleostei
Clupeocephala
Osteoglossomorpha
Elopomorpha
B Otophysa
Citharinoidei
Characoidei
Characiformes
Gymnotiformes
Siluriformes
C Sister to Neoteleostei
Argentiniformes
Salmoniformes
Esociformes
Stomiatiformes
Osmeriformes
Galaxiiformes
Neoteleostei
D Sister to Acanthopterygii
Acanthopterygii
Lampriformes
Zeiogadaria
Polymixiiformes
Percopsiformes
E Sister to Percomorphaceae
Trachichthyiformes
Percomorphaceae
Holocentriformes
Beryciformes
F Atherinomorpha
Atheriniformes
Beloniformes
Cyprinodontiformes
500
400
300
200
100
0
Millions of Years

accumulated mutations, possibly enhancing the non-linearity. Therefore, Hughes et al., (2018) avoided using paralogues genes in their phylogeny.

Paralogous genes are found throughout the domains of life; however, a couple of clades are more exposed to the effects of paralogy due to whole genome duplication (WGD) events, also known as polyploidization. The plant kingdom is the most renowned clade of WGD, where the upper estimates of polyploidy in the flowering plants (Angiosperms) are 30-35% and the lower estimates are 2-4% (Otto and Whitton, 2000; Stebbins, 1971), and all are paleopolyploid. Mammals seem to be very intolerant of WGD. Polyploidy occurs in 2-3% of all human pregnancies, but almost every case result in either miscarriages or death short time after delivery. The oldest human with a recorded case of complete WGD (92 chromosomes) survived until the age of 27 weeks (Arvidsson et al., 1986). Despite WGD are deleterious for mammals, it has been speculated to be fundamental for the success of vertebrates. First postulated by Ohno (1970), the 2R hypothesis (coined by Holland et al., (1994)) states that the vertebrate genome is composed by two rounds of WGD, thus modern vertebrate genomes reflect the state of paleopolyploid. This hypothesis was hotly debated in the late 90's, and with the advent of modern sequencing technologies and increase in computational power, it gained popularity. Kasahara (2007) concluded that the 2R hypothesis is true, however, some of the cited works within these studies have lost some of the relevance to the conclusion. This regard the HOX genes (Abbasi, 2015). Even though the literature is not fully conclusive on the topic of vertebrate WGD, it is conclusive regarding the palaeopolyploidization of teleosts.

Basally, the teleosts experienced a WGD, termed the teleost specific (TS) WGD. Three lines of inquiry support this claim: I – high number of HOX genes, II - molecular clock analyses, estimating the TS-WGD to 350 - 320 mya and III - whole genome sequence analyses, reviewed in Glasauer and Neuhauss (2014). Further, WGD events have shaped the path of teleost evolution, with WGD occurring in both salmonids and cyprinids (Glasauer and

Neuhauss, 2014). The Salmonidae experienced a WGD event approximately 50 - 80 mya (Alexandrou et al., 2013; Johnson et al., 1987), and the LCA of the common carp and goldfish approximately 5.6 -11.3 mya (Wang et al., 2012; Zhang et al., 2013c). Additionally, some loaches (Cobitidae) and suckers (Catostomidae) also experienced WGD events (Ferris and Whitt, 1977; Uyeno and Smith, 1972). With more whole genome sequencing of teleosts, it is expected that more WGD events will be unveiled.

Aims of the study

The aims of this study were to investigate early immune responses in lumpfish (*Cyclopterus lumpus*) upon bacterial exposure and characterize the major pro-inflammatory cytokines. The objectives were as follows:

- Establish a lumpfish sequence database and protocols for handling the big data set
- Investigate innate immune responses in lumpfish
    - Global transcriptome analysis of early immune responses in lumpfish leukocytes upon exposure to *V. anguillarum* O1
    - In-depth mapping of major responding immune system pathways
- Identify and characterize IL-1 family members, IL-6 and TNF-α in lumpfish
    - Molecular characterization of gene, cDNA and peptide sequences
    - Study the phylogeny of the cytokines
    - Establish qPCR assay for the cytokines
    - Measure transcript levels of the cytokines in normal tissues and leukocytes by qPCR
    - Measure effects of PAMPs on the expression of these cytokines

Major findings in paper I, II and III

- The lumpfish transcriptome consisted of 346430 transcripts (**paper I**).
- In the lumpfish transcriptome 2490 genes belonged to immune system processes. Of them 956 genes were innate immune response genes (**paper I**).
- Quality assessment of DEG-analysis of lumpfish HKL after exposure to *V. anguillarum* was determined by principal component analysis (PCA) and clustered heatmap. The DEG consisted of 34280 genes, of which approximately 28% of the genes at 6 hours post exposure (hpe) and 45% of the genes at 24 hpe were significantly regulated (adjusted p-value < 0.05) and most of the variance was due to the experimental variables time and *V. anguillarum* exposure (**paper I**).
- Among the most regulated lumpfish genes after exposure to *V. anguillarum* were genes controlling pro-inflammatory processes; e.g. cytokines, TLR5S and complement factors (**paper I**).
- In addition to TLR5S, 12 TLRs, adaptor molecules and key molecules in the NF-κB and MAPK signaling pathways were identified (**paper I and III**).
- The lumpfish IL-1 family members; IL-1β, IL-18, nIL-1F and IL-1Fm2, and its receptors; IL-1R1, IL-1R2, IL-1R3, IL-1R4, IL-R5 and IL-1R9 were identified. The lumpfish IL-1 family shared the characteristics of other species within Perciformes, except that IL-1Fm2 in lumpfish lacks major parts of the N-terminal peptide sequence. The phylogenetic analysis placed the lumpfish genes within their respective clades and unveiled that IL-1Fm2 is most closely related to the IL-1β3 clade (**paper I and III**).
- Lumpfish TNF-α were identified and molecularly characterized. The gene contained four exons, the TNF signature sequence and the expected protein structure. The phylogenetic analysis placed lumpfish TNF-α within its expected clade, further, it demonstrated for the first time the lack of the typical TACE cut site in all TNF-α sequences within Ostariophysi (**paper I and II**).

- The lumpfish IL-6 gene sequence had a similar structure to other IL-6 genes. However, two isoforms were identified; one typical (IL-6 i1) and one alternatively retaining an intron (IL-6 i2). The latter contained a signal peptide first revealed after proteolytic cleavage, possibly performed by caspase 1. The phylogenetic analysis placed lumpfish IL-6 within their expected clades, further, it demonstrated for the first time the presence of a salmonid IL-6 gene duplication (**paper I and II**).
- The gene expression of the IL-1 family, IL-6 and TNF-α were characterized. Throughout 16 tissues, HKLs and PBLs all the examined genes were constitutively expressed. IL-1β and IL-1Fm2 were significantly lower expressed than nIL-1F and IL-18. The highest level of TNF-α and IL-6 transcripts were measured in immune organs, followed by surface tissues and lowest in other organs, except IL-6 in eye and brain where the highest levels of IL-6 were measured (**paper II and III**).
- Upon stimulation of IL-1 family, IL-6 and TNF-α with differing PAMPs; flagellin, pam3csk4, FSL-1, poly (I:C), CpG, GpC and ssPoly(U), IL-1β, nIL-1F, IL-6 and TNF-α were similarly differentially expressed, highly by flagellin and moderately by poly (I:C) and CpG, and to a limited extent by Pam3CSK3. The examined PAMPs did not elicit any response of IL-1Fm2 and IL-18 (**paper II and III**).

Discussion

In the present thesis, an explorative study of early innate immune responses in lumpfish leukocytes upon exposure to *V. anguillarum* has been performed using global transcriptome analyses, unveiling the underlying mechanisms of transduction of infective signals. Furthermore, the major pro-inflammatory cytokines of lumpfish have been characterized. The first phase of this study was a global characterization of the early anti-bacterial responses of lumpfish HKLs. The second phase of this study was continuing the notion of early immune responses of lumpfish HKLs, focusing in detail on the major pro-inflammatory cytokines. The pro-inflammatory cytokines have been instrumental to the development of a wide range of fish health disciplines; infection medicine, immunology and physiology. All these disciplines will be important for the continued improvement of the lumpfish fish health biology.

The sequenced lumpfish transcriptome consisted of 516 million reads, which is considered deep sequencing. In the context of RNA sequencing of bacteria exposed teleosts to date Jiang et al., (2016) are the only authors surpassing this depth (Sudhagar et al., 2018). In addition to containing information about the major gene activities, a deep transcriptome encompasses information regarding low expressing genes.

The assembled lumpfish transcriptome consisted of 346430 transcripts among 221659 trinity-genes. This gene number is far higher than expected considering its genome consists of 50 chromosomes (Li and Clyburne, 1977). This is the same number of chromosomes possessed by zebrafish, and the number of protein-encoding genes in zebrafish is about 26000 (Collins et al., 2012). Assuming the same genomic properties of lumpfish as with zebrafish, the number of assembled genes was approximately 8.5 times higher than expected. This was an intended consequence since a more relaxed collapsing algorithm would keep more low coverage genes in the assembled transcriptome. The extremely high number of genes in the transcriptome can therefore be a technical artifact.

It may also represent splicing variants. Independent of the cause, the number of genes is inflated and does not refer to the true biology. In general, when assessing number of genes in a *de novo* transcriptome, one should read them in relative and not absolute terms.

The assembled transcriptome was functionally annotated through a BLAST (basic local alignment search tool) based algorithm, utilizing manually curated mammalian biased databases such as e.g. SWISS-PROT and UNIPROT. Fish specific and novel genes are routinely ignored in such databases, however, the quality of the annotated genes is generally high. In the lumpfish transcriptome, the functional annotation consisted of 37895 gene ontology (GO) enriched genes. Within "biological process" the distribution of prevalent level 2 terms was as expected, except for metabolic process that was higher. As we *a priori* were interested in the immune system, we focused on the GO level 2 term 'immune system process'. It contained 2490 enriched genes, and the most abundant daughter-term 'immune response' containing 1354 genes. Within this level 3 GO term, the level 4 GO term 'innate immune response' was most abundant and included 956 genes.

The global DEG analysis revealed major differences across both tested variables – *V. anguillarum* exposure and time, as seen in both the PCA plot and the hierarchical clustering. As expected, the HKLs mounted a more extensive and potent response at 24 hpe compared to 6 hpe to *V. anguillarum.* The number of statically significant DEG increased from 9033 to 15225 genes over the time course in this study. In relative terms, DEG increased from 28% at 6 hpe to 45% at 24 hpe. Interestingly, only 16% of the DEGs (5389) were significantly regulated at both time points; perhaps reflecting important nuances in the early responses in lumpfish HKLs exposed to *V. anguillarum*, or time-dependent confounding variables, such as the HKLs adapting to the primary culture environment. Although such confounding variables contributed to the observed variance, the immunological effect of the experiment was clear. GO enrichment of the DEGs

revealed that upregulated genes at 6 hpe over-represented the GO-terms response to lipopolysaccharide, inflammatory response and regulation of intracellular signal. And, at 24 hpe the most over-represented GO terms included response to stimulus, defense response, response to stress, positive regulation of immune system processes and regulation of intracellular signal transduction. The GO enriched DEGs clearly showed involvement of the immune system through diverse mechanisms. Interestingly, GO terms related to IL-4 were over-represented at both 6 and 24 hpe.

Among the KEGG-pathways involved in detection of pathogens, the complement cascade and TLR pathway were the most upregulated in the *V. anguillarum* exposed HKLs. This is in congruence with other transcriptomic works on percomorph fish injected with *V. anguillarum* (Zhang et al., 2015; Zhao et al., 2016). However, a transcriptomic work in turbot studying the intestinal barrier alteration and pathogen entry upon immersion of *V. anguillarum,* did report a considerable downregulation of complement factors and did not mention the TLRs (Gao et al., 2016). Although all these works are performed in different species, this inconsistency seems to be an effect of challenge route. It seems likely that the effects reported in the present study, and those reported by Zhao et al., (2016) and Zhang et al., (2015), reflect the biological state of a systemic infection stage, while the effects reported by Gao et al., (2016) seems to reflect a local intestinal specific response.

The complement cascade can be activated by three different pathways; the classical, the lectin and the alternative pathway. In contrast to mammals, the alternative complement pathway titers are several orders of magnitude higher in teleosts (Sunyer and Tort, 1995). Many lumpfish genes belonging to the classical and alternative pathway were among the most highly differentially expressed genes. The complement factor H (CFH), complement factor 8A and B and complement factor B were the top four upregulated genes at 24 hpe 410, 265 and 203 times the control value, respectively. C1QA and C, GPR1 and C2 were the four most downregulated genes at 24 hpe, 0.022, 0.027, 0.057 and 0.074 compared

to the control, respectively. Complement factor H allows factor I to degrade C3b into iC3b, which binds to pathogenic membranes. In turn, iC3b binds to CR3, thereby enhancing phagocytosis, respiratory burst and antigen uptake. Interestingly, the CR3 was downregulated approximately 6.3 times the control value at 24 hpe. This contradicting expression value of CR3 might be a negative feedback loop. The complement factors 8 A and B are involved in the forming of the membrane attack complex. Complement factor B is also an integral part of the alternative complement pathway as it non-covalently binds to C3, forming C3 convertase upon factor D processing, and if the requisite environmental conditions are met, it forms C5 convertase. The alternative pathway is completely dependent on the alternative C3 and C5 convertases (Boshra et al., 2006). The most down-regulated genes were involved in the classical and lectin pathway. The DEG analysis showed a very clear picture; the alternative complement cascade is very important in the lumpfish HKL response to *V. anguillarum*.

The TLR pathway is initiated by PAMP binding of a TLR. In the KEGG reference pathway the human TLRs are entered, which is not fully representative of the lumpfish pathway. In the present study, 13 TLRs were identified and included in the TLR pathway analysis. The phylogenetic analysis confirmed the identification of the lumpfish TLRs, and conclusively proved the existence of TLR1, 2, 3, 5S, 5M, 7, 8, 9, 13, 14, 21, 22 and 28 in the lumpfish. Furthermore, we identified most of the members in the TLR signaling pathway. The DEG of the TLR signaling pathway clearly indicated that MYD88 and NF-κB dependent TLR signaling were the primarily activated signaling pathway in lumpfish HKLs during exposure to *V. anguillarum* . This was supported by the high upregulations of gene transcripts at 24 hpe of the pro-inflammatory cytokines; IL-1β (315.2), IL-6 (137.2), IL-8 (104) and TNF-α (30), the NF-κB signaling pathway genes; NF-κB inhibitor alpha (10.5) and NF-κB (5), and TLR5S (119.5). Interestingly the other TLRs were either not, slightly (TLR 2, 7, 14, and 21, ranging from 0.8 – 0.29) or severely downregulated (TLR13, 0.027) at 24 hpe. High upregulation of TLR5S upon bacterial exposure has previously been reported in rainbow

trout, gilthead seabream and flounder (Jayaramu et al., 2017; Munoz et al., 2013; Tsujita et al., 2004). In addition, the MAPK pathway genes MP2K6 and MP2K3 were downregulated (0.4) and (0.2). All the mentioned regulation levels were significant with adjusted p-value < 0.05. Among the downregulated TLRs in lumpfish with reported bacterial TLR-ligand were TLR 2 and 13. Teleost TLR2 ligands are lipopeptides, Pam_3CSK_4, PGN and LTA (Basu et al., 2012; Quiniou et al., 2013; Ribeiro et al., 2010; Samanta et al., 2012), and teleost TLR13 ligand is bacterial RNA (Liang et al., 2018). These are components of *V. anguillarum,* and it is highly interesting that lumpfish HKLs down-regulates these receptors. Some possible explanations could include the following hypotheses: 1) Lumpfish TLR2 and 13 do not share the ligand specificity of other described teleost TLR2 and 13. 2) The cells expressing TLR2 and 13 are selectively removed by a confounding variable, such as adaptation to the primary culture environment. 3) TLR2 and 13 competitively bind the adaptor proteins of TLR5 and thereby function as decoys for the TLR5 adaptor proteins. This could possibly lead to TLR5:flagellin complexes not being able to bind their adaptor proteins, due to too low concentration of free adaptor proteins, and thus termination/potency-reduction of the signaling cascade. The leukocytes needs to reduce the levels of TLR2 and 13 in order to maintain full potency of the TLR5 signal transduction. Independent of this hypothesis ,it is clear that lumpfish HKL's responses to *V. anguillarum* are highly dependent on TLR5, and that flagellin is likely the most efficient PAMP to protect against *V. anguillarum* infection. However, if hypothesis 3 is true, the consequence is that other PAMPs would not, or only slightly, elicit a protective response, as their receptors would be downregulated upon *V. anguillarum* infection.

The cytokines produced downstream of the TLR signaling pathway, IL-1β, IL-6, IL-8 and TNF-α, are all pro-inflammatory. These cytokines are known to be important in septic diseases, of which vibriosis is associated to (Frans et al., 2011). IL-8, also known as CXCL8, is an important chemotactic factor for neutrophils which are the most prevalent professional phagocytic cells in the immune system (Baggiolini and Clark-Lewis, 1992). The

chemotactic capacity of IL-8 has been demonstrated in cyprinids and is also associated with increased superoxide production of recruited cells (De Oliveira et al., 2015; De Oliveira et al., 2013a; De Oliveira et al., 2013b; Van Der Aa et al., 2010). Teleosts IL-8 has been reviewed by Bird and Tafalla (2015). In the transcriptome we observed some conflicting evidence regarding IL-1β. The previously mentioned transcript was extremely upregulated, but other automatic annotated IL-1β transcripts had low or no regulation at all. It was therefore necessary to perform deeper characterization of these transcripts and identify the true genes behind them (**paper III**). This conflicting state of the transcripts also highlighted the need for full description of the IL-1 family, to ensure future users of the lumpfish transcriptome would not accidentally select the wrong IL-1 family member.

Further, the NF-κB and MAPK signaling pathways and their regulation in lumpfish HKLs upon exposure to *V. anguillarum* were characterized. Most members of both signaling pathways were identified (**paper III**). As previously described for the TLR pathway, the DEG analysis consisted of genes belonging to the canonical part of the NF-κB signaling pathway. Interestingly, we identified three differentially regulated transcripts of TNFSF11a, also known as RANKL (Receptor activator of nuclear factor kappa-B ligand) regulated at 24 hpe 0.16, 1.22 and 11.16 times the control level. The DEG analysis of the MAPK signaling pathway displayed upregulation of the transcription factor belonging to classical MAP kinase pathway, JNK (c-Jun N-terminal kinase) and p38 MAP kinase pathway. These pathways all lead to an increased proliferation, differentiation and inflammation (Burotto et al., 2014).

The characterization of the IL-1 family members clearly proved the existence of the four expected teleost members in the lumpfish transcriptome; IL-1β, IL-18, nIL-1F and IL-1Fm2. In addition, the teleost receptors of the IL-1 family were identified; IL-1R1, IL-R2, IL-1R4, IL-1R5, DIGIRR and IL1-R3, the latter two only partial sequences. All the lumpfish IL-1 ligands contained the IL-1 signature sequence. As expected, the lumpfish IL-1β sequence

contained a propeptide, but not a caspase-1 cut site, as observed for other teleost IL-1 β , but in contrast to IL-1 β in mammals (Zou and Secombes, 2016). The gene organization of IL-1β showed that it is a type II IL-1β containing five exons. Lumpfish IL-18 also possesses five exons like other IL-18 sequences. A caspase-1 cut site was identified in lumpfish nIL-1F, in addition to two thrombin cut sites, previously suggested to be involved in the processing of trout nIL-1F (Wang et al., 2009). Lumpfish nIL-1F possesses seven exons, like other teleost nIL1F sequences (Zou and Secombes, 2016). Interestingly, the lumpfish IL-1Fm2 contained a shortened peptide sequence compared with other teleost sequences due to a stop codon after the first 36 bp of the coding sequence. The remaining transcript coded for a shortened IL-1Fm2 peptide sequence. It lacks the second exon and the majority of the third exon compared to IL-1Fm2 other species. This exon structure is unique for lumpfish. The loci of IL-1 ligands were identified in the lumpfish draft-genome (Knutsen, 2018). Synteny analysis showed that they mostly displayed similar co-localization as other teleosts (**paper III**).

The phylogenetic analysis of the IL-1 ligands conclusively proved the identification of the IL-1 family members in lumpfish. Interestingly, the present study for the first time identified the nIL-1F gene in non-teleost species – namely in Chondrichthyes and Sarcopterygii species. This is highly interesting as IL-1Ra and nIL-1F have been argued to not share an orthologous relationship, despite having similar function (Wang et al., 2009; Yao et al., 2015). The results in the present study clearly place nIL-1F in the evolutionary tree before the tetrapod divergence, implying that nIL-1F predates IL-1Ra. Further, it may imply that nIL-1F is the ancestor of IL-1Ra. The lack of similarity between nIL-1F and IL-1Ra might be explained by a gene-duplication followed by non-functionalization of the paralog most like nIL-1F. Also, the observed IL-1Fm2 phylogeny of Angosto et al., (2014) was observed in the present study (**paper III).**

Although the IL-1 ligands were constitutively expressed in tissues, there were not observed any significant tissue dependent gene-expression of the IL-1 family members in 16 lumpfish tissues and the two primary leukocyte cultures. However, IL-18 and nIL-1F were significantly overall higher expressed than IL-1β and IL-1Fm2. In the PAMP-stimulation experiment, IL-1Fm2 and IL-18 were barely induced, this is in congruence with the sparse literature as these cytokines are known to only be weakly induced by PAMPs and pathogens in teleosts (Angosto et al., 2014; Perez-Cordon et al., 2014; Zou et al., 2004). Interestingly, nIL-1F has shown to inhibit the expression of IL-1β in other teleosts, and has a similar expression profile as IL-1β across tissues (Wang et al., 2009; Yao et al., 2015). In the present study, IL-1β and nIL-1F expression levels were modulated in a similar pattern, highly induced by flagellin, moderately by CpG and poly(I:C) and weakly by Pam_3CSK_4 (**paper III**).

Gene organization of lumpfish TNF-α displayed the typical traits of teleosts TNF-α type I. This was also observed regarding the peptide characteristics. Within Teleostei there have been identified two types of TNF-α. Moreover, in certain clades such as Cyprininae and Salmonidae even more TNF-α genes have been identified. The phylogenetic analysis of lumpfish TNF-α with all presently available full-length teleost TNF-α sequence reproduced the previously known phylogenetic properties of the teleost TNF-α: two neoteleost clades, two Salmoniformes specific and two Cyprinidae specific clades (**paper II**).

Two lumpfish IL-6 isoforms were identified. One isoform displayed a conventional peptide sequence (IL6 i1), while the other isoform retained the first intron (IL6 i2). Interestingly, the predicted lumpfish IL-6 i2 sequence contained a signal peptide sequence, as expected, however this was first revealed after proteolytic cleavage, indicating that lumpfish IL-6 i2 is dependent on post-translational modification in order to gain its functionality. A capase-1 cut site was predicted in a region allowing for the aforementioned unveiling of the signal peptide. These predictions lead us to hypothesize that lumpfish IL-6 i2 is dependent on

caspase-1 processing. This hypothesis should be tested experimentally. Interestingly, the phylogenetic analysis of lumpfish and other teleost IL-6 revealed two clades within Salmoniformes. Eggestøl et al., 2020 is the first report of two IL-6 paralogs within Salmoniformes (**paper II**).

The gene expression profiling of lumpfish TNF-α and IL-6 in normal tissues and primary leukocyte cultures revealed an interesting pattern. Both genes were highly expressed in immune organs, followed by surface tissues and lowest in other internal organs, such as liver, muscle and gonad. However, the highest levels of lumpfish IL-6 were detected in brain and eye - the only organs where IL-6 expression surpassed TNF-α expression. In general, TNF-α transcripts were more prevalent than IL-6 transcripts in lumpfish tissues. This is highly interesting considering the PAMP stimulation of lumpfish IL-6 and TNF-α. Lumpfish IL-6 was considerably more potently regulated than lumpfish TNF-α (**paper II**).

Concluding remarks

A lumpfish transcriptome database was established, consisting of 346430 transcripts, among them 956 innate immune genes,. We found that the lumpfish innate immune responses are potent. The early responses against the extracellular bacteria *V. anguillarum*, are dominated by the alternative complement pathway, the TLR5S induced TLR signaling, chiefly through the canonical NF-κB pathway, leading to the production of the hallmark pro-inflammatory cytokines; IL-1β, TNF-α and IL-6. These cytokines are known to increase phagocytosis, proliferation and inflammation. The qPCR-assays for quantitative measurements of the cytokines were established. Four IL-1 ligands and several IL-1Rs were identified in lumpfish, and possess the typical traits found within teleosts. The phylogenetic analysis split the IL-1β clade according to their type, lumpfish IL-1β being placed within type I. Further, the present study describes nIL-1F for the first time outside of Teleostei. Lumpfish TNF-α also possesses the typical teleost traits, however some slight possible discrepancies have been described regarding lumpfish IL-6, as one of its isoforms are predicted to contain a caspase 1 cut site. Also, the present study contains the first evidence of IL-6 paralogs in Salmoniformes. If the speculations regarding IL-6 i2 processing represents true biology, then lumpfish IL-6 may be an unprecedented cytokine in evolution, being a pro- and anti-inflammatory cytokine with its kinetics dependent on caspase 1 processing. The qPCR data of the normal lumpfish tissues showed that IL-1β and IL-1Fm2 is lower expressed than nIL-1F and IL-18, and that TNF-α is higher expressed than IL-6, except for brain and eye. The PAMP stimulation of the lumpfish leukocytes potently regulated IL-1β, TNF-α, IL-6 and nIL-1F, in a parallel pattern, while IL-1Fm2 and IL18 were not. Our data constitute an important tool to further elucidate cytokine functions, protein-protein interactions and the underlying mechanisms for regulation of these molecules in lumpfish.

Knowledge of the immune system contribute to increased welfare of lumpfish, as it enables development of immune prophylactic measures, such as vaccination and

stimulation, and it increases our understanding of the lumpfish responses to disease. Further, this knowledge is also of comparative interest as lumpfish represent a phylogenetic group that is poorly described immunologically.

References

Aas, I.B., Austbø, L., König, M., Syed, M., Falk, K., Hordvik, I., Koppang, E.O., 2014. Transcriptional characterization of the T cell population within the salmonid interbranchial lymphoid tissue. Immunol. 193, 3463-3469. https://doi.org/10.4049/jimmunol.1400797

Abbasi, A.A., 2015. Diversification of four human HOX gene clusters by step-wise evolution rather than ancient whole-genome duplications. Dev. Genes Evol. 225, 353-357. https://doi.org/10.1007/s00427-015-0518-z

Abel, A.M., Yang, C., Thakar, M.S., Malarkannan, S., 2018. Natural Killer cells: development, maturation, and clinical utilization. Front. Immunol. 9, 1869-1869. https://doi.org/10.3389/fimmu.2018.01869

Aggarwal, B.B., 2003. Signalling pathways of the TNF superfamily: a double-edged sword. Nat. Rev.s Immunol. 3, 745-756. https://doi.org/10.1038/nri1184

Alarcon, M., Gulla, S., Rosaeg, M.V., Rønneseth, A., Wergeland, H., Poppe, T.T., Nilsen, H., Colquhoun, D.J., 2016a. Pasteurellosis in lumpsucker (*Cyclopterus lumpus*), farmed in Norway. J. Fish Dis. 39, 489-495. https://doi.org/10.1111/jfd.12366

Alarcon, M., Thoen, E., Poppe, T.T., Borno, G., Mohammad, S.N., Hansen, H., 2016b. Co-infection of *Nucleospora cyclopteri* (Microsporidia) and *Kudoa islandica* (Myxozoa) in farmed lumpfish (*Cyclopterus lumpus* L.) in Norway: a case report. J. Fish Dis. 39, 411-418. https://doi.org/10.1111/jfd.12372

Alexandrou, M.A., Swartz, B.A., Matzke, N.J., Oakley, T.H., 2013. Genome duplication and multiple evolutionary origins of complex migratory behavior in Salmonidae. Mol. Phylogenet. Evol. 69, 514-523. https://doi.org/10.1016/j.ympev.2013.07.026

Angosto, D., Lopez-Castejon, G., Lopez-Munoz, A., Sepulcre, M.P., Arizcun, M., Meseguer, J., Mulero, V., 2012. Evolution of inflammasome functions in vertebrates: Inflammasome and caspase-1 trigger fish macrophage cell death but are dispensable for the processing of IL-1beta. Innate Immun. 18, 815-824. https://doi.org/10.1177/1753425912441956

Angosto, D., Montero, J., Lopez-Munoz, A., Alcaraz-Perez, F., Bird, S., Sarropoulou, E., Abellan, E., Meseguer, J., Sepulcre, M.P., Mulero, V., 2014. Identification and functional characterization of a new IL-1 family member, IL-1Fm2, in most evolutionarily advanced fish. Innate Immun. 20, 487-500. https://doi.org/10.1177/1753425913501011

Arvidsson, C.G., Hamberg, H., Johnsson, H., Myrdal, U., Anneren, G., Brun, A., 1986. A boy with complete triploidy and unusually long survival. Acta Paediatr. Scand. 75, 507-510.

Baeyens, K.J., De Bondt, H.L., Raeymaekers, A., Fiers, W., De Ranter, C.J., 1999. The structure of mouse tumour-necrosis factor at 1.4 A resolution: towards modulation of its selectivity and trimerization. Acta Crystallogr. D Biol. Crystallogr. 55, 772-778. https://doi.org/10.1107/s0907444998018435

Baggiolini, M., Clark-Lewis, I., 1992. Interleukin-8, a chemotactic and inflammatory cytokine. FEBS Lett. 307, 97-101. https://doi.org/10.1016/0014-5793(92)80909-z

Bai, J.-S., Li, Y.-W., Deng, Y., Huang, Y.-Q., He, S.-H., Dai, J., Zhao, S.-Z., Dan, X.-M., Luo, X.-C., 2017. Molecular identification and expression analysis of TLR5M and TLR5S from orange-spotted grouper (*Epinephelus coioides*). Fish Shellfish Immunol. 63, 97-102. https://doi.org/https://doi.org/10.1016/j.fsi.2017.01.037

Barton, G.M., Kagan, J.C., Medzhitov, R., 2006. Intracellular localization of Toll-like receptor 9 prevents recognition of self DNA but facilitates access to viral DNA. Nat. Immunol. 7, 49-56. https://doi.org/10.1038/ni1280

Bassity, E., Clark, T.G., 2012. Functional identification of dendritic cells in the teleost model, rainbow trout (*Oncorhynchus mykiss*). PLoS One. 7, e33196-e33196. https://doi.org/10.1371/journal.pone.0033196

Basu, M., Kumar, M., Samanta, M., 2013. Toll-like receptor (TLR) 4 in mrigal (*Cirrhinus mrigala*): response to lipopolysaccharide treatment and *Aeromonas hydrophila* infection. Int. Res. J. Bio. Sci. 2, 20-27.

Basu, M., Swain, B., Sahoo, B.R., Maiti, N.K., Samanta, M., 2012. Induction of toll-like receptor (TLR) 2, and MyD88-dependent TLR- signaling in response to ligand stimulation and bacterial infections in the Indian major carp, mrigal (*Cirrhinus mrigala*). Mol. Biol. Rep. 39, 6015-6028. https://doi.org/10.1007/s11033-011-1415-9

Bergman, A.M., 1909. Die rote Beulenkrankheit des Aals. 2, 10-54.

Betancur, R., Broughton, R., Wiley, E, Carpenter, K., Lopez, J., Li, C., Holcroft, N., 2013. The Tree of Life and a New Classification of Bony Fishes. PLoS Curr. https://doi.org/10.1371/currents.tol.53ba26640df0ccaee75bb165c8c26288.

Bi, D., Wang, Y., Gao, Y., Li, X., Chu, Q., Cui, J., Xu, T., (2018). Recognition of Lipopolysaccharide and Activation of NF-κB by Cytosolic Sensor NOD1 in Teleost Fish. Front Immunol. 9 (1413). http://doi.org/10.3389/fimmu.2018.01413

Bird, S., Tafalla, C., 2015. Teleost Chemokines and Their Receptors. Biology (Basel). 4, 756-784. https://doi.org/10.3390/biology4040756

Bird, S., Zou, J., Savan, R., Kono, T., Sakai, M., Woo, J., Secombes, C., 2005. Characterisation and expression analysis of an interleukin 6 homologue in the

Japanese pufferfish*, Fugu rubripes*. Dev. Comp. Immunol. 29, 775-789. https://doi.org/10.1016/j.dci.2005.01.002

Bist, P., Dikshit, N., Koh, T.H., Mortellaro, A., Tan, T.T., Sukumaran, B., 2014. The Nod1, Nod2, and Rip2 axis contributes to host immune defense against intracellular *Acinetobacter baumannii* infection. Infect. Immun. 82, 1112-1122. https://doi.org/10.1128/iai.01459-13

Biswas, G., Bilen, S., Kono, T., Sakai, M., Hikima, J.-I., 2016. Inflammatory immune response by lipopolysaccharide-responsive nucleotide binding oligomerization domain (NOD)-like receptors in the Japanese pufferfish (*Takifugu rubripes*). Dev. Comp. Immunol. 55, 21-31. https://doi.org/https://doi.org/10.1016/j.dci.2015.10.008

Biswas, G., Kinoshita, S., Kono, T., Hikima, J., Sakai, M., 2015. Evolutionary evidence of tumor necrosis factor super family members in the Japanese pufferfish (*Takifugu rubripes*): Comprehensive genomic identification and expression analysis. Mar. Genomics. 22, 25-36. https://doi.org/10.1016/j.margen.2015.03.003

Bo, Y.X., Song, X.H., Wu, K., Hu, B., Sun, B.Y., Liu, Z.J., Fu, J.G., 2015. Characterization of interleukin-1beta as a proinflammatory cytokine in grass carp *(Ctenopharyngodon idella*). Fish Shellfish Immunol. 46, 584-595. https://doi.org/10.1016/j.fsi.2015.07.024

Bobe, J., Goetz, F.W., 2001. Molecular cloning and expression of a TNF receptor and two TNF ligands in the fish ovary. Comp. Biochem. Physiol. B Biochem. Mol. Biol. 129, 475-481. https://doi.org/10.1016/S1096-4959(01)00353-0

Bode, C., Zhao, G., Steinhagen, F., Kinjo, T., Klinman, D.M., 2011. CpG DNA as a vaccine adjuvant. Expert review of vaccines. 10, 499-511. https://doi.org/10.1586/erv.10.174

Boraschi, D., Italiani, P., Weil, S., Martin, M., 2018. The Family of the Interleukin-1 Receptors. Immunol Rev 281, (1) 197-232. https://doi.org/10.1111/imr.12606.

Bornø, G., Linaker, L., (red.), 2015. Fiskehelserapporten 2014, Vetrinærinstituttet

Boshra, H., Li, J., Sunyer, J.O., 2006. Recent advances on the complement system of teleost fish. Fish Shellfish Immunol. 20, 239-262. https://doi.org/10.1016/j.fsi.2005.04.004

Brinkmann, V., Reichard, U., Goosmann, C., Fauler, B., Uhlemann, Y., Weiss, D.S., Weinrauch, Y., Zychlinsky, A., 2004. Neutrophil extracellular traps kill bacteria. Science. 303, 1532-1535. https://doi.org/10.1126/science.1092385

Burotto, M., Chiou, V.L., Lee, J.M., Kohn, E.C., 2014. The MAPK pathway across different malignancies: a new perspective. Cancer. 120, 3446-3456. https://doi.org/10.1002/cncr.28864

Cai, Z.H., Song, L.S., Gao, C.P., Wu, L.T., Qiu, L.H., Xiang, J.H., 2003. Cloning and expression of tumor necrosis factor (TNFalpha) cDNA from red seabream (*Pagrus major*). Sheng Wu Hua Xue Yu Sheng Wu Wu Li Xue Bao (Shanghai). 35, 1111-1116.

Castellana, B., Iliev, D.B., Sepulcre, M.P., Mackenzie, S., Goetz, F.W., Mulero, V., Planas, J.V., 2008. Molecular characterization of interleukin-6 in the gilthead seabream (*Sparus aurata*). Mol. Immunol. 45, 3363-3370. https://doi.org/10.1016/j.molimm.2008.04.012

Castro, R., Tafalla, C., 2015. 2 - Overview of fish immunity, in: Beck, B.H., Peatman, E. (Eds.), Mucosal Health in Aquaculture. Academic Press, San Diego, pp. 3-54.

Cavin, J.M., Donahoe, S.L., Frasca, S., Jr., Innis, C.J., Kinsel, M.J., Kurobe, T., Naples, L.M., Nyaoke, A., Poll, C.P., Weber, E.P., 3rd, 2012. *Myxobolus albi* infection in cartilage of captive lumpfish (*Cyclopterus lumpus*). J. Vet. Diagn. Invest. 24, 516-524. https://doi.org/10.1177/1040638712440990

Chaves-Pozo, E., Pelegrin, P., Garcia-Castillo, J., Garcia-Ayala, A., Mulero, V., Meseguer, J., 2004. Acidophilic granulocytes of the marine fish gilthead seabream (*Sparus aurata* L.) produce interleukin-1beta following infection with *Vibrio anguillarum*. Cell Tissue Res. 316, 189-195. https://doi.org/10.1007/s00441-004-0875-9

Chen, H.H., Lin, H.T., Foung, Y.F., Han-You Lin, J., 2012. The bioactivity of teleost IL-6: IL-6 protein in orange-spotted grouper (*Epinephelus coioides*) induces Th2 cell differentiation pathway and antibody production. Dev. Comp. Immunol. 38, 285-294. https://doi.org/10.1016/j.dci.2012.06.013

Chin, A.I., Dempsey, P.W., Bruhn, K., Miller, J.F., Xu, Y., Cheng, G., 2002. Involvement of receptor-interacting protein 2 in innate and adaptive immune responses. Nature. 416, 190-194. https://doi.org/10.1038/416190a

Collins, J.E., White, S., Searle, S.M., Stemple, D.L., 2012. Incorporating RNA-seq data into the zebrafish Ensembl genebuild. Genome Res. 22, 2067-2078. https://doi.org/10.1101/gr.137901.112

Costa, M.M., Maehr, T., Diaz-Rosales, P., Secombes, C.J., Wang, T., 2011. Bioactivity studies of rainbow trout (*Oncorhynchus mykiss*) interleukin-6: effects on macrophage growth and antimicrobial peptide gene expression. Mol. Immunol. 48, 1903-1916. https://doi.org/10.1016/j.molimm.2011.05.027

Costa, M.M., Pereiro, P., Wang, T., Secombes, C.J., Figueras, A., Novoa, B., 2012. Characterization and gene expression analysis of the two main Th17 cytokines (IL-17A/F and IL-22) in turbot, *Scophthalmus maximus*. Dev. Comp. Immunol. 38, 505-516. https://doi.org/10.1016/j.dci.2012.09.002

De Oliveira, S., Lopez-Munoz, A., Martinez-Navarro, F.J., Galindo-Villegas, J., Mulero, V., Calado, A., 2015. Cxcl8-l1 and Cxcl8-l2 are required in the zebrafish defense against

Salmonella typhimurium. Dev. Comp. Immunol. 49, 44-48. https://doi.org/10.1016/j.dci.2014.11.004

De Oliveira, S., Reyes-Aldasoro, C.C., Candel, S., Renshaw, S.A., Mulero, V., Calado, A., 2013a. Cxcl8 (IL-8) mediates neutrophil recruitment and behavior in the zebrafish inflammatory response. J. Immunol. 190, 4349-4359. https://doi.org/10.4049/jimmunol.1203266

De Oliveira, S., Reyes-Aldasoro, C.C., Candel, S., Renshaw, S.A., Mulero, V., Calado, A., 2013b. Cxcl8 (IL-8) mediates neutrophil recruitment and behavior in the zebrafish inflammatory response. J. Immunol. 190, 4349-4359. https://doi.org/10.4049/jimmunol.1203266

Denes, A., Lopez-Castejon, G., Brough, D., 2012. Caspase-1: is IL-1 just the tip of the ICEberg? Cell Death Dis. 3, e338. https://doi.org/10.1038/cddis.2012.86

Dinarello, C.A., 1999. IL-18: A TH1 -inducing, proinflammatory cytokine and new member of the IL-1 family. J. Allergy Clin. Immunol. 103, 11-24. https://doi.org/https://doi.org/10.1016/S0091-6749(99)70518-X

Ding, Y., Ao, J., Ai, C., Chen, X., 2016. Molecular and functional identification of three interleukin-17A/F (IL-17A/F) homologues in large yellow croaker (*Larimichthys crocea*). Dev. Comp. Immunol. 55, 221-232. https://doi.org/10.1016/j.dci.2015.09.010

Du, L., Feng, S., Yin, L., Wang, X., Zhang, A., Yang, K., Zhou, H., 2015. Identification and functional characterization of grass carp IL-17A/F1: An evaluation of the immunoregulatory role of teleost IL-17A/F1. Dev. Comp. Immunol. 51, 202-211. https://doi.org/10.1016/j.dci.2015.03.014

Earnshaw, W.C., Martins, L.M., Kaufmann, S.H., 1999. Mammalian caspases: structure, activation, substrates, and functions during apoptosis. Annu. Rev. Biochem. 68, 383-424. https://doi.org/10.1146/annurev.biochem.68.1.383

Eggestøl, H.Ø., Lunde, H.S., Haugland, G.T., 2019. TLR and TLR signaling in lumpfish (*Cyclopterus lumpus* L.). Poster, 19th EAFP meeting 2019. Porto, Portugal.

Eggestøl, H.Ø., Lunde, H.S., Haugland, G.T., 2020. The pro-inflammatory cytokines TNF-α and IL-6 in lumpfish (*Cyclopterus lumpus* L.) -identification, molecular characterization, phylogeny and gene expression analyses. Dev Comp Immunol. 105, 103608

Eggestøl, H.Ø., Lunde, H.S., Rønneseth, A., Fredman, D., Petersen, K., Mishra, C.K., Furmanek, T., Colquhoun, D.J., Wergeland, H.I., Haugland, G.T., 2018. Transcriptome-wide mapping of signaling pathways and early immune responses in lumpfish leukocytes upon in vitro bacterial exposure. Sci. Rep. 8, 5261. https://doi.org/10.1038/s41598-018-23667-x

Eimon, P.M., Kratz, E., Varfolomeev, E., Hymowitz, S.G., Stern, H., Zha, J., Ashkenazi, A., 2006. Delineation of the cell-extrinsic apoptosis pathway in the zebrafish. Cell Death Differ. 13, 1619-1630. https://doi.org/10.1038/sj.cdd.4402015

Ellul, R.M., Bulla, J., Brudal, E., Colquhoun, D.J., Wergeland, H., Rønneseth, A., 2019a. Protection and antibody reactivity in lumpsucker (*Cyclopterus lumpus* L.) following vaccination against *Pasteurella* sp. Fish Shellfish Immunol. 95:650-658. http://doi: 10.1016/j.fsi.2019.11.016

Ellul, R.M., Walde, C., Haugland, G.T., Wergeland, H., Rønneseth, A., 2019b. Pathogenicity of *Pasteurella* sp. in lumpsuckers (*Cyclopterus lumpus* L.). J. Fish Dis. 42, 35-46. https://doi.org/10.1111/jfd.12905

Emmerich, R., Webel, E., 1894. Über eine durch Bacterien erzeugte Seuche unter den Forellen. Hyg. Bakteriol. 21, 1-21.

Esteban, M.Á., Cuesta, A., Chaves-Pozo, E., Meseguer, J., 2015. Phagocytosis in teleosts. Implications of the new cells involved. Biology. 4, 907-922. https://doi.org/10.3390/biology4040907

Evans, D.L., Jaso-Friedmann, L., 1992. Nonspecific cytotoxic cells as effectors of immunity in fish. Annu. Rev. Fish Dis. 2, 109-121. https://doi.org/https://doi.org/10.1016/0959-8030(92)90059-7

Fan, S., Chen, S., Liu, Y., Lin, Y., Liu, H., Guo, L., Lin, B., Huang, S., Xu, A., 2008. Zebrafish TRIF, a golgi-localized protein, participates in IFN induction and NF-kappaB activation. J. Immunol. 180, 5373-5383. https://doi.org/10.4049/jimmunol.180.8.5373

Farmer, J.J., Michael Janda, J., Brenner, F.W., Cameron, D.N., Birkhead, K.M., 2015. Vibrio, Bergey's Manual of Systematics of Archaea and Bacteria, pp. 1-79.

Feng, S., Cokus, S.J., Zhang, X., Chen, P.Y., Bostick, M., Goll, M.G., Hetzel, J., Jain, J., Strauss, S.H., Halpern, M.E., Ukomadu, C., Sadler, K.C., Pradhan, S., Pellegrini, M., Jacobsen, S.E., 2010. Conservation and divergence of methylation patterning in plants and animals. Proc. Natl. Acad. Sci. U. S. A. 107, 8689-8694. https://doi.org/10.1073/pnas.1002720107

Ferris, S.D., Whitt, G.S., 1977. Duplicate gene expression in diploid and tetraploid loaches (Cypriniformes, Cobitidae). Biochem. Genet. 15, 1097-1112.

Forlenza, M., Magez, S., Scharsack, J.P., Westphal, A., Savelkoul, H.F., Wiegertjes, G.F., 2009. Receptor-mediated and lectin-like activities of carp (*Cyprinus carpio*) TNF-alpha. J. Immunol. 183, 5319-5332. https://doi.org/10.4049/jimmunol.0901780

Frans, I., Michiels, C.W., Bossier, P., Willems, K.A., Lievens, B., Rediers, H., 2011. *Vibrio anguillarum* as a fish pathogen: virulence factors, diagnosis and prevention. J. Fish Dis. 34, 643-661. https://doi.org/10.1111/j.1365-2761.2011.01279.x

Fujiki, K., Nakao, M., Dixon, B., 2003. Molecular cloning and characterisation of a carp (*Cyprinus carpio*) cytokine-like cDNA that shares sequence similarity with IL-6 subfamily cytokines CNTF, OSM and LIF. Dev. Comp. Immunol. 27, 127-136. https://doi.org/10.1016/S0145-305x(02)00074-5

Gao, C., Fu, Q., Su, B., Zhou, S., Liu, F., Song, L., Zhang, M., Ren, Y., Dong, X., Tan, F., Li, C., 2016. Transcriptomic profiling revealed the signatures of intestinal barrier alteration and pathogen entry in turbot (*Scophthalmus maximus*) following *Vibrio anguillarum* challenge. Dev. Comp. Immunol. 65, 159-168. https://doi.org/https://doi.org/10.1016/j.dci.2016.07.007

Garcia-Castillo, J., Pelegrin, P., Mulero, V., Meseguer, J., 2002. Molecular cloning and expression analysis of tumor necrosis factor alpha from a marine fish reveal its constitutive expression and ubiquitous nature. Immunogenetics. 54, 200-207. https://doi.org/10.1007/s00251-002-0451-y

Glasauer, S.M., Neuhauss, S.C., 2014. Whole-genome duplication in teleost fishes and its evolutionary consequences. Mol Genet Genomics. 289, 1045-1060. https://doi.org/10.1007/s00438-014-0889-2

Glenney, G.W., Wiens, G.D., 2007. Early diversification of the TNF superfamily in teleosts: genomic characterization and expression analysis. J. Immunol. 178, 7955-7973. https://doi.org/10.4049/jimmunol.178.12.7955

Granja, A.G., Leal, E., Pignatelli, J., Castro, R., Abos, B., Kato, G., Fischer, U., Tafalla, C., 2015. Identification of Teleost Skin CD8alpha+ Dendritic-like Cells, Representing a

Potential Common Ancestor for Mammalian Cross-Presenting Dendritic Cells. J. Immunol. 195, 1825-1837. https://doi.org/10.4049/jimmunol.1500322

Grayfer, L., Walsh, J.G., Belosevic, M., 2008. Characterization and functional analysis of goldfish (*Carassius auratus* L.) tumor necrosis factor-alpha. Dev. Comp. Immunol. 32, 532-543. https://doi.org/10.1016/j.dci.2007.09.009

Guethmundsdottir, S., Vendramin, N., Cuenca, A., Sigurethardottir, H., Kristmundsson, A., Iburg, T.M., Olesen, N.J., 2019. Outbreak of viral haemorrhagic septicaemia (VHS) in lumpfish (*Cyclopterus lumpus*) in Iceland caused by VHS virus genotype IV. J. Fish Dis. 42, 47-62. https://doi.org/10.1111/jfd.12910

Gulla, S., 2016. Helsestatus for rensefisk i 2016. Vetrinærinstituttet, https://www.fhf.no, Presentation of health status of cleaner fish in 2016.

Gulla, S., 2017. Introductory studies on bacterial agents infecting cleaner fish, Norwegian Veterinary Institute. Norwegian University of Life Sciences, Ås.

Gulla, S., Lund, V., Kristoffersen, A.B., Sorum, H., Colquhoun, D.J., 2016. vapA (A-layer) typing differentiates *Aeromonas salmonicida* subspecies and identifies a number of previously undescribed subtypes. J. Fish Dis. 39, 329-342. https://doi.org/10.1111/jfd.12367

Hajam, I.A., Dar, P.A., Shahnawaz, I., Jaume, J.C., Lee, J.H., 2017. Bacterial flagellin—a potent immunomodulatory agent. Exp. Mol. Med. 49, e373-e373. https://doi.org/10.1038/emm.2017.172

Haugarvoll, E., Bjerkås, I., Nowak, B.F., Hordvik, I., Koppang, E.O., 2008. Identification and characterization of a novel intraepithelial lymphoid tissue in the gills of Atlantic salmon. J. Anat. 213, 202-209. https://doi.org/10.1111/j.1469-7580.2008.00943.x

Haugland, G.T., Jakobsen, R.A., Vestvik, N., Ulven, K., Stokka, L., Wergeland, H.I., 2012a. Phagocytosis and respiratory burst activity in lumpsucker (*Cyclopterus lumpus* L.) leucocytes analysed by flow cytometry. PLoS One. 7, e47909. https://doi.org/10.1371/journal.pone.0047909

Haugland, G.T., Jordal, A.E., Wergeland, H.I., 2012b. Characterization of small, mononuclear blood cells from salmon having high phagocytic capacity and ability to differentiate into dendritic like cells. PLoS One. 7, e49260. https://doi.org/10.1371/journal.pone.0049260

Haugland, G.T., Olsen, A.-B., Rønneseth, A., Andersen, L., 2017. Lumpfish (*Cyclopterus lumpus* L.) develop amoebic gill disease (AGD) after experimental challenge with *Paramoeba perurans* and can transfer amoebae to Atlantic salmon (Salmo salar L.). Aquaculture. 478, 48-55. https://doi.org/https://doi.org/10.1016/j.aquaculture.2016.04.001

Haugland, G.T., Rønneseth, A., Wergeland, H.I., 2014. Flow cytometry analyses of phagocytic and respiratory burst activities and cytochemical characterization of leucocytes isolated from wrasse (*Labrus bergylta* A.). Fish Shellfish Immunol. 39, 51-60. https://doi.org/10.1016/j.fsi.2014.04.023

Haugland, G.T., Rønneseth, A., Wergeland, H., 2018. Immunology and vaccinology of lumpfish and wrasse, in: Treasurer, J. (Ed.), Cleaner fish biology and aquaculture applications. 5M Publishing Ltd., UK, pp. 258-280.

Helfman, G., Collette, B.B., Facey, D.E., Bowen, B.W., 2009. The diversity of fishes: biology, evolution, and ecology. John Wiley & Sons.

Hirono, I., Nam, B.H., Kurobe, T., Aoki, T., 2000. Molecular cloning, characterization, and expression of TNF cDNA and gene from Japanese flounder *Paralychthys olivaceus*. J. Immunol. 165, 4423-4427. https://doi.org/10.4049/jimmunol.165.8.4423

Holland, P.W., Garcia-Fernandez, J., Williams, N.A., Sidow, A., 1994. Gene duplications and the origins of vertebrate development. Dev. Suppl., 125-133.

Hong, S., Li, R., Xu, Q., Secombes, C.J., Wang, T., 2013. Two types of TNF-alpha exist in teleost fish: phylogeny, expression, and bioactivity analysis of type-II TNF-alpha3 in rainbow trout *Oncorhynchus mykiss*. J. Immunol. 191, 5959-5972. https://doi.org/10.4049/jimmunol.1301584

Hong, S., Peddie, S., Campos-Pérez, J.J., Zou, J., Secombes, C.J., 2003. The effect of intraperitoneally administered recombinant IL-1β on immune parameters and resistance to *Aeromonas salmonicida* in the rainbow trout (*Oncorhynchus mykiss*). Dev. Comp. Immunol. 27, 801-812. https://doi.org/https://doi.org/10.1016/S0145-305X(03)00056-9

Hong, S., Zou, J., Collet, B., Bols, N.C., Secombes, C.J., 2004. Analysis and characterisation of IL-1β processing in rainbow trout*, Oncorhynchus mykiss*. Fish Shellfish Immunol. 16, 453-459. https://doi.org/https://doi.org/10.1016/j.fsi.2003.08.002

Hu, W., Wu, W., Sun, S., Liu, Z., Li, A., Gao, L., Liu, X., Liu, D., Deng, H., Zhao, B., Liu, B., Pang, Q., 2019. Identification and characterization of a TNF receptor-associated factor in *Dugesia japonica*. Gene. 681, 52-61. https://doi.org/10.1016/j.gene.2018.09.038

Huang, R., Dong, F., Jang, S., Liao, L., Zhu, Z., Wang, Y., 2012. Isolation and analysis of a novel grass carp toll-like receptor 4 (tlr4) gene cluster involved in the response to grass carp reovirus. Dev. Comp .Immunol. 38, 383-388. https://doi.org/https://doi.org/10.1016/j.dci.2012.06.002

Hughes, L.C., Orti, G., Huang, Y., Sun, Y., Baldwin, C.C., Thompson, A.W., Arcila, D., Betancur, R.R., Li, C., Becker, L., Bellora, N., Zhao, X., Li, X., Wang, M., Fang, C., Xie, B., Zhou, Z., Huang, H., Chen, S., Venkatesh, B., Shi, Q., 2018. Comprehensive phylogeny

of ray-finned fishes (Actinopterygii) based on transcriptomic and genomic data. Proc. Natl. Acad. Sci. U. S. A. 115, 6249-6254. https://doi.org/10.1073/pnas.1719358115

Huising, M.O., Kruiswijk, C.P., Van Schijndel, J.E., Savelkoul, H.F., Flik, G., Verburg-Van Kemenade, B.M., 2005. Multiple and highly divergent IL-11 genes in teleost fish. Immunogenetics. 57, 432-443. https://doi.org/10.1007/s00251-005-0012-2

Huising, M.O., Stet, R.J., Savelkoul, H.F., Verburg-Van Kemenade, B.M., 2004. The molecular evolution of the interleukin-1 family of cytokines; IL-18 in teleost fish. Dev. Comp. Immunol. 28, 395-413. https://doi.org/10.1016/j.dci.2003.09.005

Inohara, N., Koseki, T., Lin, J., Del Peso, L., Lucas, P.C., Chen, F.F., Ogura, Y., Nunez, G., 2000. An induced proximity model for NF-kappa B activation in the Nod1/RICK and RIP signaling pathways. J. Biol. Chem. 275, 27823-27831. https://doi.org/10.1074/jbc.M003415200

Jang, J.-H., Shin, H.W., Lee, J.M., Lee, H.-W., Kim, E.-C., Park, S.H., 2015. An Overview of Pathogen Recognition Receptors for Innate Immunity in Dental Pulp. Mediators Inflamm. 2015, 794143-794143. https://doi.org/10.1155/2015/794143

Jang, J.H., Kim, H., Kim, Y.J., Cho, J.H., 2016. Molecular cloning and functional analysis of nucleotide-binding oligomerization domain-containing protein 1 in rainbow trout, *Oncorhynchus mykiss*. Fish Shellfish Immunol. 51, 53-63. https://doi.org/https://doi.org/10.1016/j.fsi.2016.02.012

Jang, Y.H., Subramanian, D., Heo, M.S., 2014. Efficacy of formalin-killed *Pseudomonas anguilliseptica* vaccine on immune gene expression and protection in farmed olive flounder, *Paralichthys olivaceus*. Vaccine. 32, 1808-1813. https://doi.org/10.1016/j.vaccine.2014.01.088

Jayaramu, P.K., Tripathi, G., Pavan Kumar, A., Keezhedath, J., Pathan, M.K., Kurcheti, P.P., 2017. Studies on expression pattern of toll-like receptor 5 (TLR5) in *Edwardsiella tarda* infected *Pangasianodon hypophthalmus*. Fish Shellfish Immunol. 63, 68-73. https://doi.org/10.1016/j.fsi.2017.01.041

Jiang, Y., Feng, S., Zhang, S., Liu, H., Feng, J., Mu, X., Sun, X., Xu, P., 2016. Transcriptome signatures in common carp spleen in response to *Aeromonas hydrophila* infection. Fish Shellfish Immunol. 57, 41-48. https://doi.org/10.1016/j.fsi.2016.08.013

Johansen, L., Colquhoun, D.J., Hansen, H., Hildre, S., Wergeland, H., Mikalsen, H.E., 2016. Analyse av sykdomsrelatert risiko forbundet med bruk av villfanget og oppdrettet rensefisk for kontroll av lakselus, NOFIMA, Tromsø, Norway. [In Norwegian]

Johnson, K.R., Wright, J.E., Jr., May, B., 1987. Linkage relationships reflecting ancestral tetraploidy in salmonid fish. Genetics. 116, 579-591.

Jordan, S.C., Ammerman, N., Choi, J., Huang, E., Toyoda, M., Kim, I., Wu, G., Vo, A., 2018. Interleukin 6: pathogenic potential and therapeutic approaches in autoimmunity and transplant rejection, eLS, 1-12.

Jung, H.M., Castranova, D., Swift, M.R., Pham, V.N., Venero Galanternik, M., Isogai, S., Butler, M.G., Mulligan, T.S., Weinstein, B.M., 2017. Development of the larval lymphatic system in zebrafish. Development. 144, 2070. https://doi.org/10.1242/dev.145755

Kadowaki, T., Harada, H., Sawada, Y., Kohchi, C., Soma, G., Takahashi, Y., Inagawa, H., 2009. Two types of tumor necrosis factor-alpha in bluefin tuna (*Thunnus orientalis*) genes: Molecular cloning and expression profile in response to several immunological stimulants. Fish Shellfish Immunol. 27, 585-594. https://doi.org/10.1016/j.fsi.2008.12.006

Kaneda, M., Odaka, T., Suetake, H., Tahara, D., Miyadai, T., 2012. Teleost IL-6 promotes antibody production through STAT3 signaling via IL-6R and gp130. Dev. Comp. Immunol. 38, 224-231. https://doi.org/10.1016/j.dci.2012.02.002

Kasahara, M., 2007. The 2R hypothesis: an update. Curr. Opin. Immunol. 19, 547-552. https://doi.org/10.1016/j.coi.2007.07.009

Kawai, T., Akira, S., 2007. TLR signaling. Semi.n Immunol. 19, 24-32. https://doi.org/10.1016/j.smim.2006.12.004

Kawasaki, T., Kawai, T., 2014. Toll-like receptor signaling pathways. Front. Immunol. 5, 461. https://doi.org/10.3389/fimmu.2014.00461

Kenny, E.F., O'Neill, L.A., 2008. Signalling adaptors used by toll-like receptors: an update. Cytokine. 43, 342-349. https://doi.org/10.1016/j.cyto.2008.07.010

Kim, M.S., Hwang, Y.J., Yoon, K.J., Zenke, K., Nam, Y.K., Kim, S.K., Kim, K.H., 2009. Molecular cloning of rock bream (*Oplegnathus fasciatus*) tumor necrosis factor-alpha and its effect on the respiratory burst activity of phagocytes. Fish Shellfish Immunol. 27, 618-624. https://doi.org/10.1016/j.fsi.2009.07.007

Kim, Y.-G., Park, J.-H., Shaw, M.H., Franchi, L., Inohara, N., Núñez, G., 2008. The cytosolic sensors nod1 and nod2 are critical for bacterial recognition and host defense after exposure to toll-like receptor ligands. Immunity. 28, 246-257. https://doi.org/https://doi.org/10.1016/j.immuni.2007.12.012

Kinoshita, S., Biswas, G., Kono, T., Hikima, J., Sakai, M., 2014. Presence of two tumor necrosis factor (tnf)-alpha homologs on different chromosomes of zebrafish (*Danio rerio*) and medaka (*Oryzias latipes*). Mar Genomics. 13, 1-9. https://doi.org/10.1016/j.margen.2013.10.004

Knutsen, T.M., 2018. Lumpfish (*Cyclopterus lumpus*) draft genome assembly, Figshare pubishing tool, https://doi.org/DOI:10.6084/M9.FIGSHARE.7301546

Kobayashi, K., Inohara, N., Hernandez, L.D., Galan, J.E., Nunez, G., Janeway, C.A., Medzhitov, R., Flavell, R.A., 2002. RICK/Rip2/CARDIAK mediates signalling for receptors of the innate and adaptive immune systems. Nature. 416, 194-199. https://doi.org/10.1038/416194a

Kono, T., Korenaga, H., Sakai, M., 2011. Genomics of fish IL-17 ligand and receptors: a review. Fish Shellfish Immunol. 31, 635-643. https://doi.org/10.1016/j.fsi.2010.11.028

Kono, T., Zou, J., Bird, S., Savan, R., Sakai, M., Secombes, C.J., 2006. Identification and expression analysis of lymphotoxin-beta like homologues in rainbow trout *Oncorhynchus mykiss*. Mol. Immunol. 43, 1390-1401. https://doi.org/10.1016/j.molimm.2005.07.037

Kristmundsson, A., Freeman, M.A., 2014. Negative effects of *Kudoa islandica* n. sp. (Myxosporea: Kudoidae) on aquaculture and wild fisheries in Iceland. Int. J. Parasitol. Parasites Wildl. 3, 135-146. https://doi.org/10.1016/j.ijppaw.2014.06.001

Kryvi, H., Totland, G.K., 1997. Fiskeanatomi. Høyskoleforlaget AS - Norwegian Academic Press, Kistiansand, Norway.

Kumar, H., Kawai, T., Akira, S., 2009. Toll-like receptors and innate immunity. Biochem. Biophys. Res. Commun. 388, 621-625. https://doi.org/10.1016/j.bbrc.2009.08.062

Kuzmich, N.N., Sivak, K.V., Chubarev, V.N., Porozov, Y.B., Savateeva-Lyubimova, T.N., Peri, F., 2017. TLR4 signaling pathway modulators as potential therapeutics in inflammation and sepsis. Vaccines. 5 https://doi.org/10.3390/vaccines5040034

Laing, K.J., Purcell, M.K., Winton, J.R., Hansen, J.D., 2008. A genomic view of the NOD-like receptor family in teleost fish: identification of a novel NLR subfamily in zebrafish. BMC Evol. Biol. 8, 42. https://doi.org/10.1186/1471-2148-8-42

Laing, K.J., Wang, T., Zou, J., Holland, J., Hong, S., Bols, N., Hirono, I., Aoki, T., Secombes, C.J., 2001. Cloning and expression analysis of rainbow trout *Oncorhynchus mykiss* tumour necrosis factor-alpha. Eur. J. Biochem. 268, 1315-1322. https://doi.org/10.1046/j.1432-1327.2001.01996.x

Leifer, C.A., Kennedy, M.N., Mazzoni, A., Lee, C., Kruhlak, M.J., Segal, D.M., 2004. TLR9 is localized in the endoplasmic reticulum prior to stimulation. The Journal of Immunology. 173, 1179-1183. https://doi.org/10.4049/jimmunol.173.2.1179

Lepen Pleic, I., Secombes, C.J., Bird, S., Mladineo, I., 2014. Characterization of three pro-inflammatory cytokines, TNFalpha1, TNFalpha2 and IL-1beta, in cage-reared Atlantic bluefin tuna *Thunnus thynnus*. Fish Shellfish Immunol. 36, 98-112. https://doi.org/10.1016/j.fsi.2013.10.011

Li, J., Barreda, D.R., Zhang, Y.-A., Boshra, H., Gelman, A.E., Lapatra, S., Tort, L., Sunyer, J.O., 2006. B lymphocytes from early vertebrates have potent phagocytic and microbicidal abilities. Nat. Immunol. 7, 1116-1124. https://doi.org/10.1038/ni1389

Li, M., Clyburne, S., 1977. New cell line from the marine lumpfish, *Cyclopterus lumpus*. J. Fish. Boards of Canada. 34, 134-139.

Li, M.F., Zhang, J., 2016. CsTNF1, a teleost tumor necrosis factor that promotes antibacterial and antiviral immune defense in a manner that depends on the conserved receptor binding site. Dev. Comp. Immunol. 55, 65-75. https://doi.org/10.1016/j.dci.2015.10.010

Li, X.-D., Chen, Z.J., 2012. Sequence specific detection of bacterial 23S ribosomal RNA by TLR13. Elife. 1, e00102.

Li, X., Jia, Z., Wang, W., Wang, L., Liu, Z., Yang, B., Jia, Y., Song, X., Yi, Q., Qiu, L., Song, L., 2017a. Glycogen synthase kinase-3 (GSK3) regulates TNF production and haemocyte phagocytosis in the immune response of Chinese mitten crab *Eriocheir sinensis*. Dev. Comp. Immunol. 73, 144-155. https://doi.org/10.1016/j.dci.2017.03.022

Li, X., Wang, S., Qi, J., Echtenkamp, S.F., Chatterjee, R., Wang, M., Boons, G.-J., Dziarski, R., Gupta, D., 2007. Zebrafish peptidoglycan recognition proteins are bactericidal amidases essential for defense against bacterial infections. Immunity. 27, 518-529. https://doi.org/10.1016/j.immuni.2007.07.020

Li, Y., Li, Y., Cao, X., Jin, X., Jin, T., 2017b. Pattern recognition receptors in zebrafish provide functional and evolutionary insight into innate immune signaling pathways. Cell. Mol. Immunol. 14, 80-89. https://doi.org/10.1038/cmi.2016.50

Lie, K., Tørresen, O., Solbakken, M., Rønnestad, I., Tooming-Klunderud, A., Nederbragt, A., Jentoft, S., Sæle, O., 2018. Loss of stomach, loss of appetite? Sequencing of the ballan wrasse (*Labrus bergylta*) genome and intestinal transcriptomic profiling illuminate the evolution of loss of stomach function in fish. BMC Genomics 19(1): http://doi.org/186.10.1186/s12864-018-4570-8

Liang, Y., Ding, X., Yu, X., Wang, Y., Zhou, Y., He, J., Shi, Y., Zhang, Y., Lin, H., Lu, D., 2018. Identification and functional characterization of Toll-like receptor 13 from orange-spotted grouper (*Epinephelus coioides*). Fish Shellfish Immunol. 74, 309-317. https://doi.org/https://doi.org/10.1016/j.fsi.2017.12.054

Liu, J., Cao, D., Liu, Y., Li, Z., Si, Y., Wang, Z., Zhang, Q., Yu, H., Wang, X., 2018. Expression and functional analysis of receptor-interacting serine/threonine kinase 2 (RIP2) in

Japanese flounder (*Paralichthys olivaceus*). Fish Shellfish Immunol. 75, 327-335. https://doi.org/10.1016/j.fsi.2018.02.021

Lou, D.Q., Lesbordes, J.C., Nicolas, G., Viatte, L., Bennoun, M., Van Rooijen, N., Kahn, A., Renia, L., Vaulont, S., 2005. Iron- and inflammation-induced hepcidin gene expression in mice is not mediated by Kupffer cells in vivo. Hepatology. 41, 1056-1064. https://doi.org/10.1002/hep.20663

Lu, X.J., Chen, Q., Yang, G.J., Chen, J., 2015. The TNFalpha converting enzyme (TACE) from ayu (*Plecoglossus altivelis*) exhibits TNFalpha shedding activity. Mol. Immunol. 63, 497-504. https://doi.org/10.1016/j.molimm.2014.10.010

Lugo-Villarino, G., Balla, K.M., Stachura, D.L., Banuelos, K., Werneck, M.B., Traver, D., 2010. Identification of dendritic antigen-presenting cells in the zebrafish. Proc. Natl. Acad. Sci. U. S. A. 107, 15850-15855. https://doi.org/10.1073/pnas.1000494107

Magnadottir, B., 2006. Innate immunity of fish (overview). Fish Shellfish Immunol. 20, 137-151. https://doi.org/10.1016/j.fsi.2004.09.006

Manz, M.G., 2018. Plasmacytoid dendritic cells: origin matters. Nat. Immunol. 19, 652-654. https://doi.org/10.1038/s41590-018-0143-x

Marcos-Lopez, M., Donald, K., Stagg, H., Mccarthy, U., 2013. Clinical Vibrio anguillarum infection in lumpsucker *Cyclopterus lumpus* in Scotland. Vet. Rec. 173, 319. https://doi.org/10.1136/vr.101763

Marcos-Lopez, M., Ruane, N.M., Scholz, F., Bolton-Warberg, M., Mitchell, S.O., Murphy O'sullivan, S., Irwin Moore, A., Rodger, H.D., 2017. *Piscirickettsia salmonis* infection in cultured lumpfish (*Cyclopterus lumpus* L.). J. Fish Dis. 40, 1625-1634. https://doi.org/10.1111/jfd.12630

Marinus, M.G., Løbner-Olesen, A., 2014. DNA Methylation. EcoSal. Plus. 6, 10.1128/ecosalplus.ESP-0003-2013. https://doi.org/10.1128/ecosalplus.ESP-0003-2013

Mathew, J.A., Guo, Y.X., Goh, K.P., Chan, J., Verburg-Van Kemenade, B.M., Kwang, J., 2002. Characterisation of a monoclonal antibody to carp IL-1beta and the development of a sensitive capture ELISA. Fish Shellfish Immunol. 13, 85-95.

Matsuo, A., Oshiumi, H., Tsujita, T., Mitani, H., Kasai, H., Yoshimizu, M., Matsumoto, M., Seya, T., 2008. Teleost TLR22 recognizes RNA duplex to induce IFN and protect cells from birnaviruses. J. Immunol. 181, 3474-3485. https://doi.org/10.4049/jimmunol.181.5.3474

McMillan, D.N., Secombes, C.J., 1997. Isolation of rainbow trout (*Oncorhynchus mykiss*) intestinal intraepithelial lymphocytes (IEL) and measurement of their cytotoxic activity. Fish Shellfish Immunol. 7, 527-541. https://doi.org/https://doi.org/10.1006/fsim.1997.0099

Meager, A., Wadhwa, M., 2013. Interleukins, eLS., 1-18

Meijer, A.H., Gabby Krens, S.F., Medina Rodriguez, I.A., He, S., Bitter, W., Ewa Snaar-Jagalska, B., Spaink, H.P., 2004. Expression analysis of the toll-like receptor and TIR domain adaptor families of zebrafish. Mol. Immunol. 40, 773-783. https://doi.org/https://doi.org/10.1016/j.molimm.2003.10.003

Midtlyng, P.J., 1996. A field study on intraperitoneal vaccination of Atlantic salmon (*Salmo salar* L.) against furunculosis. Fish Shellfish Immunol. 6, 553-595.

Minton, K. (2018). "LC3 anchors TLR9 signalling." Nat. Rev. Immunol. 18(7) 418-419 http://doi.org/10.1038/s41577-018-0019-1

Mitchell, S., Vargas, J., Hoffmann, A., 2016. Signaling via the NFkappaB system. Wiley Interdiscip. Rev. Syst. Biol. Med. 8, 227-241. https://doi.org/10.1002/wsbm.1331

Mogensen, T.H., 2009. Pathogen recognition and inflammatory signaling in innate immune defenses. Clin. Microbiol. Rev. 22, 240-273. https://doi.org/10.1128/CMR.00046-08

Munoz, I., Sepulcre, M.P., Meseguer, J., Mulero, V., 2013. Molecular cloning, phylogenetic analysis and functional characterization of soluble Toll-like receptor 5 in gilthead seabream, *Sparus aurata*. Fish Shellfish Immunol. 35, 36-45. https://doi.org/10.1016/j.fsi.2013.03.374

Murphy, K., Weaver, C., 2012. Janeway's immunobiology, 8 ed. Garland Science.

Nam, B.H., Byon, J.Y., Kim, Y.O., Park, E.M., Cho, Y.C., Cheong, J., 2007. Molecular cloning and characterisation of the flounder (*Paralichthys olivaceus*) interleukin-6 gene. Fish Shellfish Immunol. 23, 231-236. https://doi.org/10.1016/j.fsi.2006.10.001

Nemeth, E., Rivera, S., Gabayan, V., Keller, C., Taudorf, S., Pedersen, B.K., Ganz, T., 2004. IL-6 mediates hypoferremia of inflammation by inducing the synthesis of the iron regulatory hormone hepcidin. J. Clin. Invest. 113, 1271-1276. https://doi.org/10.1172/jci20945

Neumann, S., Scheurich, P., Maier, O., 2013. Tumour Necrosis Factors, eLS., 1-14.

Nie, L., Cai, S.-Y., Shao, J.-Z., Chen, J., 2018. Toll-like receptors, associated biological roles, and signaling networks in non-mammals. Front. Immunol. 9 https://doi.org/10.3389/fimmu.2018.01523

Novoa, B., Bowman, T.V., Zon, L., Figueras, A., 2009. LPS response and tolerance in the zebrafish (*Danio rerio*). Fish Shellfish Immunol. 26, 326-331. https://doi.org/https://doi.org/10.1016/j.fsi.2008.12.004

Norwegian Directory of Fisheries, 2018. Salg av oppdrettet rensefisk 2012-2018. https://www.fiskeridir.no/Akvakultur/Tall-og-analyse/Akvakulturstatistikk-tidsserier/Rensefisk

Ogryzko, N.V., Renshaw, S.A., Wilson, H.L., 2014. The IL-1 family in fish: swimming through the muddy waters of inflammasome evolution. Dev. Comp. Immunol. 46, 53-62. https://doi.org/10.1016/j.dci.2014.03.008

Ohno, S., 1970. Evolution by gene duplication. Springer, Berlin.

Okamura, H., Kashiwamura, S.-I., Tsutsui, H., Yoshimoto, T., Nakanishi, K., 1998. Regulation of interferon-γ production by IL-12 and IL-18. Curr. Opin. Immunol. 10, 259-264. https://doi.org/https://doi.org/10.1016/S0952-7915(98)80163-5

Oldenburg, M., Krüger, A., Ferstl, R., Kaufmann, A., Nees, G., Sigmund, A., Bathke, B., Lauterbach, H., Suter, M., Dreher, S., Koedel, U., Akira, S., Kawai, T., Buer, J., Wagner, H., Bauer, S., Hochrein, H., Kirschning, C.J., 2012. TLR13 recognizes bacterial 23S rRNA devoid of erythromycin resistance–forming modification. Science. 337, 1111-1115. https://doi.org/10.1126/science.1220363

O'Neill, L., and A. G. Bowie, A., 2007. The family of five: TIR-domain-containing adaptors in Toll-like receptor signalling. Nat. Rev. Immunol. 7(5): 353-http://doi.org/364.10.1038/nri2079

Ordas, M.C., Costa, M.M., Roca, F.J., Lopez-Castejon, G., Mulero, V., Meseguer, J., Figueras, A., Novoa, B., 2007. Turbot TNFalpha gene: molecular characterization and biological activity of the recombinant protein. Mol. Immunol. 44, 389-400. https://doi.org/10.1016/j.molimm.2006.02.028

Oshiumi, H., Matsuo, A., Matsumoto, M., Seya, T., 2008. Pan-vertebrate toll-like receptors during evolution. Curr. Genomics. 9, 488-493. https://doi.org/10.2174/138920208786241234

Otto, S.P., Whitton, J., 2000. Polyploid incidence and evolution. Annu. Rev. Genet. 34, 401-437. https://doi.org/10.1146/annurev.genet.34.1.401

Palti, Y., 2011. Toll-like receptors in bony fish: from genomics to function. Dev. Comp. Immunol. 35, 1263-1272. https://doi.org/10.1016/j.dci.2011.03.006

Palti, Y., Rodriguez, M.F., Gahr, S.A., Purcell, M.K., Rexroad, C.E., Wiens, G.D., 2010. Identification, characterization and genetic mapping of TLR1 loci in rainbow trout (*Oncorhynchus mykiss*). Fish Shellfish Immunol. 28, 918-926. https://doi.org/https://doi.org/10.1016/j.fsi.2010.02.002

Paria, A., Deepika, A., Sreedharan, K., Makesh, M., Chaudhari, A., Purushothaman, C.S., Thirunavukkarasu, A.R., Rajendran, K.V., 2016. Identification of Nod like receptor C3 (NLRC3) in Asian seabass, *Lates calcarifer*: Characterisation, ontogeny and expression analysis after experimental infection and ligand stimulation. Fish Shellfish Immunol. 55, 602-612. https://doi.org/https://doi.org/10.1016/j.fsi.2016.06.029

Park, J.-H., Kim, Y.-G., Mcdonald, C., Kanneganti, T.-D., Hasegawa, M., Body-Malapel, M., Inohara, N., Núñez, G., 2007. RICK/RIP2 mediates innate immune responses induced through Nod1 and Nod2 but not TLRs. J. Immunol. 178, 2380-2386. https://doi.org/10.4049/jimmunol.178.4.2380

Parthier, C., Stelter, M., Ursel, C., Fandrich, U., Lilie, H., Breithaupt, C., Stubbs, M.T., 2014. Structure of the Toll-Spatzle complex, a molecular hub in Drosophila development and innate immunity. Proc. Natl. Acad. Sci. U. S. A. 111, 6281-6286. https://doi.org/10.1073/pnas.1320678111

Peddie, S., Zou, J., Cunningham, C., Secombes, C.J., 2001. Rainbow trout (*Oncorhynchus mykiss*) recombinant IL-1beta and derived peptides induce migration of head-kidney leucocytes in vitro. Fish Shellfish Immunol. 11, 697-709. https://doi.org/10.1006/fsim.2001.0348

Pelegrin, P., Chaves-Pozo, E., Mulero, V., Meseguer, J., 2004. Production and mechanism of secretion of interleukin-1β from the marine fish gilthead seabream. Dev. Comp. Immunol. 28, 229-237. https://doi.org/https://doi.org/10.1016/j.dci.2003.08.002

Percy, M.G., Grundling, A., 2014. Lipoteichoic acid synthesis and function in gram-positive bacteria. Annu. Rev. Microbiol. 68, 81-100. https://doi.org/10.1146/annurev-micro-091213-112949

Pereiro, P., Balseiro, P., Romero, A., Dios, S., Forn-Cuni, G., Fuste, B., Planas, J.V., Beltran, S., Novoa, B., Figueras, A., 2012. High-throughput sequence analysis of turbot (*Scophthalmus maximus*) transcriptome using 454-pyrosequencing for the discovery of antiviral immune genes. PLoS One. 7, e35369. https://doi.org/10.1371/journal.pone.0035369

Perez-Cordon, G., Estensoro, I., Benedito-Palos, L., Calduch-Giner, J.A., Sitja-Bobadilla, A., Perez-Sanchez, J., 2014. Interleukin gene expression is strongly modulated at the local level in a fish-parasite model. Fish Shellfish Immunol. 37, 201-208. https://doi.org/10.1016/j.fsi.2014.01.022

Pietretti, D., Wiegertjes, G.F., 2014. Ligand specificities of Toll-like receptors in fish: indications from infection studies. Dev. Comp. Immunol. 43, 205-222. https://doi.org/10.1016/j.dci.2013.08.010

Powell, A., Treasurer, J.W., Pooley, C.L., Keay, A.J., Lloyd, R., Imsland, A.K., Garcia De Leaniz, C., 2018. Use of lumpfish for sea-lice control in salmon farming: challenges and opportunities. Rev. Fish. Sci. Aquac. 10, 683-702. https://doi.org/10.1111/raq.12194

Praveen, K., Evans, D.L., Jaso-Friedmann, L., 2006. Constitutive expression of tumor necrosis factor-alpha in cytotoxic cells of teleosts and its role in regulation of cell-mediated cytotoxicity. Mol. Immunol. 43, 279-291. https://doi.org/10.1016/j.molimm.2005.01.012

Purcell, M.K., Smith, K.D., Hood, L., Winton, J.R., Roach, J.C., 2006. Conservation of toll-like receptor signaling pathways in teleost fish. Comp. Biochem. Physiol. Part D Genomics Proteomics. 1, 77-88. https://doi.org/10.1016/j.cbd.2005.07.003

Qu, F., Xiang, Z., Zhou, Y., Qin, Y., 2017. A molluscan TNF receptor-associated factor 2 (TRAF2) was involved in host defense against immune challenges. Fish Shellfish Immunol. 71, 105-115. https://doi.org/10.1016/j.fsi.2017.09.076

Quiniou, S.M., Boudinot, P., Bengten, E., 2013. Comprehensive survey and genomic characterization of toll-like receptors (TLRs) in channel catfish, *Ictalurus punctatus*: identification of novel fish TLRs. Immunogenetics. 65, 511-530. https://doi.org/10.1007/s00251-013-0694-9

Rebl, A., Goldammer, T., Seyfert, H.M., 2010. Toll-like receptor signaling in bony fish. Vet. Immunol. Immunopathol. 134, 139-150. https://doi.org/10.1016/j.vetimm.2009.09.021

Reid, C.W., Vinogradov, E., Li, J., Jarrell, H.C., Logan, S.M., Brisson, J.R., 2012. Structural characterization of surface glycans from *Clostridium difficile*. Carbohydr. Res. 354, 65-73. https://doi.org/10.1016/j.carres.2012.02.002

Reis, M.I., Do Vale, A., Pereira, P.J., Azevedo, J.E., Dos Santos, N.M., 2012. Caspase-1 and IL-1beta processing in a teleost fish. PLoS One. 7, e50450. https://doi.org/10.1371/journal.pone.0050450

Ribeiro, C.M., Hermsen, T., Taverne-Thiele, A.J., Savelkoul, H.F., Wiegertjes, G.F., 2010. Evolution of recognition of ligands from Gram-positive bacteria: similarities and differences in the TLR2-mediated response between mammalian vertebrates and teleost fish. J. Immunol. 184, 2355-2368. https://doi.org/10.4049/jimmunol.0900990

Roca, F.J., Ramakrishnan, L., 2013. TNF dually mediates resistance and susceptibility to mycobacteria via mitochondrial reactive oxygen species. Cell. 153, 521-534. https://doi.org/10.1016/j.cell.2013.03.022

Ross, M.H., Pawlina, W., 2011. Digesitive system II: Esophagus and gastintestinal tract, Histology: A text and Atlas with Correlated Cell and Molecular Biology, 6 ed. Lippincott Williams & Wilkins, pp. 568-627.

Ryan, G.B., Majno, G., 1977. Acute inflammation. A review. Am. J. Clin. Pathol. 86, 183-276.

Rønneseth, A., Ghebretnsae, D.B., Wergeland, H.I., Haugland, G.T., 2015. Functional characterization of IgM+ B cells and adaptive immunity in lumpfish (*Cyclopterus lumpus* L.). Dev. Comp. Immunol. 52, 132-143. https://doi.org/10.1016/j.dci.2015.05.010

Rønneseth, A., Haugland, G.T., Colquhoun, D.J., Brudal, E., Wergeland, H.I., 2017. Protection and antibody reactivity following vaccination of lumpfish (*Cyclopterus lumpus* L.) against atypical *Aeromonas salmonicida*. Fish Shellfish Immunol. 64, 383-391. https://doi.org/https://doi.org/10.1016/j.fsi.2017.03.040

Saeij, J.P.J., Stet, R.J.M., De Vries, B.J., Van Muiswinkel, W.B., Wiegertjes, G.F., 2003. Molecular and functional characterization of carp TNF: a link between TNF polymorphism and trypanotolerance? Dev. Comp. Immunol. 27, 29-41. https://doi.org/10.1016/s0145-305x(02)00064-2

Salinas, I., 2015. The mucosal immune system of teleost gish. Biology. 4, 525-539. https://doi.org/10.3390/biology4030525

Samanta, M., Swain, B., Basu, M., Panda, P., Mohapatra, G.B., Sahoo, B.R., Maiti, N.K., 2012. Molecular characterization of toll-like receptor 2 (TLR2), analysis of its inductive expression and associated down-stream signaling molecules following ligands exposure and bacterial infection in the Indian major carp, rohu (*Labeo rohita*). Fish Shellfish Immunol. 32, 411-425. https://doi.org/https://doi.org/10.1016/j.fsi.2011.11.029

Santos, M.D., Yasuike, M., Kondo, H., Hirono, I., Aoki, T., 2008. Teleostean IL11b exhibits complementing function to IL11a and expansive involvement in antibacterial and antiviral responses. Mol. Immunol. 45, 3494-3501. https://doi.org/10.1016/j.molimm.2008.02.004

Sarkar, A., Duncan, M., Hart, J., Hertlein, E., Guttridge, D.C., Wewers, M.D., 2006. ASC Directs NF-κB Activation by Regulating Receptor Interacting Protein-2 (RIP2) Caspase-1 Interactions. J. Immunol. 176, 4979-4986. https://doi.org/10.4049/jimmunol.176.8.4979

Sasai, M., Yamamoto, M., 2013. Pathogen recognition receptors: ligands and signaling pathways by toll-like receptors. Int. Rev. Immunol. 32, 116-133. https://doi.org/10.3109/08830185.2013.774391

Savan, R., Kono, T., Igawa, D., Sakai, M., 2005. A novel tumor necrosis factor (TNF) gene present in tandem with theTNF-alpha gene on the same chromosome in teleosts. Immunogenetics. 57, 140-150. https://doi.org/10.1007/s00251-005-0768-4

Savan, R., Sakai, M., 2004. Presence of multiple isoforms of TNF alpha in carp (*Cyprinus carpio* L.): genomic and expression analysis. Fish Shellfish Immunol. 17, 87-94. https://doi.org/10.1016/j.fsi.2003.11.001

Scapigliati, G., Fausto, A.M., Picchietti, S., 2018. Fish Lymphocytes: An Evolutionary Equivalent of Mammalian Innate-Like Lymphocytes? Front. Immunol. 9 (971) https://doi.org/10.3389/fimmu.2018.00971

Scholz, F., Fringuelli, E., Bolton-Warberg, M., Marcos-Lopez, M., Mitchell, S., Prodhol, P., Moffet, D., Savage, P., Murphy O'sullivan, S., I, O.C., Mccarthy, E., Rodger, H.D., 2017. First record of *Tetramicra brevifilum* in lumpfish (*Cyclopterus lumpus*, L.). J. Fish Dis. 40, 757-771. https://doi.org/10.1111/jfd.12554

Scholz, F., Glosvik, H., Marcos-Lopez, M., 2018. Cleaner fish health, in: Treasurer, J. (Ed.), Cleaner fish biology and aquaculture applications. 5M Publishing Ltd., UK, pp. 221-257.

Schroder, K., Tschopp, J., 2010. The inflammasomes. Cell. 140, 821-832. https://doi.org/https://doi.org/10.1016/j.cell.2010.01.040

Secombes, C.J., Wang, T., Bird, S., 2011. The interleukins of fish. Dev. Comp. Immunol. 35, 1336-1345. https://doi.org/10.1016/j.dci.2011.05.001

Secombes, C.J., Wang, T., Bird, S., 2016. Vertebrate cytokines and their evolution, in: Malagoli, D. (Ed.), The evolution of the immune system. Academic Press, pp. 87-150.

Seger, R., Krebs, E.G., 1995. The MAPK signaling cascade. The FASEB Journal. 9, 726-735. https://doi.org/10.1096/fasebj.9.9.7601337

Sepulcre, M.P., Alcaraz-Perez, F., Lopez-Munoz, A., Roca, F.J., Meseguer, J., Cayuela, M.L., Mulero, V., 2009. Evolution of lipopolysaccharide (LPS) recognition and signaling: fish TLR4 does not recognize LPS and negatively regulates NF-kappaB activation. J. Immunol. 182, 1836-1845. https://doi.org/10.4049/jimmunol.0801755

Sepulcre, M.P., Lopez-Castejon, G., Meseguer, J., Mulero, V., 2007. The activation of gilthead seabream professional phagocytes by different PAMPs underlines the

behavioural diversity of the main innate immune cells of bony fish. Mol. Immunol. 44, 2009-2016. https://doi.org/10.1016/j.molimm.2006.09.022

Sha, Z., Abernathy, J.W., Wang, S., Li, P., Kucuktas, H., Liu, H., Peatman, E., Liu, Z., 2009. NOD-like subfamily of the nucleotide-binding domain and leucine-rich repeat containing family receptors and their expression in channel catfish. Dev. Comp. Immunol. 33, 991-999. https://doi.org/https://doi.org/10.1016/j.dci.2009.04.004

Sims, J.E., Nicklin, M.J., Bazan, J.F., Barton, J.L., Busfield, S.J., Ford, J.E., Kastelein, R.A., Kumar, S., Lin, H., Mulero, J.J., Pan, J., Pan, Y., Smith, D.E., Young, P.R., 2001. A new nomenclature for IL-1-family genes. Trends Immunol. 22, 536-537.

Skjæveland, I., Iliev, D.B., Strandskog, G., Jorgensen, J.B., 2009. Identification and characterization of TLR8 and MyD88 homologs in Atlantic salmon (*Salmo salar*). Dev. Comp. Immunol. 33, 1011-1017. https://doi.org/10.1016/j.dci.2009.04.007

Skoge, R.H., Brattespe, J., Økland, A.L., Plarre, H., Nylund, A., 2018. New virus of the family Flaviviridae detected in lumpfish (*Cyclopterus lumpus*). Arch. Virol. 163, 679-685. https://doi.org/10.1007/s00705-017-3643-3

Småge, S.B., Frisch, K., Brevik, Ø.J., Watanabe, K., Nylund, A., 2016. First isolation, identification and characterisation of *Tenacibaculum maritimum* in Norway, isolated from diseased farmed sea lice cleaner fish *Cyclopterus lumpus* L. Aquaculture. 464, 178-184. https://doi.org/https://doi.org/10.1016/j.aquaculture.2016.06.030

Solbakken, M.H., Torresen, O.K., Nederbragt, A.J., Seppola, M., Gregers, T.F., Jakobsen, K.S., Jentoft, S., 2016. Evolutionary redesign of the Atlantic cod (*Gadus morhua* L.) Toll-like receptor repertoire by gene losses and expansions. Sci. Rep. 6, 25211. https://doi.org/10.1038/srep25211

Soleto, I., Fischer, U., Tafalla, C., Granja, A.G., 2018. Identification of a potential common ancestor for mammalian cross-presenting dendritic dells in teleost respiratory surfaces. Front. Immunol. 9, 59. https://doi.org/10.3389/fimmu.2018.00059

Spits, H., Cupedo, T., 2012. Innate Lymphoid Cells: Emerging Insights in Development, Lineage Relationships, and Function. Annu. Rev. Immunol. 30(1): 647-75. https://doi.org/10.1146/annurev-immunol-020711-075053.

Stebbins, G.L., 1971. Chromosomal evolution in higher plants. Chromosomal evolution in higher plants.

Stein, C., Caccamo, M., Laird, G., Leptin, M., 2007. Conservation and divergence of gene families encoding components of innate immune response systems in zebrafish. Genome Biol. 8, R251. https://doi.org/10.1186/gb-2007-8-11-r251

Su, J., Yang, C., Xiong, F., Wang, Y., Zhu, Z., 2009. Toll-like receptor 4 signaling pathway can be triggered by grass carp reovirus and *Aeromonas hydrophila* infection in rare minnow *Gobiocypris rarus*. Fish Shellfish Immunol. 27, 33-39. https://doi.org/https://doi.org/10.1016/j.fsi.2009.02.016

Sudhagar, A., Kumar, G., El-Matbouli, M., 2018. Transcriptome analysis based on RNA-Seq in understanding pathogenic mechanisms of diseases and the immune system of fish: a comprehensive review. Int. J. Mol. Sci. 19 https://doi.org/10.3390/ijms19010245

Sullivan, C., Charette, J., Catchen, J., Lage, C.R., Giasson, G., Postlethwait, J.H., Millard, P.J., Kim, C.H., 2009. The gene history of zebrafish tlr4a and tlr4b is predictive of their divergent functions. J. Immunol. 183, 5896-5908. https://doi.org/10.4049/jimmunol.0803285

Sullivan, C., Postlethwait, J.H., Lage, C.R., Millard, P.J., Kim, C.H., 2007. Evidence for evolving Toll-IL-1 receptor-containing adaptor molecule function in vertebrates. J. Immunol. 178, 4517-4527. https://doi.org/10.4049/jimmunol.178.7.4517

Sunyer, J.O., Tort, L., 1995. Natural hemolytic and bactericidal activities of sea bream *Sparus aurata* serum are effected by the alternative complement pathway. Vet. Immunol. Immunopathol. 45, 333-345. https://doi.org/10.1016/0165-2427(94)05430-z

Tacchi, L., Musharrafieh, R., Larragoite, E.T., Crossey, K., Erhardt, E.B., Martin, S.a.M., Lapatra, S.E., Salinas, I., 2014. Nasal immunity is an ancient arm of the mucosal immune system of vertebrates. Nature Comm. 5, 5205. https://doi.org/10.1038/ncomms6205

Tafalla, C., et al., (2013). Adjuvants and immunostimulants in fish vaccines: current knowledge and future perspectives. Fish Shellfish Immunol. 35(6): 1740-1750. http://doi.org/10.1016/j.fsi.2013.02.029

Taechavasonyoo, A., Hirono, I., Kondo, H., 2013. The immune-adjuvant effect of Japanese flounder *Paralichthys olivaceus* IL-1beta. Dev. Comp. Immunol. 41, 564-568. https://doi.org/10.1016/j.dci.2013.07.003

Takano, T., Hwang, S.D., Kondo, H., Hirono, I., Aoki, T., Sano, M., 2010. Evidence of molecular toll-like receptor mechanisms in teleosts. Fish Pathol. 45, 1-16.

Takano, T., Kondo, H., Hirono, I., Saito-Taki, T., Endo, M., Aoki, T., 2006. Identification and characterization of a myeloid differentiation factor 88 (MyD88) cDNA and gene in Japanese flounder, *Paralichthys olivaceus*. Dev. Comp. Immunol. 30, 807-816. https://doi.org/10.1016/j.dci.2005.11.003

Takeuchi, O., Akira, S., 2010. Pattern recognition receptors and inflammation. Cell. 140, 805-820. https://doi.org/https://doi.org/10.1016/j.cell.2010.01.022

Tanaka, T., Narazaki, M., Kishimoto, T., 2014. IL-6 in inflammation, immunity, and disease. Cold Spring Harb Perspect Biol. 6, a016295. https://doi.org/10.1101/cshperspect.a016295

Thornberry, N.A., Bull, H.G., Calaycay, J.R., Chapman, K.T., Howard, A.D., Kostura, M.J., Miller, D.K., Molineaux, S.M., Weidner, J.R., Aunins, J., Et Al., 1992. A novel heterodimeric cysteine protease is required for interleukin-1 beta processing in monocytes. Nature. 356, 768-774. https://doi.org/10.1038/356768a0

Thornberry, N.A., Lazebnik, Y., 1998. Caspases: enemies within. Science. 281, 1312-1316. https://doi.org/10.1126/science.281.5381.1312

Ting, J.P.Y., Lovering, R.C., Alnemri, E.S., Bertin, J., Boss, J.M., Davis, B.K., Flavell, R.A., Girardin, S.E., Godzik, A., Harton, J.A., Hoffman, H.M., Hugot, J.-P., Inohara, N., Mackenzie, A., Maltais, L.J., Nunez, G., Ogura, Y., Otten, L.A., Philpott, D., Reed, J.C., Reith, W., Schreiber, S., Steimle, V., Ward, P.A., 2008. The NLR gene family: a standard nomenclature. Immunity. 28, 285-287. https://doi.org/https://doi.org/10.1016/j.immuni.2008.02.005

Tsujita, T., Tsukada, H., Nakao, M., Oshiumi, H., Matsumoto, M., Seya, T., 2004. Sensing bacterial flagellin by membrane and soluble orthologs of toll-like receptor 5 in rainbow trout (*Onchorhynchus mykiss*). J. Biol. Chem. 279, 48588-48597. https://doi.org/10.1074/jbc.M407634200

Uehara, A., Sugawara, Y., Kurata, S., Fujimoto, Y., Fukase, K., Kusumoto, S., Satta, Y., Sasano, T., Sugawara, S., Takada, H., 2005. Chemically synthesized pathogen-associated molecular patterns increase the expression of peptidoglycan recognition

proteins via toll-like receptors, NOD1 and NOD2 in human oral epithelial cells. Cell. Microbiol. 7, 675-686. https://doi.org/10.1111/j.1462-5822.2004.00500.x

Uyeno, T., Smith, G.R., 1972. Tetraploid origin of the karyotype of catostomid fishes. Science. 175, 644-646. https://doi.org/10.1126/science.175.4022.644

Van Der Aa, L.M., Chadzinska, M., Tijhaar, E., Boudinot, P., Verburg-Van Kemenade, B.M., 2010. CXCL8 chemokines in teleost fish: two lineages with distinct expression profiles during early phases of inflammation. PLoS One. 5, e12384. https://doi.org/10.1371/journal.pone.0012384

Van Der Sar, A.M., Stockhammer, O.W., Van Der Laan, C., Spaink, H.P., Bitter, W., Meijer, A.H., 2006. MyD88 innate immune function in a zebrafish embryo infection model. Infect. Immun. 74, 2436-2441. https://doi.org/10.1128/iai.74.4.2436-2441.2006

Varela, M., Dios, S., Novoa, B., Figueras, A., 2012. Characterisation, expression and ontogeny of interleukin-6 and its receptors in zebrafish (*Danio rerio*). Dev. Comp. Immunol. 37, 97-106. https://doi.org/10.1016/j.dci.2011.11.004

Veerdonk, F.V.D., Netea, M., 2013. New insights in the immunobiology of IL-1 family members. Front. Immunol. 4, 167.

Vojtech, L.N., Scharping, N., Woodson, J.C., Hansen, J.D., 2012. Roles of inflammatory caspases during processing of zebrafish interleukin-1beta in *Francisella noatunensis* infection. Infect. Immun. 80, 2878-2885. https://doi.org/10.1128/iai.00543-12

Vollmer, W., Blanot, D., De Pedro, M.A., 2008. Peptidoglycan structure and architecture. FEMS Microbiol. Rev. 32, 149-167. https://doi.org/10.1111/j.1574-6976.2007.00094.x

Walde, C., Gulla, S., Hansen, H., Mjølnerød, E., Bornø, G., 2019. The health of cleaner fish (In norwegian), Fish health report 2018, 119-125, The Norwegian Veterinary Institute.

Walport, M.J., 2001. Complement. New Engl J Med. 344, 1058-1066. https://doi.org/10.1056/nejm200104053441406

Wang, J., Zhang, Z., Liu, J., Li, F., Chang, F., Fu, H., Zhao, J., Yin, D., 2015a. Structural characterization and evolutionary analysis of fish-specific TLR27. Fish Shellfish Immunol. 45, 940-945. https://doi.org/10.1016/j.fsi.2015.06.017

Wang, J.T., Li, J.T., Zhang, X.F., Sun, X.W., 2012. Transcriptome analysis reveals the time of the fourth round of genome duplication in common carp (*Cyprinus carpio*). BMC Genomics. 13, 96. https://doi.org/10.1186/1471-2164-13-96

Wang, K., Mu, Y., Qian, T., Ao, J., Chen, X., 2013. Molecular characterization and expression analysis of toll-like receptor 1 from large yellow croaker (*Pseudosciaena crocea*). Fish Shellfish Immunol. 35, 2046-2050. https://doi.org/https://doi.org/10.1016/j.fsi.2013.10.022

Wang, T., Bird, S., Koussounadis, A., Holland, J.W., Carrington, A., Zou, J., Secombes, C.J., 2009. Identification of a novel IL-1 cytokine family member in teleost fish. J. Immunol. 183, 962-974. https://doi.org/10.4049/jimmunol.0802953

Wang, T., Jiang, Y., Wang, A., Husain, M., Xu, Q., Secombes, C.J., 2015b. Identification of the salmonid IL-17A/F1a/b, IL-17A/F2b, IL-17A/F3 and IL-17N genes and analysis of their expression following in vitro stimulation and infection. Immunogenetics. 67, 395-412. https://doi.org/10.1007/s00251-015-0838-1

Wang, T., Martin, S.A., Secombes, C.J., 2010. Two interleukin-17C-like genes exist in rainbow trout *Oncorhynchus mykiss* that are differentially expressed and modulated. Dev. Comp. Immunol. 34, 491-500. https://doi.org/10.1016/j.dci.2009.11.011

Wang, T., Secombes, C.J., 2009. Identification and expression analysis of two fish-specific IL-6 cytokine family members, the ciliary neurotrophic factor (CNTF)-like and M17

genes, in rainbow trout *Oncorhynchus mykiss*. Mol. Immunol. 46, 2290-2298. https://doi.org/10.1016/j.molimm.2009.04.003

Wang, X., Li, C., Thongda, W., Luo, Y., Beck, B., Peatman, E., 2014. Characterization and mucosal responses of interleukin 17 family ligand and receptor genes in channel catfish *Ictalurus punctatus*. Fish Shellfish Immunol. 38, 47-55. https://doi.org/10.1016/j.fsi.2014.02.020

Wang, Y., Bi, X., Chu, Q., Xu, T., 2016a. Discovery of toll-like receptor 13 exists in the teleost fish: Miiuy croaker (Perciformes, Sciaenidae). Dev. Comp. Immunol. 61, 25-33. https://doi.org/https://doi.org/10.1016/j.dci.2016.03.005

Wang, Y., Li, J., Han, J., Shu, C., Xu, T., 2016b. Identification and characteristic analysis of TLR28: A novel member of the TLR1 family in teleost. Dev. Comp. Immunol. 62, 102-107. https://doi.org/10.1016/j.dci.2016.05.001

Wang, Y., Xu, G., Han, J., Xu, T., 2016c. miR-200a-3p regulates TLR1 expression in bacterial challenged miiuy croaker. Dev. Comp. Immunol. 63, 181-186. https://doi.org/https://doi.org/10.1016/j.dci.2016.06.004

Wei, X., Li, B., Wu, L., Yin, X., Zhong, X., Li, Y., Wang, Y., Guo, Z., Ye, J., 2018. Interleukin-6 gets involved in response to bacterial infection and promotes antibody production in Nile tilapia (*Oreochromis niloticus*). Dev. Comp. Immunol. 89, 141-151. https://doi.org/10.1016/j.dci.2018.08.012

Wei, Y.C., Pan, T.S., Chang, M.X., Huang, B., Xu, Z., Luo, T.R., Nie, P., 2011. Cloning and expression of toll-like receptors 1 and 2 from a teleost fish, the orange-spotted grouper *Epinephelus coioides*. Vet. Immunol. Immunopathol. 141, 173-182. https://doi.org/https://doi.org/10.1016/j.vetimm.2011.02.016

Whittaker, B.A., Consuegra, S., Garcia De Leaniz, C., 2018. Genetic and phenotypic differentiation of lumpfish (*Cyclopterus lumpus*) across the North Atlantic: implications for conservation and aquaculture. PeerJ. 6, e5974-e5974. https://doi.org/10.7717/peerj.5974

Whyte, S.K., 2007. The innate immune response of finfish – A review of current knowledge. Fish Shellfish Immunol. 23, 1127-1151. https://doi.org/https://doi.org/10.1016/j.fsi.2007.06.005

Wiklund, T., Dalsgaard, I., 1998. Occurrence and significance of atypical *Aeromonas salmonicida* in non-salmonid and salmonid fish species: a review. Dis. Aquat. Organ. 32, 49-69. https://doi.org/10.3354/dao032049

Wolf, A.J., Underhill, D.M., 2018. Peptidoglycan recognition by the innate immune system. Nat. Rev. Immunol. 18, 243. https://doi.org/10.1038/nri.2017.136

Wu, X.Y., Xiang, L.X., Huang, L., Jin, Y., Shao, J.Z., 2008. Characterization, expression and evolution analysis of toll-like receptor 1 gene in pufferfish (*Tetraodon nigroviridis*). Int. J. Immunogenet. 35, 215-225. https://doi.org/10.1111/j.1744-313X.2008.00759.x

Wu, Y., Zhou, Y., Cao, Z., Sun, Y., Chen, Y., Xiang, Y., Wang, L., Zhang, S., Guo, W., 2019. Comparative analysis of the expression patterns of IL-1beta, IL-11, and IL-34 in golden pompano (*Trachinotus ovatus*) following different pathogens challenge. Fish Shellfish Immunol. 93, 863-870. https://doi.org/10.1016/j.fsi.2019.08.018

Xie, J., Belosevic, M., 2015. Functional characterization of receptor-interacting serine/threonine kinase 2 (RIP2) of the goldfish (*Carassius auratus* L.). Dev. Comp. Immunol. 48, 76-85. https://doi.org/https://doi.org/10.1016/j.dci.2014.09.006

Xie, J., Hodgkinson, J.W., Katzenback, B.A., Kovacevic, N., Belosevic, M., 2013. Characterization of three Nod-like receptors and their role in antimicrobial responses

of goldfish (Carassius auratus L.) macrophages to *Aeromonas salmonicida* and *Mycobacterium marinum*. Dev. Comp. Immunol. 39, 180-187. https://doi.org/https://doi.org/10.1016/j.dci.2012.11.005

Xu, T., Wang, Y., Li, J., Shu, C., Han, J., Chu, Q., 2016a. Comparative genomic evidence for duplication of TLR1 subfamily and miiuy croaker TLR1 perceives LPS stimulation via MyD88 and TIRAP. Fish Shellfish Immunol. 56, 336-348.

Xu, X.-Y., Shen, Y.-B., Fu, J.-J., Yu, H.-Y., Huang, W.-J., Lu, L.-Q., Li, J.-L., 2016b. MicroRNA-induced negative regulation of TLR-5 in grass carp, *Ctenopharyngodon idella*. Sci. Rep. 6, 18595. https://doi.org/10.1038/srep18595

Yang, Q., Sun, Y., Su, X., Li, T., Xu, T., 2016. Characterization of six IL-17 family genes in miiuy croaker and evolution analysis of vertebrate IL-17 family. Fish Shellfish Immunol. 49, 243-251. https://doi.org/10.1016/j.fsi.2015.12.031

Yao, F., Yang, X., Wang, X., Wei, H., Zhang, A., Zhou, H., 2015. Molecular and functional characterization of an IL-1beta receptor antagonist in grass carp (*Ctenopharyngodon idella*). Dev. Comp. Immunol. 49, 207-216. https://doi.org/10.1016/j.dci.2014.11.016

Yin, Z., Kwang, J., 2000. Carp interleukin-1 beta in the role of an immuno-adjuvant. Fish Shellfish Immunol. 10, 375-378. https://doi.org/10.1006/fsim.1999.0241

Zhang, A., Chen, D., Wei, H., Du, L., Zhao, T., Wang, X., Zhou, H., 2012. Functional characterization of TNF-alpha in grass carp head kidney leukocytes: induction and involvement in the regulation of NF-kappaB signaling. Fish Shellfish Immunol. 33, 1123-1132. https://doi.org/10.1016/j.fsi.2012.08.029

Zhang, G., Meredith, T.C., Kahne, D., 2013a. On the essentiality of lipopolysaccharide to Gram-negative bacteria. Curr Opin Microbiol. 16, 779-785. https://doi.org/10.1016/j.mib.2013.09.007

Zhang, J., Kong, X., Zhou, C., Li, L., Nie, G., Li, X., 2014. Toll-like receptor recognition of bacteria in fish: ligand specificity and signal pathways. Fish Shellfish Immunol. 41, 380-388. https://doi.org/10.1016/j.fsi.2014.09.022

Zhang, J., Liu, S., Rajendran, K.V., Sun, L., Zhang, Y., Sun, F., Kucuktas, H., Liu, H., Liu, Z., 2013b. Pathogen recognition receptors in channel catfish: III Phylogeny and expression analysis of toll-like receptors. Dev. Comp. Immunol. 40, 185-194. https://doi.org/https://doi.org/10.1016/j.dci.2013.01.009

Zhang, L., Gao, Z., Yu, L., Zhang, B., Wang, J., Zhou, J., 2018. Nucleotide-binding and oligomerization domain (NOD)-like receptors in teleost fish: Current knowledge and future perspectives. J. Fish Dis. 41, 1317-1330. https://doi.org/10.1111/jfd.12841

Zhang, L., Wang, C.C., 2014. Inflammatory response of macrophages in infection. Hepatobiliary Pancreat. Dis. Int. 13, 138-152.

Zhang, S., Cui, P., 2014. Complement system in zebrafish. Dev. Comp. Immunol. 46, 3-10. https://doi.org/10.1016/j.dci.2014.01.010

Zhang, X., Wang, S., Chen, S., Chen, Y., Liu, Y., Shao, C., Wang, Q., Lu, Y., Gong, G., Ding, S., Sha, Z., 2015. Transcriptome analysis revealed changes of multiple genes involved in immunity in *Cynoglossus semilaevis* during *Vibrio anguillarum* infection. Fish Shellfish Immunol. 43, 209-218. https://doi.org/https://doi.org/10.1016/j.fsi.2014.11.018

Zhang, X., Zhang, Y., Zheng, X., Kuang, Y., Zhao, Z., Zhao, L., Li, C., Jiang, L., Cao, D., Lu, C., Xu, P., Sun, X., 2013c. A consensus linkage map provides insights on genome character and evolution in common carp (*Cyprinus carpio* L.). Mar Biotechnol (NY). 15, 275-312. https://doi.org/10.1007/s10126-012-9485-9

Zhao, C., Fu, M., Wang, C., Jiao, Z., Qiu, L., 2016. RNA-Seq analysis of immune-relevant genes in *Lateolabrax japonicus* during *Vibrio anguillarum* infection. Fish Shellfish Immunol. 52, 57-64. https://doi.org/https://doi.org/10.1016/j.fsi.2016.02.032

Zhu, L.Y., Nie, L., Zhu, G., Xiang, L.X., Shao, J.Z., 2013. Advances in research of fish immune-relevant genes: a comparative overview of innate and adaptive immunity in teleosts. Dev. Comp. Immunol. 39, 39-62. https://doi.org/10.1016/j.dci.2012.04.001

Zou, J., Bird, S., Truckle, J., Bols, N., Horne, M., Secombes, C., 2004. Identification and expression analysis of an IL-18 homologue and its alternatively spliced form in rainbow trout (*Oncorhynchus mykiss*). Eur. J. Biochem. 271, 1913-1923. https://doi.org/10.1111/j.1432-1033.2004.04101.x

Zou, J., Peddie, S., Scapigliati, G., Zhang, Y., Bols, N.C., Ellis, A.E., Secombes, C.J., 2003a. Functional characterisation of the recombinant tumor necrosis factors in rainbow trout, *Oncorhynchus mykiss*. Dev. Comp. Immunol. 27, 813-822. https://doi.org/https://doi.org/10.1016/S0145-305X(03)00077-6

Zou, J., Secombes, C.J., 2016. The function of fish cytokines. Biology. 5 https://doi.org/10.3390/biology5020023

Zou, J., Secombes, C.J., Long, S., Miller, N., Clem, L.W., Chinchar, V.G., 2003b. Molecular identification and expression analysis of tumor necrosis factor in channel catfish (*Ictalurus punctatus*). Dev. Comp. Immunol. 27, 845-858. https://doi.org/https://doi.org/10.1016/S0145-305X(03)00085-5

Zou, J., Wang, T., Hirono, I., Aoki, T., Inagawa, H., Honda, T., Soma, G.I., Ototake, M., Nakanishi, T., Ellis, A.E., Secombes, C.J., 2002. Differential expression of two tumor necrosis factor genes in rainbow trout, *Oncorhynchus mykiss*. Dev. Comp. Immunol. 26, 161-172. https://doi.org/https://doi.org/10.1016/S0145-305X(01)00058-1

Zou, P.F., Chang, M.X., Li, Y., Xue, N.N., Li, J.H., Chen, S.N., Nie, P., 2016. NOD2 in zebrafish functions in antibacterial and also antiviral responses via NF-κB, and also MDA5, RIG-I and MAVS. Fish Shellfish Immunol. 55, 173-185. https://doi.org/https://doi.org/10.1016/j.fsi.2016.05.031

Øvergard, A.C., Nepstad, I., Nerland, A.H., Patel, S., 2012. Characterisation and expression analysis of the Atlantic halibut (*Hippoglossus hippoglossus* L.) cytokines: IL-1beta, IL-6, IL-11, IL-12beta and IFNgamma. Mol. Biol. Rep. 39, 2201-2213. https://doi.org/10.1007/s11033-011-0969-x

Øverland, H.S., Pettersen, E.F., Rønneseth, A., Wergeland, H.I., 2010. Phagocytosis by B-cells and neutrophils in Atlantic salmon (*Salmo salar* L.) and Atlantic cod (*Gadus morhua* L.). Fish Shellfish Immunol. 28, 193-204. https://doi.org/https://doi.org/10.1016/j.fsi.2009.10.021

I

SCIENTIFIC REPORTS

OPEN

Transcriptome-wide mapping of signaling pathways and early immune responses in lumpfish leukocytes upon *in vitro* bacterial exposure

Received: 19 October 2017
Accepted: 16 March 2018
Published online: 27 March 2018

Håvard Ø. Eggestøl[1], Harald S. Lunde[1], Anita Rønneseth[1], David Fredman[2], Kjell Petersen[2], Charitra K. Mishra[2], Tomasz Furmanek[2], Duncan J. Colquhoun[1,3], Heidrun I. Wergeland[1] & Gyri T. Haugland[1]

We performed RNA sequencing, identified components of the immune system and mapped early immune responses of lumpfish (*Cyclopterus lumpus*) leukocytes following *in vitro* exposure to the pathogenic bacterium *Vibrio anguillarum* O1. This is the first characterization of immune molecules in lumpfish at the gene level. *In silico* analyses revealed that genes encoding proteins involved in pathogen recognition, cell signaling and cytokines in mammals and teleosts are conserved in lumpfish. Unique molecules were also identified. Pathogen recognition components include 13 TLRs, several NLRs and complement factors. Transcriptome-wide analyses of immune responses 6 and 24 hours post bacterial exposure revealed differential expression of 9033 and 15225 genes, respectively. These included TLR5S, IL-1β, IL-8, IL-6, TNFα, IL-17A/F3, IL-17C and several components of the complement system. The data generated will be valuable for comparative studies and make an important basis for further functional analyses of immune and pathogenicity mechanisms. Such knowledge is also important for design of immunoprophylactic measures in lumpfish, a species of fish now farmed intensively for use as cleaner-fish in Atlantic salmon (*Salmo salar*) aquaculture.

Teleost fish, the earliest evolutionary group with an immune system exerting both innate and adaptive immunity, is highly diverse, consisting of more than 32 000 species. The innate immune system in fish, like mammals, consists of a variety of molecules and immune cells that provide the first line of defense against microbial attack through recognition of potential pathogens. Recognition and degradation of microbes followed by induction of inflammation are essential processes for clearance of microbes and onset of adaptive immune responses. The innate immune system is triggered by complement factors, antibodies and/ or pattern recognition receptor (PRR) recognition of pathogen-associated molecular patterns (PAMPs) such as nucleic acid structures unique to bacteria and virus (CpG DNA, dsRNA), diverse proteins (flagellin), lipopolysaccharide, lipoteichoic acid and peptidoglycan.

While recognition of potential pathogens by complement factors and antibodies lead to increased phagocytic activity of host cells and degradation of invading microbes, recognition of PAMPs by PRRs ensures, through production of cytokines, that the elicited immune response is tailored to the invading pathogen. The major families of PRRs are the Toll-like receptors (TLRs), Nucleotide binding and oligomerization domain (NOD)- like receptors (NLRs), retinoic acid inducible gene I (RIG-I)- like receptors (RLRs), C-type lectin receptors (CLRs) and absent in melanoma 2 (AIM2)- like receptors (ALRs)[1,2]. In teleost fish, the TLRs is the most studied family of the PRRs and an enormous diversity has been identified in teleosts (reviewed in[1,3,4]). This diversity is suggested to be driven by adaptation to specific environments and host-intrinsic factors[3]. Teleosts possess orthologues to mammalian TLRs, with the exception of TLR6 and TLR10 which have not yet been identified in fish and the existence of a

[1]Department of Biology, University of Bergen, Bergen, Norway. [2]Computational biology unit, Department of Informatics, University of Bergen, Bergen, Norway. [3]Norwegian Veterinary Institute, Oslo, Norway. Correspondence and requests for materials should be addressed to G.T.H. (email: Gyri.Haugland@bio.uib.no)

functional TLR4 in fish is subject to discussion. In addition, several TLRs are unique for the teleosteii i.e. TLR18-23, 25–28[4,5]. Fish and amphibians also have a soluble version of TLR5, termed TLR5S[6] in addition to a membrane bound TLR5 (TLR5M). TLR5 has been identified in all investigated teleost species, with the exception of the *Paracanthopterygii*[7]. From functional studies and functional inference based on sequence homology indicate that fish TLR1, TLR2, TLR5, TLR5S, TLR9, TLR21, TLR28[5,8,9] recognize bacterial ligands. In general, ligand binding initiates downstream cell signaling mediated via adapter proteins MyD88, MAL, TRIF, TRAM and SARM[10], resulting in activation of transcription factors NFκB, IRF3/7, CREB and AP1, finally resulting in production of proinflammatory cytokines like TNFα, IL-12 IL-1β and IL-18 and/or interferons. There is currently little information regarding the downstream cell signaling pathways following activation of the fish-specific TLRs.

As for the TLR family, some NLRs also play a role in antimicrobial immune responses. NOD-like receptors are described in several species of fish including, but not exclusively, zebrafish, channel catfish, Japanese pufferfish and rainbow trout[11–16]. The NLRs described in fish are NOD1, NOD2, NLRC3, NLRC5, NLRCX and NLRC. Importantly, NLRC in fish is different from mammalian NLRC and as many as several hundred genes have been reported from one species[13]. There are, however, few functional studies of NLRs in fish and there is currently little knowledge of the downstream signaling after activation and how the receptors and signaling are regulated.

The transcriptome of lumpfish, as a representative for *Cyclopteridae* is highly valuable as this group is poorly characterized genetically and no reference genome or immune gene sequences are available in public databases. Also, it is not clear whether they belong to the suborder *Cottoidei* within the order *Perciformes*[17] or within the order *Scorpaniformes*[18]. In addition to being interesting for comparative studies, mapping of the lumpfish immune system is important for basic immunological studies and for the rational design of immunoprophylactic measures for this species. In recent years, there has been a tremendous increase in the production of farmed lumpfish in Europe and Canada[19], due to its ability to eat lice from farmed Atlantic salmon (*Salmo salar* L.)[20]. In Norway alone, the number of lumpfish farmed increased from 0.4 million in 2012 to approximately 15 million in 2016[21].

Large scale farmed lumpfish mortalities due to bacterial disease are reported[22] and development of vaccines protecting against the most common pathogens is ongoing[23]. The level of total immunoglobulin M (IgM) in lumpfish sera is lower compared to species like salmon[24,25], but it has been shown that lumpfish has the ability to produce specific antibodies upon immunization[25] and that vaccination has an effect[26]. Previous studies have also shown that innate immune functions like phagocytosis and respiratory burst are efficient in lumpfish[27] and that IgM^+ B-cells display phagocytic ability[25]. More knowledge about the underlying mechanisms of the immune system of lumpfish at the individual gene level and their immune responses upon bacterial infection is required as this will form the basis for development of immunoprophylactic measures and immune stimulation. Therefore, to characterize the immediate and early induced innate response in this species, lumpfish leukocytes were exposed to the bacterium *Vibrio anguillarum* serotype O1, a known fish pathogen, for 6 and 24 hours, and RNA sequencing was performed followed by *de novo* transcriptome assembly and differential gene expression analysis.

Results

Illumina sequencing and de novo transcriptome assembly. Sequencing of RNA isolated from non-treated head kidney leukocytes (HKL) and HKL exposed to *Vibrio* resulted in 516 million reads. Reads of low quality, low complexity, containing adapter sequence, matching ribosomal or mitochondrial sequences were discarded. The resulting transcriptome consisted of 433 million assembled bases in 346,430 transcripts from 221,659 trinity genes. The median transcript length was 585 bases, mean length 1.25 kb and N50 of 2.5 kb. The RNA sequencing reads after trimming, the differential gene expression data and the assembled transcriptome are submitted to Array Express under accession number E-MTAB-6388.

Annotation of predicted proteins and functional annotation of the Trinity genes. Genes within the assembled transcriptome were annotated using Trinotate. Putative gene functions were identified by Gene ontology (GO) analysis. Of the 221,659 Trinity genes 37,895 were assigned minimum one Gene ontology (GO)-term. GO mapping resulted in 62 GO categories presented in Fig. 1. The GO-terms containing the highest number of genes were binding (23786), organelle (20995), cellular process (25011) and biological regulation (19578). The GO-term 'immune system processes' contained 2490 Trinity genes and includes genes involved in the development or function of the immune system e.g. immune response, leukocyte activation, activation of immune response and immune effector process (Fig. 1b). The most abundant immune system process was "innate immune response" which included 956 genes.

Global differential gene expression (DEG) analysis upon bacterial exposure. To gain more information of the early induced innate immune responses in lumpfish, leukocytes were subjected to differential gene expression (DEG) analysis 6 and 24 hrs post bacterial exposure. Principal component analysis (Fig. 2a) revealed a major difference between exposed and non-exposed samples at both time points. This can be seen in the heat map following hierarchical clustering of the DEGs (Fig. 2b). The immune response was stronger and more extensive at 24 hours post exposure (hpe) (Fig. 2c) compared to 6 hpe (Fig. 2d). The number of statistically (p-value < 0.05) and biologically (p-value < 0.05 and fold change >4) significantly regulated genes was higher at 24 hpe compared to 6 hpe (Fig. 2e). The number of genes that were statistically differentially expressed at 24 hpe was 15225 genes (44%) compared to 9033 genes (26%) 6 hpe (Fig. 2e and f). As shown in the Venn diagram, 5389 (16%) genes were significantly differentially expressed at both time points (Fig. 2f).

GO enrichment analysis showed that among the upregulated transcripts at 24 hpe, GO-terms with lowest p-value were; response to stimulus (log10 p-value −19.7), defense response (log10 p-value −18.9), response to stress (log10 p-value −17.1), positive regulation of immune system processes (log10 p-value −16.6) and regulation of intracellular signal transduction (log10 p-value −16.1) (Fig. 3a). Among downregulated transcripts at 24 hpe, the GO-terms with lowest p-value were; "small molecule biosynthetic process" (log10 p-value −11.3),

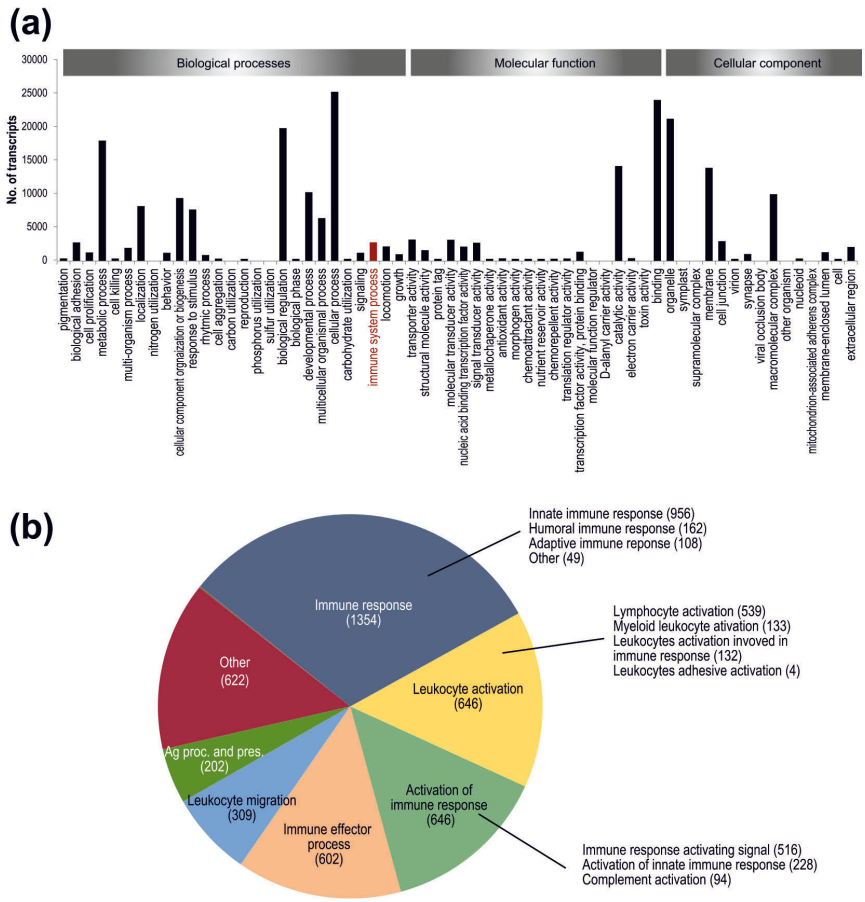

Figure 1. Gene Ontology (GO) analyses of annotated genes in the lumpfish transcriptome. (**a**) The annotated genes were divided into the main GO-terms Biological processes, Molecular function and cellular components and further divided into subcategories. (**b**) Pie chart of the GO term distribution among the annotated genes in the lumpfish transcriptome in the GO term immune system process.

"single-organism process" (log10 p-value −9.8), "response to interleukin 4" (log10 p-value −7.9), "cytokinesis" (log10 p-value −7.3) and "defense response"(log10 p-value −7.0) (Fig. 3b). For upregulated transcripts at 6 hpe, the GO-terms with lowest p-values were; "response to lipopolysaccharide" (log10 p-value −10.4), "inflammatory response" (log10 p-value −9.7), "response to biotic stimulus" (log10 p-value −9.4), "regulation of intracellular signal transduction" (log10 p-value −8.1) and "response to external stimulus" (log10 p-value −8.1) (Fig. 3c). For downregulated transcripts at 6 hpe, the p-values were not as low as at 24 hpe (Fig. 3d).

Analyses of KEGG pathways belonging to the immune system were performed (Table 1). Several genes were identified for each KEGG ID, and thus, the number of lumpfish genes in DEG was higher than the number of KEGG IDs in DEG (Table 1). Further, the 20 most significantly regulated genes at 24 and 6 hpe (based on p-values) were identified (Supplemental Table 1). At 24 hours, the most significantly regulated gene was TLR5S, followed by interleukin 8 (IL-8) which is also known as neutrophil chemotactic factor and an uncharacterized protein. From blast search the uncharacterized protein likely belongs to the interleukin 6 (IL-6) family, most closely related to Leukemia Inhibitory factor (LIF) (Supplemental Table 1).

The 50 most up- and down-regulated genes at each time point were identified (Supplemental Tables 2–5). Many of the upregulated immune genes at 24 hpe were cytokines such as IL-1β, IL-6, IL-8 and IL-17, or belonged to either the complement cascade (CFH, CFB, C8a, C8b and C5) or the TLR pathway (TLR5s). Other studies have shown that members of the NLR family of pattern recognition receptors also recognize bacterial antigens and regulation of genes encoding these receptors was investigated. The response of NOD1, NOD2 and other NLRs

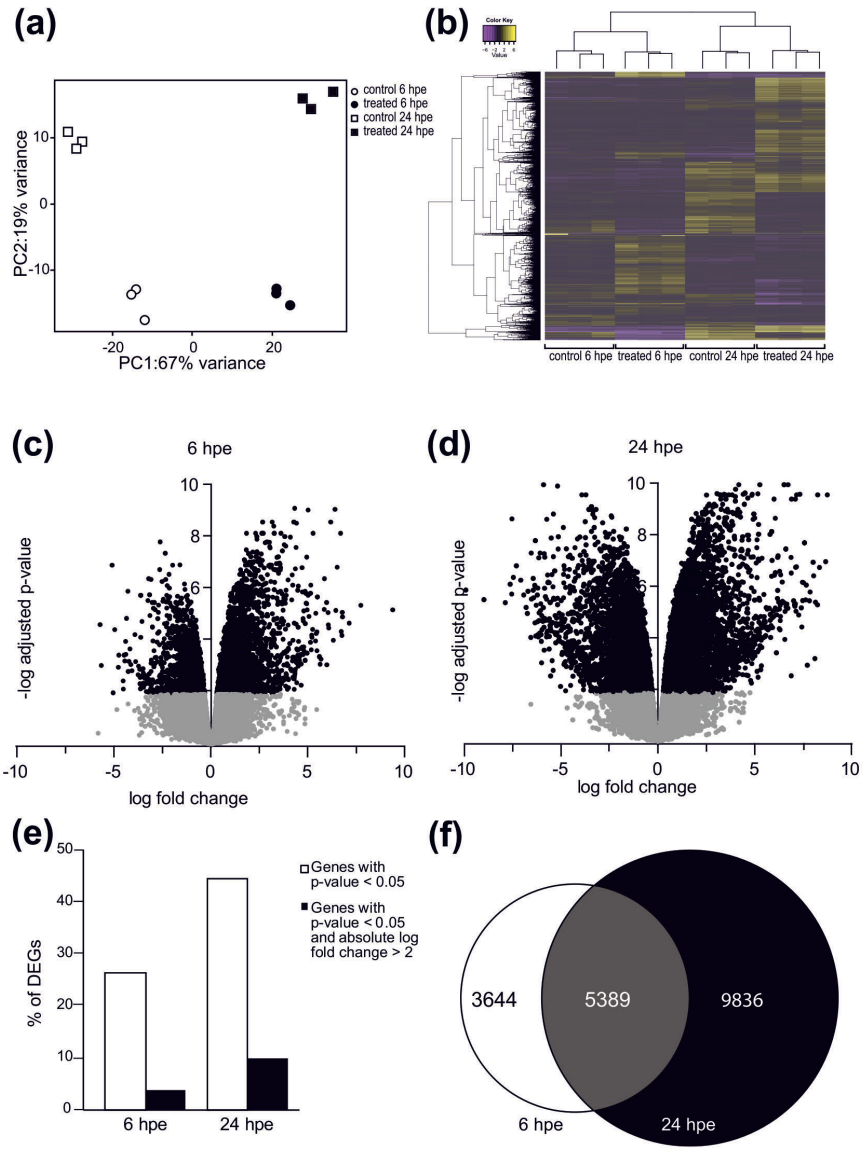

Figure 2. Differential gene expression (DEG) analysis 6 hrs and 24 hrs post bacterial exposure. (**a**) Principal component analysis. PC1 is time and PC2 is treatment. White circles are non-treated controls 6 hpe, black circles are treated samples 6 hpe, white squares are non-treated controls 24 hpe and black circles are treated samples 24 hpe. (**b**) Heatmap of transcriptome profiling data of non-treated controls versus bacterial exposed samples 6 and 24 hpe. (**c**) Volcano plot of DEGs 6 hpe. Significantly regulated genes are shown as black dots. Non-significantly regulated genes are shown as grey dots. (**d**) Volcano plot of DEGs 24 hpe. Significantly regulated genes are shown as black dots. Non-significantly regulated genes are shown as grey dots. (**e**) Percentage of DEGs that were significantly regulated (p-value < 0.05) at 6 hpe and 24 hpe are shown in black bars. Percentages of statistically significantly regulated (p-value < 0.05) DEG with an absolute log fold change >2. (**f**) Venn diagram showing the number of DEGs at the different time point. Only those that were statistically significant are shown. White = 6 hpe, black = 24 hpe and dark grey = genes that were significantly regulated at both time points.

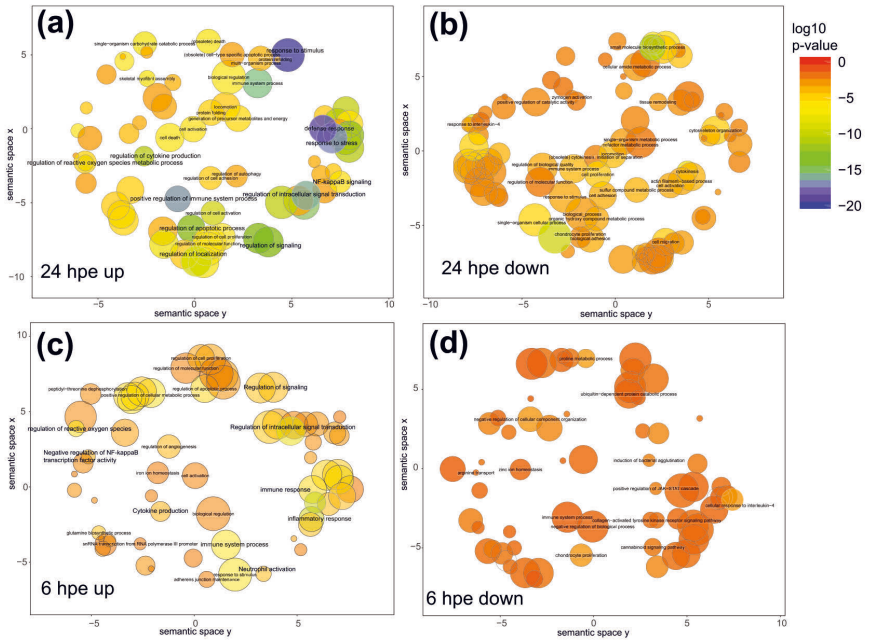

Figure 3. Enrich GO-analysis 6 and 24 hours post bacterial exposure. Semantic plots of up and down regulated (log fold change >2 and p-value < 0.001) enriched GO terms at 6 and 24 hours post exposure, generated through REVIGO. Enrichment p-value is plotted in red, through yellow and green to blue; where blue is the smallest p-value and red the biggest p-value. Size of the circles correlates to the semantic size of the GO terms.

were very weakly regulated or non-responsive (data not shown). Since the most regulated genes belonged to the complement cascade and TLR signaling, these pathways were investigated at the individual gene level.

Complement cascade. The complement system can be activated by three biochemical pathways; the classical complement pathway, the alternative complement pathway and the lectin pathway. Many genes encoding complement proteins were identified in lumpfish (shown in Fig. 4a and listed in Table 1), including components such as C3, C6 and C7. The differential gene expression analyses showed that upon exposure to *V. anguillarum* complement factor responses were higher at 24 hpe compared to 6hpe (Fig. 4b). The most upregulated genes were the regulatory factors complement factor H (CFH) and complement factor B (CFB), complement components C5, vitronectin (VTN) and complement factors 8a and 8b. The latter are subunits of the membrane attack complex responsible for lysis of microbes. Also, complement factor P, which is a positive regulator for C3 and C5 convertases was also upregulated at 24 hpe. The most highly downregulated genes were complement C1q subcomponent subunit A (C1QA) and subunit C (C1QC) which are part of the classical pathway, in addition to complement components C2 (Fig. 4b). Lumpfish genes verified (by blast) as belonging to the complement cascade are given in Supplemental Table 6.

TLRs and TLR signaling. The TLR family of signaling PRRs plays an essential role in the early innate immune response against both bacteria and viruses. In the lumpfish transcriptome, 13 TLRs were identified; TLR1, 2, 3, 5 M, 5 S, 7, 8, 9, 13, 14, 21, 22 and 28 (Fig. 5, Table 2). Activation of TLRs initiates intracellular signaling resulting in production of inflammatory cytokines and co-stimulatory molecules important in early pro-inflammatory responses, chemotaxis and activation of T cells. Many of the molecules involved in the TLR signaling pathway were identified in lumpfish (Fig. 6), including the adaptor proteins MyD88, TRIF (also known as TICAM1) and TIRAP (also known as MAL). TICAM 2 (TRAM) was not identified. All transcripts listed in Table 2 were annotated following a BLAST search against NCBI's non-redundant database, for which the hit with highest total score is included in the Table. MyD88, TRIF and TIRAP were full-length, but for SARM only two short non-overlapping fragments were identified.

Members of the tumor necrosis factor receptor (TNFR)-associated factor (TRAF) family are important mediators of various signaling pathways, including the TLR signaling pathway. The TRAFs identified in lumpfish were TRAF2-6. Further, IRAK1, 3 and 4 were identified. Also, main components of the two downstream signaling routes, NF-κB signaling; NEMO, IKKA, IKKB, IKB, p50 and p65 and MAPK-signaling pathways; MKKs, ERK, JNK, p38, c-fos Jun were identified (Fig. 6 and Table 2). Components that were not mapped through batch mapping in the KEGG pathway database were searched for manually in the lumpfish transcriptome using synonyms

KEGG pathway	KEGG ID	No. of KEGG IDs in reference pathway	No. of KEGG IDs in DEG	No. of lumpfish genes in DEG	6 hpe		24 hpe	
					Upreg. genes	Downreg. genes	Upreg. genes	Downreg. genes
Hematopoietic cell lineage	K04640	80	35	70	10	19	36	18
Complement and coagulation cascades	K04610	78	33	57	10	15	23	18
Platelet activation	K04611	89	73	223	43	34	69	74
Toll-like receptor signaling pathway	K04620	76	54	124	28	41	29	56
Toll and Imd signaling pathway	K04624	47	21	74	12	20	13	29
NOD-like receptor signaling pathway	K04621	136	92	239	48	66	46	105
RIG-I-like receptor signaling pathway	K04622	53	39	96	22	31	22	45
Cytosolic DNA-sensing pathway	K04623	51	29	44	11	15	13	17
Natural killer cell mediated cytotoxicity	K04650	81	41	146	33	31	52	45
Antigen processing and presentation	K04612	41	27	71	5	21	18	19
T cell receptor signaling pathway	K04660	85	59	206	36	48	55	86
Th1 and Th2 cell differentiation	K04658	67	44	116	19	42	36	43
B cell receptor signaling pathway	K04662	57	42	122	30	31	32	54
Fc epsilon RI signaling pathway	K04664	47	31	98	25	20	27	38
Fc gamma R-mediated phagocytosis	K04666	58	48	211	41	46	73	71
Leukocyte transendothelial migration	K04670	75	58	171	27	47	59	57
Intestinal immune network for IgA prod.	K04672	37	14	32	6	9	12	7
Chemokine signaling pathway	K04062	153	83	259	53	64	73	102

Table 1. Overview of identified lumpfish genes in immune system pathways*. *KEGG pathways in category 5.1.

or sequences from related species. Activation of NF-κB induces production of the pro-inflammatory cytokines, while activation of MAPK has impact on several immune functions including proliferation, differentiation, survival, apoptosis, chemoattraction and production of inflammatory mediators. TNFα, IL-1β, IL-6 and IL-12 were among the cytokines identified in the lumpfish transcriptome. Also, the chemokines IL-8 and MIP1 β (macrophage inflammatory protein, also known as CCL4) were identified. The genes most upregulated at both 6 hpe and 24 hpe included proinflammatory cytokines (IL-1β, IL-6, TNFα), a homologue of IL-17 (IL-17C1), IL-8 and the soluble form of TLR5 (TLR5S) (Supplemental Tables 2 and 4). Members of the NFκβ pathway, but not the MAPK pathway were upregulated (Fig. 6b). Interestingly, another IL-17 homologue (IL17A/F3) was one of the most down-regulated immune genes at 24 hpe (Supplemental Table 3). TLR13 (logFC −5.21) and TLR2 (logFC −2.74) were down-regulated at 24 hpe and 6 hpe, respectively.

Discussion

The innate immune system is of major importance for fish as aquatic vertebrates are generally more heavily exposed to pathogens than terrestrial vertebrates and the adaptive defenses are less efficient in aquatic vertebrates. The major humoral components essential for innate defense in vertebrates are antibodies and the complement system which tag and kill invading microbes and promote inflammatory responses[28]. Furthermore, conserved structures on potential pathogenic organisms such as flagellin are recognized by the host's PRRs and trigger intracellular signaling pathways which results in production of inflammatory cytokines and initiation of adaptive immune responses tailored to the infecting agent.

To obtain information of the gene repertoire in lumpfish head kidney leukocytes and early anti-bacterial immune responses, leukocytes were exposed to the pathogenic bacterium *V.anguillarum* O1 and RNA was isolated 6 and 24 hpe. *De novo* transcriptome assembly and global differential gene expression revealed that the complement system and TLR signaling pathway were the most highly upregulated innate immune processes. Another family of PRRs involved in bacterial recognition is NLRs. *In vivo* challenge experiments in other teleost species have shown that expression of NOD1 and NOD2 is upregulated in several tissues after bacterial infection[29,30]. Lumpfish NLRs were either non-regulated or weakly downregulated. The functions and roles of NLRs in lumpfish upon bacterial infection should, therefore, be further explored. The ligand specificity of the expanded fish-specific NLRC family reported from several fish species is currently unknown and it will be exciting to elucidate their role and importance in fish immunity.

Several components of the complement cascade were identified within the lumpfish transcriptome as shown in Fig. 4. Most genes belonging to the classical and alternative pathway were identified, but not the mannose-binding lectin (MBL) involved in the lectin pathway. Of the complement receptors, CR1, CR3, CR4 and C5AR1 were identified, but not complement receptor CR2. This is similar to other fish species (summarized in[28]). In humans it is known that the complement system cross-talks with other pathways and modulates adaptive immune responses[31,32]. Information regarding cross-talk between pathways and involvement of B and T cells in fish are scarce, and discrimination of some components, in example C1r/C1s, requires functional analyses at the protein level.

In the lumpfish transcriptome, TLR1, −2, −3, −5 (membrane-bound and soluble), −7, −8, −9, −13, −14, −21, −22 and −28 were identified. All lumpfish TLR transcripts, with the exception of TLR22, encoded full-length sequences. Phylogenetic analyses (Fig. 5) show that lumpfish TLRs group together with the order

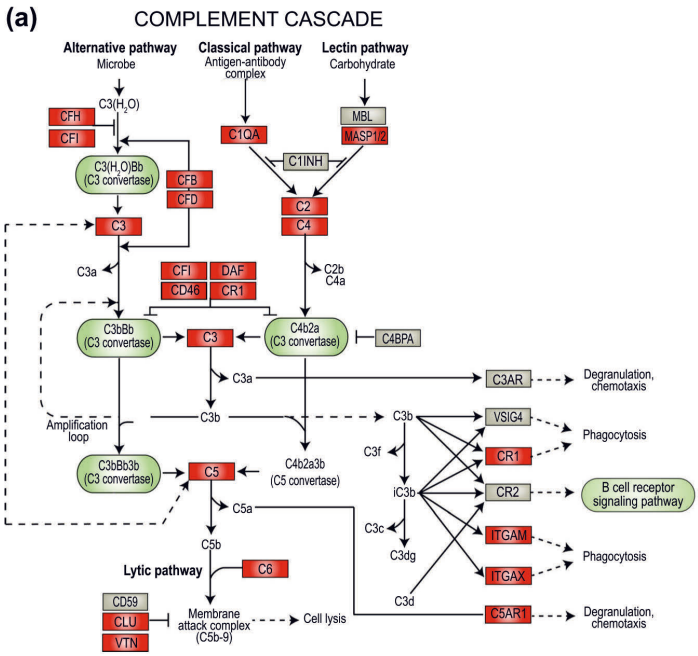

Figure 4. An overview of the complement cascade in lumpfish (**a**) The molecules in the complement cascade identified in lumpfish are shown with red boxes, those that are not yet identified are shown in grey. The figure is modified from KEGG map04610[63]. (**b**) Differential gene expression analyses of members of the complement cascade 6 hrs and 24 hrs post exposure (hpe). Only those that are statistically significant regulated (p-value < 0.05) are shown. The color gradient represents highly upregulated (dark brown) to highly downregulated (dark blue) genes. The exact values are given for each gene. The genes are sorted by fold regulation at 24 hpe.

Perciformes, most closely with orange-spotted grouper (*Epinephelus coioides*). While some teleost TLRs are orthologues of mammalian counterparts, equivalents to human TLR6 and TLR10 have not yet been found in fish. Many of the TLRs in fish are not present in mammals. These include TLR5S, −14, −18, −19, −20, −21, −22, −23, −24, −25, −26, −27 and −28, and of these, some are fish-specific (TLR18-23, 25–28). The soluble variant of TLR5 is widely present in teleosts and has been identified in several species such as rainbow trout[33], catfish[34,35], gilthead seabream[36], flounder[37] and orange spotted grouper[38]. Since *V. anguillarum* is a flagellated bacterium, it was not unexpected that TLR5S was highly upregulated during early immune responses. Actually, it was the most significantly regulated gene at 24 hpe and among the most significantly upregulated genes at 6 hpe (Supplemental Table 1). In lumpfish leukocytes, TLR5M was not significantly regulated either at 6 hpe or 24 hpe. This is similar to the situation in rainbow trout where expression of TLR5S, but not TLR5M, was induced by *V.anguillarum* and purified recombinant *V.anguillarum* flagellin[33]. Upregulation of TLR5S transcripts during bacterial exposure is reported in other fish species[35,36]. Humans do not have TLR5S, but the innate immune response to flagellin mediated by human TLR5M is similar to that of teleost fishes[39]. Interestingly, a study of Tsujita and colleagues showed that TLR5S from rainbow trout amplifies the human TLR5 response via physical binding to flagellin[40]. How TLR5S initiates downstream signaling is not yet known, but a hypothetical mechanism has been suggested in which TLR5S binds circulating flagellin and transports it to TLR5M. In this way danger signals are amplified in a similar manner to LPS recognition by human TLR4 and the soluble factors LBP and CD14[41]. It is known that activation of TLR5 in mammals results in activation of NF-kappa-B and production of proinflammatory cytokines. The DEG analyses of lumpfish leukocytes indicated that the NF-κB signaling pathway, not the MAPK signaling pathway, was activated, as inhibitors of both nuclear factor kappa-B kinase alpha (NFKBIA, also known as IκBα and IKKA) and NFκB were highly upregulated. DEG analysis showed that IKKA was upregulated at both 6 hpe and 24 hpe, while NFkB was most highly upregulated at 24 hpe. Gene expressions of transcripts involved in the MAPK signaling pathway, such as MP2K3 and MP2K6, showed little change (after 6 hpe) or were downregulated (after 24 hpe). It will be interesting to investigate whether regulation of the TLR5 signaling pathway is conserved, or whether teleosts have developed another regulatory mechanism than mammals.

The cytokines that were most differentially regulated were IL-1β, IL-8, IL-6, TNF-α, one of the IL-17A/F3 and IL17C1. All were highly upregulated, except IL17A/F3 which was barely differentially regulated at 6 hpe and highly downregulated at 24 hpe. IL-1β has diverse functions including being a major regulator of inflammatory

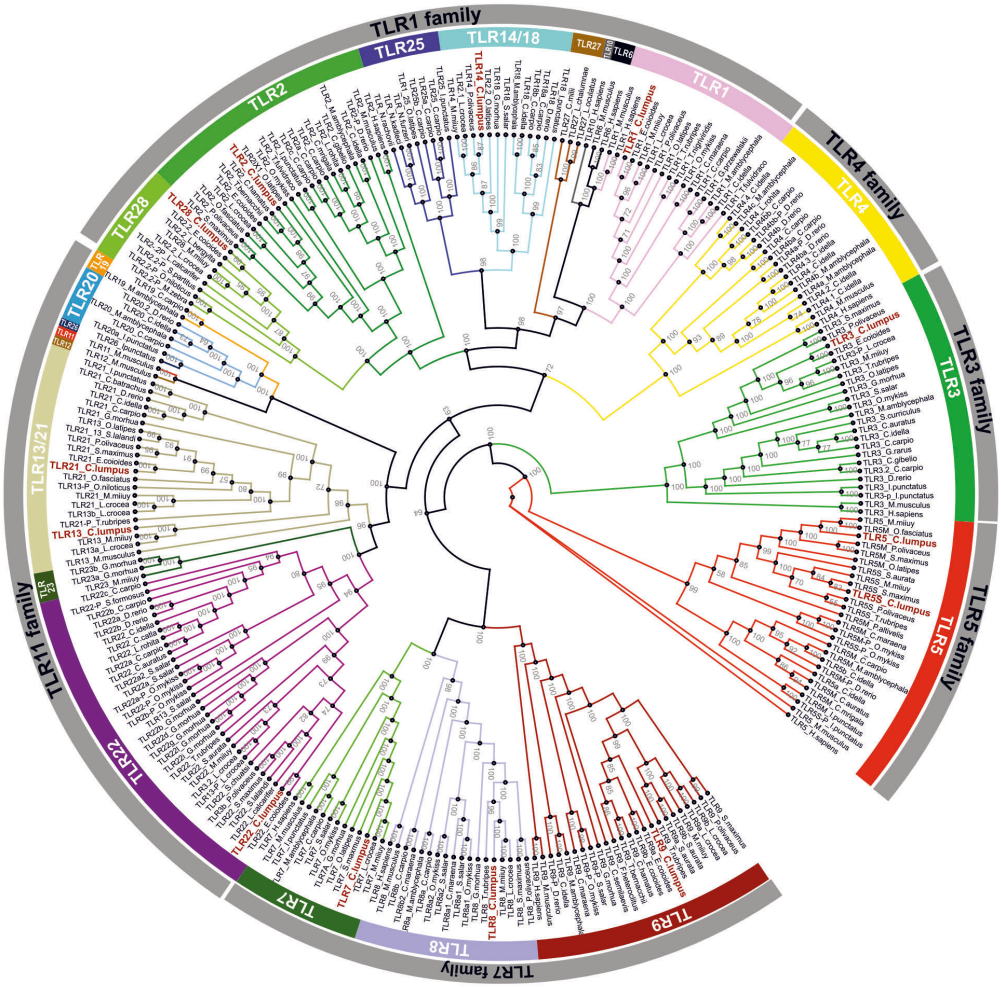

Figure 5. Phylogenetic tree of TLRs. Full-length TLR sequences in public databases were included in the phylogenetic analyses. The TLRs are divided into families and subtypes. The TLRs identified in the lumpfish transcriptome is shown by red letters, including TLR1, −2, −3, −5 (membrane-bound and soluble), −7, −8, −9, −13, −14, −21, −22 and −28. The full-length name of the species and accession numbers of the sequences in the Figure is given in Supplemental Tables 7 and 8.

processes. It is a chemoattractant for fish leukocytes, it stimulates chemokine production in cells following infection and is known to induce expression of TNF-α. Further, IL-1β also modulates differentiation of T helper 17 cells (Th17) and expression of IL-17 family members[42,43]. Th17 cells are a subset of activated CD4 + T cells and are known to play a role in mucosal immunity and tissue inflammation. In mice, in addition to IL-1β, IL-6 and the transcription factor RORγt, transforming growth factor β1 (TGF-β1) is required for differentiation of Th17 cells. In humans, RORγt and Th17 polarization was induced by IL-1β and enhanced by IL-6, but suppressed by TGF-β1 and IL-12[44]. Although the exact regulation of Th17 cells in fish is not yet understood, it is widely accepted that fish have Th17 cells as all the major components of mammalian Th17 cell development are present in fish, including Th17 driver cytokines (IL-6, TGF- β1, IL-21 and IL-23), transcription factor (RORγ) and effector cytokines (IL17A/F, IL-22)[42,45]. Since some of the Th17 components in fish have multiple isoforms, it has been suggested that an even more complex Th17 type responses and regulation are present in fish compared to mammals[45].

The most highly regulated cytokine in lumpfish leukocytes following bacterial exposure belonged to the IL-17 family. IL-17A/F3 was highly downregulated 24 hpe, while one of the IL-17C proteins, IL-17C1, was the most upregulated transcript, at 6 hpe and 24 hpe. IL-17 cytokines are central mediators of inflammatory responses and have been functionally characterized in jawed and jawless vertebrates and in invertebrates such as molluscs,

Gene-ID	Name	KEGG ID	Top BLAST hit			
			Description	E-value	Species	Accession number
Pathogen recognition receptors						
TR65368|c1_g16	TLR1	K05398	Toll-like receptor 1	0	*Notothenia coriiceps*	XP_010775742.1
TR39054|c0_g2	TLR2	K10159	Toll-like receptor 2	0	*Oplegnathus fasciatus*	AFZ81806
TR25266|c0_g1	TLR3	K05401	Toll-like receptor 3	0	*Epinephelus coioides*	AEX01718
TR27403|c4_g1	TLR5M	K10168	toll-like receptor 5 membrane bound	0	*Oplegnathus fasciatus*	AQT26515
TR41627|c0_g1	TLR5S	K10168	PRED: toll-like receptor 5	0	*Notothenia coriiceps*	XP_010788825
TR35019|c2_g2	TLR7	K05404	PRED: toll-like receptor 7	0	*Notothenia coriiceps*	XP_010771824
TR35019|c2_g2	TLR8	K10170	PRED: toll-like receptor 7	0	*Notothenia coriiceps*	XP_010771824
TR74757|c0_g1	TLR9	K10161	Toll-like receptor 9B	0	*Epinephelus lanceolatus*	AJW66344
TR14442|c0_g1	TLR13	—	Toll-like receptor 13	0	*Lates calcarifer*	XP_018537347
TR7225|c0_g1	TLR14	—	Toll-like receptor 14	0	*Larimichtys crocea*	XP_010735448
TR59969|c0_g1	TLR21	—	Toll-like receptor 21	0	*Epinephelus lanceolatus*	AJW66342
TR32827|c0_g1	TLR22	—	Toll-like receptor 22	0	*Epinephelus coioides*	AGA84053
TR50658|c1_g2	TLR28	—	Toll-like receptor 2–2	0	*Epinephelus coioides*	AIS23533
TR22563|c0_g3	LBP/BPI	K05399	Bactericidal permeability-increasing protein	0	*Oplegnathus fasciatus*	BAM21037
Intracellular signaling molecules						
TR12120|c0_g1	AKT1	K04456	Unnamed protein product, partial	3.22E-34	*Tetraodon nigroviridis*	CAG10696
TR31506|c0_g2	CASP8	K04398	Caspase-8-like	1.82E-76	*Labrus bergylta*	XP_020505530
TR59882|c1_g1	FADD	K02373	FAS-associated death domain protein-like	1.75E-36	*Lates calcarifer*	XP_018527571
TR33817|c1_g1	IKKa	K04467	Inhibitor of NFk-B kinase subunit alpha-like	1.04E-39	*Labrus bergylta*	XP_020482453
TR52372|c4_g2 TR71389|c0_g1	IKKb IKKb	K07209 K04734	IKKbeta IKKbeta alpha	4.37E-161 7.36E-128	*Siniperca chuatsi* *Epinephelus coioides*	ADK47101 AKN59236
TR27462|c0_g1	IKKE	K07211	PRED: inhibitor of NFkappa-B kinase E	0	*Lates calcarifer*	XP_018542264
TR109249|c0_g1	IRAK1	K04730	Interleukin-1 receptor activated kinase 1	3.98E-34	*Siniperca chuatsi*	ACN64942
TR49087|c0_g1	IRAK4	K04733	Interleukin-1 receptor-associated kinase 4	9.13E-35	*Trachidermus fasciatus*	AFH88675
TR16021|c2_g2	IRF3	K05411	Interferon regulatory factor 3	1.07E-57	*Dicentrarchus labrax*	CBN81356
TR53466|c0_g1	IRF5	K09446	Interferon regulatory factor 5	4.38E-108	*Oplegnathus fasciatus*	AFZ93894
TR129437|c0_g1	IRF7	K09447	Interferon regulatory factor 7	0	*Epinephelus coioides*	ADA57613
TR80028|c2_g8	M3K7	K04427	PRED: MAP3K7_isoform X1	1.66E-05	*Stegastes partitus*	XP_008299748
TR129360|c0_g1	MAP3K8	K04415	PRED: MAP3K8	6.49E-47	*Notothenia coriiceps*	XP_010779244
TR10769|c1_g13	MK01	K04371	PRED: MAPkinase 1	4.28E-09	*Pundamilia nyererei*	XP_005730582
TR83303|c0_g1	MK08	K04440	MAPkinase 8B	1.15E-88	*Larimichthys crocea*	KKF10666
TR8373|c0_g1	MP2K1	K04368	Dual specificity MAPkinase kinase 1-like	2.94E-18	*Oncorhynchus kisutch*	XP_020331169
TR24160|c1_g1	MP2K2	K04369	PRED: dual specificity MAP kinase kinase 2	1.30E-70	*Stegastes partitus*	XP_008275716
TR24160|c1_g1	MP2K3	K04430	Dual specificity MAP kinase kinase 4	0	*Larimichthys crocea*	KKF28316
TR10914|c0_g1	MP2K4	K04430	Dual specificity MAP kinase kinase 4-like	0	*Monopterus albus*	XP_020467371
TR11220|c0_g1	MP2K6	K04433	PRED: dual specificity MAP kinase kinase 6-like	0	*Larimichthys crocea*	XP_019116692
TR69482|c2_g12	MP2K7	K04431	PRED: dual specificity MAP kinase kinase 7	3.15E-21	*Notothenia coriiceps*	XP_010776556
TR70736|c1_g1	MyD88	K04729	Myeloid differentiation factor 88	1.14E-163	*Oplegnathus fasciatus*	AQT26514
TR52312|c2_g4	NEMO	K07210	NFkappa-B kinase essential modifier 2	0	*Epinephelus coioides*	AKN59239
TR19609|c0_g2	NFKB1	K02580	PRED: nuclear factor NF-kappa-B p100 subunit	5.71E-13	*Astyanax mexicanus*	XP_007258829

Continued

Gene-ID	Name	KEGG ID	Top BLAST hit			
			Description	E-value	Species	Accession number
TR105668|c0_g1	P3KCA	K00922	PRED: PIK3 catalytic subunit gamma isoform-like	8.43E-70	*Notothenia coriiceps*	XP_010777483
TR102536|c0_g1	P85A	K02649	PIK3 regulatory subunit alpha-like, partial	7.35E-62	*Labrus bergylta*	XP_020514940
TR34005|c0_g1	PMK1	K04441	PRED: MAPkinase 11-like isoform X2	2.63E-45	*Salmo salar*	XP_014008787
TR106991|c0_g1	RAC1	K04392	Unnamed protein product, partial	3.34E-11	*Mus musculus*	BAC38272
TR24024|c0_g3	RIPK1	K02861	PRED: serine/threonine-protein kinase Nek8-like	2.01E-118	*Lates calcarifer*	XP_018555349
TR18988|c3_g2	STAT1	K11220	PRED: STAT1-alpha/beta isoform X4	1.81E-109	*Larimichthys crocea*	XP_010745394
TR101399|c0_g1	TAB1	K04403	PRED: TAB1	7.18E-18	*Paralichthys olivaceus*	XP_019958222
TR18998|c1_g2	TAB2	K04404	TAK1-binding protein 2	0	*Epinephelus coioides*	AKN59234
TR86999|c0_g2	TBK1	K05410	PRED: serine/threonine-protein kinase TBK1	1.05E-09	*Larimichthys crocea*	XP_019126730
TR33723|c0_g2	TF65	K04735	p65 transcription factor	5.99E-93	*Siniperca chuatsi*	ABW84004
TR1276|c0_g1	TICAM1	K05842	PRED: TIR domain-containing adapter molecule 1	0	*Larimichthys crocea*	XP_010736595
TR53144|c0_g1	TIRAP	K05403	PRED: TIRAP	2.27E-77	*Lates calcarifer*	XP_018554351
TR15941|c0_g6	TOLLIP	K05402	PRED: toll-interacting protein-like, partial	4.72E-57	*Notothenia coriiceps*	XP_010779552
TR27389|c3_g2	TRAF3	K03174	PRED: TNF receptor-associated factor 3	1.0E-148	*Lutjanus sanguineus*	APJ7747
TR49717|c0_g1	TRAF6	K03175	TNF receptor-associated factor 6, partial	4.00E-174	*Gasterosteus aculeatus*	ABJ15863
Extracellular signaling molecules						
TR102531|c0_g1	CC-like	K14625	PRED: C-C motif chemokine 17-like	9.90E-60	*Notothenia coriiceps*	XP_010784217
TR155750|c0_g1	CC-like	K05512	PRED: C-C motif chemokine 26-like	3.34E-26	*Cynoglossus semilaevis*	XP_008332070
TR71759|c1_g1	CC-like	K12964	PRED: monocyte chemotactic protein 1B-like	1.28E-34	*Oreochromis niloticus*	XP_019216385
TR1773|c1_g1	CC-like	K12964	C-C motif chemokine 14 precursor	1.22E-28	*Anoplopoma fimbria*	ACQ58688
TR4483|c0_g1	CC-like	K16595	PRED: C-C motif chemokine 4 homolog	1.53E-27	*Lates calcarifer*	XP_018542538
TR26820|c0_g1	CC-like	K12964	C-C motif chemokine 3 precursor	3.86E-48	*Anoplopoma fimbria*	ACQ58878
TR135792|c0_g1	CXC-like	K05416	C-X-C motif chemokine 10 precursor	3.00E-56	*Anoplopoma fimbria*	ACQ59055
TR88050|c0_g1	CXC-like	NA	PRED: C-X-C motif chemokine 11-like	1.12E-41	*Stegastes partitus*	XP_008294834
TR19700|c0_g1	CXC-like	K05506	Interleukin-8 like protein	5.53E-39	*Oplegnathus fasciatus*	BAM99883
TR25958|c0_g1	IL12A	K05406	PRED: uncharacterized protein LOC109630380	7.13E-71	*Paralichthys olivaceus*	XP_019944119
TR24065|c1_g2	IL12B	K05425	Interleukin 12p40	1.80E-54	*Oplegnathus fasciatus*	AIB04025
TR14360|c3_g2	IL1B	K04519	Interleukin-1 beta	8.98E-138	*Trachidermus fasciatus*	AFH88676
TR87818|c0_g1	IL6	K05405	Interleukin-6	3.04E-94	*Epinephelus coioides*	AFE62919
TR13890|c0_g3	IL8	K10030	Interleukin-8 precursor	2.95E-33	*Anoplopoma fimbria*	ACQ57874
TR50382|c0_g2	JUN	K04448	PRED: transcription factor AP-1-like	4.29E-62	*Notothenia coriiceps*	XP_010795740
TR29865|c0_g1	nIL1F1	NA	New interleukin-1 family member, partial	5.58E-57	*Gasterosteus aculeatus*	CCV66728
TR69814|c0_g2	TNFa	K03156	Tumor necrosis factor alpha	4.71E-120	*Oplegnathus fasciatus*	ACM69339
TR42972|c0_g1	FOS	K04379	PRED: proto-oncogene c-Fos-like isoform X1	9.07E-89	*Larimichthys crocea*	XP_010733543
TR37206|c0_g2	CD40	K03160	TNF receptor superfam member 5-like isoform X2	1.51E-26	*Labrus bergylta*	XP_020504780
TR1121|c5_g7	CD80/86	K05413	PRED: CD276 antigen-like	1.53E-78	*Lates calcarifer*	XP_018537117

Table 2. Verified TLRs in lumpfish and genes in TLR signaling pathway. *Pathway: ko04620.

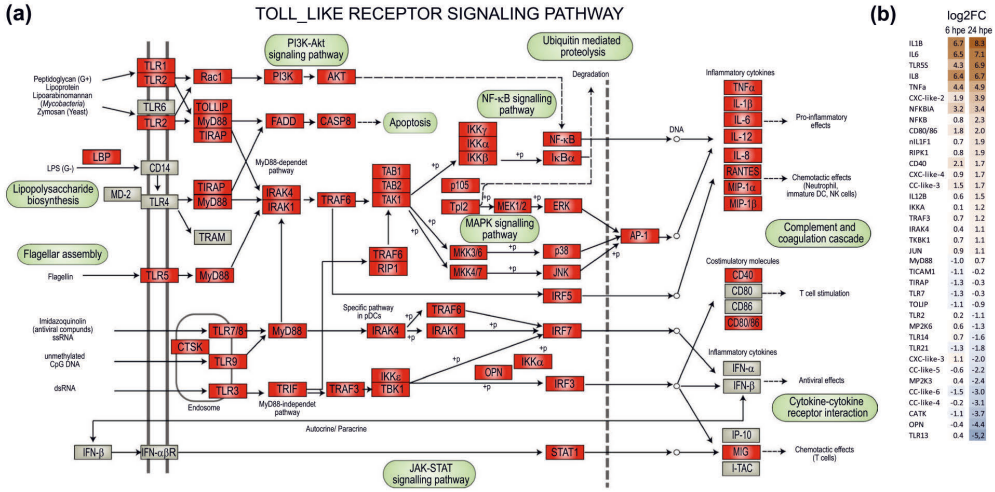

Figure 6. An overview of the Toll-like receptor signaling pathway in lumpfish (**a**) The molecules in the TLR signaling pathway identified in lumpfish are shown with red boxes, those that are not yet identified are shown in grey. The figure is modified from KEGG map04620[63]. (**b**) Differential gene expression analyses of members of the TLR pathway 6 hrs and 24 hrs post exposure (hpe). Only those that are statistically significant regulated (p-value < 0.05) are shown. The color gradient represents highly upregulated (dark brown) to highly downregulated (dark blue) genes. The exact values are given for each gene. The genes are sorted by fold regulation at 24 hpe.

nematodes and arthropods[46–51]. Teleost fish have several IL-17 molecules including IL17A and IL-17F, termed IL17A/F1-3, IL-17B, IL17C and IL17D[42,52]. One IL-17 originally termed IL-17N[53] is likely to represent a fourth IL-17A/F member. An IL17E equivalent has thus far not been identified in fish, but two IL17C genes have been reported in rainbow trout[48] and Japanese pufferfish[54]. Two IL-17C-like genes were also identified in lumpfish, but no IL-17E. It has been suggested that an ancient IL17C may have diverged into IL-17C and IL-17E in early mammals, whereas two IL-17C genes can be present in teleosts. Although relatively few studies have reported bioactivity of the IL-17 molecules in fish, studies from different species suggest that while IL-17 proteins play a role in innate immunity, they may have evolved specialized roles. Recombinant IL-17A/F from grass carp and trout can increase expression of proinflammatory cytokines in isolated head kidney leukocytes[55] and splenocytes[56], respectively, while IL-17D in grass carp increase expression of IL-1β, IL-8, TNF-α but not IL-6 (reviewed in[42]).

In summary, our transcriptomic data suggests that the complement system recognized the pathogenic bacterium and activated subunits of the membrane attack complex (MAC) which is a prerequisite for formation of a MAC complex at the surface of the microbe and thereafter cell lysis. Also, complement receptors involved in phagocytosis, degranulation and chemotaxis were upregulated which is related to the need to recruit host phagocytic cells for clearance of the bacterium. One of the most highly upregulated genes was IL-8 which is a chemokine involved in chemotaxis and attraction of neutrophilic cells. Another immediate innate immune response essential to prevent infection is promotion of inflammation and production of cytokines that ensures the immune response is tailored to the infecting microbe. Our study suggests that TLR5S recognized flagellin and triggered downstream signaling through the NFk-B signaling pathway resulting in production of pro-inflammatory cytokines (IL-1β, TNFα, IL-6, IL-12 and IL-17). IL-12 is needed for activation of naïve T-cells and IL-17 induces production of chemokines. Our transcriptomic data adds valuable information about the immune responses in lumpfish during the early stages of a bacterial infection. Functional analysis of the proteins involved in the signaling pathways is however necessary to gain further insight into the role of specific proteins and the interaction between them.

The lumpfish transcriptome presented provides a valuable base for comparative and phylogenetic analyses as lumpfish is a representative of the infraorder *Cottoidea*, a phylogenetic group which is poorly characterized immunologically and genetically. Furthermore, the lumpfish is a novel and a very important species for aquaculture since it is used for sea-lice control in salmon farming[19]. Although production of lumpfish has generally been successful, there have been challenges with large-scale mortality due to bacterial infections[22]. Vaccines against selected lumpfish pathogens are in use[23,26], but more knowledge of the lumpfish immune system and responses to bacterial exposure at the individual gene level is important. Thus, the identification of immune genes, transcriptome–wide mapping of signaling pathways and early immune responses presented here are highly valuable as they provide a basis for development of more efficient immune prophylactic measures and provide important tools for evaluation of the efficacy of different prophylactic measures.

Materials and Methods

The work in the presented manuscript was performed on cells isolated from dead fish. The fish were sacrificed with a sharp blow to the head which is an appropriate procedure under Norwegian law. All experiments were performed in accordance with relevant guidelines and regulations. Rearing of fish under normal, optimal conditions does not require ethical approval under Norwegian law (FOR 1996- 01- 15 no. 23)

Fish. Farmed lumpfish (*C. lumpus* L.) were provided from Fjord Forsk Sogn AS, a commercial breeder in Sogn & Fjordane County, Norway. The fish were kept in a 500 L tank at the Aquatic and Industrial Laboratory (ILAB) within the High-Technology Centre in Bergen under normal rearing conditions with a light regime 12 h light: 12 h dark. The water temperature was 8 °C, salinity 34 PSU and a minimum of 77% oxygen saturation in the outlet water. The fish were fed with the commercial dry feed Amber Neptune (1.5 mm).

Bacterial culture. *Vibrio anguillarum* serotype O1 (8752) isolated from moribund lumpfish after a disease-outbreak in 2012 in Møre & Romsdal county in Norway was cultured in tryptic soy broth containing 2% NaCl at 20 °C, 200 rpm until late log phase. The bacterium was washed once in PBS and re-suspended in L-15 + medium without antibiotics.

Isolation of leukocytes and *in vitro* bacterial exposure. Head kidney leukocytes were isolated as described previously using discontinuous Percoll gradients[27]. Both left and right kidney lobes from 15 fish were included. Cell number, viability and aggregation factor was determined using a CASY Cell Counter™ (Innovatis AG). For *in vitro* bacterial exposure, 5×10^6 cells in L-15 + medium without antibiotics were added to each well in a 24-well plate (Nunc) and mixed with the bacterium *V. anguillarum* O1 (MOI 1:10) in a total volume of 0.5 mL. In wells with non-exposed cells, medium was added instead of bacterial cells. The plates were incubated at 15 °C. After 1.5 hour, pencillin/streptomycin was added to each well and the plates were further incubated until 6 hrs and 24 hours post bacterial exposure. In order to obtain an as comprehensive transcriptome as possible, a sample with leukocytes exposed with infectious pancreatic necrosis virus for 24 hrs was also included. This sample was used for the *de novo* transcriptome assembly, but was not part of the DEG analysis. Following incubation, the plates were centrifuged for 10 min at 200 × g. The supernatants were removed and lysis buffer was added directly to the wells. The lysates were stored at −80 °C prior to RNA isolation.

Isolation of total RNA. Total RNA was isolated using GeneElute Mammalian Total RNA miniprep kit (Sigma) according to the manufacturer's instructions. Samples were treated with DNase I (Sigma) to removed traces of genomic DNA and the concentration of total RNA determined in a Nanodrop®ND-1000 UV-Vis spectrophotometer (Nanodrop Technologies). Total RNA extracts from three-five fish were pooled, in total 5 µg per pooled sample. For each time point three parallels were prepared for RNA sequencing. The pooled RNA (5 µg) was cleaned using RNA clean & concentrator-5 (zymo research) according to the manufacturer's instructions and the quality of the RNA were determined in an Agilent 2100 bioanalyzer. RNA isolated from virus infected leukocytes was kept separately. The RQI values were in the range 6.3–9.3.

Transcriptome sequencing, assembly and annotation. The Norwegian High Throughput Sequencing Centre prepared sequencing libraries using TruSeq™RNA sample Preparation kit (Illumina®) according to the manufacturer's protocol and performed paired-end strand-specific sequencing on the Illumina HiSeq platform with a 125 bp read length, resulting in a total of 516 million reads. Read quality was first assessed using FastQC, and Trinity's option for read trimming by quality was included during assembly (trimmomatic). Reads of low quality, low complexity, containing adapter sequence, matching ribosomal or mitochondrial sequences were discarded. Transcripts were assembled using Trinity v2.0.6[57] with read normalization enabled and library type specified, otherwise keeping default settings. Known contaminants (*Vibrio* and IPNV) were removed from the assembly using blast. During the analyses, other non-eukaryotic sequences were discovered and additionally removed from the expression value matrices, with a more generic contaminant removal procedure[58]. More information on all steps of the sequencing data processing is given in Supplemental methods. The resulting transcriptome consisted of 433 million assembled bases in 346,430 transcripts from 221,659 "genes". The median transcript length was 585 bases, mean length 1.25 kb and N50 of 2.5 kb. Following assembly transcripts were annotated with BLAST matches, protein domains and GO terms using the Trinotate toolkit (https://trinotate.github.io).

Bioinformatical analyses. Gene ontology mapping was performed in J-express Gene expression analysis software. Detailed information about the gene included in each category was obtained using Quick GO, which is a fast browser for Gene Ontology terms and annotation (http://www.ebi.ac.uk/QuickGO/GTerm?id=GO:0006954#term=annotation). Verification of the annotation of the transcripts was performed with BLAST search (https://blast.ncbi.nlm.nih.gov/Blast.cgi), multiple sequence alignment (MSA) using PAGAN v.0.61[51]. The phylogenetic tree was constructed from MSA by maximum likelihood with IQ-TREE 1.5.4[59] using automatic model selection[60] followed by 100,000 ultrafast bootstraps[61]. An overview of the species and accession numbers included in the phylogenetic analyses are given in Supplemental Tables 7 and 8, respectively. Pathway analyses were performed using KEGG[61–63]. KEGG pathways analysis[64] was performed by annotating the transcripts using BLAST against KO genes in KEGG, downloaded 08.02.2017. Transcripts with a BLAST score of 300 and above against KO genes in KEGG were mapped to the KEGG pathways as described in the KEGG Mapper tool. Transcript abundances for three biological replicates for treatment and control at 6 and 24 hpe were estimated using RSEM as part of the Trinity pipeline (Supplementary results of Trinity RSEM). The read count estimates were used as a basis for differential expression analysis using the Limma R-package[65]. Only genes with at least 10 reads in at least three samples were considered for differential expression analysis (34280 of 221659

assembled genes). Fold changes between groups and adjusted p-values (BH correction for multiple testing) were exported for downstream analyses. The DEG analyses were visualized in Graph-Pad prism 5. GO enrichment was calculated using GO-seq.[66] and visualized in REVIGO.

The datasets generated during the current study are available in Array Express repository.

References

1. Aoki, T., Hikima, J., Hwang, S. D. & Jung, T. S. Innate immunity of finfish: primordial conservation and function of viral RNA sensors in teleosts. *Fish Shellfish Immunol* **35**, 1689–1702 (2013).
2. Brubaker, S. W., Bonham, K. S., Zanoni, I. & Kagan, J. C. Innate immune pattern recognition: a cell biological perspective. *Annu Rev Immunol* **33**, 257–290 (2015).
3. Solbakken, M. H., Voje, K. L., Jakobsen, K. S. & Jentoft, S. Linking species habitat and past palaeoclimatic events to evolution of the teleost innate immune system. *Proc Biol Sci* **284**, 20162810 (2017).
4. Zhang, J. *et al*. Toll-like receptor recognition of bacteria in fish: ligand specificity and signal pathways. *Fish Shellfish Immunol* **41**, 380–388 (2014).
5. Wang, Y., Li, J., Han, J., Shu, C. & Xu, T. Identification and characteristic analysis of TLR28: A novel member of the TLR1 family in teleost. *Dev Comp Immunol* **62**, 102–107 (2016).
6. Roach, J. C. *et al*. The evolution of vertebrate Toll-like receptors. *Proc Natl Acad Sci USA* **102**, 9577–9582 (2005).
7. Solbakken, M. H., Rise, M. L., Jakobsen, K. S. & Jentoft, S. Successive Losses of Central Immune Genes Characterize the Gadiformes' Alternate Immunity. *Genome Biol Evol* **8**, 3508–3515 (2016).
8. Pietretti, D. & Wiegertjes, G. F. Ligand specificities of Toll-like receptors in fish: indications from infection studies. *Dev Comp Immunol* **43**, 205–222 (2014).
9. Quiniou, S. M., Boudinot, P. & Bengten, E. Comprehensive survey and genomic characterization of Toll-like receptors (TLRs) in channel catfish, *Ictalurus punctatus*: identification of novel fish TLRs. *Immunogenetics* **65**, 511–530 (2013).
10. O'Neill, L. A. & Bowie, A. G. The family of five: TIR-domain-containing adaptors in Toll-like receptor signalling. *Nat Rev Immunol* **7**, 353–364 (2007).
11. Alvarez, C. A. *et al*. Insights into the diversity of NOD-like receptors: Identification and expression analysis of NLRC3, NLRC5 and NLRX1 in rainbow trout. *Mol Immunol* **87**, 102–113 (2017).
12. Biswas, G., Bilen, S., Kono, T., Sakai, M. & Hikima, J. Inflammatory immune response by lipopolysaccharide-responsive nucleotide binding oligomerization domain (NOD)-like receptors in the Japanese pufferfish (*Takifugu rubripes*). *Dev Comp Immunol* **55**, 21–31 (2016).
13. Howe, K. *et al*. Structure and evolutionary history of a large family of NLR proteins in the zebrafish. *Open Biol* **6**, 160009 (2016).
14. Laing, K. J., Purcell, M. K., Winton, J. R. & Hansen, J. D. A genomic view of the NOD-like receptor family in teleost fish: identification of a novel NLR subfamily in zebrafish. *BMC Evol Biol* **8**, 42 (2008).
15. Rajendran, K. V. *et al*. Pathogen recognition receptors in channel catfish: I. Identification, phylogeny and expression of NOD-like receptors. *Dev Comp Immunol* **37**, 77–86 (2012).
16. Stein, C., Caccamo, M., Laird, G. & Leptin, M. Conservation and divergence of gene families encoding components of innate immune response systems in zebrafish. *Genome Biol* **8**, R251 (2007).
17. Betancur-R. R. *et al*. The tree of life and a new classification of bony fishes. *PLoS Curr* **5** ecurrents.tol.53ba26640df0ccaee75bb165c8c26288 (2013).
18. Nelson, J. S., Grande, T. C. & Wilson, M. V. H. *Fishes of the world, 5th Edition*. Order *Scorpaniformes*, 467–495 (Wiley, 2016).
19. Powell, A. *et al*. Use of lumpfish for sea-lice control in salmon farming: challenges and opportunities. *Reviews in aquaculture* https://doi.org/10.1111/raq.12194 (2017).
20. Imsland, A. K. *et al*. The use of lumpfish (*Cyclopterus lumpus* L.) to control sea lice (*Lepeophtheirus salmonis* Krøyer) infestations in intensively farmed Atlantic salmon (*Salmo salar* L.). *Aquaculture* **424-425**, 18–23 (2014).
21. Norwegian Directorate of Fisheries. Sales of farmed cleanerfish 2012-2016. http://www.fiskeridir.no/English/Aquaculture/Statistics/Cleanerfish-Lumpfish-and-Wrasse (2017).
22. Hjeltnes, B., Bornø, G., Jansen, M. D., Haukaas, A. & Walde, C. S. The Health Situation in Norwegian Aquaculture 2016 (2017).
23. Haugland, G. T., Rønneseth, A. & Wergeland, H. I. in *Cleaner Fish biology and aquaculture application* (ed Jim Treasurer) Immunology and vaccinology of lumpfish and wrasse (5m Publishing, *in print*).
24. Bilal, S., Lie, K. K., Karlsen, O. A. & Hordvik, I. Characterization of IgM in Norwegian cleaner fish (lumpfish and wrasses). *Fish Shellfish Immunol* **59**, 9–17 (2016).
25. Rønneseth, A., Ghebretnsae, D. B., Wergeland, H. I. & Haugland, G. T. Functional characterization of IgM^+ B cells and adaptive immunity in lumpfish (*Cyclopterus lumpus* L.). *Dev Comp Immunol* **52**, 132–143 (2015).
26. Rønneseth, A., Haugland, G. T., Colquhoun, D. J., Brudal, E. & Wergeland, H. I. Protection and antibody reactivity following vaccination of lumpfish (*Cyclopterus lumpus* L.) against atypical Aeromonas salmonicida. *Fish Shellfish Immunol* **64**, 383–391 (2017).
27. Haugland, G. T. *et al*. Phagocytosis and respiratory burst activity in lumpsucker (*Cyclopterus lumpus* L.) leucocytes analysed by flow cytometry. *PLoS One* **7**, e47909 (2012).
28. Nakao, M., Tsujikura, M., Ichiki, S., Vo, T. K. & Somamoto, T. The complement system in teleost fish: progress of post-homolog-hunting researches. *Dev Comp Immunol* **35**, 1296–1308 (2011).
29. Li, J., Gao, Y. & Xu, T. Comparative genomic and evolution of vertebrate NOD1 and NOD2 genes and their immune response in miiuy croaker. *Fish Shellfish Immunol* **46**, 387–397 (2015).
30. Li, M. *et al*. Expression profiles of NODs in channel catfish (*Ictalurus punctatus*) after infection with *Edwardsiella tarda*, *Aeromonas hydrophila*, *Streptococcus iniae* and channel catfish hemorrhage reovirus. *Fish Shellfish Immunol* **33**, 1033–1041 (2012).
31. Kemper, C. & Atkinson, J. P. T-cell regulation: with complements from innate immunity. *Nat Rev Immunol* **7**, 9–18 (2007).
32. Ricklin, D., Hajishengallis, G., Yang, K. & Lambris, J. D. Complement: a key system for immune surveillance and homeostasis. *Nat Immunol* **11**, 785–797 (2010).
33. Tsujita, T. *et al*. Sensing bacterial flagellin by membrane and soluble orthologs of Toll-like receptor 5 in rainbow trout (*Onchorhynchus mykiss*). *J Biol Chem* **279**, 48588–48597 (2004).
34. Baoprasertkul, P., Xu, P., Peatman, E., Kucuktas, H. & Liu, Z. Divergent Toll-like receptors in catfish (*Ictalurus punctatus*): TLR5S, TLR20, TLR21. *Fish Shellfish Immunol* **23** (2007).
35. Jayaramu, P. K. *et al*. Studies on expression pattern of toll-like receptor 5 (TLR5) in *Edwardsiella tarda* infected *Pangasianodon hypophthalmus*. *Fish Shellfish Immunol* **63**, 68–73 (2017).
36. Munoz, I., Sepulcre, M. P., Meseguer, J. & Mulero, V. Molecular cloning, phylogenetic analysis and functional characterization of soluble Toll-like receptor 5 in gilthead seabream, *Sparus aurata*. *Fish Shellfish Immunol* **35**, 36–45 (2013).
37. Moon, J. Y. *et al*. Maximal transcriptional activation of piscine soluble Toll-like receptor 5 by the NF-kappaB subunit p65 and flagellin. *Fish Shellfish Immunol* **31** (2011).
38. Bai, J. S. *et al*. Molecular identification and expression analysis of TLR5M and TLR5S from orange-spotted grouper (*Epinepheluscoioides*). *Fish Shellfish Immunol* **63**, 97–102, https://doi.org/10.1016/j.fsi.2017.01.037 (2017).
39. Hayashi, F. *et al*. The innate immune response to bacterial flagellin is mediated by Toll-like receptor 5. *Nature* **410**, 1099–1103 (2001).
40. Tsujita, T. *et al*. Fish soluble Toll-like receptor (TLR)5 amplifies human TLR5 response via physical binding to flagellin. *Vaccine* **24**, 2193–2199 (2006).

41. Rebl, A., Goldammer, T. & Seyfert, H. M. Toll-like receptor signaling in bony fish. *Vet Immunol Immunopathol* **134**, 139–150 (2010).
42. Secombes, C. J., Wang, T. & Bird, S. in *The evolution of the immune system* (ed D. Malagoli) Vertebrate cytokines and their evolution, 87–150 (Elsevier, 2016).
43. Zou, J. & Secombes, C. J. The Function of Fish Cytokines. *Biology (Basel)* **5**, 23 (2016).
44. Acosta-Rodriguez, E. V., Napolitani, G., Lanzavecchia, A. & Sallusto, F. Interleukins 1beta and 6 but not transforming growth factor-beta are essential for the differentiation of interleukin 17-producing human T helper cells. *Nat Immunol* **8**, 942–949 (2007).
45. Wang, T. & Secombes, C. J. The cytokine networks of adaptive immunity in fish. *Fish Shellfish Immunol* **35**, 1703–1718 (2013).
46. Das, S. & Khader, S. *Yin and yang of interleukin-17 in host immunity to infection* [version 1; referees: 2 approved]. F1000Research **6** (F1000 Feculty Rev), 741 (2017).
47. Buckley, K. M. *et al.* IL17 factors are early regulators in the gut epithelium during inflammatory response to *Vibrio* in the sea urchin larva. *Elife* **6**, e23481 (2017).
48. Wang, T., Martin, S. A. & Secombes, C. J. Two interleukin-17C-like genes exist in rainbow trout *Oncorhynchus mykiss* that are differentially expressed and modulated. *Dev Comp Immunol* **34**, 491–500 (2010).
49. Lee, J. *et al.* IL-17E, a novel proinflammatory ligand for the IL-17 receptor homolog IL-17Rh1. *J Biol Chem* **276**, 1660–1664 (2001).
50. Li, H. *et al.* Cloning and characterization of IL-17B and IL-17C, two new members of the IL-17 cytokine family. *Proc Natl Acad Sci USA* **97**, 773–778 (2000).
51. Starnes, T., Broxmeyer, H. E., Robertson, M. J. & Hromas, R. Cutting edge: IL-17D, a novel member of the IL-17 family, stimulates cytokine production and inhibits hemopoiesis. *J Immunol* **169**, 642–646 (2002).
52. Kono, T., Korenaga, H. & Sakai, M. Genomics of fish IL-17 ligand and receptors: a review. *Fish Shellfish Immunol* **31**, 635–643 (2011).
53. Wang, T. *et al.* Identification of the salmonid IL-17A/F1a/b, IL-17A/F2b, IL-17A/F3 and IL-17N genes and analysis of their expression following *in vitro* stimulation and infection. *Immunogenetics* **67**, 395–412 (2015).
54. Korenaga, H., Kono, T. & Sakai, M. Isolation of seven IL-17 family genes from the Japanese pufferfish Takifugu rubripes. *Fish Shellfish Immunol* **28**, 809–818 (2010).
55. Du, L. *et al.* Identification and functional characterization of grass carp IL-17A/F1: An evaluation of the immunoregulatory role of teleost IL-17A/F1. *Dev Comp Immunol* **51**, 202–211 (2015).
56. Monte, M. M., Wang, T., Holland, J. W., Zou, J. & Secombes, C. J. Cloning and characterization of rainbow trout interleukin-17A/F2 (IL-17A/F2) and IL-17 receptor A: expression during infection and bioactivity of recombinant IL-17A/F2. *Infect Immun* **81**, 340–353 (2013).
57. Grabherr, M. G. *et al.* Full-length transcriptome assembly from RNA-Seq data without a reference genome. *Nat Biotechnol* **29**, 644–652 (2011).
58. Gladyshev, E. A., Meselson, M. & Arkhipova, I. R. Massive horizontal gene transfer in bdelloid rotifers. *Science* **329**, 1210–1213 (2008).
59. Nguyen, L. T., Schmidt, H. A., von Haeseler, A. & Minh, B. Q. IQ-TREE: a fast and effective stochastic algorithm for estimating maximum-likelihood phylogenies. *Mol Biol Evol* **32**, 268–274 (2015).
60. Kalyaanamoorthy, S., Minh, B. Q., Wong, T. K. F., Von Haeseler, A. & Jermiin, L. S. ModelFinder: Fast model selection for accurate phylogenetic estimates. *Nat Methods* **14**, 587–589 (2017).
61. Minh, B. Q., Nguyen, M. A. & von Haeseler, A. Ultrafast approximation for phylogenetic bootstrap. *Mol Biol Evol* **30**, 1188–1195 (2013).
62. Kanehisa, M., Furumichi, M., Tanabe, M., Sato, Y. & Morishima, K. KEGG: new perspectives on genomes, pathways, diseases and drugs. *Nucleic Acids Res* **45**, D353–D361 (2017).
63. Kanehisa, M. & Goto, S. KEGG: Kyoto Encyclopedia of Genes and Genomes. *Nucleic Acids Res.* **28**, 27–30 (2000).
64. Kanehisa, M., Goto, S., Sato, Y., Furumichi, M. & Tanabe, M. KEGG for integration and interpretation of large-scale molecular data sets. *Nucleic Acids Res* **40**, D109–114 (2012).
65. Ritchie, M. E. *et al.* Limma powers differential expression analyses for RNA-sequencing and microarray studies. *Nucleic Acids Res.* **47**, e47 (2015).
66. Young, M. D., Wakefield, M. J., Smyth, G. K. & Oshlack, A. Goseq: Gene Ontology Testing for RNA-seq Datasets. https://bioconductor.org/packages/devel/bioc/vignettes/goseq/inst/doc/goseq.pdf (2012).

Acknowledgements

The sequencing service was provided by the Norwegian Sequencing Centre (www.sequencing.uio.no), a national technology platform hosted by the University of Oslo and supported by the "Functional Genomics" and "Infrastructure" programs of the Research Council of Norway and the Southeastern Regional Health Authorities. Funding: Research Council in Norway (Grant 244148/E40, GTH) and University of Bergen.

Author Contributions

G.T.H., D.F. A.R. and H.I.W. planned the experiment; G.T.H. and A.R. performed the *in vitro* bacterial exposure experiment and sample preparation for RNA sequencing; H.Ø.E., G.T.H., H.S.L., D.F., C.K.M., K.P., T.F. performed bioinformatics and analyzed the results. D.J.C. provided material for the *in vitro* bacterial exposure experiment; G.T.H. wrote the initial draft of the manuscript; all co-authors contributed to proofreading and editing the manuscript.

Additional Information

Supplementary information accompanies this paper at https://doi.org/10.1038/s41598-018-23667-x.

Competing Interests: The authors declare no competing interests.

Publisher's note: Springer Nature remains neutral with regard to jurisdictional claims in published maps and institutional affiliations.

II

Developmental and Comparative Immunology 105 (2020) 103608

Contents lists available at ScienceDirect

Developmental and Comparative Immunology

journal homepage: www.elsevier.com/locate/devcompimm

The proinflammatory cytokines TNF-α and IL-6 in lumpfish (*Cyclopterus lumpus* L.) -identification, molecular characterization, phylogeny and gene expression analyses

Håvard Øritsland Eggestøl*, Harald S. Lunde, Gyri Teien Haugland**

Department of Biological Sciences, Bergen High-Technology Center, University of Bergen, PO Box 7803, NO-5020, Bergen, Norway

ARTICLE INFO

Keywords:
Proinflammatory cytokines
Lumpsucker
Tumor necrosis-factor
Interleukin
Cleaner fish
Teleost
Phylogeny
Innate immune system
Responses
PAMP
PRR
Tissue dependence
Genomic organization

ABSTRACT

The proinflammatory cytokines TNF-α and IL-6 are important mediators of inflammatory reactions and orchestrators of the immune system in vertebrate. In this study, we have identified TNF-α and IL-6 in lumpfish, molecular characterized them at mRNA and gene level, performed homology modelling and measured their gene expression in different tissues and upon *in vitro* stimulation. A comprehensive phylogenetic analysis of TNF-α teleost sequences give novel insight into the TNF –α biology. Interestingly, we identified two isoforms of luIL-6. In normal tissue and leukocyte, the level of luTNF-α transcripts was higher than luIL-6. The expression pattern were parallel, except for brain, eye and gonad, and they displayed a similar induction pattern upon exposure to PAMPs, being most highly upregulated by flagellin. This is the first in-depth characterization of TNF and IL-6 in lumpfish. In recent years, lumpfish has become an important species for the aquaculture industry and establishment of qPCR-assays of luTNF-α and luIL-6 provide a valuable tool to measure effect of immune modulation, such as vaccination, microbiological disease and physiological trials. Lumpfish is also interesting for comparative studies as it represent a phylogenetic group that is poorly described immunologically.

1. Introduction

Tumor necrosis factor alpha (TNF-α) is a pleiotropic pro-inflammatory cytokine involved in regulation of the immune response and immune system homeostasis. Also, it is a major mediator of apoptosis, cell proliferation and differentiation, and it is also involved in sleep (Dubravec et al., 1990; Krueger et al., 1998; Warner and Libby, 1989; Young et al., 1987). TNF-α is expressed as a membrane bound peptide that is enzymatically cleaved by TNF convertase (TACE), also known as ADAM17. In mice (*Mus muscelus*) the biological active peptide of TNF-α is a homotrimer with a molecular weight of 51.81 kDa. The solved crystal structures (1.4 Å resolution) of the mature murine TNF-α has revealed important receptor binding surfaces at amino acid (aa) 30–34 and 144–147 and that one 2-propanol molecule, stabilized by Tyr-119 in each monomer, is trapped inside the trimeric channel (Baeyens et al., 1999).

TNF is an ancient gene identified and characterized in several invertebrates, such as planarians, mollusks and arthropods (Hu et al., 2019; Li et al., 2017; Qu et al., 2017), as well as in vertebrate species. Among fish, TNF-α has been identified and characterized in salmonids (Bobe and Goetz, 2001; Zou et al., 2002), carp fishes (Eimon et al., 2006; Grayfer et al., 2008; Saeij et al., 2003; Savan and Sakai, 2004; Zhang et al., 2012), Japanese flounder (*Paralychthys olivaceus*) (Hirono et al., 2000), gilthead seabream (*Sparus aurata*) (Garcia-Castillo et al., 2002) as well as ayu fish (*Plecoglossus altivelis*) (Uenobe et al., 2007), bluefin tuna (*Thunnus orientalis* and *Thunnus thynnus)* (Kadowaki et al., 2009; Lepen Pleic et al., 2014), channel catfish (*Icatalarus punctatus*) (Zou et al., 2003b), tilapia (*Oreochromis niloticus*) (Praveen et al., 2006), turbot (*Scophthalmus maximus*) (Ordas et al., 2007) and rock bream (*Oplegnathus fasciatus*) (Kim et al., 2009).

Several paralogs of TNF-α have been identified in teleosts. Hong et al. (2013) divided between Type I and II, the former being structurally similar to the ancient TNF-α, while the latter type II contained a shortened pre-TACE extracellular stalk and two aa inserted between β-sheet 9 and 10. They showed that type I TNF-α is co-localized with TNF-N and gabbr1a in zebrafish, while type II TNF-α is co-localized with SCAM1L and gabbr1b. Furthermore, Hong et al. (2013) suggested that type II can be heterofunctional as the shortened stalk possibly could inhibit the TACE-action, leaving the type II in a transmembrane form.

* Corresponding author.
** Corresponding author.
E-mail addresses: Havard.Eggestol@uib.no (H.Ø. Eggestøl), Gyri.Haugland@uib.no (G.T. Haugland).

https://doi.org/10.1016/j.dci.2020.103608
Received 19 August 2019; Received in revised form 3 January 2020; Accepted 3 January 2020
Available online 07 January 2020

Moreover, they also speculated that this would leave type I as mainly a secreted cytokine.

TNF-α is constitutively expressed in most examined teleost tissue. Bluefin tuna (both Pacific and Atlantic), salmonid fishes and common carp have at least two TNFα paralogs (Hong et al., 2013; Kadowaki et al., 2009; Laing et al., 2001; Lepen Pleic et al., 2014; Saeij et al., 2003; Savan and Sakai, 2004). Hong et al. (2013) observed a higher gene expression of TNF-α1 (type 1) compared to TNF-α2 (type 1) and TNF-α3 (type 2) in most examined tissues in rainbow trout. In Pacific tuna, TNF2 (type II), but not TNF1 (type I), showed a tissue dependent gene expression (Kadowaki et al., 2009). Lepen Pleic et al. (2014) did not observe any tissue dependent gene expression of the TNF-α paralogs in Atlantic tuna.

In a stimulation experiment in Pacific tuna, where head kidney leukocytes (HKLs) were exposed to various pathogen-associated molecular patterns (PAMPs), type I TNF-α did not exhibit any altered expression, while type II TNFα showed moderate upregulation by lipopolysaccharide (LPS), phytohemagglutinin, concanavalin A, pokeweed mitogen and phorbol myristate acetate (Kadowaki et al., 2009). Most examined teleost TNF-α are positively regulated by LPS. Other PAMPs also induces TNF-α levels *in vitro* in teleosts, but consensus reduction or induction patterns of non-LPS PAMPs in different species have not yet been unveiled. This is likely due to the same PAMPs is not included in the different studies. Recombinant teleost TNF-α exhibit pro-inflammatory properties, such as IL-1β is upregulated in all examined species, trout TNF-α induce expression of IL-8, IL-17C and cox-2 genes and rock bream HKLs display elevated capability of receptor-mediated phagocytosis upon stimulation with TNF-α (Kim et al., 2009; Li and Zhang, 2016; Zhang et al., 2012; Zou et al., 2003a). In an *in vivo* experiment in tongue sole, elevated levels of IL-1, IL-6, IL-8, IL-27, Toll-like receptor (TLR) 9 and galectin-3-binding protein (G3BP) transcripts were measured in kidney upon injection with a recombinant TNF homologue (Li and Zhang, 2016). Further, Li and Zhang (2016) showed that the receptor binding sites are essential for TNF function, as observed in mammals.

IL-6 has both pro- and anti-inflammatory activities. It was first described as a B cell stimulatory factor, capable of inducing differentiation of B cells to plasma cells and have thereby been linked to antibody production in vertebrates (Hirano et al., 1985, 1986; Kaneda et al., 2012). In mammals IL-6 function as a hepatocyte stimulating factor and a capable inducer of acute phase proteins (Andus et al., 1987; Gauldie et al., 1987).

IL-6 has been identified in several teleosts such as Japanese pufferfish (*Takifugu rubripes*) (Bird et al., 2005), rainbow trout (Iliev et al., 2007), olive flounder (Nam et al., 2007), gilthead seabream (Castellana et al., 2008), zebrafish (Varela et al., 2012), orange-spotted grouper (*Epinephelus coicoides*) (Chen et al., 2012), Atlantic halibut (Øvergard et al., 2012) and Nile tilapia (Wei et al., 2018). These studies report varying tissue expression of IL-6. Studies using conventional PCR reports some absence of IL-6 expression in certain tissues (Castellana et al., 2008; Fujiki et al., 2003; Nam et al., 2007), while later, studies utilizing quantitative PCR reports constitutive expression of IL-6. The relative distribution of IL-6 is highest in lymphoid and central nervous system (CNS) organs, and lowest in liver. In all examined teleosts, IL-6 contains 4 exons and 5 introns.

It has been reported that IL-6 elicits antibody production and regulation of differentiation of naïve T helper (T_h) cells into T_h2 cells *in vivo* in orange-spotted grouper (Chen et al., 2012). The involvement of IL-6 in the promotion of antibody production has also been reported in Nile tilapia (Wei et al., 2018) and Japanese pufferfish (Kaneda et al., 2012). Several works reports IL-6 up-regulation after exposure to pathogens in teleosts; *Streptococcus agalactia* in *in vitro* Nile tilapia, *Edwardisella tarda* in *in vivo* olive founder and *Vibrio anguillarum* in *in vivo* gilthead seabream (Castellana et al., 2008; Nam et al., 2007; Wei et al., 2018). Up-regulation of IL-6 is also observed post stimulation with several PAMPs in teleosts including LPS, bacterial DNA, peptidoglycan, imiquimod and poly (I:C) (Bird et al., 2005; Castellana et al., 2008; Chen et al., 2012; Varela et al., 2012; Wei et al., 2018; Øvergard et al., 2012).

Table 1
Used primers in this study.

Gene	Direction	5′-sequence-3′	Application
RPS20	Forward	GGAGAAGAGCCTGAAGGTGAAG	qPCR
	Reverse	GAGTTTTCCTGGTGGTGATGC	qPCR
IL6	Forward	GAAGACACGCCCACCGACAT	qPCR
	Reverse	GCCCCGCCTGCTCCTCACCT	qPCR
	Forward	GACCGGATGGCTGACGCAA	Sanger sequencing
	Reverse	ACCCAATTTCCACAAGGTAGTGCT	Sanger sequencing
TNFα	Forward	CCACACCACGTTGAGGCAGATCA	qPCR
	Reverse	CCTTGACCGCTTCTCCACTCCA	qPCR
	Forward	GCTGGAAGCACCTGAAGACTCAGACAC	Sanger sequencing
	Reverse	TTGTATCGTGTATGTTACGACCGCATA	Sanger sequencing

Table 2
qPCR assay performance.

Gene	α	Efficiency	R^2	Ampl. size
RPS20	−3299	2,01	0,999	74
IL6	−3398	1,95	0,998	58
TNFα	−3409	1,96	0,996	117

Lumpfish is a representative of the poorly described phylogenetic clade of teleosts, the *Cottales*. Furthermore, it is a novel species for the farming industry in Europe (Powell et al., 2018). The production is successful, but it suffers from high mortality due to bacterial diseases caused by *V. anguillarum*, atypical *Aeromonas salmonicida*, *Pasteurella* sp. and *Pseudomonas anguilliseptica* (Scholz et al., 2018; Walde et al., 2019). Thus, immunological studies in lumpfish is interesting for both phylogenetic, comparative and applied science. In the current study, we have characterized TNF- α and IL-6 in lumpfish. We have examined their tissue - and PAMP dependent gene expression, performed phylogenetic analyses and described their molecular properties.

2. Materials and methods

2.1. Identification of lumpfish (lu) TNF-α and IL-6

In a previous study (Eggestøl et al., 2018) we performed RNA sequencing and *de novo* transcriptome assembly of lumpfish leukocytes, yielding a tri-layered database structure divided into contigs, genes and transcripts. In the current study, we have used this transcriptome as our database to search for TNF-α and IL-6 in lumpfish, and performed a tBLAST-n search utilizing the human TNFα (P01275) and human IL6 (P05231) as our query sequences and chose the top gene ID among the transcript hits. Among that gene ID, we performed a BLAST-X search on all its transcripts against NCBI's non-redundant database and chose the transcript ID with the highest BLAST score among the full-length sequences. Sanger sequencing (see 2.3) verified the sequences.

2.2. Bioinformatical analyses

The phylogenetic analyses included, in addition to the luTNF-α and luIL-6 sequences, all annotated teleost TNF-α and IL-6 sequences in INSDC (Karsch-Mizrachi et al., 2018), human and mouse sequences, and the top 100 hits of a tBLAST-n searches against INSDC's non-

Fig. 1. Nucleotide and deduced amino acid sequences for lumpfish TNF-α. gDNA specific sequence is represented with lower case, cDNA sequence is represented with upper case and coding cDNA sequence is represented with bold. Introns are indicated by ellipses at both ends, AT rich elements are indicated by underlining, double underlining indicates the polyadenylation signal, and the endotoxin responsive motifs are boxed.

redundant database using the lumpfish and zebrafish sequences as queries. In addition for TNF-α, the top 100 hits of a tBLAST-n searches against INSDC's non-redundant database using the Arctic char (*Salvelinus alpinus*) sequences as queries. A preliminary MUSCLE (Edgar, 2004) multiple sequence alignment (MSA) was conducted in order to identify and remove duplicate or inadequate (low quality, partial etc.) sequences, yielding 178 TNF-α and 80 IL-6 sequences for the phylogenetic analyses. Based on these sequences a MUSCLE MSA was made

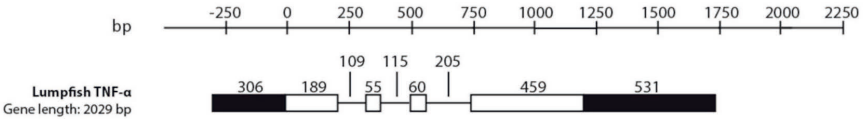

Fig. 2. Genomic organization of lumpfish TNF-α. The zero point is defined as start of peptide coding DNA sequence (CDS). Black boxes represent UTRs, white boxes represents exons and lines represents introns. Numbers represents the number of nucleotides of the corresponding element and parenthesized numbers represent the gene length.

and a maximum likelihood phylogenetic tree utilizing IQ-TREE (Nguyen et al., 2015) with automatic model selection (Kalyaanamoorthy et al., 2017) was constructed (Figs. 7 and 8 and Supplementary Figs. S1 and S2). Bootstrapping was conducted with 100 000 replicates to assess clade support (Minh et al., 2013).

In order to compare the predicted amino acid sequence of luTNF-α and luIL-6 and to identify conserved regions, a MSA was made using the CLUSTALΩ algorithm (Sievers and Higgins, 2014) in which the lumpfish sequences were compared with TNF-α and IL-6 from all teleost sequences fully characterized in the published scientific literature, in addition to human and mouse sequences. In addition, for IL-6, the Tanaka's snailfish (*Liparis tanakae*) sequence were added. Identification of the functional domains was performed by InterProScan (Jones et al., 2014), using the entries from the SMART database (Letunic and Bork, 2018), with the following exceptions: TMHMM used for transmembrane prediction (http://www.cbs.dtu.dk/services/TMHMM/), SignalP-5.0 for signal peptide prediction (http://www.cbs.dtu.dk/services/SignalP-5.0/) and Peptide Cutter for enzyme cleavage site prediction (https://web.expasy.org/peptide_cutter/). Prediction of molecular weight and isoelectric point were performed by ExPASy tool Compute pI/Mw (https://web.expasy.org/compute_pi/).

Scaffolds including luTNF-α and luIL-6 genes, were found by BLAST searching the lumpfish genome with luTNF-α and luIL-6 transcripts in Galaxy (Camacho et al., 2009; Cock et al., 2015; Knutsen, 2018). Intron-exon boundaries were predicted by aligning cDNA and gene sequences and adjusting the introns according to the GT …. AG rule. UTR's were determined by aligning the transcript sequences with the predicted aa sequences.

The tertiary structure of the lumpfish sequences were modeled with SWISS-MODEL (Waterhouse et al., 2018), and fit to murine crystal structures (TNF-α - 2tnf.1.C and IL-6 - 2l3y.1.A). The models and templates were displayed using ICM-Browser 3.8–7b © (MolSoft L.L.C.).

2.3. Sanger sequencing

Sanger sequencing was performed by amplifying the relevant genomic DNA sequence through a high fidelity polymerase chain reaction (PCR) in a 2720 Thermal Cycler (Applied Biosystems, California, USA), using specific primers (Table 1) and Phusion High-Fidelity polymerase (ThermoFischer Scientific) according to the manufactures instructions. The DNA products were extracted from a 1% agarose gel containing GelRed® (Biothium, Fremont, USA). The sequencing reaction was run using the BigDye™ Terminator v3.1 (Applied Biosystems), according to the manufactures instructions and sequenced using the 3730XL Analyzer (Applied Biosystems) at the DNA sequencing Facility at the High-Technology Centre, Bergen, Norway.

2.4. Fish and rearing conditions

Farmed, unvaccinated lumpfish were provided by Vest Aqua base, Norway. The fish were kept at the rearing facilities at the Aquatic and Industrial Laboratory (ILAB), Bergen High-Technology Centre, Bergen, Norway, under normal optimal rearing facilities at a temperature of 8–9 °C, salinity of 34‰ and 12:12 h light:dark. The water flow were 300–400 l per hour and the outlet water had a minimum of 77% oxygen saturation. The fish were fed with commercial dry feed for lumpfish (3 mm pellets).

2.5. Tissue sampling and homogenization

In order to study the normal gene expression in different tissues 16 tissues were collected from fish (n = 7) with an average size of 245.7 ± 49 g and 18.1 ± 1.1 cm,; skin mucus, skin, muscle, thymus, gill filament, gill arch, tongue, liver, spleen, gonad, head kidney (left lobe), heart, pyloric caeca, gut, eye and brain. Up to 40 mg tissue were immediately put in 0.3 ml of fresh lysis buffer in FastPrep® Tubes (MP Biomedicals, USA) containing 3 SS Metal Beads Lysing Matrix (MP Biomedicals, USA) and homogenized in the 24x FastPrep-24™ 5G (MP Biomedicals, USA). Additional 0.4 ml fresh lysis buffer was added after homogenization, according to the manufactures RNA isolation protocol. Isolation of total RNA and cDNA synthesis are described in Section 2.8.

2.6. Leukocyte isolation

For *in vitro* stimulation, leukocytes were isolated from peripheral blood and head kidney from six lumpfish that weighed 282.7 ± 56.5 g and measured 18.5 ± 1.1 cm. The fish were killed by a sharp blow to the head. Leukocytes were isolated from peripheral blood (0.7 ml), collected from *vena caudalis,* as described previously (Haugland et al., 2012). Briefly, the blood was transferred to heparinized containers and diluted to a total volume of 5 ml Leibovitz L-15+ (L-15 media without L-Glutamine adjusted to 370 mOsm by adding 5% (v/v) of a solution consisting of 0.41 M NaCl 0.33 M $NaHCO_3$ and 0.66 5 (w/v) D-glucose) supplemented with 100 μg/ml genatamicin (Lonza Biowhittaker Verviers, Belgium), 10 U/ml heparin (Lonza Biowhittaker Verviers, Belgium) and 15 mM HEPES (Sigma-Aldrich, St. louis, USA)). For isolation of HKL, the anterior 1 cm of the right head kidney lobe was transferred to a gentleMACS™ C tube (Miltenyi Biotec, Germany) containing 3 ml L-15 + medium and dissociated by gentleMACS™ Dissociator (Miltenyi Biotec, Köln, Germany) on the default program D. After dissociation, the cell suspension were placed on discontinuous Percoll gradients, 3 ml 1.070 g/ml Percoll™ (GE Healthcare, Uppsala, Sweden) solution overlaid with 2.5 ml 1.050 g/ml Percoll solution, and centrifuged at 400 g and 4 °C for 40 min. The leukocyte fraction were transferred to a new tube and washed once with L15 + media, centrifuged at 200 g and 4 °C for 10 min, resuspended in L15 + media and counted by CASY® Modell TT cell counter (Innovatis AG, Reutlingen, Germany). All leukocytes samples showed viability over 95% and low levels of aggregation.

2.7. Leukocyte stimulation with PAMPs

Each leukocyte sample in the *in vitro* stimulation experiment was split into eight wells in 24-well plates, each containing 4×10^7 leukocytes and the following PAMPs: 0.3 μg/ml Pam3CSK4 (InvivoGen, San Diego, USA), 0.1 μg/ml FSL-1 (InvivoGen, San Diego, USA), 20 μg/ml Fla-BS (InvivoGen, San Diego, USA), 50 μg/ml poly (I:C) HMW (InvivoGen, San Diego, USA), 10 μg/ml ssPolyU/LyoVec™ (InvivoGen, San Diego, USA), 1 μM CpG-B: T*C*G*T*C*G*T*T*T*T*G*T*C*G*T*T*T*T*G*T*C*G*T*T* (Eurogentech) or 1 μM GpC-B: T*G*C*T*G*C*T*T*T*T*G*T*G*C*T*T*T*T*G*T*G*C*T*T* (Eurogentech), in a total volume of 500 μl of L15 + media. To the non-stimulated control sample, L15 + was added

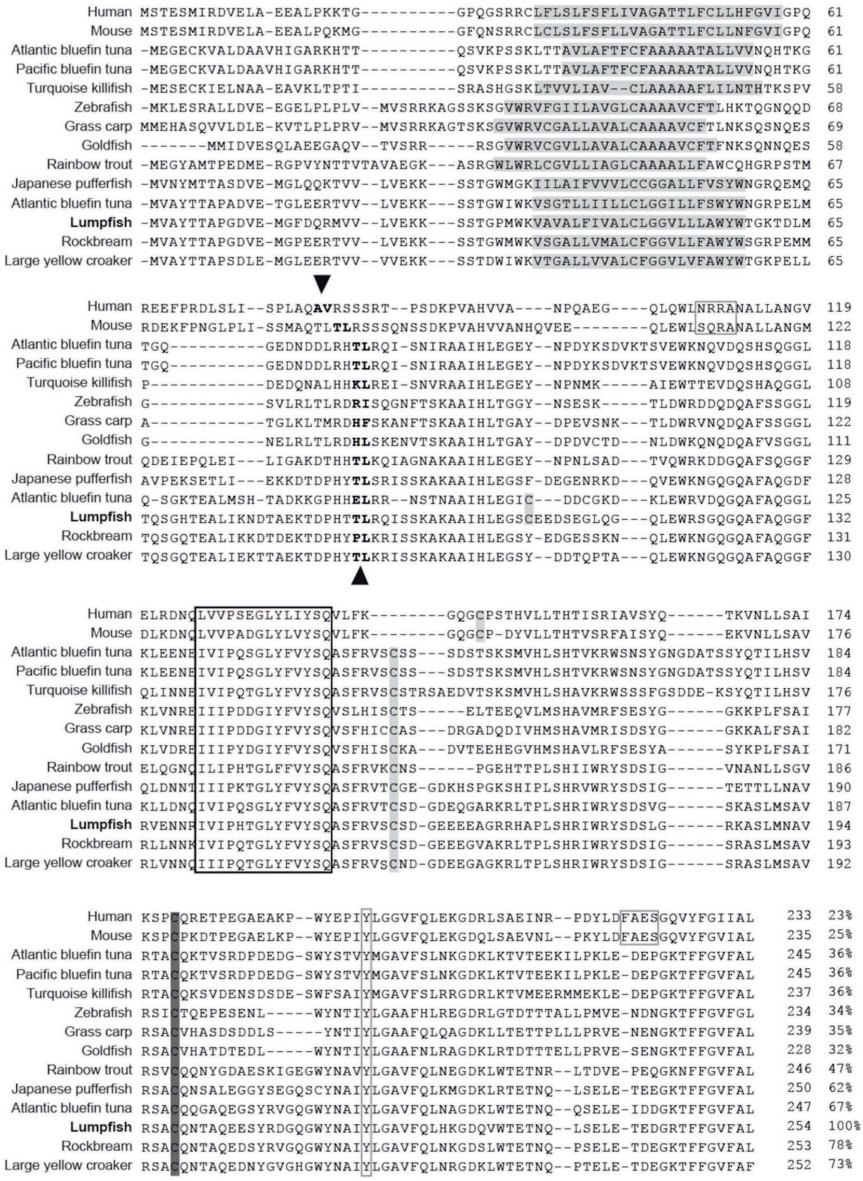

Fig. 3. Multiple alignment of lumpfish TNF-α sequence with other reported teleost, human and murine TNF-α sequences. Cysteine residues is vertically shaded and family signature is boxed in black. Receptor binding surfaces in mammals is boxed in grey. The transmembrane domain is horizontally shaded. The putative TACE cleavage site are in bold type and indicated by arrowheads. Amino acid similarity percentage with lumpfish TNF-α is written as percentage at the end of the respective alignment.

instead of PAMPs. The plates were covered by Microseal® 'B' seal Seals (Bio-Rad, United Kingdom) and incubated at 15 °C. After 18 h, the supernatants were transferred to Eppendorf tubes and centrifuged at 400 g in 10 min at 15 °C. To both the wells and cell pellets 250 μl of lysis solution for total RNA kit (Sigma-Aldrich, St. Louis, USA) were added and subsequently mixed. The lysates were stored at −80 °C.

2.8. Total RNA extraction and cDNA synthesis

Total RNA was isolated using GenElute™ Mammalian Total RNA Miniprep kit (Sigma-Aldrich, St. Louis, USA) according to the manufacturer's instructions and treated by DNase I (up to 2500 ng RNA per reaction) (Sigma-Aldrich, St. Louis, USA) according to the

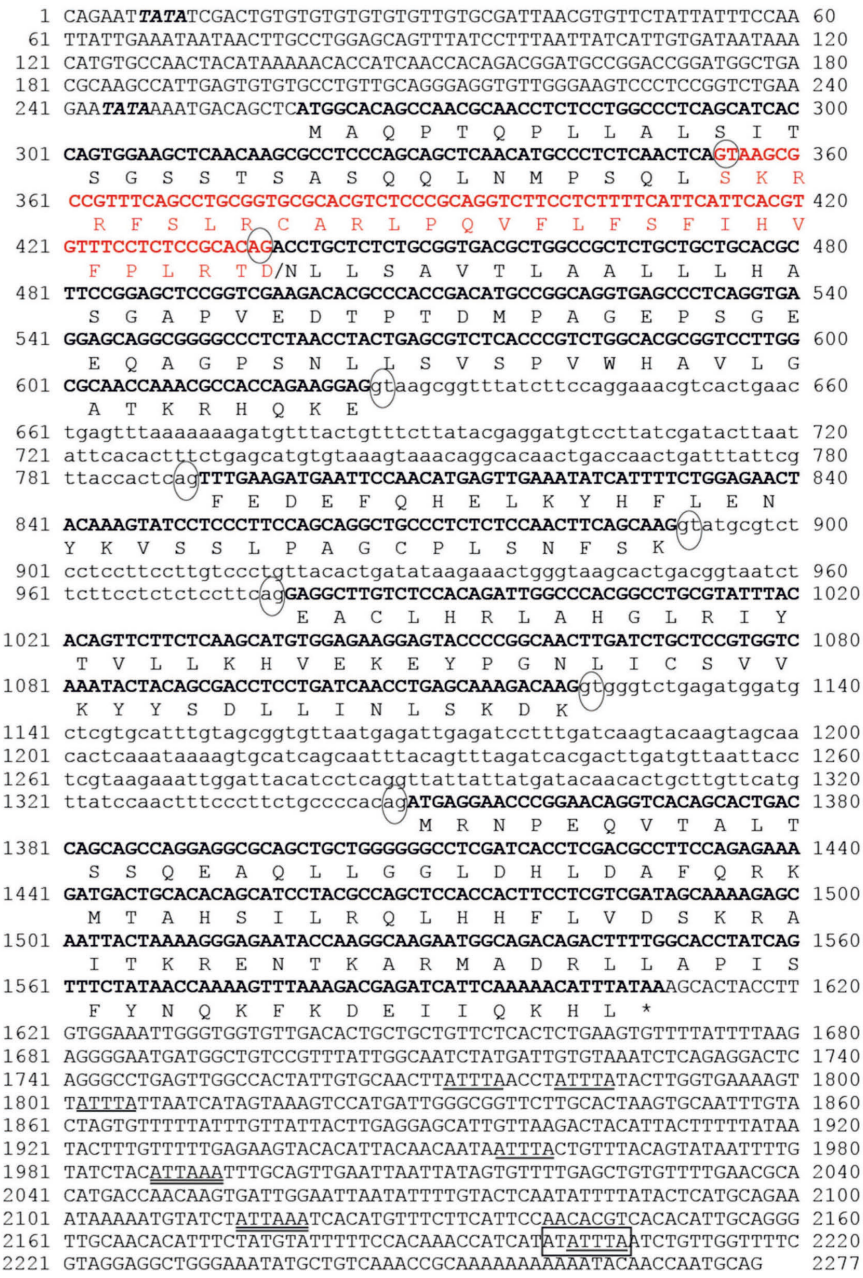

Fig. 4. Nucleotide and deduced amino acid sequences for lumpfish IL-6. gDNA specific sequence is represented with lower case, cDNA sequence is represented with upper case and coding cDNA sequence is represented with bold. Alternatively retained intron are indicated with red letters. Introns are indicated by ellipses at both end, AT rich elements are indicated by underlining, double underlining indicates the polyadenylation signal, the endotoxin responsive motifs are boxed and a TATA box is shown in bold italic. (For interpretation of the references to color in this figure legend, the reader is referred to the Web version of this article.)

manufacturer's instructions. The DNase treated RNA was analyzed on a 1% agarose gel containing GelRed® (Biothium, Fremont, USA) to ensure that all traces of genomic DNA were removed, and to validate the integrity and the quality of the RNA. The RNA concentration and purity was measured in a NanoDrop™ 2000 spectrophotometer (Thermo Fisher Scientific, Waltham, USA). Furthermore, RNA (< 1000 ng/reaction) was reverse-transcribed into cDNA using cDNA synthesis kit (Quantabio, Beverly, USA) according to the manufacturer's instructions.

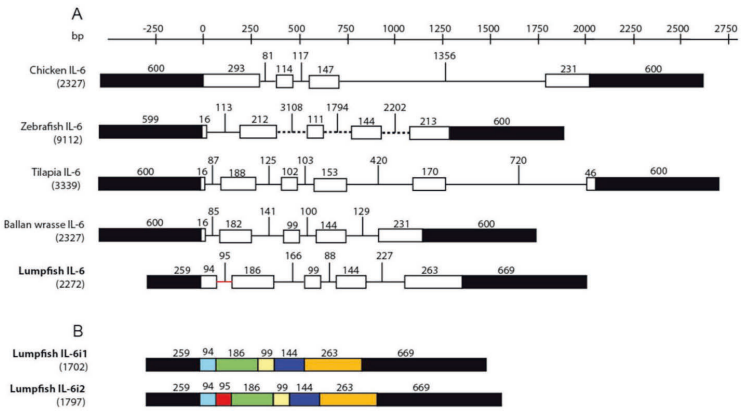

Fig. 5. Genomic organization of IL-6 (A) and transcript organization of luIL-6 (B). The zero point is defined as start of peptide coding DNA sequence (CDS). Black boxes represent UTRs, Numbers represents the number of nucleotides of the corresponding element and parenthesized numbers represent the gene or transcript length. In Fig. 5**A,** white boxes represents exon, black lines represents introns and red lines represents alternatively retained intron. Dashed lines does not correspond with intron length. In Fig. 5**B,** shared exons are represented with same colored boxes, and the alternatively retained intron is represented with a red box. (For interpretation of the references to color in this figure legend, the reader is referred to the Web version of this article.)

2.9. Quantitative PCR (qPCR)

Gene expression were measured by quantitative polymerase chain reaction (qPCR) performed in a C1000 Touch Thermal Cycler with CFX96 Real-Time System (Bio-Rad, Hercules, California) using SYBR Green Jumpstart® Taq DNA Readymix® (Sigma-Aldrich, St. Louis, USA). The pipetting was performed using the PipetMAX 268 (Gilson, Wisconsin, USA). All primers (Table 1) were custom DNA Oligos delivered from Sigma-Aldrich (St. Louis, USA). The target genes assays were optimized for specificity (> 10 000 signal to noise ratio) and efficiency (approximately 2). The performance of the best assay for each gene is reported in Table 2. For relative quantification, the target genes were normalized against the house keeping gene ribosomal protein subunit 20 (RPS20). The qPCR reaction (25 µl) contained 12.5 µl of 2 x SYBR Green Jumpstart® Taq DNA ReadyMix®, 10 µl cDNA (2 ng for RPS20 and 20 ng for target genes), 1 µl (10 µM) of forward and reverse primers and 0.5 µl nuclease-free water (Sigma-Aldrich, St. Louis, USA). The cycling conditions were 94 °C for 5 min followed by 40 cycles of 94 °C for 15 s and 60 °C for 1 min, finishing with a 4 °C hold until termination. For each run, melting curve analyses were performed for each amplicon to ensure the specificity of the primers. Each sample were analyzed by triplicate master mixes. For each master mix a non-template control (NTC) was included to ensure no contamination of the reagents, and a non-reverse transcriptase control (NRT, cDNA reaction without reverse transcriptase) was included to ensure a complete degradation of genomic DNA. For the normal tissue experiment, mean normalized expression (MNE) values were calculated by the ΔCt method (equation (1)), and for the leukocyte stimulation experiment, fold MNE values were calculated by the ΔΔCt method (equation (2)). E is an abbreviation for the assay efficiency, x is any observed Ct value for sample x and y is any observed Ct value for control group sample y.

$$\Delta Ct_x = \frac{E_{target}{}^{-\bar{x}}}{E_{reference}{}^{-\bar{x}}} \quad (1)$$

$$\Delta\Delta Ct_{xy} = \frac{\frac{E_{target}{}^{-\bar{x}}}{E_{reference}{}^{-\bar{x}}}}{\frac{E_{target}{}^{-\bar{y}}}{E_{reference}{}^{-\bar{y}}}} \quad (2)$$

2.10. Statistical analysis

Both qPCR datasets were analyzed by two-way ANOVA in IBM® SPSS® Statistics (version 25.0.0.2) on log10 transformed data. The normal tissue set were followed up by Bonferroni corrected pairwise comparisons and the ligand stimulation set were followed up by Tukey's honest square difference post hoc test. F values refers to the F statistic, df values refers to the degrees of freedom, p values refer to the probability that the statistical summary of the population is equal or more extreme than the observed values of the sample, given that the null hypothesis is true (p values less than 5% is considered significant), and η^2 refers to the effect size, or how much the relevant variable explains the observed variance.

3. Results

3.1. Sequence and structure analysis of luTNF-α and luIL-6

The full-length cDNA sequence of luTNF-α (GenBank accession No: MN093126) composed of 1600 bp with a 5′-untranslated region (UTR) of 306 bp, an open reading frame (ORF) of 762 bp encoding 254 aa and a 3′-UTR of 531 bp containing six AT rich elements, two endotoxin responsive motifs and one polyadenylation signal. The luTNF-α gene was 2031 bp and contained four exons (Figs. 1 and 2). In the translated aa sequence, a transmembrane domain (35–57) and a tumor necrosis factor family domain (96–254) were identified (Fig. 3). Comparative analysis with other TNF-α aa sequences identified a putative TACE cleavage site in luTNF-α (Thr86 and Leu87), resulting in a mature peptide of 168 aa with a theoretic molecular weight of 18.9 kDa and isoelectric point of pH 5.6. Two cysteine residues, known from other species to be involved in the correct folding of the mature peptide, were also present in the luTNF-α. In addition, lumpfish like Atlantic Bluefin tuna contain a cysteine in position 106 and 102, respectively (Fig. 3).

One luIL-6 gene was identified (GenBank accession No: MN093126), having two isoforms. The luIL-6 gene, 2277 bp, contained five exons and four introns (Figs. 4 and 5A). The first exon in luIL-6 is 94 bp (Fig. 5A). This is longer than other non-cyclopteridae/lipridae teleost sequences in which the first exon is typically only 16 bp. The full-length cDNA sequence of the first isoform of luIL-6 (luIL-6 i1) was composed of 1702 bp with a 5′-UTR of 259 bp, an ORF of 775 bp encoding 289 aa and a 3′-UTR of 669 bp containing five AT rich elements, one endotoxin responsive motifs and two polyadenylation signals (Figs. 4 and 5B). The full-length cDNA sequence of the second IL-6 isoform (luIL-6 i2) in lumpfish contained the first intron of the luIL-6 gene, it was composed of 1797 bp, it contained an ORF of 870 bp encoding 289 aa and is a case of alternative intron retention (Figs. 4 and 5B). In the translated aa sequences, the IL-6 family signature sequence were identified. In addition in IL-6 i2, a Caspase 1 cleavage site between position 60 and 61 (DL) (Fig. 6). In the c-termini product a signal peptide sequence were predicted (99.4% probability), but not in the native luIL-6 i2 form (0.6% probability). In IL-6 i1 a signal peptide sequence was predicted with 19% probability. The mature peptides without the predicted signal

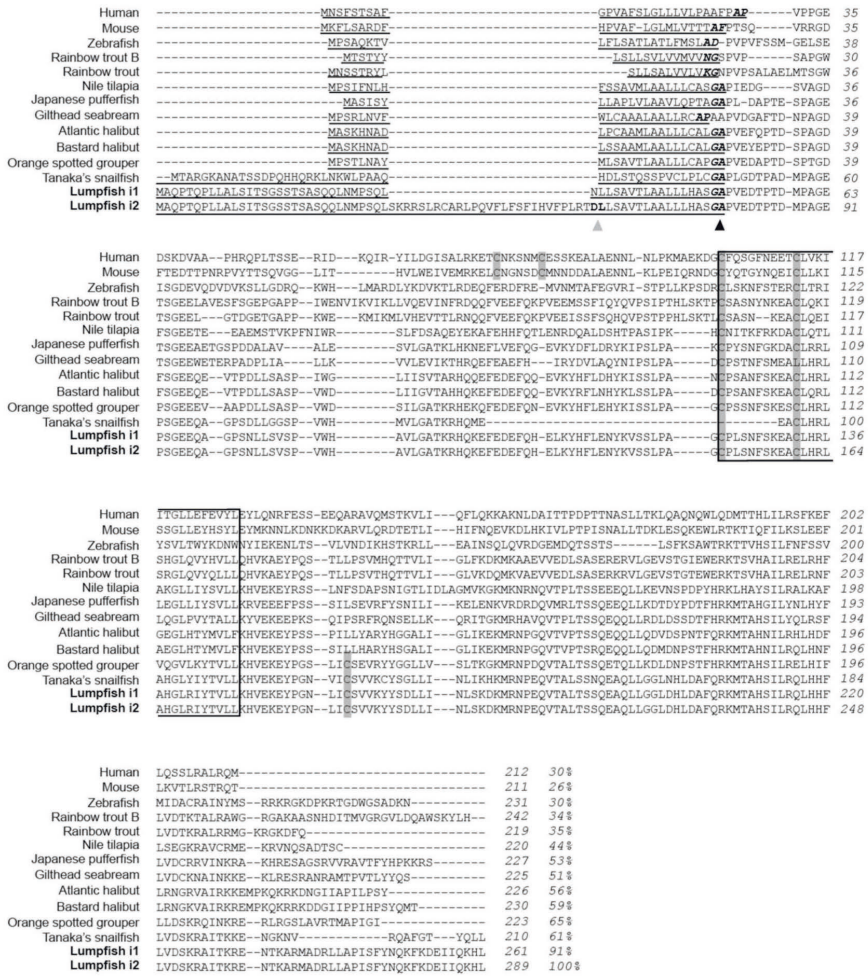

Fig. 6. Multiple alignment of lumpfish IL-6 sequence with other reported teleost, human and murine IL-6 sequences. Cysteine residues are vertically shaded and family signature is boxed in black. Earlier reported and predicted signal peptides is underlined. Putative intron converted aa is horizontally dark grey shaded and UTR converted aa is light grey shaded. Bold letters and grey arrowhead indicate predicted caspase 1 cleavage site. Bold italicized letters and black arrowhead indicate predicted signal peptidase cleavage site. Amino acid similarity percentage with lumpfish IL-6 is written as percentage at the end of the respective alignment.

sequences have a theoretic molecular weight of 24.2 kDa and isoelectric point of pH 7.94. Comparative analysis with other IL-6 sequences revealed that both isoforms of luIL-6 has two conservative cysteine residues. The first cysteine pair in human and mouse are absent in teleosts. Interestingly, 11 positions after the IL-6 family signature sequence, a cysteine residue is present in IL-6 in lumpfish like orange-spotted grouper and Tanaka's snailfish.

3.2. Phylogenetic analysis luTNF-α and luIL-6

The phylogenetic position of luTNF-α was determined through a maximum-likelihood based phylogram (Fig. 7). The teleost TNF-α sequences were divided into three main clades. Clade II contained sequences belonging to *Elopomorpha*, *Osteoglossomorpha* and *Clupeiiformes*, the most basal members of *Teleostei* in this tree. The other teleost sequences were clustered into two clades, corresponding to the TNF-α type-definition proposed for rainbow trout by Hong et al. (2013), clade III and IV. Further, two intra-*Salmonidae* clades of both type I (clade III. a and III. b) and type II (clade IV. a and IV. b) were present, and two intra-*Cyprinae* clades of type II (clade IV. c and IV. d) were also present. LuTNF-α was clustered within the neoteleost clade containing type I TNF-α members (clade III).

The phylogenetic position of luIL-6 was determined through a maximum-likelihood based phylogram (Fig. 8). LuIL-6 was clustered together with other neoteleostei IL-6 sequences. The IL-6 tree reflected the teleost specie tree (clade I, II and III), with the exception of salmoniformes sequences, where two intra-*Salmonidae* clades were present (clade III. a and III. b).

3.3. Homology modelling based structure determination of luTNF-α and IL-6

The structural comparison of luTNF-α monomer with its murine counterpart (Fig. 9) revealed a three-dimensional structure consisting of

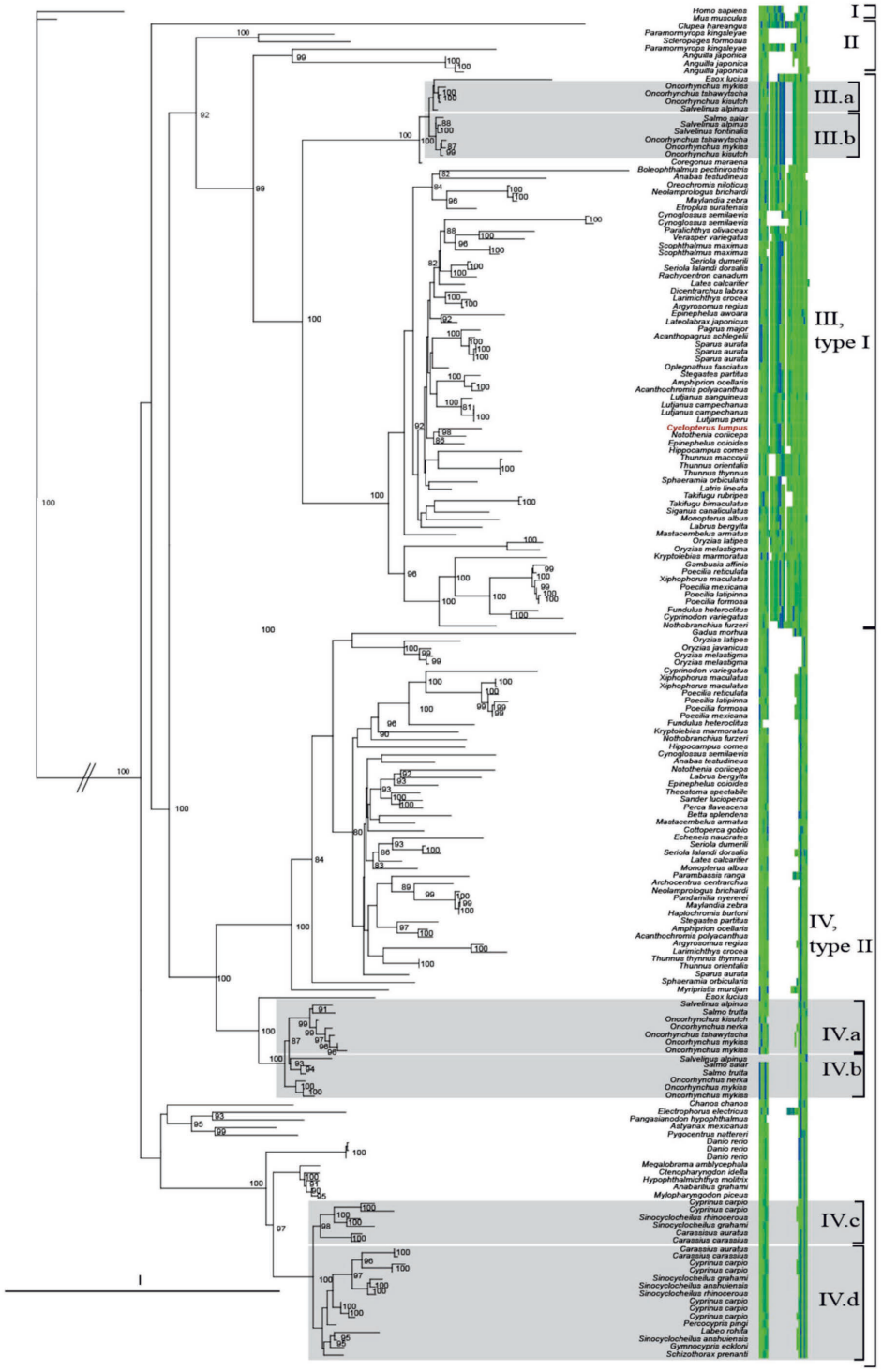

(caption on next page)

Fig. 7. Phylogenetic tree of teleost TNF-α utilizing human and mouse as outgroup. Phylogenetic distance is indicated by branch length and decimal numbers (> 0.1), fat bar indicates distance of 1 amino acid per sequence site. Whole numbers refer to bootstrap values (> 80) of 100000 iterations. Accession numbers are given in the full phylogenetic trees (Supplementary Fig. S1 A, B). Ten clades are indicated by brackets and roman numbers; I – mammalian sequences, II - Elopomorpha, osteoglossomorpha and clupeiiformes sequences, III – type I teleost sequences not present in clade II, IV – type II teleost sequences not present in clade II, V and IV – intra-*Salmonidae* specific type I clades, IIV and IIX – intra-*Salmonidae* specific type II clades, IX and X – intra-*Cyprinidae* specific clades. The intra-clades have been shaded with grey boxes. Alignment defining type affiliation are to the right of the species. Amino acids are colored according to their buried index, dark blue are buried and bright green are not. (For interpretation of the references to color in this figure legend, the reader is referred to the Web version of this article.)

two anti-parallel β-pleated sheets, forming a jellyroll motif, which is the typical protein structure of the TNF-family. LuTNF-α contained a third cysteine residue, only found in lumpfish and Atlantic Bluefin tuna TNF-α1. Due to spatial prediction of this cysteine residue, it is not likely that it contribute in any stabilizing disulfide bridges within the monomer, but it may have a stabilizing function in the trimer, if TNF-α in teleosts have similar quaternary structure as their mammalian counterparts.

The structural comparison of LuIL-6 with its murine counterpart (Fig. 9) showed that LuIL-6 has four conserved α-helices, the typical protein structure of the IL-6 family. LuIL-6 contains a third cysteine residue, presently only found in lumpfish, Tanaka's snailfish and orange spotted grouper IL-6 (Fig. 5). This cysteine residue is placed spatially different from the second cysteine pair known from mammals. The model does not predict the di-sulfide bridge between the first cysteine pair. However, the spatial placement could allow a di-sulfide bridge in luIL-6.

3.4. Gene expression profiling of luTNF- α and luIL-6 in normal tissues

In order to gain insights into the expression of luTNF-α and luIL-6 in different tissues during normal conditions, qPCR assays for luTNF-α and luIL-6 were designed. LuRPS-20 was used as reference gene in a simplex qPCR setup (Fig. 10). Transcripts of all three genes were measured in all examined leukocytes and tissues. A two-way ANOVA showed that TNF-α expression was dependent on tissue (F (17 186) = 8.048, p = 5.5E-16, η^2 = 0.447). The highest level of TNF-α transcripts was measured in HKL. It was significantly different from liver, gonad, muscle and gut. The lowest level was measured in gonad and it was significantly different from gill arch, gill filament, HK, heart, HKL, PBL, skin mucus, skin, spleen, thymus and tongue (Fig. 10A). Similar to TNF- α, IL-6 expression was also dependent on tissue (F (17 186) = 8.849, p = 1.8E-16, η^2 = 0.447). The highest level of IL-6 transcripts was in brain. It was significantly different from liver, muscle, gut, gill arch, gill filament, gonad, HK, pyloric caeca, skin, skin mucus, tongue. IL6 was expressed at its lowest in gut, being significantly different from brain, eye, gill arch, gill filament, gonad, HK, heart, HKL, PBL, skin, skin mucus, spleen and thymus. (Fig. 10B). A direct comparison showed that the expression level of TNF-α was higher than IL-6 in HKL and all examined organs except brain, eye, gonad and PBL (Fig. 10C). PBL consisted of only two samples due to isolation issues, and therefore should be exempted from questions regarding significance. The statistical analyses showed that there is a significant effect of both tissue and gene F (17, 186) = 4.278, p = 2.5E-7, η^2 = 0.281.

3.5. Modulation of luTNF-α and luIL-6 expression upon exposure to different PAMPs

To further our knowledge of luTNF- α and luIL-6, we stimulated HKL with seven different ligands (Fig. 11). In general, luIL-6 induction was higher than luTNF-α and flagellin was the most potent inducer of luTNF-α resulting in 16.8 times upregulation (p = 3.12E-15) and luIL-6 at 91.8 upregulation (p = 1.65E-7) compared with the control. LuTNF-α was also significantly positively regulated by CpG (p = 0.0031) (Fig. 11A). Although, luIL-6 responded higher than luTNF-α, it varied too much to produce statistically significant results for the more moderate inducers of lumpfish HKLs. The ANOVA analysis showed that the examined PAMPs caused significant changes in the expression of both luTNF-α (F (7, 64) = 25.463, p = 3E-16, η^2 = 0.736) and luIL6 (F (7, 64) = 9.218, p = 9E-8, η^2 = 0.500). Also, there was slightly different induction patterns between the genes (F (7, 64) = 2.214, p = 0.044, η^2 = 0.195). Both PAM3CSK4 and poly (I:C) was significant inducers of the average measurement of luTNF-α and luIL-6 expression in HKL (Fig. 11B).

4. Discussion

In this study lumpfish TNF-α and IL-6 were identified and characterized. LuTNF-α exhibited all the hallmark traits of teleost TNF-α including four exons and a TNF signature sequence. In addition to a canonical IL-6 (luIL-6i1) which is similar to IL-6 in other species (Bird et al., 2005; Castellana et al., 2008; Chen et al., 2012; Fujiki et al., 2003; Iliev et al., 2007; Kaneda et al., 2012; Nam et al., 2007; Varela et al., 2012; Wei et al., 2018; Øvergard et al., 2012), an alternative isoform retaining the first intron were identified (luIL-6i2) for the first time in teleost IL-6 sequences. The luIL-6 gene have five exons and four introns, of which intron 1 is alternatively retained in lu-IL6 i2. The first exon in luIL-6 is larger than IL-6 in non-cyclopteidae/lipridae teleosts containing 94 bp while the first exon contains 16 bp commonly (Valera et al. 2012). Further, luIL-6 has a much shorter 5′UTR of 259 bp, while other IL-6 sequences typically have 600 bp (Fig. 5). This suggests that the reading frame have been shifted 78 bp upstream in luIL-6, and a reduction of the 5′UTR have occurred. The close lumpfish relative Tanaka's snailfish also contains an elongated IL-6 n-termini entailing that the elongated exon is a feature shared by *Cyclopteridae* and *Lipridae* (Fig. 6). The alternative isoform contained a potential Caspase 1 cleavage site, and *in sillico* analyses indicated that caspase 1 processing is required to produce a signal peptide containing lu-IL6 i2 form. This may lead to four different functionally fates; I – IL-6 i2 is dysfunctional, II – IL-6 is functional intracellularly, III – IL-6 is functional and secreted independent of the Golgi apparatus, and IV – IL6 i2 is functional and is dependent on caspase 1 processing in order to be secreted. If fate IV is true, the kinetics of luIL-6 would have bimodal distribution where the extracellular levels would fluctuate as a consequence of luIL-I i1 levels, and upon recruitment of the inflammasome the levels would increase as the stores of luIL-6 i2 would be converted to IL-6 that is secretable. These fates should be tested experimentally.

Lu TNF-α and IL-6 contain conserved cysteine residues, as other teleosts, suggesting they have disulfide bridges. In addition, both examined lumpfish genes contains another cysteine residue, shared with a few teleosts.

Teleosts have undergone several WGDs. The first teleost-specific (TS) WGD occurred basally in teleosts approximately 320 million years ago (mya), later a *Salmonidae*-specific (SS) WGD occurred approximately 80 mya and most recently a *cyprinae*-specific (CS) WGD occurred 8 mya, reviewed in Ravi and Venkatesh (2018). These WGD are important events, providing additional genetic raw material to evolution giving rise to novel phenotypes. The most common fate of a duplicated gene by WGD (ohnolog) is non-functionalization through accumulation of deleterious mutations. The alternative to non-functionalization is gene retention. Gene retention can take two forms: sub-functionalization; the splitting of original functions and dividing them between the ohnologs, or neo-funtionalization; one ohnolog retains the original functions while the other adopts innovative functions. Species radiated post SS-WGD have probably retained approximately 50% of their

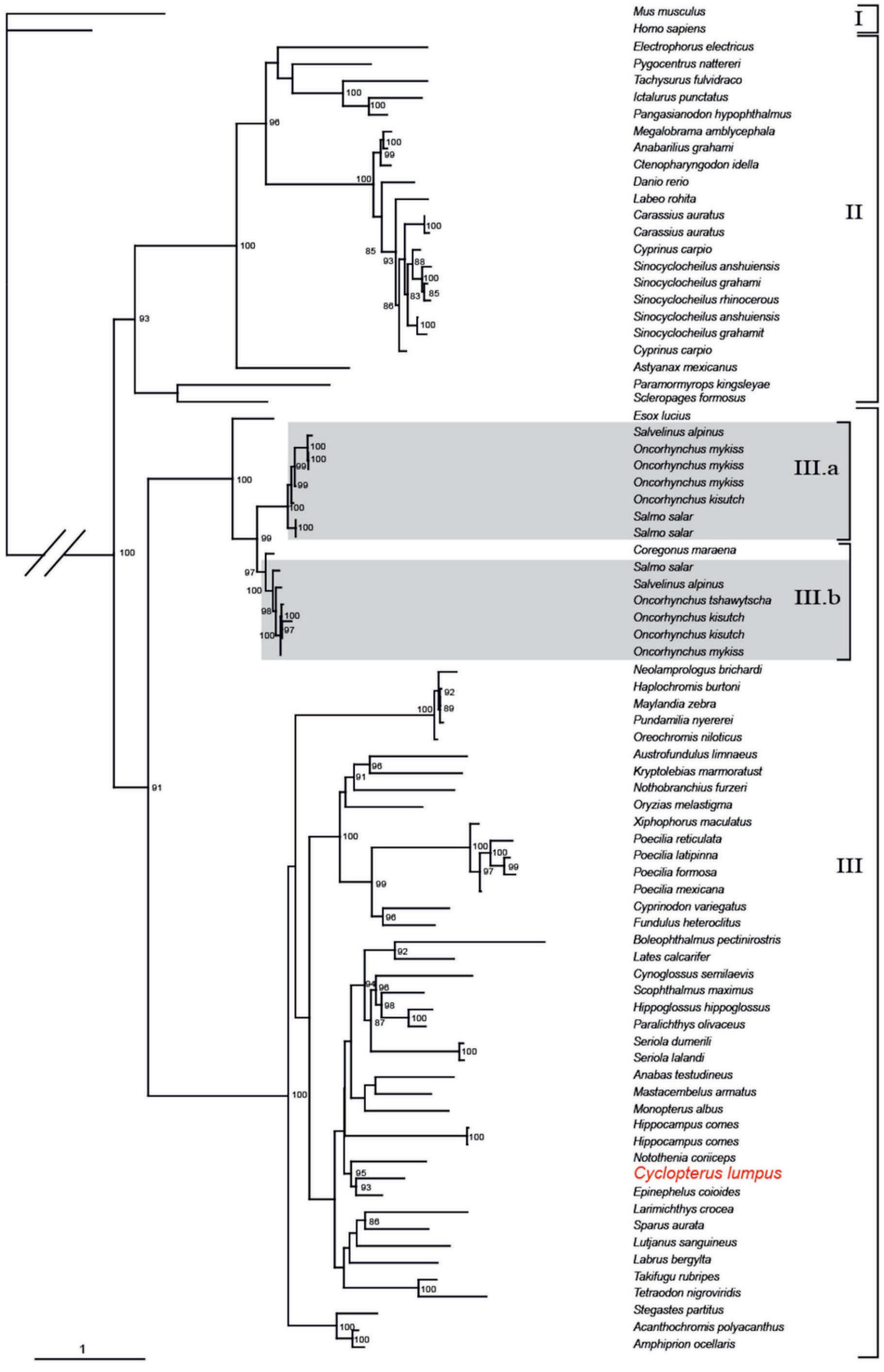

(caption on next page)

Fig. 8. Phylogenetic tree of teleost IL-6 amino acid sequences, utilizing human and mouse as outgroup. Phylogenetic distance is indicated by branch length and decimal numbers (> 0.1), fat bar indicates distance of 1 amino acid per sequence site. Whole numbers refer to bootstrap values (> 80) of 100000 iterations. Accession numbers are given in the full phylogenetic trees (Supplementary Fig. S2). Five clades are indicated by brackets and roman numbers; I – mammalian sequences, II - Elopomorpha, osteoglossomorpha and otomorpha sequences, III – euteleostomorpha sequences, IV and V – intra-*Salmonidae* specific clades. The intra-clades have been shaded with grey boxes.

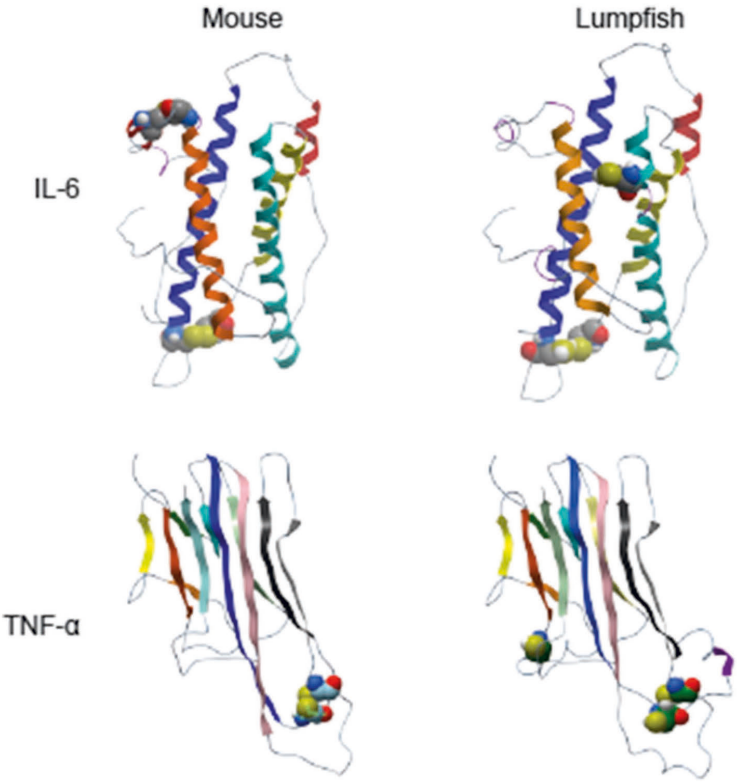

Fig. 9. Tertiary structure models of lumpfish TNF-α and IL-6 peptide sequences using murine templates (respectively: 2tnf.1.C and 2l3y.1.A). α-Helices, β-sheets and sidechain atoms of cysteine residues are varyingly colored, the peptide backbone are in colored in grey.

duplicated genes (Allendorf, 1978), unsurprisingly this have effects in the phylogeny of both TNF-α and IL-6. For IL-6 we observed two intra-*Salmonidae* clades (clade III. a and III. b in Fig. 8) and for TNF-α we observed four intra-*Salmonidae* clades, distributed evenly between one type I clade (clade III. a and III. b in Fig. 7) and one type II clade (clade IV. a and IV. b in Fig. 7) according to the definition by Kadowaki et al. (2009). Due to the members present in both clades, these splits likely rose from the SS-WGD. The IL-6 *Salmonidae* clades are the first evidence of the existence of two IL-6 paralogs within *Salmoniformes.* We also identified two intra-*Cyprinae* clades for TNF-α (clade IV. c and IV. d in Fig. 7). Due to the members present in both clades, it is likely rising from the CS-WGD. Moreover regarding TNF-α, we also observed that all teleosts not belonging to *Elopomorpha*, *Osteoglossomorpha* and *Clupeiiformes* were divided into two clades (clade III and IV in Fig. 7) according to the type affiliation defined by Kadowaki et al. (2009). It is likely that this occurred because of the TS-WGD. The fate of these paralogs had likely not been resolved before the first species were delineated, explaining the more random type affiliation of clade II in Fig. 7. According to the functional suggestion made by Hong et al. (2013) regarding the function of type II TNF-α: "The fish type-II TNF-α has a short stalk that may impact on its enzymatic release or restrict it to a membrane-bound form", the members of clade IV may not function, or have a reduced activity, as a secreted pro-inflammatory cytokine. Highly interestingly all sequences belonging to *Ostariophysi* are exclusively type II TNF-α. This may have profound consequences for the TNF-α biology of the popular model-organism zebrafish and the most important aquaculture species – the cyprinids – of which 44.7 million tonnes were produced in 2017, at a value of 98 billion USD (FAO, 2019).

As expected for important immune genes, both TNF-α and IL-6 is highly expressed in immune organs such as kidney, spleen, thymus and PBL, in lumpfish and other studied teleosts (reviewed Zou and Secombes (2016) and Secombes et al. (2016)). An association of high IL-6 levels and neurological tissues were also observed in lumpfish, as the highest IL-6 expressing organs were brain and eye. High IL-6 levels in brain is also reported from Atlantic halibut (Øvergard et al., 2012). Interestingly, the liver during normal conditions has been identified in several papers as a low TNF-α and IL-6 expressing organ in teleosts. This might be due to the liver being a central vascular organ, and high levels of pro-inflammatory cytokines are known to cause chronical disease. This position is supported by our study as liver was the lowest expressing organ for both genes. In general luTNF-α was significantly

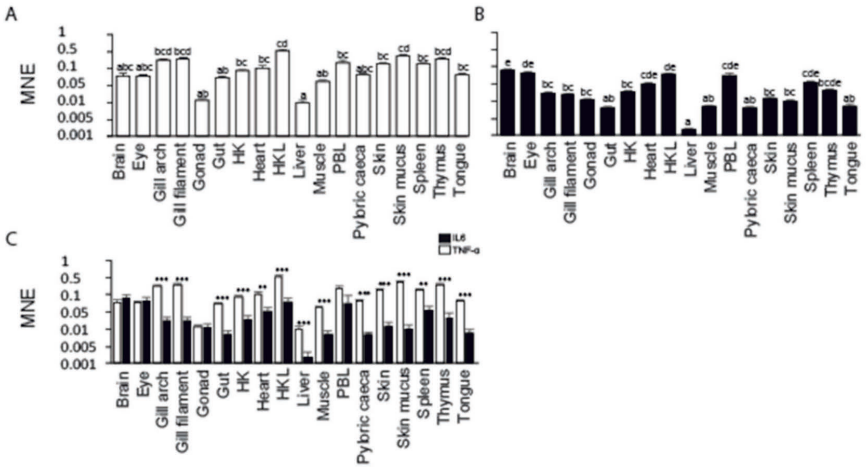

Fig. 10. Tissue distribution of relative expression of luTNF-α and luIL-6 to luRPS20. All data are log10-transfomed in advance of plotting. Error bars denote 1 standard error of the mean (SEM). Differing letters above bars denotes a significant relationship (Bonferroni corrected α-level = 0.05). Full name of abbreviated tissues: HK – Head Kidney, HKL – Head Kidney Leucocytes and PBL – Peripheral Blood Leococytes. **A.** Tissue distribution of IL-6. **B.** Tissue distribution of TNF-α. **C.** Comparison of genes within each tissue. Stars denotes significant comparisons (*p > 0.05, **P > 0.01, ***p > 0.001).

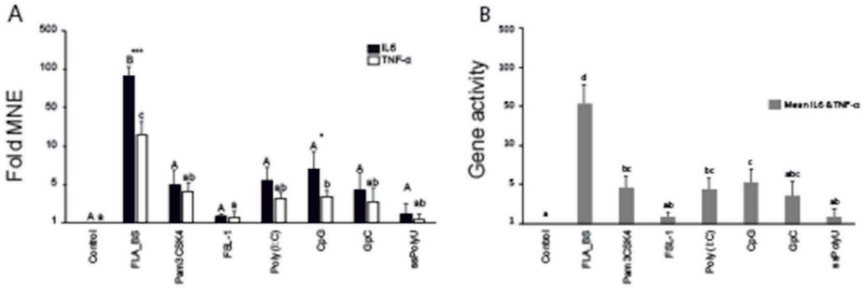

Fig. 11. TNF-α and IL-6 stimulated gene expression post PAMP stimulation in HKLs. All data are log10-transformed in advance of plotting. Error bars denote 1 standard error of the mean (SEM). Differing letters above bars denotes a significant relationship (Bonferroni corrected α-level = 0.05) between PAMPs. **A.** Gene separated PAMP stimulation. Uppercase letters denote TNF-α dependent, lowercase letters denote IL-6 dependent significant relationship between different PAMPs. Stars denotes significant comparisons between genes with the same PAMP treatment (*p > 0.05, **P > 0.01, ***p > 0.001). **B.** PAMP inducible gene activity, in terms of average TNF-α and IL-6 expression.

higher expressed than luIL-6, with the exception of the brain, eye and gonad, suggesting a strong tissue preference of some high TNF-α and/or IL-6 expressing cells or some tissue dependent regulation mechanisms. Moreover, regarding IL-6, several studies have shown high level of IL-6 transcripts in the teleost brain. Øvergard et al. (2012) reported the highest abundance of IL-6 transcripts in the brain, and Varela et al. (2012) revealed a clear appearance of IL-6 transcripts in neuromasts and suggested a role for IL-6 in neurogenesis in zebrafish (Wei et al., 2018). In addition to high expression in immune organs, luTNF-α was also highly expressed in epithelial organs such as; gill, ILT, skin and skin mucus, perhaps reflecting a higher concentration of TNF-α^+ sentinel immune cells in these organs. IL-6 was more potently stimulated than TNF-α, however IL-6 was expressed in a more varyingly manner. These data underpin the known IL-6 behavior; causing more complex downstream effects than TNF-α. Both genes were highly affected by the tested PAMPs.

Knowledge of pro-inflammatory cytokines and innate immunity in lumpfish is interesting from both a comparative and applied perspective. In the current study, we have identified and characterized TNF-α and IL-6 in lumpfish. Since both genes were highly affected by the tested PAMPs, our study suggests that functional feed containing immune stimulants may be an effective prophylactic measure against bacterial and viral diseases in lumpfish. Our analyses form an important basis for further functional analyses and the qPCR assays are valuable to measure effect of immunostimulation and early immune responses in lumpfish. Lumpfish is a novel and economically important species for the farming industry due to its use as cleaner fish. However high mortality caused by bacterial infections is a severe problem. Therefore, to further our understanding of the host-pathogen interactions and the immune system in lumpfish is of major importance.

Acknowledgement

We want to thank Mark M. Powell for valuable discussion about the statistical analyses. The project has been financed by the Research Council in Norway (grant 244148/E40, GTH) and the Univeristy of Bergen.

Appendix A. Supplementary data

Supplementary data to this article can be found online at https://doi.org/10.1016/j.dci.2020.103608.

References

Allendorf, F.W., 1978. Protein polymorphism and the rate of loss of duplicate gene expression. Nature 272, 76–78. https://doi.org/10.1038/272076a0.

Andus, T., Geiger, T., Hirano, T., Northoff, H., Ganter, U., Bauer, J., Kishimoto, T., Heinrich, P.C., 1987. Recombinant human B cell stimulatory factor 2 (BSF-2/IFN-beta 2) regulates beta-fibrinogen and albumin mRNA levels in Fao-9 cells. FEBS Lett. 221, 18–22. https://doi.org/10.1016/0014-5793(87)80344-7.

Baeyens, K.J., De Bondt, H.L., Raeymaekers, A., Fiers, W., De Ranter, C.J., 1999. The structure of mouse tumour-necrosis factor at 1.4 A resolution: towards modulation of its selectivity and trimerization. Acta Crystallogr. Sect. D Biol. Crystallogr. 55, 772–778. https://doi.org/10.1107/s0907444998018435.

Bird, S., Zou, J., Savan, R., Kono, T., Sakai, M., Woo, J., Secombes, C., 2005. Characterisation and expression analysis of an interleukin 6 homologue in the Japanese pufferfish, *Fugu rubripes*. Dev. Comp. Immunol. 29, 775–789. https://doi.org/10.1016/j.dci.2005.01.002.

Bobe, J., Goetz, F.W., 2001. Molecular cloning and expression of a TNF receptor and two TNF ligands in the fish ovary. Comp. Biochem. Physiol. B Biochem. Mol. Biol. 129, 475–481. https://doi.org/10.1016/S1096-4959(01)00353-0.

Camacho, C., Coulouris, G., Avagyan, V., Ma, N., Papadopoulos, J., Bealer, K., Madden, T.L., 2009. BLAST+: architecture and applications. BMC Bioinf. 10, 421. https://doi.org/10.1186/1471-2105-10-421.

Castellana, B., Iliev, D.B., Sepulcre, M.P., Mackenzie, S., Goetz, F.W., Mulero, V., Planas, J.V., 2008. Molecular characterization of interleukin-6 in the gilthead seabream (*Sparus aurata*). Mol. Immunol. 45, 3363–3370. https://doi.org/10.1016/j.molimm.2008.04.012.

Chen, H.H., Lin, H.T., Foung, Y.F., Han-You Lin, J., 2012. The bioactivity of teleost IL-6: IL-6 protein in orange-spotted grouper (*Epinephelus coioides*) induces Th2 cell differentiation pathway and antibody production. Dev. Comp. Immunol. 38, 285–294. https://doi.org/10.1016/j.dci.2012.06.013.

Cock, P.J., Chilton, J.M., Gruning, B., Johnson, J.E., Soranzo, N., 2015. NCBI BLAST+ integrated into Galaxy. GigaScience 4, 39. https://doi.org/10.1186/s13742-015-0080-7.

Dubravec, D.B., Spriggs, D.R., Mannick, J.A., Rodrick, M.L., 1990. Circulating human peripheral blood granulocytes synthesize and secrete tumor necrosis factor alpha. Proc. Natl. Acad. Sci. U.S.A. 87, 6758–6761. https://doi.org/10.1073/pnas.87.17.6758.

Edgar, R.C., 2004. MUSCLE: a multiple sequence alignment method with reduced time and space complexity. BMC Bioinf. 5, 113. https://doi.org/10.1186/1471-2105-5-113.

Eggestøl, H.Ø., Lunde, H.S., Rønneseth, A., Fredman, D., Petersen, K., Mishra, C.K., Furmanek, T., Colquhoun, D.J., Wergeland, H.I., Haugland, G.T., 2018. Transcriptome-wide mapping of signaling pathways and early immune responses in lumpfish leukocytes upon in vitro bacterial exposure. Sci. Rep. 8, 5261. https://doi.org/10.1038/s41598-018-23667-x.

Eimon, P.M., Kratz, E., Varfolomeev, E., Hymowitz, S.G., Stern, H., Zha, J., Ashkenazi, A., 2006. Delineation of the cell-extrinsic apoptosis pathway in the zebrafish. Cell Death Differ. 13, 1619–1630. https://doi.org/10.1038/sj.cdd.4402015.

Fisheries and aquaculture software, 2019. FishStatJ - Software for Fishery and Aquaculture Statistical Time Series. http://www.fao.org/fishery/statistics/global-aquaculture-production/en, Accessed date: 15 November 2019.

Fujiki, K., Nakao, M., Dixon, B., 2003. Molecular cloning and characterisation of a carp (*Cyprinus carpio*) cytokine-like cDNA that shares sequence similarity with IL-6 subfamily cytokines CNTF, OSM and LIF. Dev. Comp. Immunol. 27, 127–136. https://doi.org/10.1016/S0145-305x(02)00074-5.

Garcia-Castillo, J., Pelegrin, P., Mulero, V., Meseguer, J., 2002. Molecular cloning and expression analysis of tumor necrosis factor alpha from a marine fish reveal its constitutive expression and ubiquitous nature. Immunogenetics 54, 200–207. https://doi.org/10.1007/s00251-002-0451-y.

Gauldie, J., Richards, C., Harnish, D., Lansdorp, P., Baumann, H., 1987. Interferon beta 2/B-cell stimulatory factor type 2 shares identity with monocyte-derived hepatocyte-stimulating factor and regulates the major acute phase protein response in liver cells. Proc. Natl. Acad. Sci. U.S.A. 84, 7251–7255. https://doi.org/10.1073/pnas.84.20.7251.

Grayfer, L., Walsh, J.G., Belosevic, M., 2008. Characterization and functional analysis of goldfish (*Carassius auratus* L.) tumor necrosis factor-alpha. Dev. Comp. Immunol. 32, 532–543. https://doi.org/10.1016/j.dci.2007.09.009.

Haugland, G.T., Jakobsen, R.A., Vestvik, N., Ulven, K., Stokka, L., Wergeland, H.I., 2012. Phagocytosis and respiratory burst activity in lumpsucker (Cyclopterus lumpus L.) leucocytes analysed by flow cytometry. PLoS One 7, e47909. https://doi.org/10.1371/journal.pone.0047909.

Hirano, T., Taga, T., Nakano, N., Yasukawa, K., Kashiwamura, S., Shimizu, K., Nakajima, K., Pyun, K.H., Kishimoto, T., 1985. Purification to homogeneity and characterization of human B-cell differentiation factor (BCDF or BSFp-2). Proc. Natl. Acad. Sci. U.S.A. 82, 5490–5494. https://doi.org/10.1073/pnas.82.16.5490.

Hirano, T., Yasukawa, K., Harada, H., Taga, T., Watanabe, Y., Matsuda, T., Kashiwamura, S., Nakajima, K., Koyama, K., Iwamatsu, A., et al., 1986. Complementary DNA for a novel human interleukin (BSF-2) that induces B lymphocytes to produce immunoglobulin. Nature 324, 73–76. https://doi.org/10.1038/324073a0.

Hirono, I., Nam, B.H., Kurobe, T., Aoki, T., 2000. Molecular cloning, characterization, and expression of TNF cDNA and gene from Japanese flounder *Paralychthys olivaceus*. J. Immunol. 165, 4423–4427. https://doi.org/10.4049/jimmunol.165.8.4423.

Hong, S., Li, R., Xu, Q., Secombes, C.J., Wang, T., 2013. Two types of TNF-alpha exist in teleost fish: phylogeny, expression, and bioactivity analysis of type-II TNF-alpha3 in rainbow trout *Oncorhynchus mykiss*. J. Immunol. 191, 5959–5972. https://doi.org/10.4049/jimmunol.1301584.

Hu, W., Wu, W., Sun, S., Liu, Z., Li, A., Gao, L., Liu, X., Liu, D., Deng, H., Zhao, B., Liu, B., Pang, Q., 2019. Identification and characterization of a TNF receptor-associated factor in *Dugesia japonica*. Gene 681, 52–61. https://doi.org/10.1016/j.gene.2018.09.038.

Iliev, D.B., Castellana, B., Mackenzie, S., Planas, J.V., Goetz, F.W., 2007. Cloning and expression analysis of an IL-6 homolog in rainbow trout (*Oncorhynchus mykiss*). Mol. Immunol. 44, 1803–1807. https://doi.org/10.1016/j.molimm.2006.07.297.

Jones, P., Binns, D., Chang, H.Y., Fraser, M., Li, W., Mcanulla, C., Mcwilliam, H., Maslen, J., Mitchell, A., Nuka, G., Pesseat, S., Quinn, A.F., Sangrador-Vegas, A., Scheremetjew, M., Yong, S.Y., Lopez, R., Hunter, S., 2014. InterProScan 5: genome-scale protein function classification. Bioinformatics 30, 1236–1240. https://doi.org/10.1093/bioinformatics/btu031.

Kadowaki, T., Harada, H., Sawada, Y., Kohchi, C., Soma, G., Takahashi, Y., Inagawa, H., 2009. Two types of tumor necrosis factor-alpha in bluefin tuna (*Thunnus orientalis*) genes: molecular cloning and expression profile in response to several immunological stimulants. Fish Shellfish Immunol. 27, 585–594. https://doi.org/10.1016/j.fsi.2008.12.006.

Kalyaanamoorthy, S., Minh, B.Q., Wong, T.K.F., Von Haeseler, A., Jermiin, L.S., 2017. ModelFinder: fast model selection for accurate phylogenetic estimates. Nat. Methods 14, 587–589. https://doi.org/10.1038/nmeth.4285.

Kaneda, M., Odaka, T., Suetake, H., Tahara, D., Miyadai, T., 2012. Teleost IL-6 promotes antibody production through STAT3 signaling via IL-6R and gp130. Dev. Comp. Immunol. 38, 224–231. https://doi.org/10.1016/j.dci.2012.02.002.

Karsch-Mizrachi, I., Takagi, T., Cochrane, G., 2018. The international nucleotide sequence database collaboration. Nucleic Acids Res. 46, D48–D51. https://doi.org/10.1093/nar/gkx1097.

Kim, M.S., Hwang, Y.J., Yoon, K.J., Zenke, K., Nam, Y.K., Kim, S.K., Kim, K.H., 2009. Molecular cloning of rock bream (*Oplegnathus fasciatus*) tumor necrosis factor-alpha and its effect on the respiratory burst activity of phagocytes. Fish Shellfish Immunol. 27, 618–624. https://doi.org/10.1016/j.fsi.2009.07.007.

Knutsen, T.M., 2018. Lumpfish (*Cyclopterus lumpus*) Draft Genome Assembly, Figshare Pubishing Tool. https://doi.org/10.6084/M9.FIGSHARE.7301546.

Krueger, J.M., Fang, J., Taishi, P., Chen, Z., Kushikata, T., Gardi, J., 1998. Sleep. A physiologic role for IL-1 beta and TNF-alpha. Ann. N. Y. Acad. Sci. 856, 148–159. https://doi.org/10.1111/j.1749-6632.1998.tb08323.x.

Laing, K.J., Wang, T., Zou, J., Holland, J., Hong, S., Bols, N., Hirono, I., Aoki, T., Secombes, C.J., 2001. Cloning and expression analysis of rainbow trout *Oncorhynchus mykiss* tumour necrosis factor-alpha. Eur. J. Biochem. 268, 1315–1322. https://doi.org/10.1046/j.1432-1327.2001.01996.x.

Lepen Pleic, I., Secombes, C.J., Bird, S., Mladineo, I., 2014. Characterization of three pro-inflammatory cytokines, TNFalpha1, TNFalpha2 and IL-1beta, in cage-reared Atlantic bluefin tuna *Thunnus thynnus*. Fish Shellfish Immunol. 36, 98–112. https://doi.org/10.1016/j.fsi.2013.10.011.

Letunic, I., Bork, P., 2018. 20 years of the SMART protein domain annotation resource. Nucleic Acids Res. 46, D493–D496. https://doi.org/10.1093/nar/gkx922.

Li, M.F., Zhang, J., 2016. CsTNF1, a teleost tumor necrosis factor that promotes antibacterial and antiviral immune defense in a manner that depends on the conserved receptor binding site. Dev. Comp. Immunol. 55, 65–75. https://doi.org/10.1016/j.dci.2015.10.010.

Li, X., Jia, Z., Wang, W., Wang, L., Liu, Z., Yang, B., Jia, Y., Song, X., Yi, Q., Qiu, L., Song, L., 2017. Glycogen synthase kinase-3 (GSK3) regulates TNF production and haemocyte phagocytosis in the immune response of Chinese mitten crab *Eriocheir sinensis*. Dev. Comp. Immunol. 73, 144–155. https://doi.org/10.1016/j.dci.2017.03.022.

Minh, B.Q., Nguyen, M.A., Von Haeseler, A., 2013. Ultrafast approximation for phylogenetic bootstrap. Mol. Biol. Evol. 30, 1188–1195. https://doi.org/10.1093/molbev/mst024.

Nam, B.H., Byon, J.Y., Kim, Y.O., Park, E.M., Cho, Y.C., Cheong, J., 2007. Molecular cloning and characterisation of the flounder (*Paralichthys olivaceus*) interleukin-6 gene. Fish Shellfish Immunol. 23, 231–236. https://doi.org/10.1016/j.fsi.2006.10.001.

Nguyen, L.T., Schmidt, H.A., Von Haeseler, A., Minh, B.Q., 2015. IQ-TREE: a fast and effective stochastic algorithm for estimating maximum-likelihood phylogenies. Mol. Biol. Evol. 32, 268–274. https://doi.org/10.1093/molbev/msu300.

Ordas, M.C., Costa, M.M., Roca, F.J., Lopez-Castejon, G., Mulero, V., Meseguer, J., Figueras, A., Novoa, B., 2007. Turbot TNFalpha gene: molecular characterization and biological activity of the recombinant protein. Mol. Immunol. 44, 389–400. https://doi.org/10.1016/j.molimm.2006.02.028.

Øvergard, A.C., Nepstad, I., Nerland, A.H., Patel, S., 2012. Characterisation and expression analysis of the Atlantic halibut (*Hippoglossus hippoglossus* L.) cytokines: IL-1beta, IL-6, IL-11, IL-12beta and IFNgamma. Mol. Biol. Rep. 39, 2201–2213. https://doi.org/10.1007/s11033-011-0969-x.

Powell, A., Treasurer, J.W., Pooley, C.L., Keay, A.J., Lloyd, R., Imsland, A.K., Garcia De Leaniz, C., 2018. Use of lumpfish for sea-lice control in salmon farming: challenges and opportunities. Rev. Aquac. 10, 683–702. https://doi.org/10.1111/raq.12194.

Praveen, K., Evans, D.L., Jaso-Friedmann, L., 2006. Constitutive expression of tumor necrosis factor-alpha in cytotoxic cells of teleosts and its role in regulation of cell-mediated cytotoxicity. Mol. Immunol. 43, 279–291. https://doi.org/10.1016/j.molimm.2005.01.012.

Qu, F., Xiang, Z., Zhou, Y., Qin, Y., 2017. A molluscan TNF receptor-associated factor 2 (TRAF2) was involved in host defense against immune challenges. Fish Shellfish Immunol. 71, 105–115. https://doi.org/10.1016/j.fsi.2017.09.076.

Ravi, V., Venkatesh, B., 2018. The divergent genomes of teleosts. Annu. Rev. Anim. Biosci. 6, 47–68. https://doi.org/10.1146/annurev-animal-030117-014821.

Saeij, J.P.J., Stet, R.J.M., De Vries, B.J., Van Muiswinkel, W.B., Wiegertjes, G.F., 2003. Molecular and functional characterization of carp TNF: a link between TNF

polymorphism and trypanotolerance? Dev. Comp. Immunol. 27, 29–41. https://doi.org/10.1016/s0145-305x(02)00064-2.
Savan, R., Sakai, M., 2004. Presence of multiple isoforms of TNF alpha in carp (*Cyprinus carpio* L.): genomic and expression analysis. Fish Shellfish Immunol. 17, 87–94. https://doi.org/10.1016/j.fsi.2003.11.001.
Scholz, F., Glosvik, H., Marcos-Lopez, M., 2018. Cleaner fish health. In: Treasurer, J. (Ed.), Cleaner Fish Biology and Aquaculture Applications. 5M Publishing Ltd., UK, pp. 221–257.
Secombes, C.J., Wang, T., Bird, S., 2016. Vertebrate cytokines and their evolution. In: Malagoli, D. (Ed.), The Evolution of the Immune System. Academic Press, pp. 87–150.
Sievers, F., Higgins, D.G., 2014. Clustal omega. Curr. Protoc. Bioinform. 48, 3. https://doi.org/10.1002/0471250953.bi0313s48. 13.11-13.13.16.
Uenobe, M., Kohchi, C., Yoshioka, N., Yuasa, A., Inagawa, H., Morii, K., Nishizawa, T., Takahashi, Y., Soma, G., 2007. Cloning and characterization of a TNF-like protein of *Plecoglossus altivelis* (ayu fish). Mol. Immunol. 44, 1115–1122. https://doi.org/10.1016/j.molimm.2006.07.281.
Varela, M., Dios, S., Novoa, B., Figueras, A., 2012. Characterisation, expression and ontogeny of interleukin-6 and its receptors in zebrafish (Danio rerio). Dev. Comp. Immunol. 37, 97–106. https://doi.org/10.1016/j.dci.2011.11.004.
Walde, C., Gulla, S., Hansen, H., Mjølnerød, E., Bornø, G., 2019. Fish Health Report 2018. The Health of Cleaner Fish (In Norwegian), vols. 119–125 The Norwegian Veterinary Institute.
Warner, S.J., Libby, P., 1989. Human vascular smooth muscle cells. Target for and source of tumor necrosis factor. J. Immunol. 142, 100–109.
Waterhouse, A., Bertoni, M., Bienert, S., Studer, G., Tauriello, G., Gumienny, R., Heer, F.T., De Beer, T.a.P., Rempfer, C., Bordoli, L., Lepore, R., Schwede, T., 2018. SWISS-MODEL: homology modelling of protein structures and complexes. Nucleic Acids Res. 46, W296–W303. https://doi.org/10.1093/nar/gky427.
Wei, X., Li, B., Wu, L., Yin, X., Zhong, X., Li, Y., Wang, Y., Guo, Z., Ye, J., 2018. Interleukin-6 gets involved in response to bacterial infection and promotes antibody production in Nile tilapia (*Oreochromis niloticus*). Dev. Comp. Immunol. 89, 141–151. https://doi.org/10.1016/j.dci.2018.08.012.
Young, J.D., Liu, C.C., Butler, G., Cohn, Z.A., Galli, S.J., 1987. Identification, purification, and characterization of a mast cell-associated cytolytic factor related to tumor necrosis factor. Proc. Natl. Acad. Sci. U.S.A. 84, 9175–9179. https://doi.org/10.1073/pnas.84.24.9175.
Zhang, A., Chen, D., Wei, H., Du, L., Zhao, T., Wang, X., Zhou, H., 2012. Functional characterization of TNF-alpha in grass carp head kidney leukocytes: induction and involvement in the regulation of NF-kappaB signaling. Fish Shellfish Immunol. 33, 1123–1132. https://doi.org/10.1016/j.fsi.2012.08.029.
Zou, J., Secombes, C.J., 2016. The function of fish cytokines. Biology 5. https://doi.org/10.3390/biology5020023.
Zou, J., Wang, T., Hirono, I., Aoki, T., Inagawa, H., Honda, T., Soma, G.I., Ototake, M., Nakanishi, T., Ellis, A.E., Secombes, C.J., 2002. Differential expression of two tumor necrosis factor genes in rainbow trout, *Oncorhynchus mykiss*. Dev. Comp. Immunol. 26, 161–172. https://doi.org/10.1016/S0145-305X(01)00058-1.
Zou, J., Peddie, S., Scapigliati, G., Zhang, Y., Bols, N.C., Ellis, A.E., Secombes, C.J., 2003a. Functional characterisation of the recombinant tumor necrosis factors in rainbow trout, *Oncorhynchus mykiss*. Dev. Comp. Immunol. 27, 813–822. https://doi.org/10.1016/S0145-305X(03)00077-6.
Zou, J., Secombes, C.J., Long, S., Miller, N., Clem, L.W., Chinchar, V.G., 2003b. Molecular identification and expression analysis of tumor necrosis factor in channel catfish (*Ictalurus punctatus*). Dev. Comp. Immunol. 27, 845–858. https://doi.org/10.1016/S0145-305X(03)00085-5.

III

Interleukin-1 ligands and receptors in lumpfish (*Cyclopterus lumpus* L.): molecular characterization, phylogeny, gene expression and transcriptome analyses

Håvard Ø. Eggestøl[1*], Harald S. Lunde[1], Tim Martin Knutsen[2] and Gyri T. Haugland[1*]

[1] Department of Biological Sciences, Bergen High-Technology Centre, University of Bergen, PO box 7803, NO-5020 Bergen, Norway
[2] Aquagen AS, P.O. Box 1240, NO-7462 Trondheim, Norway

***Corresponding authors:** Havard.Eggestol@uib.no, Gyri.Haugland@uib.no

Keywords: IL-1 beta[1], IL-18[2], nIL-1F[3], IL-1Fm2[4], IL-1R[5], lumpsucker[6], innate immune responses[7], inflammation[8]

Abstract

The interleukin (IL)-1 family play a fundamental role as immune system modulators. Our previous transcriptome-analyses of leukocytes from lumpfish (*Cyclopterus lumpus* L.) showed that IL-1β was among the most highly upregulated genes following bacterial exposure. In the present study, we characterized IL-1 signaling pathways, identified and characterized four ligands of the IL-1 family in lumpfish; IL-1β, IL-18 and the two fish specific IL-1 family members nIL-1F and IL-1Fm2, both at mRNA and gene levels. Furthermore, a comprehensive phylogenetic analysis of 277 IL-1 ligands showed that nIL-1F, in common with IL-1β, likely represents an ancestral gene, as representatives for nIL-1F were found in cartilaginous and lobe-finned fish, in addition to teleosts. This shows that nIL-1F is not exclusively present in teleosts as previously suggested. IL-1Fm2 is identified only in the most evolutionary advanced teleosts, and is most closely related to type I IL-1 β. Furthermore, we have determined transcription levels of the IL-1 ligands in leukocytes and 16 different tissues, and their responses upon *in vitro* stimulation with seven different ligands. In addition, we have identified the IL-1 receptors IL-1R1, IL-1R2, IL-1R4 (ST2/IL-33 receptor/IL-1RL), IL-1R5 (IL-18R1) and partial sequences of DIGIRR and IL-1R3 (IL-RAcP). Identification of immune molecules and description of innate responses in lumpfish is interesting for comparative and evolutionary studies and our study constitutes a solid basis for further functional analyses of IL-1 ligands and receptors in lumpfish. Furthermore, since lumpfish are now farmed in large numbers to be used as cleaner fish for removal of sea lice on farmed salmon, in-depth knowledge

of key immune molecules, signaling pathways and innate immune responses is needed, as the basis for design of efficient immune prophylactic measures such as vaccination.

1 Introduction

Cytokines belonging to the IL-1 family are key mediators of the body's response to microbial invasion, inflammation, immunological reactions and tissue injury. In mammals, the IL-1 family consists of 11 cytokines. Of these, seven have pro-inflammatory activity (IL-1α, IL-1β, IL-18, IL-33, IL-36α, IL-36β and IL-36γ), three are antagonistic (IL-1Ra which is also known as IL-1RN, IL-36RN and IL-38) and one has anti-inflammatory properties (IL-37) (1). Of these, only IL-1β and IL-18, also referred to as IL-1F2 and IL-1F4, respectively, have been identified in teleosts thus far. Fish have, however, multiple paralogues of many cytokines (2) and multiple IL-1β have been identified in several fish species, including channel catfish (3), salmon, trout (4, 5) and carp (3, 6). The genes encoding IL-1β in teleost fish are divided into two groups (type I and II) based on the number of exon/intron and synteny analyses (4, 7). Gene expression studies of IL-1β have shown that it is significantly upregulated in immune tissues, in primary cultures and cell lines in response to immunostimulants, immune response modifiers and/or pathogens (reviewed in (2)).

IL-18 contains an IL-1 like signature sequence and has, like IL-1β, 12 β-sheet strands that form a β-trefoil structure (8). IL-18 has been described in trout and identified in other species like Japanese – and green spotted pufferfish (9) and seabass (2). In trout, like in mammals, IL-18 is constitutively expressed in a wide range of tissues (9). Transcription of IL-18 is not modulated by LPS, poly(I:C) or trout recombinant IL-1β in head kidney leukocytes (HKL) and a macrophage cell line. A shorter, alternative spliced transcript of IL-18 is, on the other hand, upregulated in RTG-2 cells (a fibroblast cell line from rainbow trout) after stimulation with LPS or poly(I:C), suggesting that proteolytic cleavage may be crucial for mediating a biologically active IL-18 in fish, as in mammals (7). Mammalian IL-18 has multiple functions in both innate and adaptive immunity, such as induction of IFN-γ in Th1 and NK cells, promotion of T and NK cell maturation and neutrophil activation. Recently, it was also shown that IL-18 is also involved in Th2 responses (10). In fish, the functions of IL-18 are less understood (9).

The teleost specific IL-1 family members are termed novel IL-1 family members (nIL-1F, also known as nIL-1Fm) and IL-1 family member 2 (IL-1Fm2) (11-14). nIL-1F has been identified in three-spined stickleback (*Gasterosteus aculeatus*), European seabass (*Dicentrarchus labrax*), Japanese flounder (*Paralichthys olivaceus*), Nile tilapia (*Oreochromis niloticus*), southern platyfish (*Xiphophorus maculatus*), Japanese puffer (*Takifugu rubripes*), spotted green pufferfish (*Tetraodon nigroviridis*), Japanese rice fish (*Oryzias latipes*), rainbow trout (*Oncorhynchus mykiss*), zebrafish (Danio rerio), channel catfish (*Ictalurus punctatus*) and grass carp (*Ctenopharyngodon idella*) (11-14). Thus far, IL-1Fm2 has only been identified in the most evolutionary advanced fishes, such as gilthead seabream (*Sparus aurata*), European seabass, three-spined stickleback, Nile tilapia, southern platyfish, Japanese rice fish and Japanese flounder (11). nIL-1F and IL-1Fm2 show low sequence identity with IL-1β, but contain the IL-1 family signature [FC]-x-S- [ASLV]-x(2)- [FYLIV]- [LI]- [SCA]-T-x(7)- [LIVM] (prosite, PDOC00226) and a β-trefoil structure with β -sheets. It has been suggested that nIL-1F antagonizes IL-1β activity similar to IL-1Ra in mammals (13-15).

In mammals, IL-1β and IL-18 are produced as pro-peptides and require proteolytic cleavage for activation. The IL-1β precursor is cleaved typically with cytosol caspase-1/ interleukin-1 converting enzyme (ICE) between the aspartate amino acid at position 116 and alanine at position 117 to form mature proteins. Alternatively, pro-IL1β can also be cleaved by enzymes like granzyme A, trypsin, chymase, elastase, cathepsin G, collagenase, matrix metalloproteases or serine proteases (2). Fish and other non-mammalian species do not have the conserved Asp^{116}. Caspases are, however, also involved in processing of IL-1 β in fish. In zebrafish, Caspases A and B cleave IL-1β at position D104 and D122. Alternatively, zebrafish caspase B cleaves IL1β at position D88 instead of D104 (16). Sea bass caspase-1 cleaves proIL-1β at D100 (17). It has been suggested that IL-18 in fish, as in mammals, needs proteolytic processing to become a functionally active protein. Potential ICE cut sites have been predicted for IL-18 and nIL-1F, but functional analyses are required to verify this (9, 13, reviewed in 7). Gilthead seabream IL-1Fm2 is processed before being released, but the mechanism is not known as it does not have a conserved caspase-1 processing site and neither inhibitors of pan-caspase nor caspase-1 inhibit its processing (11).

The IL-1 receptor (IL-1R) family comprises 10 members and includes cytokine-specific receptors, co-receptors and inhibitory receptors (18-20). A novel receptor nomenclature has been

proposed by Boraschi et al. (18) and will be followed here. There are two types of receptors that bind mammalian IL-1α/β: type I IL-1 receptor (IL-1R1) which binds to the accessory receptor protein IL-1R3 (also known as IL-1RAcP and IL-1RAP) and type II IL-1 receptor (IL-1R2), which also binds to IL-1R3. IL-1R2 is a decoy receptor that is structurally incapable of signaling (21) due to the lack of an intracellular domain. Thus, IL-1R2 serves as a negative regulator, both by competing with IL-1R1 for IL-1β and by complexing with IL-1R3, preventing dimerization of IL-1R3 with IL-1R1. Interaction between IL-1R1 and IL-1R3 is needed for downstream signaling from IL-1R1 after IL-1β binding. Both IL-1R1 and IL-1R2, in addition to IL-1R3 are described in fish, such as miiuy croaker (*Miichthys miiuy*), grass carp, Atlantic salmon (*Salmo salar*), orange-spotted grouper (*Epinephelus coioides*), gilthead seabream, rainbow trout, Japanese flounder (22, 23, 24, reviewed in 7). The IL-18 receptor in mammals consists of two subunits, IL-1R5 (also known as IL18Rα) and IL-1R7 (IL-18Rβ), while in fish, only one IL-18 receptor, IL-18R1, has been described thus far (7). In mammals, the soluble IL-18-binding protein (IL-18BP) regulates IL-18 activity (25). In grass carp, IL1R8, two isoforms of IL1R9 and IL1R10 have also been described (24). nIL-1F binds to the type I IL-1β receptor competing with IL-1β (14). The receptor for IL-1Fm2 is not yet identified.

The aim of the current study was to identify and characterize IL-1 family ligands and receptors in lumpfish, as well as the signaling pathways NF-κB and MAPK to gain further insight into the role of the IL-1 family in innate immunity. In addition, a comprehensive phylogenetic analysis was performed to investigate the evolution of IL-1 ligands.

2 Materials and methods

2.1. *Fish and rearing conditions*

Unvaccinated, farmed lumpfish were provided by Fjord Forsk Sogn AS, a commercial breeder in Sogn & Fjordane County, Norway and kept in a 500 L tank in the rearing facilities at the Industrial and Aquatic Laboratory (ILAB) at Bergen High-Technology Centre under normal optimal rearing conditions, with an average temperature of 10.7 ±1.7°C, oxygen level of 88 ± 6.4 % (n= 147 days),

salinity of 34 PPT and light regime 12 h light: 12 h dark. The fish were fed with dry commercial feed (Gemma Silk (3 mm) Skretting, Norway).

2.2. Tissue sampling and homogenization

The fish (282.7 ± 56.5 g and 18.5 ±1.1 cm) were randomly selected and killed by a sharp blow to the head, which is an appropriate procedure under Norwegian law. Peripheral blood (0.7 mL) was collected from the *vena caudalis* and transferred to heparinised containers. Skin mucus was harvested by scraping a sterile scalpel blade along the most lateral skin on the left side of the fish. The skin sample was dissected from a square, were the cranial-ventral corner touched the third skin knot. The muscle sample was harvested from the underlying white musculature. Thymus was harvested by scraping the most cranial-dorsolateral surface tissue of the mouth cavity with a sterile scalpel. Gill tissues, sampled from the second gill arch on the left side, consisted of filaments from the most caudal point on the gill arch. The gill arch sample consisted of the most proximal millimeter of the gill filament, intra-branchial tissue and the gill arch. The tongue, liver, spleen, pyloric caeca, heart and gut were dissected out aseptically. The posterior piece of the testes or ovary constituted the gonad sample. A posterior section of the right lobe constituted the head kidney sample. The eye sample was the area of the eye surrounding the end of the *nervus opticus*. A section of the *medulla oblongata* constituted the brain sample. Homogenization of the tissue-samples was performed as described previously (26). Briefly, up to 40 mg of tissue were transferred to FastPrep Tubes containing SS metal beads lysing matrix (MP biomedicals) and lysisbuffer and homogenized in a FastPrep-24 5G homogenizator (MP biomedicals).

2.3 Isolation of leukocytes and in vitro stimulation

Peripheral blood leukocytes (PBL) and head kidney leukocytes (HKL), were isolated from lumpfish (n=8) using discontinuous Percoll gradients as described previously (27). A gentleMACS Dissociator (Miltenyi Biotec) was used to homogenize of the head kidney tissues. For the *in vitro* stimulation experiment, HKLs (4 x 10^7 cells/well) were added to 24-well plates and stimulated for

18 hours at 15 °C with seven different ligands: 0.3 µg/ml triacylated lipopeptide (Pam3CSK4, Invivogen), 0.1 µg/ml diacylated lipopeptide (FSL-1, Invivogen), 20 µg/ml flagellin (FLA-BS, Invivogen), 50 µg/ml poly(I:C) (tlrl-pic, Invivogen), 10 µg/mg ssPoly (U)/LyoVec (Invivogen), 2 µM CpG (Eurogentec) or 2 µM GpC (Eurogentec). A leukocyte sample with medium added instead of ligands represented the non-stimulated control.

2.4. RNA isolation and cDNA synthesis

Total RNA was isolated from tissues and leukocytes using GenElute Mammalian Total RNA miniprep kit (Sigma) and treated with DNase I (Sigma) according to the manufacturer's instructions. A maximum of 2500 ng RNA was used per 10 µl DNase reaction. To ensure that all traces of genomic DNA were removed from the samples and to validate the integrity and quality of the RNA, DNase treated RNA was assessed on a 1% agarose gel containing GelRed (Biotium) and quantified in a NanoDrop®ND 1000 UV-Vis spectrophotometer (NanoDrop Technologies). Subsequently, the RNA was reverse transcribed into cDNA using a qScript cDNA synthesis kit (Quanta Biosciences) according to the manufacturer's instructions using maximum 1000 ng RNA per 20 µl reaction. The synthesized cDNA samples were stored at -20°C.

2.5. Quantitative PCR (qPCR)

qPCR was performed using a C1000 Touch Thermal Cycler with CFX96 Real-Time System (BioRad) using SYBR green JumpStart Taq Ready Mix kit for quantitative PCR (Sigma) and custom desalt primers from Sigma (see Table 1). The PCR reaction contained 12.5 µl 2xSYBR Green JumpStart Taq Ready Mix, 10 µl cDNA (2 ng/µl for target genes and 0.2 ng/µl for reference genes), 1 µl (10 mM) forward and reverse primer and 0.5 µl nuclease and salt free water (Sigma). The reactions were thermo-cycled for 94 °C at 5 minutes, followed by 40 cycles of 15 seconds at 94 °C and 1 minute at 60 °C, until melt curve analysis were performed. Two-fold dilution curves (80 ng-0.16 ng for the target and reference gene) were made for efficiency (E) calculations. Three parallel reactions were performed for all genes. Negative controls without template (NTC) and

cDNA reactions without reverse transcriptase (-RT) were included for all master mixes. The –RT reaction ensured that the primers did not bind non-specifically.

The gene expression in normal tissues were calculated by the ΔCq-method (Equation 1). The *in vitro* stimulation experiment was calculated by the ΔΔCq-method (Equation 2). All gene expression calculations utilized the housekeeping gene RPS20 as reference gene. Stability of the reference gene across tissues is shown in Supplemental Table 1.

Equation 1: $$\Delta Ct_x = \frac{E_{target}{}^{-\bar{x}}}{E_{reference}{}^{-\bar{x}}}$$

Equation 2: $$\Delta\Delta Ct_{xy} = \frac{\frac{E_{target}{}^{-\bar{x}}}{E_{reference}{}^{-\bar{x}}}}{\frac{E_{target}{}^{-\bar{y}}}{E_{reference}{}^{-\bar{y}}}}$$

2.6. Statistics

qPCR data were analyzed by two-way ANOVA in IBM® SPSS® Statistics (version 25.0.0.2) on log10 transformed data. The normal tissue data were followed up by Bonferroni corrected pairwise comparisons and the ligand stimulation data were followed up by Tukey's honest square difference post hoc test. F values refers to the F statistic, df values refers to the degrees of freedom, p values refer to the probability that the statistical summary of the population is equal or more extreme than the observed values of the sample, given that the null hypothesis is true ($p < 0.05$ is considered significant), and η^2 refers to the effect size, or how much the relevant variable explains the observed variance.

2.7 Sequence identification and database mining

Individual transcripts in the transcriptome were annotated with BLAST matches, protein domains and GO terms using the Trinotate toolkit (https//trinotate.github.io). The annotated transcriptome and differential gene expression (DEG)-data have been submitted to Array Express under accession number E-MTAB-6388.

194 Automatic annotated transcripts of IL-1β and nIL-1F in lumpfish were identified in a
195 previous study (34). Further searches within the transcriptome using known sequences of IL-18,
196 IL-1Fm2 and IL-1 family receptors from other fish species, gave hits to several transcripts.
197 Candidate sequences were identified by BLASTX against NCBI's non-redundant database and by
198 phylogenetic analysis, which included all known full teleost sequences and swiss-prot entries for
199 humans and mice. In order to perform multiple sequence alignment and phylogenetic analysis,
200 sequences were mined from NCBI's protein database. Analysis of IL-1 family ligands was
201 restricted to those from teleosts and the top 100 BLASTP hits using the lumpfish IL-1 family ligand
202 sequences against NCBIs non-redundant database, in addition to sequences from (13) and (11).
203 Replicate sequences, sequences <100 aa (amino acids) and >400 aa and severely deviating
204 sequences were removed. This constituted a database of 273 teleost IL-1 family sequences, in
205 addition to IL-1 and IL-18 sequences from humans and mouse (Suppl. Fig 5 and Suppl. Table 4).

206

207 *2.8. Bioinformatic analysis*

208 Multiple sequence alignment was performed using MUSCLE (28) in UGENE (29). The
209 phylogenetic maximum likelihood tree was constructed with IQ-TREE (30) using automatic model
210 selection (31), followed by 100 000 bootstraps (32). An overview of species and gene identifier
211 (GI) numbers included in the phylogenetic analysis are included in Suppl. Figure 5 and Suppl.
212 Table 4. Domain predictions were performed using InterproScan (33). Transcriptome-wide DEG
213 analyses of the signaling pathways NF-κB (KEGG map04064) and MAPK (KEGG map 04010)
214 upon bacterial exposure were performed using data generated in Eggestøl et al. (34) and KEGG
215 pathway analysis/KEGG Mapper tool as described previously (34). The synteny analyses were
216 performed using Genomics (35). β-sheets in IL-1 β and IL-18 were identified using the human
217 sequences as reference. The β-sheets in nIL-1F and IL-1Fm2 were predicted using BETApro
218 Protein Beta Sheet Predictor (http://betapro.proteomics.ics.uci.edu/). Prediction of enzymatic cut
219 sites in the lumpfish sequences were predicted using Peptide cutter
220 (https://web.expasy.org/peptide_cutter/).

221

2.9. Gene sequencing

The gene sequences of the four IL-1 family members were obtained from genome assembly (36) and/ or Sanger sequencing. A full-length IL-1 β gene was found in the assembled genome. The IL-18, nIL-1F and IL-1Fm2 genes were PCR amplified from genomic DNA (isolated using Pure Core kit A, Quiagen, according to the manufacturer's instractions) using Phusion High-Fidelity DNA polymerase (Thermo scientific) and primers shown in Table 1. PCR products were purified by gel extraction (E.N.Z.A., Omega bio-tek) and sequenced at the DNA Sequencing Facility at the High Technology Centre in Bergen, Norway. The gene structure and exon-intron boundaries were determined by comparing transcripts from RNA sequencing of head kidney leukocytes from lumpfish (34) with scaffolds from genome assembly (36) and/or sequences obtained by Sanger sequencing.

2.10. Ethics statement

The present work with lumpfish was conducted according to the approved national guidelines and performed according to prevailing animal welfare regulation. Rearing of fish under normal, optimal conditions does not require ethical approval under Norwegian law (FOR 1996-01-15 nr 23). All work in this manuscript has been done on tissues and cells harvested from dead fish. Fish were sacrificed with a sharp blow to the head, which is an appropriate procedure under Norwegian law.

3 Results

3.1. DEG analysis of the NF-kappa B – and MAPK signaling pathways

IL-1 β was the most significantly upregulated gene in lumpfish leukocytes 24 hrs post bacterial exposure (hpe) and was highly upregulated at both 6 and 24 hpe ((34); Fig. 1, Supplemental Table 2 and 3). To get further insight into the IL-1 signaling pathways, transcriptome-wide analysis of the NF-kappa B– and MAPK pathways were performed (Fig. 1A, B). Most members of both pathways were identified in lumpfish (Fig. 1, Supplemental Table 2 and 3). The DEG analysis upon

bacterial exposure showed that the transcript level of genes belonging to the canonical NF-kappa B pathway (e.g. IL-1 β, IL-8, TNFα and COX2) were most highly upregulated compared with the atypical and non-canonical pathway (Fig. 1A and Supplemental Table 2), and the level of expression was higher at 24 hpe than 6 hpe (Fig. 1A). Interestingly, IL1R2, the decoy receptor was among the most highly upregulated genes. Three TNFAIP3 transcripts were identified in the lumpfish transcriptome and these were regulated differently (Fig. 1A, Supplemental Table 2), one (TNFAIP3a) being highly upregulated (Log2 fold 2.9 and 3.5 at 6 and 24 hpe, respectively), one (TNFAIP3c) strongly downregulated at 24 hpe (Log2 fold 0 and –2.6 at 6 and 24 hpe, respectively) and one (TNFAIP3b) that was not differentially regulated. In addition to TNFAIP3c, the transcripts that were most downregulated were the lymphotoxin beta receptor TNFR superfamily member 3 (TNFR3), Tumor necrosis factor receptor superfamily member 5 (CD40) and tumor necrosis factor receptor superfamily member 11A (TNFSF11a).

In the MAPK signaling pathway, transcription factors belonging to the classical MAP kinase pathway, JNK and p38 MAP kinase pathway and ERK5 pathway were upregulated. These included; brain-derived neurotrophic factor (BDNF), nuclear factor of activated T cells 3 (NFAT4), serum response factor (SRF) and Dual specificity Map kinase phosphatase (Fig. 1B, Supplemental Table 3). Activation of these transcription factors leads to proliferation, differentiation and inflammation. The most downregulated transcripts in the MAPK signaling pathway were platelet-derived growth factor subunit B (PDGFB), transforming growth factor beta-3 (TGFB3) and the mitogen-activated kinases MAP3K12 and MK04.

3.2. Identification and molecular characterization of IL-1 family ligands in lumpfish

In the previous transcriptome-wide analysis of lumpfish leukocytes, transcripts of IL-1β and a partial sequence of a new IL-1 family member (nIL-1F) were identified ((34)). To identify and get further insight into the ligands of the IL-1 family, sequences of known IL-1 family members from other teleost species were used as query sequences to search the lumpfish transcriptome. Using this approach, another transcript of nIL-1F was identified, as well as IL-1Fm2 and IL-18. All four family members contained the IL-1 family domain (Fig. 2A). The IL-1 β transcript consisted of

1711 bp with a 759-bp open reading frame encoding a full-length protein of 252 aa (Fig. 2A, Supplemental Fig. 1). The deduced protein sequence contained an interleukin-1 propeptide (IPR00302) and the IL-1 family domain (IPR000975) (Fig. 2A). IL-1 β showed highest similarity to IL-1 β of the sculpin *Trachidermus fasciatus* (Blast E- value 1E-142, 78% identity). An IL-18 candidate was identified. The transcript of 2171 bp contained a 594-bp open reading frame encoding a 198 aa sequence that contained the IL-1 family domain and the IL-18 domain (IPR015529) (Fig. 2A, and Supplemental Fig. 2). The blast hits with highest scores were five uncharacterized proteins and IL-18 from *Miichthys miiuy*. To obtain the full-length nIL-1F, two overlapping transcripts were merged. The sequence of the merged transcript, confirmed by Sanger sequencing, was 1322 bp and contained an open reading frame of 1059 bp encoding a 352 aa sequence. The start code was determined based on identification of a Kozak sequence (5'-G/ANNAUGG-3'). nIL-1F contained the IL-1 family domain and a PDZ domain (IPR001478) (Fig. 2A, Supplemental Fig. 3). The sequence showed highest similarity to an uncharacterized protein of *Notothenia coriiceps* (Blast E value 0.0, 71% identity) and nIL-1F in *Gasterosteus aculeatus* (BLAST E value 2E-158, identity 71%). The transcript encoding the IL-1Fm2 (1168 bp) contained an open reading frame of 543-bp encoding a 180 aa sequence. The lumpfish IL-1Fm2 sequence was shorter than IL-1Fm2 sequences in *Paralichthys olivaceus* and *G. aculeatus* (Supplemental Fig. 4). A stop codon after the first predicted 11 amino acids was confirmed by Sanger sequencing. The sequence contained an IL-1 family domain (Fig. 2A). The sequence showed highest similarity to an interleukin-1 receptor antagonist protein in *Larimichthys crocea* (E- value 1<e-58, 52% identity). Caspase-1 and thrombin cut sites were only predicted in the nIL-1F sequence (Fig. 2A)

3.3. Gene structure of the IL-1 family ligands in lumpfish

Two types of IL-1β exist in fish, type I and type II, based on exon- intron structure. To determine the subtype of IL-1β in lumpfish, the gene sequence was analyzed. The IL-1 β gene in lumpfish was 3547 bp, contained five exon and four introns and is therefore a type II (Fig. 2B, Supplemental Fig. 6). IL-18 had five exons and four introns, including the conserved short exon 2 and a predicted cut site (Fig. 2B, Supplemental Fig. 7). The nIL-1F gene consisted of eight exons and seven introns

(Fig. 2B, Supplemental Fig. 8). IL-1Fm2 consisted of six exons and five introns. Interestingly, compared with other IL-1Fm2, the translated lumpfish sequence was much shorter (Fig. 2B, Supplemental Fig. 4, Supplemental Fig. 9). A stop codon was present 33 bp downstream of the start codon followed by a deletion of 270 bp that corresponded to almost two whole exons (Supplemental Fig. 4). The sequence upstream of the stop codon encoded MSDFDLSQALKR, which is similar to other IL1Fm2 sequences (Supplemental Fig. 4), showing that the stop codon and deletion is unique for lumpfish. Sanger sequencing confirmed the stop codon and deletion. Therefore, we predict that the lumpfish IL-1Fm2 consist of four exons. The first one is very short (MLQHD, due to the deletion) followed by three exons that are conserved in IL-1Fm2 sequences.

Comparison of gene structure of lumpfish IL-1 β with other type I and type II sequences confirmed that lumpfish have a type II IL-1 β (Fig. 2C). Also, the lumpfish sequence has the same intron phases as the other IL-1 β sequences. Interestingly, the typical gene structure of IL-1Fm2 sequences are very similar to the type I sequences (Fig. 2C). Due to deletion, only the three exons in the C-terminal are similar to other sequences (Fig. 2C, Supplemental Fig. 4). Lumpfish IL-1Fm2 also have an extra exon N-terminal compared with other sequences, but that may be an artifact as this region consists exclusively of “g” and “t” (Supplemental Fig. 4).

3.4. Synteny

Synteny analyses were performed for the IL-1 ligands. The locus of IL-1β in lumpfish was present on scaffold jcf7180000034562. The 5’ and 3’-end of the lumpfish IL-18 gene was present on two different scaffolds; jcf7180000029304 (position 1 to 1554) and jcf7180000030343 (position 1542-4248). Sanger sequencing was performed to obtain a full-length IL-18 gene, and the two scaffolds were combined. IL-1Fm2 was present in scaffold jcf7180000030343. nIL-1F was found on scaffold 53, contig 235.

There is a lack of well-characterized genomes from species closely related to lumpfish. In the comparative analysis, Japanese medaka, turbot, zebrafish and human were chosen as they all provide well characterized genomes of varying divergence time, approximately; 125, 125, 250 and 425 million years ago, respectively. The synteny of IL-1β was conserved among type II sequences

and located in proximity to the genes death-associated protein kinase 1 (DAPK1), phospholipid-transcporting ATPase (ATP8B5A), cyclin and CBS domain divalent metal cation transport mediator 4b (CNMM4B), cytokskeleton-associated protein 2-like (CKAP2L), purine-rich element binding protein Bb (PURBB) and histone H2A (H2AFVA) (Fig. 3). In humans, the synteny of IL-1β is different from fish, and only IL-1β and CKAP2L are shared. Human IL-1β clusters together with IL-1α and other IL-1 family ligands. Synteny of the lumpfish IL-18 scaffolds, were similar to other species, except that succinate dehydrogenase complex, subunit D, integral membrane protein a (SDHDA) and l-amino acid oxidase (LAAO) have shifted position (Fig. 3). Further, the upstream context lacks tricalbin-1 (TCB1) and sortilin related receptor 1 (SORL1). Lumpfish IL-1Fm2 possessed the same synteny as turbot, both lacking sialidase-3 (NEU3B) present in Japanese medaka (Fig. 3). Synteny analysis of nIL-1F was identical for all the species.

3.5 Phylogenetic analysis of IL-1 family members

To investigate the relationships among the IL-1 family ligands, a phylogenetic tree was constructed (Fig. 4). All full-length teleost (taxid: 32443) IL-1 sequences available in NCBI, IL-1 ligand sequences described in the literature (11, 13), and human and mouse sequences (Supplemental Fig. 5, Supplemental Table 4) were included. In addition, as many of the fish sequences are as yet uncharacterized, we included all full-length teleost hits with adequate quality from a BLAST search using the lumpfish sequences as query sequences. The phylogenetic tree showed that nIL-1F and IL-1β, share a common ancestor. (Fig. 4). The nIL1F1 clade is a separate clade with sequences from all groups of fish, including cartilaginous (Chondrichthyes) and lobe-finned fish (Sarcopterygii). This suggest that nIL-1, as IL-1β, may be an ancestral gene. IL-1β is divided into two subgroups; type II found in Neoteleostei and Protacanthopterygii, and type I found in species belonging to Elopomorpha, Otomorpha and Osteoglossomorpha (EOO), and IL-1β3 which thus far only are described from Salmoniformes. Interestingly, the IL-1β sequences from Clupeiformes cluster together with IL-1β3. IL-1Fm2, which has only been reported from modern teleosts belonging to Neoteleostei shows highest similarity to IL-1 β type I. The lumpfish sequences grouped within their expected group.

361

362 *3.6. Expression pattern of IL1β, IL-18, nIL-1F and IL-1Fm2 in tissues and leukocytes.*

363 mRNA transcript levels of the four IL-1 family ligands were measured by qPCR in sixteen tissues,
364 as well as PBL and HKL. A two-way ANOVA analysis, investigating the effect of gene and tissue,
365 showed that there was a significant effect of both gene ($F(3, 372) = 44.996$, $p = 7.8E\text{-}25$, $\eta^2 =$
366 0.266) and tissue ($F(17, 372) = 2.458$, $p=0.001$, $\eta^2 = 0.101$). An interaction effect was, however,
367 not observed ($F(51, 372) = 0.547$, $p = 0.995$, $\eta^2 =0.070$) between the factors, meaning that the
368 genes were expressed in the different tissues, but at different levels. After examining the Bonferroni
369 corrected post hoc multiple comparisons and the column chart of the tissue-independent gene
370 expression, it became apparent that the level of IL-18 and nIL-1F transcripts are statistically
371 significantly higher than IL-1β and IL-1Fm2 transcripts ($p< 0.001$) throughout the tested tissues.
372 IL-1β expression was highly variable, from an MNE value of 0.04 in tongue to more than 2.3 in
373 PBL, skin mucus, head kidney, HKL and spleen (Fig. 5 A). IL-18 and nIL-1F were abundant in
374 most of the tissues analyzed (Fig. 5 B, C). High levels of IL-18 and nIL-1F transcripts were detected
375 in skin and skin mucus, but surprisingly, also in muscle. The lowest detected level of nIL-1Fm was
376 in the gonads. In contrast to IL-1β, the lowest values of IL-18 were in head kidney, HKL and
377 spleen. The relative expression of IL-1Fm2 was generally low, except in the liver (Fig. 5 D).
378 Comparisons of the average transcript levels showed that the levels of IL-1β and IL-1Fm2 are
379 statistically significantly lower than IL-18 and nIL-1F (Fig. 5E).

380

381 *3.7. Modulation of IL1 β, nIL-1F, IL-1Fm2 and IL-18 expression in head kidney leukocytes after*
382 *stimulation with various ligands in vitro*

383 Transcriptome analyses of head kidney leukocytes upon bacterial exposure, showed that only IL-
384 1β and, to a lesser extent, nIL1F, was upregulated (33, Fig. 1A)). IL-18 was slightly, but
385 significantly, downregulated (0.3-fold change) and IL-1Fm2 was not regulated. To compare the
386 results from RNA sequencing (transcriptome data) with qPCR, we made cDNA of the RNA
387 samples (n=4) in the transcriptome analyses and performed qPCR. The results from RNA
388 sequencing correlated well with qPCR analyses (R^2-value= 0.988) (Fig. 6A). To further our

understanding of the IL-1 family members' role in innate immunity, we stimulated head kidney leukocytes with seven different ligands (Fig. 6B). IL-1β and nIL1F1 were most highly upregulated upon exposure to flagellin (FLA_BS), 100 and 12.7 fold change, respectively (p-values < 0.0001). These two genes were also highly upregulated upon exposure to poly (I:C) and CpG. nIL1Fm2 and IL-18 did not respond highly to any of the ligands, but they were both significantly upregulated upon exposure to Pam3CSK4 which is a synthetic triacylated lipopeptide (Fig. 6B). The correlation analyses between the genes, showed that the expression levels of IL-1β and nIL1F are similar. IL18 and IL-1Fm2 are similar to each other, but different from the two aforementioned genes (Fig. 6B). In summary, flagellin had the most highly significant effect on the HKL ($p < 0.001$), followed by CpG, Pam3CSK4 and poly (I:C) (Fig. 6). GpC, the diacylated lipoprotein FSL-1 and Poly(U) did not have a statistic significant effect on the expression levels of the IL-1 family members.

3.7. Identification of IL-family member receptors.

In the lumpfish transcriptome, full-length sequences of the receptors IL-1R1 (two transcripts), IL1R2, IL1R3 (also known as IL-1RAcP), IL-1R4 (also known as ST2, which bind IL-33), IL-1R5 (also known as IL-18Rα) IL-1R9 (also known as TIGIRR-2) and DIGIRR were identified (Table 3 and Fig. 7). Both IL-1R1 transcripts were significantly upregulated at 24 h post bacterial exposure. IL-1R2 was also significantly upregulated at both times points. Interestingly, both IL-1R4 and IL-1R5 were down regulated. As shown in Figure 7, the full-length IL-1R1s, IL-1R3, IL-1R4, IL-1R5 and IL-1R9 have a signal peptide, three immunoglobulin domains, a transmembrane region and an intracellular domain. IL-1R2 is similar, but lacks the intracellular domain needed for downstream signaling. Furthermore, a lumpfish transcript showing high similarity to the C-terminal of fish specific IL-1R like family member double Ig-1R related molecule (DIGIRR) was identified (Table 3), having the conserved amino acid sequences ISRSRRLIV and FWKELALAMP, similar to other described DIGIRR sequences (35). IL-18R2 and IL-36R were searched for using known sequences from teleosts but were not found in the transcriptome.

Discussion

In a previous transcriptome-wide study of lumpfish leukocytes, we identified IL-1β and a partial sequence of a new interleukin-1 family member, nIL-1F. Both were upregulated upon bacterial exposure (34). To further our understanding of the biological processes involving IL-1β, we characterized the NF-kB and MAPK pathways by identifying signaling components and performed differential gene expression analyses upon bacterial exposure. Most components of the signaling pathways were found in the lumpfish transcriptome. In addition to the pro-inflammatory cytokines (IL-1 β, TNF-α and COX-2) which were highly upregulated, two of the most highly upregulated genes were IKBA and IL-1R2, both involved in regulation of IL-1β. IL-1β is regulated both at the transcriptional – and protein level where antagonists, IL-1Ra in mammals and nIL-1F in fish, bind to the IL-1R1 and block downstream signaling (14). There are also so-called decoy receptors, as they lack an intracellular signaling domain that bind to IL-1 and prevent downstream signaling. Knowledge of the underlying mechanisms for regulation and signaling pathway is important as dysregulation can lead to acute and chronic inflammatory conditions (20, 25, 38).

Mammalian species have 11 ligands belonging to the IL-1 family. To date, only two of these are identified in fish; IL-1β and IL-18 (7). Fish have, however, two members that are unique for fish; the nIL-1F and IL-1Fm2. In the current study, we have identified and characterized full-length sequences of IL-1β, IL-18, nIL-1F and IL-1Fm2. Analysis of their predicted protein sequences showed that they all possess the IL-1 signature sequence. Interestingly, the lumpfish IL-1Fm2 is shorter than other teleost sequences. After the 12 first amino acids, a stop codon is present, and it lacks 69 amino acids N-terminally compared with Japanese flounder (Supplemental Fig. 4). The rest of the lumpfish IL-1Fm2 sequence, which encodes the IL-1 signature and the characteristic β-strands that form a beta barrel, is present and shows similarity to IL-1Fm2 described in other teleosts (11).

Gene expression analyses of the four IL-1 family members in different tissues and leukocytes from peripheral blood and head kidney in lumpfish showed that IL-18 is constitutively expressed in all tested organs. This is similar to other studies (reviewed in (7)). Upon stimulation of head kidney leukocytes with various PAMPs, there were no significant difference in expression levels of lumpfish IL-18. Lack of differential IL-18 gene expression upon stimulation in vitro with

PAMPs, recombinant proteins or pathogens has also been reported for other species such as trout (9) and sea bream (39). In chicken, IL-18 is a major growth factor for CD4+ T-cells and can stimulate their IFN-γ production. Use of IL-18 as an adjuvant in anti-viral vaccines has shown promising results (2). IL-18 is involved in both T cell type 1 and type 2 responses (10). Much less is known about the function and regulation of IL-18 in fish, but it has been suggested that alternative splicing might regulate IL-18 activity (2). IL-18BP in human is a secreted protein with high affinity for IL-18. IL-18BP is involved in down-regulation of Th1 responses, as well as controlling Th2 cytokine responses (reviewed in (25). IL-18BP candidates from different species of fish are present in public databases, but these have not yet been characterized functionally.

Our results show that nIL-1F, like IL-18, was highly expressed in most organs. Upon exposure to various PAMPs, the expression pattern to nIL-1F was similar to IL1β, being most highly upregulated upon stimulation with flagellin and CpG. Studies from other species have shown that nIL-1F inhibits expression of IL-1β rather than initiates expression of pro-inflammatory cytokines, suggesting it is an antagonist of IL-1β (13). Antagonistic effect of nIL-1F has also been demonstrated in grass carp where it binds to IL-1β receptor type 1 and attenuates IL-1 β activity in HKL (14). The other fish specific IL-1 family members, IL-1Fm2, was expressed at low levels in most studied organs in lumpfish and stimulation with different PAMPs did not cause significant differences in expression levels. Weak induction of IL-1Fm2 upon PAMP activation has also been shown in gilthead seabream (11) and Japanese flounder (12). The function of IL-1Fm2 is not fully understood, but it plays a role in innate immunity activating respiratory burst activity of phagocytes (11). Down-stream signaling of IL-1Fm2 has not yet been investigated, but crosstalk between Toll-like receptors (TLRs) and IL-1Fm2 has been suggested by (11).

Our phylogenetic analysis confirms that lumpfish possess all perciform IL-l ligands. In addition, it demonstrates that only Neoteleostei species (including Acanthopterygii, lanternfish, lizardfish and oarfish) possess IL-1Fm2. This gene is possibly a paralog of a last common ancestor (LCA) leading to IL-1β3 in salmoniforms, as it is the sister group to the IL-1Fm2 clade, and a case of neofunctionalization leading to the creation of a new gene. Alternatively, since only type II IL-1β is described in the most advanced fishes, it is tempting to speculate that IL-1Fm2 is an equivalent to type I IL-1β found in Protacanthopterygii/EOO. Further, the nIL1-F1 clade contains members from Sarcopterygii *(Latimeria chalumnae)* and Chondrichthyes *(Callorhinchus milii)*, and is placed

476 between the IL-1β and IL-18 clades, indicating that this is an old gene that stems back to before
477 the spilt of Eugnathostomata (approximately. 430 mya) and the development of the adaptive
478 immune system. It is likely that the tetrapod lineage has lost the nIL-1F gene somewhere along its
479 evolution. Interstingly, the Neoteleostei clade is placed closer to the Euteleostomorpha clade than
480 the Elopomorpha/Otomorpha/Osteoglossomorpha clade, displaying that the Otomorpha clade is
481 evolutionarily more distant to most teleosts than the ghost shark and lobe-finned fishes, in terms of
482 nIL-1F homology. It is therefore likely that Otomorpha nIL-1F gene possesses traits that are not
483 necessarily consistent with other teleost nIL-1F traits. Moreover, our analysis supports that the
484 type-division between the IL-1β sequences is a phylogenetically dependent division, as all type I
485 member are members of Otomorpha.

486 In the current study, we have also identified six IL-1R like receptors; IL-1R1 (two
487 transcripts), IL-1R2, IL-1R3, IL-1R4, IL-1R5 and IL-1R9 in addition to a double Ig IL-1R related
488 molecule (DIGIRR). Differential gene expression analyses of lumpfish HKL exposed to *V.*
489 *anguillarum*, showed that both transcripts of IL1R1, IL1R2 and IL-1R3 were significantly
490 upregulated. Of these, IL1R2, which is a negative regulator for the IL-1 system, was most highly
491 upregulated (18-fold upregulated). It is of major importance to balance amplification of innate
492 immunity and uncontrolled inflammation that can lead to diseases (reviewed in (20, 40)). In
493 mammals, IL1R2 negatively regulates IL-1 activity by different mechanisms (reviewed in (41)). In
494 short, it can act as a decoy receptor for IL-1 (both IL-1 α and IL-1 β), a dominant –negative
495 molecule and scavenger. Also, IL1R2 can bind to proIL-1α and proIL-1 β in cytoplasm and thus
496 avoid processing by caspase-1 and thus activation. Another negative regulator of the IL-1 signaling
497 in mammals is the receptor called single Ig IL-1R related molecule (SIGIRR, also known as TIR8/
498 IL-1R8). SIGIRR is also present in ancient vertebrates such as zebrafish (42). However, some fish
499 such as green spotted puffer, Japanese puffer and three-spined stickleback do not have SIGIRR,
500 but have instead a related receptor with two Ig domains called double Ig IL-1R related molecule
501 (DIGIRR) which is a negative regulator of IL-1 signaling similar to SIGIRR (37)). In lumpfish, we
502 found a DIGIRR candidate with two Ig domains and the conserved amino acids A L similar to
503 other DIGIRR sequences. An understanding of how production of cytokines is regulated, through
504 their receptors and signaling pathways, gives the potential to modulate their activity, e.g. through
505 immune stimulation.

Conclusion:

In the current study, we have identified and characterized members of the IL-1 family of cytokines, as well as their receptors and down-stream signaling pathways. Our data constitutes an important foundation for further elucidation of cytokine functions, protein-protein interactions and the underlying mechanisms for regulation of these molecules in lumpfish. In-depth knowledge of the innate and adaptive immunity will contribute to increased welfare of lumpfish as it forms the basis for development for immune prophylactic measures. Furthermore, genomic and transcriptomic data of lumpfish is also of interest as it represents a phylogenetic group (Cottales) that is usually not included in comparative and phylogenetic analyses.

Acknowledgement

We want to thank Dr. Mark M. Powell for valuable discussion about the statistical analyses and Dr. Duncan J. Colquhoun for critical reading of the manuscript. Also, we want to thank the editor and the anonymous reviewers for their invaluable suggestions on the manuscript.

References

1. C. A. Dinarello: Immunological and inflammatory functions of the interleukin-1 family. *Annu Rev Immunol*, 27, 519-50 (2009)

2. C. J. Secombes, T. Wang and S. Bird: Vertebrate cytokines and their evolution. In: *The evolution of the immune system*. Ed D. Malagoli. (2016)

3. M. Y. Engelsma, R. J. Stet, J. P. Saeij and B. M. Verburg-van Kemenade: Differential expression and haplotypic variation of two interleukin-1beta genes in the common carp (*Cyprinus carpio* L.). *Cytokine*, 22(1-2), 21-32 (2003)

4. M. Husain, S. Bird, R. van Zwieten, C. J. Secombes and T. Wang: Cloning of the IL-1beta3 gene and IL-1beta4 pseudogene in salmonids uncovers a second type of IL-1beta gene in teleost fish. *Dev Comp Immunol*, 38(3), 431-46 (2012)

5. O. Pleguezuelos, J. Zou, C. Cunningham and C. J. Secombes: Cloning, sequencing, and analysis of expression of a second IL-1beta gene in rainbow trout (*Oncorhynchus mykiss*). *Immunogenetics*, 51(12), 1002-11 (2000)

6. K. Fujiki, D. H. Shin, M. Nakao and T. Yano: Molecular cloning and expression analysis of carp (*Cyprinus carpio*) interleukin-1 beta, high affinity immunoglobulin E Fc receptor gamma subunit and serum amyloid A. *Fish Shellfish Immunol*, 10(3), 229-42 (2000)

7. J. Zou and C. J. Secombes: The Function of Fish Cytokines. *Biology (Basel)*, 5(2) (2016) doi:10.3390/biology5020023

8. A. G. Murzin: Structural principles for the propeller assembly of beta-sheets: the preference for seven-fold symmetry. *Proteins*, 14(2), 191-201 (1992)

9. J. Zou, S. Bird, J. Truckle, N. Bols, M. Horne and C. Secombes: Identification and expression analysis of an IL-18 homologue and its alternatively spliced form in rainbow trout (*Oncorhynchus mykiss*). *Eur J Biochem*, 271(10), 1913-23 (2004)

10. K. Nakanishi: Unique Action of Interleukin-18 on T Cells and Other Immune Cells. *Front Immunol*, 9, 763 (2018)

11. D. Angosto, J. Montero, A. Lopez-Munoz, F. Alcaraz-Perez, S. Bird, E. Sarropoulou, E. Abellan, J. Meseguer, M. P. Sepulcre and V. Mulero: Identification and functional characterization of a new IL-1 family member, IL-1Fm2, in most evolutionarily advanced fish. *Innate Immun*, 20(5), 487-500 (2014)

12. A. Taechavasonyoo, H. Kondo, R. Nozaki, Y. Suzuki and I. Hirono: Identification of novel interleukin 1 beta family genes in Japanese flounder *Paralichthys olivaceus*. *Fish Shellfish Immunol*, 34(1), 393-6 (2013)

13. T. Wang, S. Bird, A. Koussounadis, J. W. Holland, A. Carrington, J. Zou and C. J. Secombes: Identification of a novel IL-1 cytokine family member in teleost fish. *J Immunol*, 183(2), 962-74 (2009)

14. F. Yao, X. Yang, X. Wang, H. Wei, A. Zhang and H. Zhou: Molecular and functional characterization of an IL-1beta receptor antagonist in grass carp (*Ctenopharyngodon idella*). *Dev Comp Immunol*, 49(2), 207-16 (2015)

15. C. J. Secombes, T. Wang and S. Bird: The interleukins of fish. *Dev Comp Immunol*, 35(12), 1336-45 (2011)

16. L. N. Vojtech, N. Scharping, J. C. Woodson and J. D. Hansen: Roles of inflammatory caspases during processing of zebrafish interleukin-1beta in *Francisella noatunensis* infection. *Infect Immun*, 80(8), 2878-85 (2012)

17. M. I. Reis, A. do Vale, P. J. Pereira, J. E. Azevedo and N. M. Dos Santos: Caspase-1 and IL-1beta processing in a teleost fish. *PLoS One*, 7(11), e50450 (2012)

18. D. Boraschi, P. Italiani, S. Weil and M. U. Martin: The family of the interleukin-1 receptors. *Immunol Rev*, 281(1), 197-232 (2018)

19. J. K. Fields, S. Gunther and E. J. Sundberg: Structural Basis of IL-1 Family Cytokine Signaling. *Front Immunol*, 10, 1412 (2019)

20. J. Palomo, D. Dietrich, P. Martin, G. Palmer and C. Gabay: The interleukin (IL)-1 cytokine family--Balance between agonists and antagonists in inflammatory diseases. *Cytokine*, 76(1), 25-37 (2015)

21. F. Colotta, F. Re, M. Muzio, R. Bertini, N. Polentarutti, M. Sironi, J. G. Giri, S. K. Dower, J. E. Sims and A. Mantovani: Interleukin-1 type II receptor: a decoy target for IL-1 that is regulated by IL-4. *Science*, 261(5120), 472-5 (1993)

22. Q. Yang, Q. Chu, X. Zhao and T. Xu: Characterization of IL-1beta and two types of IL-1 receptors in miiuy croaker and evolution analysis of IL-1 family. *Fish Shellfish Immunol*, 63, 165-172 (2017)

23. X. Yang, S. Wang, L. Du, K. Yang, X. Wang, A. Zhang and H. Zhou: Molecular and functional characterization of IL-1 receptor type 2 in grass carp: a potent inhibitor of IL-1beta signaling in head kidney leukocytes. *Dev Comp Immunol*, 41(4), 738-45 (2013)

24. J. Gao, X. Jiang, J. Wang, Y. Xue, X. Li, Z. Sun, H. Wie, P. Nie, J. Zou, Q. Gao: Phylogeny and expression modulation of interleukin 1 receptors in grass carp (*Ctenopharyngodon idella*). *Dev Comp Immunol*, 99, 103401

25. C. A. Dinarello, D. Novick, S. Kim and G. Kaplanski: Interleukin-18 and IL-18 binding protein. *Front Immunol*, 4, 289 (2013)

26. H. Ø. Eggestøl, H. S. Lunde and G. T. Haugland: The proinflammatory cytokines TNF-α and IL-6 in lumpfish (*Cyclopterus lumpus* L.) -identification, molecular characterization,phylogeny and gene expression analyses. *submitted manuscript*

27. G. T. Haugland, R. A. Jakobsen, N. Vestvik, K. Ulven, L. Stokka and H. I. Wergeland: Phagocytosis and respiratory burst activity in lumpsucker (*Cyclopterus lumpus* L.) leucocytes analysed by flow cytometry. *PLoS One*, 7(10), e47909 (2012)

28. R. C. Edgar: MUSCLE: a multiple sequence alignment method with reduced time and space complexity. *BMC Bioinformatics*, 5, 113 (2004)

29. K. Okonechnikov, O. Golosova and M. Fursov: Unipro UGENE: a unified bioinformatics toolkit. *Bioinformatics*, 28(8), 1166-1167 (2012)

30. L.-T. Nguyen, H. A. Schmidt, A. von Haeseler and B. Q. Minh: IQ-TREE: A Fast and Effective Stochastic Algorithm for Estimating Maximum-Likelihood Phylogenies. *Molecular Biology and Evolution*, 32(1), 268-274 (2015)

31. S. Kalyaanamoorthy, B. Q. Minh, T. K. F. Wong, A. von Haeseler and L. S. Jermiin: ModelFinder: fast model selection for accurate phylogenetic estimates. *Nat Methods*, 14(6), 587-589 (2017)

32. B. Q. Minh, M. A. T. Nguyen and A. von Haeseler: Ultrafast Approximation for Phylogenetic Bootstrap. *Molecular Biology and Evolution*, 30(5), 1188-1195 (2013)

33. P. Jones, D. Binns, H. Y. Chang, M. Fraser, W. Li, C. McAnulla, H. McWilliam, J. Maslen, A. Mitchell, G. Nuka, S. Pesseat, A. F. Quinn, A. Sangrador-Vegas, M. Scheremetjew, S. Y. Yong, R. Lopez and S. Hunter: InterProScan 5: genome-scale protein function classification. *Bioinformatics*, 30(9), 1236-40 (2014)

34. H. Ø. Eggestøl, H. S. Lunde, A. Rønneseth, D. Fredman, K. Petersen, C. K. Mishra, T. Furmanek, D. J. Colquhoun, H. I. Wergeland and G. T. Haugland: Transcriptome-wide mapping of signaling pathways and early immune responses in lumpfish leukocytes upon in vitro bacterial exposure. *Sci Rep*, 8(1), 5261 (2018)

614 35. M. Muffato, A.Louis, C.E. Poisnel and H.R. Crollius (2010). Genomicus:a database and a
615 browser to study gene synteny in modern and ancestral genomes. *Bioinformatics*, 26 (8), 1119-
616 1121.

617 36. T.M. Knutsen, G.T. Kirubakaran, M. Mommens, T. Moen. LumpfISH (Cyclopterus
618 lumpus) draft genome assembly. Doi: 10.6084/m9.figshare.7301546.v4

619 37. Y. F. Gu, Y. Fang, Y. Jin, W. R. Dong, L. X. Xiang and J. Z. Shao: Discovery of the
620 DIGIRR gene from teleost fish: a novel Toll-IL-1 receptor family member serving as a negative
621 regulator of IL-1 signaling. *J Immunol*, 187(5), 2514-30 (2011)

622 38. M. O. Huising, R. J. M. Stet, H. F. J. Savelkoul and B. M. L. Verburg-van Kemenade: The
623 molecular evolution of the interleukin-1 family of cytokines; IL-18 in teleost fish. *Developmental*
624 *and Comparative Immunology*, 28(5), 395-413 (2004)

625 39. G. Perez-Cordon, I. Estensoro, L. Benedito-Palos, J. A. Calduch-Giner, A. Sitja-Bobadilla
626 and J. Perez-Sanchez: Interleukin gene expression is strongly modulated at the local level in a fish-
627 parasite model. *Fish Shellfish Immunol*, 37(2), 201-8 (2014)

628 40. M. Molgora, I. Barajon, A. Mantovani and C. Garlanda: Regulatory Role of IL-1R8 in
629 Immunity and Disease. *Front Immunol*, 7, 149 (2016)

630 41. C. Garlanda, C. A. Dinarello and A. Mantovani: The interleukin-1 family: back to the
631 future. *Immunity*, 39(6), 1003-18 (2013)

632 42. W. Feng, Y. F. Gu, L. Nie, D. Y. Guo, L. X. Xiang and J. Z. Shao: Characterization of
633 SIGIRR/IL-1R8 Homolog from Zebrafish Provides New Insights into Its Inhibitory Role in Hepatic
634 Inflammation. *J Immunol*, 197(1), 151-67 (2016)

635

636 **Figure legends**

637 **Figure 1.** Overview of NF-κB and MAPK signaling pathway in lumpfish. **(A)** NF-κB signaling
638 pathway (modified from KEGG map 04064) and **(B)** MAPK signaling pathway (modified from
639 KEGG map 04010).The colors of the boxes refers to the respective gene's differential expression
640 upon bacterial exposure and whether or not they are present in the lumpfish transcriptome.: grey –
641 not present, a scale ranging from deep blue (very negative, log2 fold change = -10), through white
642 (neutral, log2 fold change = 0), to brown-red (very positive, log2 fold change = 10) refers to the
643 differentially expressed genes at 24 hours. All genes that are identified in lumpfish, but not
644 significant (adjusted p-value > 0.05) regulated is shown as white boxes. Differently regulated
645 transcripts of the same gene are represented with horizontal bars within the respective gene-box.
646 The 11 most regulated genes at 24h are shown in the Tables in the Figure. See Supplemental Table
647 2 and 3 for a full list of DEG at 6 and 24 h post bacterial exposure.

Figure 2. Molecular characterization of IL-1 ligands. **(A)** Domain and cut site prediction of IL-1β, IL-18, nIL-1F and IL-1Fm2. The x-axis is the number of amino acids from N-terminus to C-terminus of the proteins. IL-1 family domain is defined as IPR00097, IL-1 propeptide as IPR00302 and PDZ domain by IPR001478. (**B)** Exon/intron structure of the IL-1 ligands. Black boxes are non-coding exons, white boxes are coding exons. Red exon indicates remnants of the deleted exon in lumpfish IL-1Fm2. Thin lines are introns. Dotted lines are not to scale. **(C)** Non-coding exons (black boxes), coding exons (white boxes) for selected IL-1 β type I and type II and IL-1Fm2 sequences. Roman numerals represent intron phases.

Figure 3. Synteny analysis of type II IL-1β, IL-18, nIL-1F and IL-1Fm2**.** Schematic diagrams showing the genomic regions containing the IL-1 ligands. Lumpfish sequences are compared with Japanese medaka, stickleback, turbot, zebrafish, platyfish and human. Conserved genes in the IL-1β and IL-18 locus in humans are shown for comparison. The IL-1 family ligands are shown in black boxes. Identical genes have same color.

Figure 4. Phylogenetic tree of IL-1β, IL-18, nIL-1F and IL-1Fm2. All full-length fish IL-1 ligands, and the human and mouse IL-1β and IL-18 sequences, are included. The phylogenetic tree was made using maximum likelihood as described in material and methods. Phylogenetic distance is indicated by branch length. Bar indicates distance of 1 substitution per amino acid site. A detailed phylogenetic tree which include sequence information (species and accession numbers) and bootstrap values (>80%) of 100000 iterations is shown in Supplemental Figure 5 and listed in Supplemental Table 4.

Figure 5. Tissue distribution of IL-1 ligand family members. Mean Normalized Expression (MNE) of the IL-1 ligands are shown relative to the reference gene (RPS20), plotted on a log10 scale. Error bars denote 1 standard deviation (SD). HKL – Head Kidney Leucocytes and PBL – Peripheral Blood Leukocytes. **(A)** IL-1β. **(B)** IL18. **(C)** nIL-1F. **(D)** IL1-Fm2. **(E)** Tissue-independent expression of IL-1 ligands. Single letters= measurement that is statistically different the other.

Figure 6. Gene expression of IL-1β, IL-18, nIL-1F and IL1-Fm2. **(A)** Correlation between log10 qPCR and RNA seq data of the IL-1 family members. **(B)** qPCR analyses of the IL-1 family members upon stimulation with various ligands. Error bars denote 1 standard deviation (SD). Stars

676 denotes significant change compared with control (* P < 0.05, ** P < 0.01, *** P < 0.001). The
677 control is set to 1.

678 **Figure 7**. IL-1 receptors. **(A)** Phylogenetic tree including IL-1 receptors identified in lumpfish and
679 in other species. Accession/trinity numbers of the sequences and bootstrap values are shown in the
680 tree. **(B)** Schematic figure of full-length IL-1Rs identified in lumpfish transcriptome. The following
681 domains are identified by interproscan: TIR domains (IPR035897) = pink, immunoglobulin
682 domains (IPR007110) = red,transmembrane domain= light blue, signal peptide= dark blue. The
683 IL1R3b sequence is not completely full-length, lacking about 10 amino acids in the N and C
684 terminals. **(C)** DEG analysis of IL-1 receptors in lumpfish upon bacterial exposure. The color of
685 the boxes reflects the DEG-value. Brown = upregulated, blue= downregulated.

686 **Supplemental Figure 1.** IL1β alignment. Alignment of IL-1β sequences from human, mouse and
687 teleosts, including the lumpfish sequence. Underlined amino acids are members of the IL-1 family
688 signature. The purple horizontal line indicates the mammalian caspase 1 cut site. β -sheets are
689 indicated by grey boxes.

690 **Supplemental Figure 2.** IL18 alignment. Alignment of IL-18 sequences from human, mouse and
691 teleosts, including the lumpfish sequence. Underlined amino acids are members of the IL-1 family
692 signature. The first purple horizontal line indicates a teleost cut site identified in Zou et al. (2004).
693 The second purple horizontal line indicates the mammalian caspase 1 or 4 cut site. Regions that
694 contain β -sheets are indicated by grey boxes.

695 **Supplemental Figure 3.** nIL-1F alignment. Alignment of teleost, including lumpfish, IL-1β
696 sequences. Underlined amino acids are members of the IL-1 family signature. The purple
697 horizontal line indicates the caspase 1 cut site predicted in the lumpfish sequence. The blue
698 horizontal lines indicate the thrombin cut sites predicted in the lumpfish sequence. β -sheets are
699 indicated by grey boxes.

700 **Supplemental Figure 4.** IL-1Fm2 alignment. Alignment of teleost, including lumpfish, IL-
701 1Fm2sequences. Underlined amino acids are members of the IL-1 family signature. β -sheets are
702 indicated by grey boxes.

Supplemental Figure 5. Phylogenetic tree of IL-1 ligands with accession numbers. The colors of the clades are similar to Fig. 4. Bootstrap values >80 % (of 100000 iterations) are shown in the tree. The lumpfish sequences are written with red letters.

Supplemental Figure 6. Nucleotide and deduced amino acid sequences for lumpfish IL-1β. gDNA specific sequence is represented with lower case, cDNA sequence with upper case and cDNA sequence is represented with bold letter. Intron-exon boundaries (gt and ag) are encircled.

Supplemental Figure 7. Nucleotide and deduced amino acid sequences for lumpfish IL-18. gDNA specific sequence is represented with lower case, cDNA sequence with upper case and cDNA sequence is represented with bold letter. Intron-exon boundaries (gt and ag) are encircled.

Supplemental Figure 8. Nucleotide and deduced amino acid sequences for lumpfish nIL-1F. gDNA specific sequence is represented with lower case, cDNA sequence with upper case and cDNA sequence is represented with bold letter. Intron-exon boundaries (gt and ag) are encircle.

Supplemental Figure 9. Nucleotide and deduced amino acid sequences for lumpfish IL-1Fm2. gDNA specific sequence is represented with lower case, cDNA sequence with upper case and cDNA sequence is represented with bold letter. Intron-exon boundaries (gt and ag) are encircled.

Table 1. Primers used for qPCR, PCR and Sanger sequencing.

Gene	Primer name	Sequence 5'-3'	Application
RPS20	RPS20_F	GGAGAAGAGCCTGAAGGTGAAG	qPCR
	RPS20_R	GAGTTTTCCTGGTGGTGATGC	qPCR
IL-1β	IL-1β_F	GACGGCGAGAAGCGGACCATAG	qPCR
	IL-1β_R	TCAGGACAACTTTCTTGAGGTCAG	qPCR
IL-18	IL-18_F	CCACCACAAGGCGCTGTTCTACA	qPCR
	IL-18_R	AGGCGGAGGACTCGAACTCGTA	qPCR
	IL-18intr_F1	CTGTTTCTTTCCAGAGTGCAAGTT	PCR and Sanger seq.
	IL-18intr_R1	TCCACCTCGTCTTTGGCTTTTTC	PCR and Sanger seq.
nIL-1F	nIL-1F_F	CAAGTCCAACTGCTTCCTCCG	qPCR
	nIL-1F_R	ATCTTCTTCAACCTCTGCTTCTCG	qPCR
	nIL-1F_F353	ATGCAAAGCGGAAGCACAGACG	PCR and Sanger seq.
	nIL-1F_R354	AAGTCTGAATGACGAAGAGGAACGATT	PCR and Sanger seq.
	nIL-1F_F355	ACAGACGCACTGGGGGCTTTTA	Sanger seq.
	nIL-1F_R356	TGAATGACGAAGAGGAACGATTC	Sanger seq.
	nIL-1F_F357	ACAGTACTCAGTTTCAGCATGGAGATG	Sanger seq.

	nIL-1F_R358	ACCTCCTCTTGGAACGAGCATCACCT	Sanger seq.
	nIL_1F_R360	AACGAGCATCACCTCGCTGGATT	Sanger seq.
	nIL-1F_F422	CACATCCATCAGTGTCAGTGGCCTCTCAGTCCTAC	PCR and Sanger seq.
IL-1Fm2	IL-1Fm2_F	GAACATCAGCGACCACGAGGACAT	qPCR
	IL-1Fm2_R	CAGGGACTCGAAGGTGTTCAGGGA	qPCR
	IL-1Fm2intr_F156	ATGAGCGACTTTGATCTGTCTCAAGC	PCR and Sanger seq.
	IL-1Fm2intr_F362	TCGTCACGGCGACACAGAACT	PCR and Sanger seq.
	IL-1Fm2intr_R363	ATCATAATGGAAACCTTCAAGCTGCACTAAA	PCR and Sanger seq.

720

721 **Table 2.** qPCR assays

Target	Y	R^2	E	qPCR-product (bp)
RPS20	-3.30	0.999	2.01	74
IL-1β	-3.45	0.999	1.95	97
IL-18	-3.27	0.999	2.02	71
nIL-1F	-3.40	0.998	1.97	90
IL-1Fm2	-3.51	0.999	1.93	85

722

723 **Table 3.** Overview of the IL1-family receptors identified in lumpfish

Name*	Alias	Lumpfish Gene-ID	BLAST hit gene	BLAST hit specie	E-value	Acc.no
IL-1R1	IL-1R1a	TR84990|c3	interleukin-1 receptor type 1-like isoform X1	*Monopterus albus*	0	XP_020469769.1
	IL-1R1b	TR22841|c1	interleukin-1 receptor type 1-like isoform X2	*Lates calcarifer*	0	XP_018551896.1
IL-1R2	IL-1R2	TR83610|c2	IL-1RII	*Miichthys miiuy*	8.00E-143	AQR55702.1
IL-1R3	IL-1RAcP/ IL-1RAP	TR35281|c1	interleukin-1 receptor accessory protein-like 1 isoX3	*Monopterus albus*	0	XP_020447933.1
IL-1R4	ST2 /IL33R	TR80915|c0	interleukin-1 receptor-like 1	*Larimichthys crocea*	0	XP_027147138.1
IL-1R5	IL-18Rα	TR33815|c1	PREDICTED: interleukin-18 receptor 1-like	*Lates calcarifer*	0	XP_018539216.1
IL-1R9	TIGIRR-2	TR47117|c0	Interleukin-1 receptor accessory protein-like iso X1	*Mastacembelus armatus*	2.00E-177	XP_026183142.1
DIGIRR	DIGIRR	TR66708|c0	double immunoglobulin IL-1R-related protein	*Gasterosteus aculeatus*	1.00E-132	ACA51853.1

724 *Same nomenclature as Boraschi et al. (18)

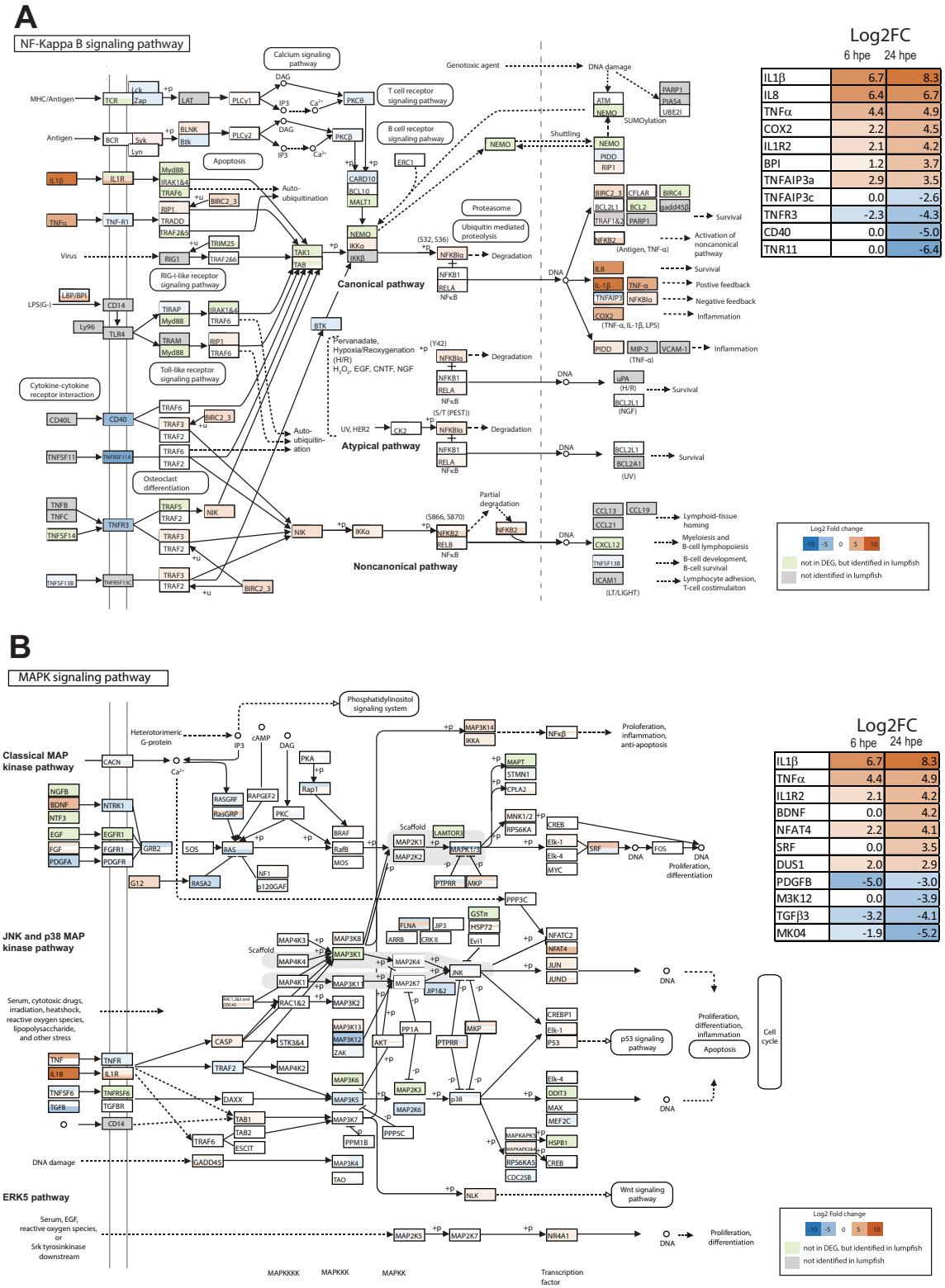
A
NF-Kappa B signaling pathway
Log2FC
6 hpe 24 hpe
IL1β 6.7 8.3
IL8 6.4 6.7
TNFα 4.4 4.9
COX2 2.2 4.5
IL1R2 2.1 4.2
BPI 1.2 3.7
TNFAIP3a 2.9 3.5
TNFAIP3c 0.0 -2.6
TNFR3 -2.3 -4.3
CD40 0.0 -5.0
TNR11 0.0 -6.4
Canonical pathway
Atypical pathway
Noncanonical pathway
Log2 Fold change
not in DEG, but identified in lumpfish
not identified in lumpfish
B
MAPK signaling pathway
Log2FC
6 hpe 24 hpe
IL1β 6.7 8.3
TNFα 4.4 4.9
IL1R2 2.1 4.2
BDNF 0.0 4.2
NFAT4 2.2 4.1
SRF 0.0 3.5
DUS1 2.0 2.9
PDGFB -5.0 -3.0
M3K12 0.0 -3.9
TGFβ3 -3.2 -4.1
MK04 -1.9 -5.2
Classical MAP kinase pathway
JNK and p38 MAP kinase pathway
ERK5 pathway
Log2 Fold change
not in DEG, but identified in lumpfish
not identified in lumpfish

Figure 1

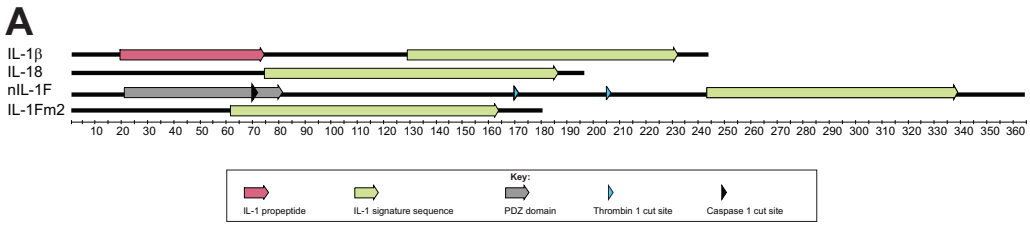
A
IL-1β
IL-18
nIL-1F
IL-1Fm2
Key:
IL-1 propeptide
IL-1 signature sequence
PDZ domain
Thrombin 1 cut site
Caspase 1 cut site

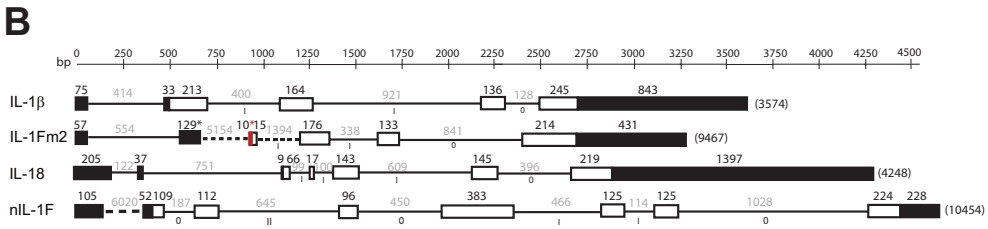
B
bp
IL-1β
IL-1Fm2
IL-18
nIL-1F

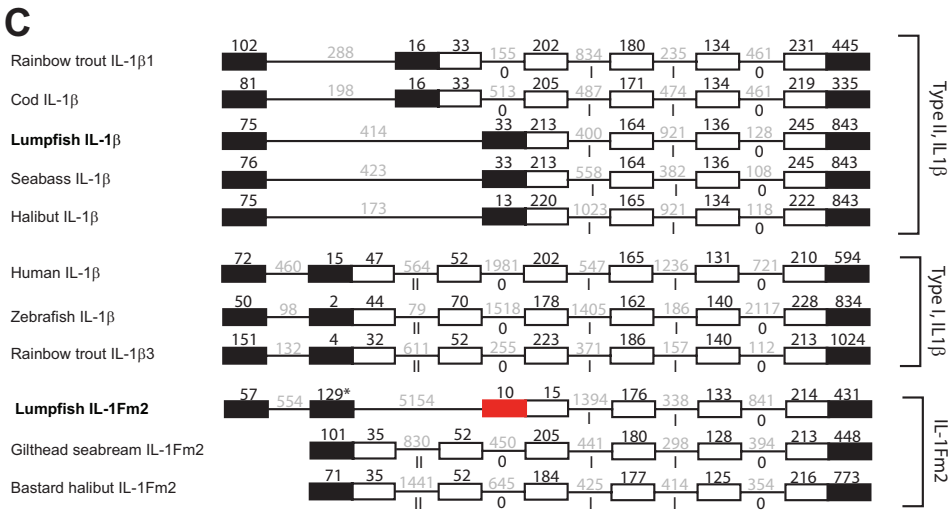
C
Rainbow trout IL-1β1
Cod IL-1β
Lumpfish IL-1β
Seabass IL-1β
Halibut IL-1β
Human IL-1β
Zebrafish IL-1β
Rainbow trout IL-1β3
Lumpfish IL-1Fm2
Gilthead seabream IL-1Fm2
Bastard halibut IL-1Fm2
Type II, IL1β
Type I, IL1β
IL-1Fm2

Figure 2

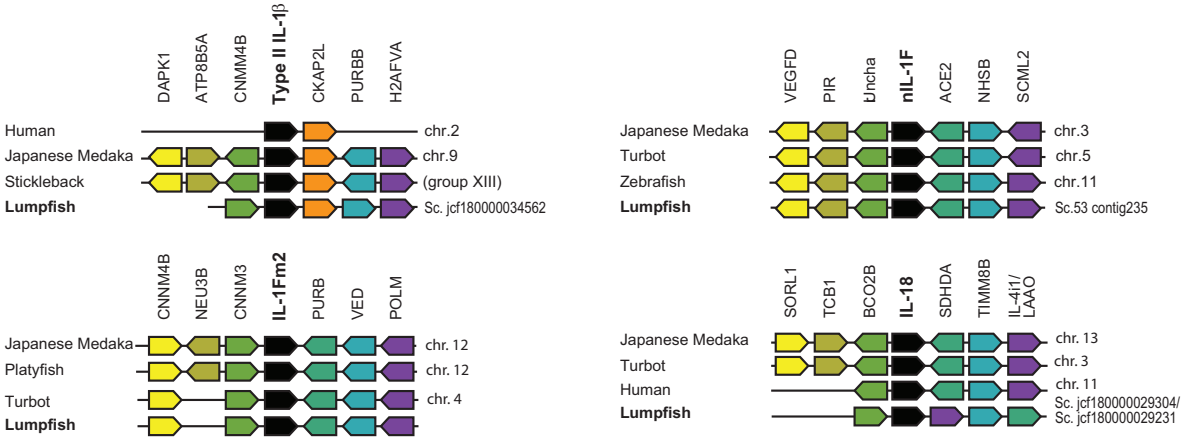
DAPK1
ATP8B5A
CNMM4B
Type II IL-1β
CKAP2L
PURBB
H2AFVA
Human
Japanese Medaka
Stickleback
Lumpfish
chr.2
chr.9
(group XIII)
Sc. jcf180000034562
VEGFD
PIR
Uncha
nIL-1F
ACE2
NHSB
SCML2
Japanese Medaka
Turbot
Zebrafish
Lumpfish
chr.3
chr.5
chr.11
Sc.53 contig235
CNNM4B
NEU3B
CNNM3
IL-1Fm2
PURB
VED
POLM
Japanese Medaka
Platyfish
Turbot
Lumpfish
chr. 12
chr. 12
chr. 4
SORL1
TCB1
BCO2B
IL-18
SDHDA
TIMM8B
IL-4i1/
LAAO
Japanese Medaka
Turbot
Human
Lumpfish
chr. 13
chr. 3
chr. 11
Sc. jcf180000029304/
Sc. jcf180000029231

Figure 3

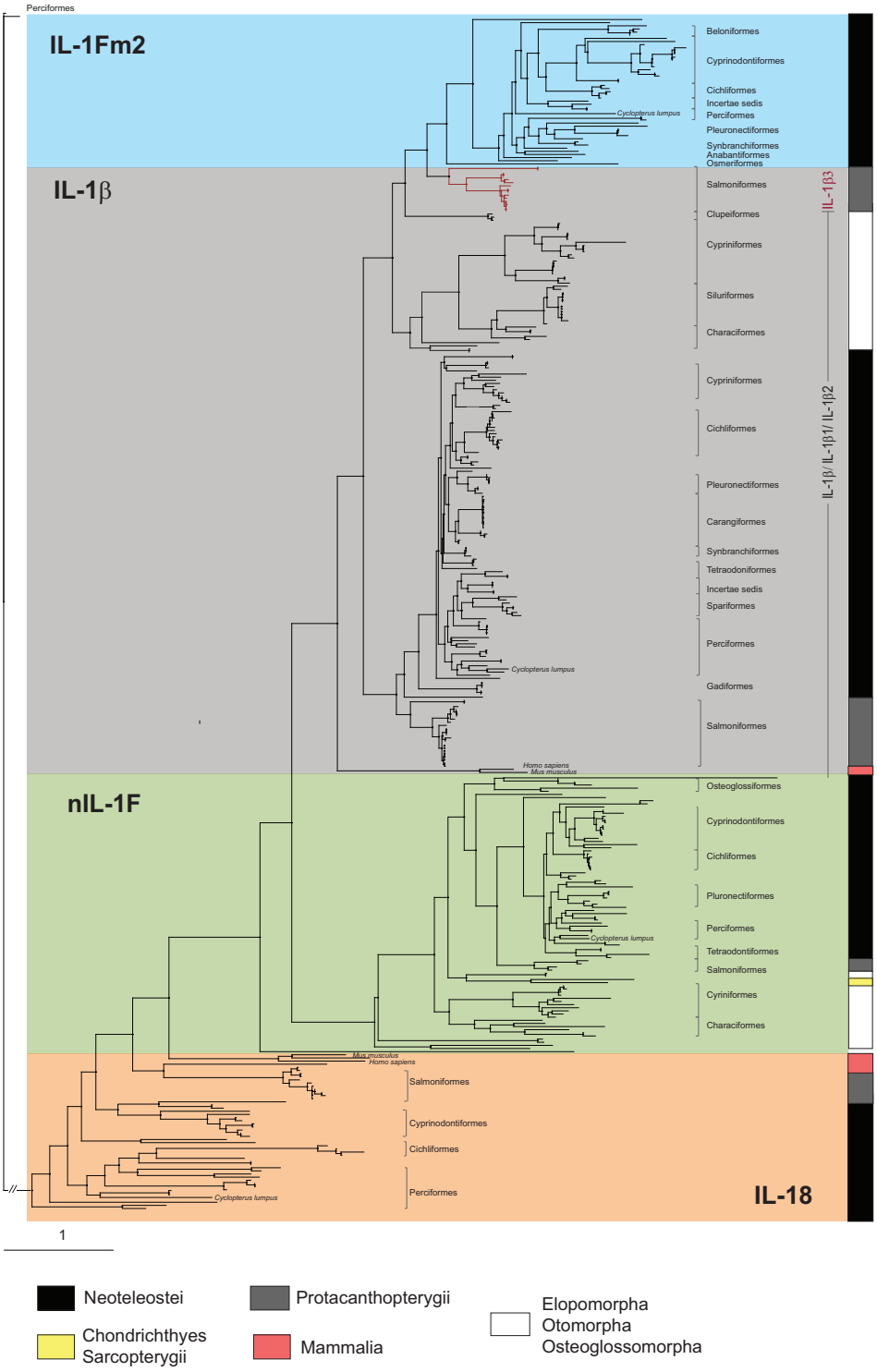
Perciformes
IL-1Fm2
Beloniformes
Cyprinodontiformes
Cichliformes
Incertae sedis
Perciformes
Cyclopterus lumpus
Pleuronectiformes
Synbranchiformes
Anabantiformes
Osmeriformes
IL-1β
Salmoniformes
Clupeiformes
Cypriniformes
Siluriformes
Characiformes
Cypriniformes
Cichliformes
Pleuronectiformes
Carangiformes
Synbranchiformes
Tetraodoniformes
Incertae sedis
Spariformes
Perciformes
Cyclopterus lumpus
Gadiformes
Salmoniformes
IL-1β3
IL-1β/ IL-1β1/ IL-1β2
Type I
Type II
Homo sapiens
Mus musculus
nIL-1F
Osteoglossiformes
Cyprinodontiformes
Cichliformes
Pluronectiformes
Perciformes
Cyclopterus lumpus
Tetraodontiformes
Salmoniformes
Cyriniformes
Characiformes
Mus musculus
Homo sapiens
Salmoniformes
Cyprinodontiformes
Cichliformes
Perciformes
Cyclopterus lumpus
IL-18
1
Neoteleostei
Chondrichthyes
Sarcopterygii
Protacanthopterygii
Mammalia
Elopomorpha
Otomorpha
Osteoglossomorpha

Figure 4

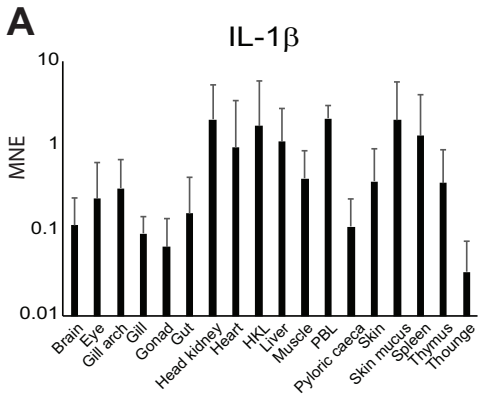
A
IL-1β
MNE
10
1
0.1
0.01
Brain
Eye
Gill arch
Gill
Gonad
Gut
Head kidney
Heart
HKL
Liver
Muscle
PBL
Pyloric caeca
Skin
Skin mucus
Spleen
Thymus
Thounge

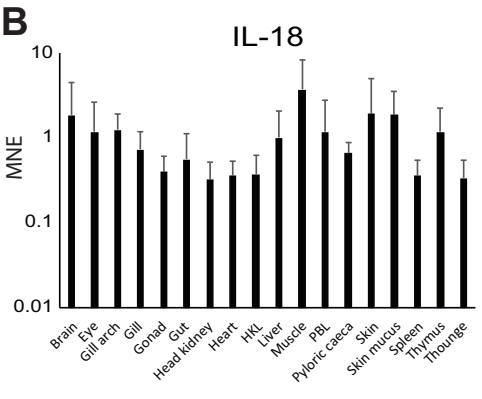
B
IL-18
MNE
10
1
0.1
0.01
Brain
Eye
Gill arch
Gill
Gonad
Gut
Head kidney
Heart
HKL
Liver
Muscle
PBL
Pyloric caeca
Skin
Skin mucus
Spleen
Thymus
Thounge

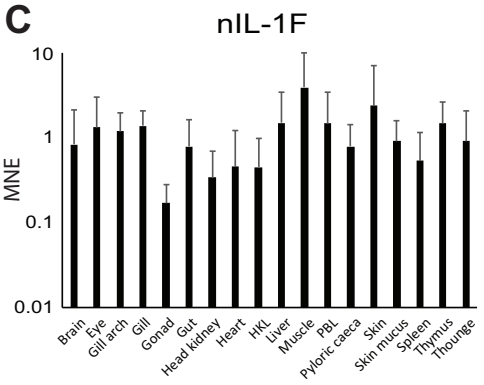
C
nIL-1F
MNE
10
1
0.1
0.01
Brain
Eye
Gill arch
Gill
Gonad
Gut
Head kidney
Heart
HKL
Liver
Muscle
PBL
Pyloric caeca
Skin
Skin mucus
Spleen
Thymus
Thounge

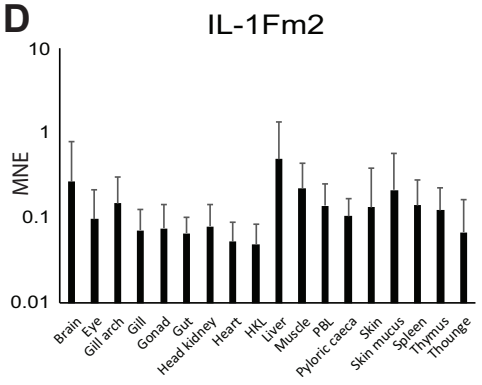
D
IL-1Fm2
MNE
10
1
0.1
0.01
Brain
Eye
Gill arch
Gill
Gonad
Gut
Head kidney
Heart
HKL
Liver
Muscle
PBL
Pyloric caeca
Skin
Skin mucus
Spleen
Thymus
Thounge

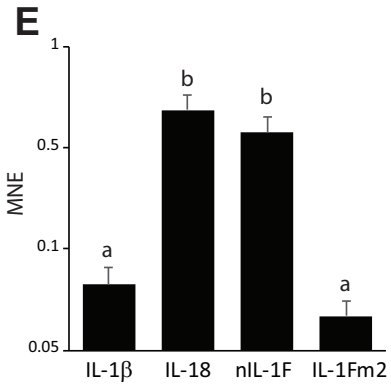
E
MNE
1
0.5
0.1
0.05
a
b
b
a
IL-1β
IL-18
nIL-1F
IL-1Fm2

Figure 5

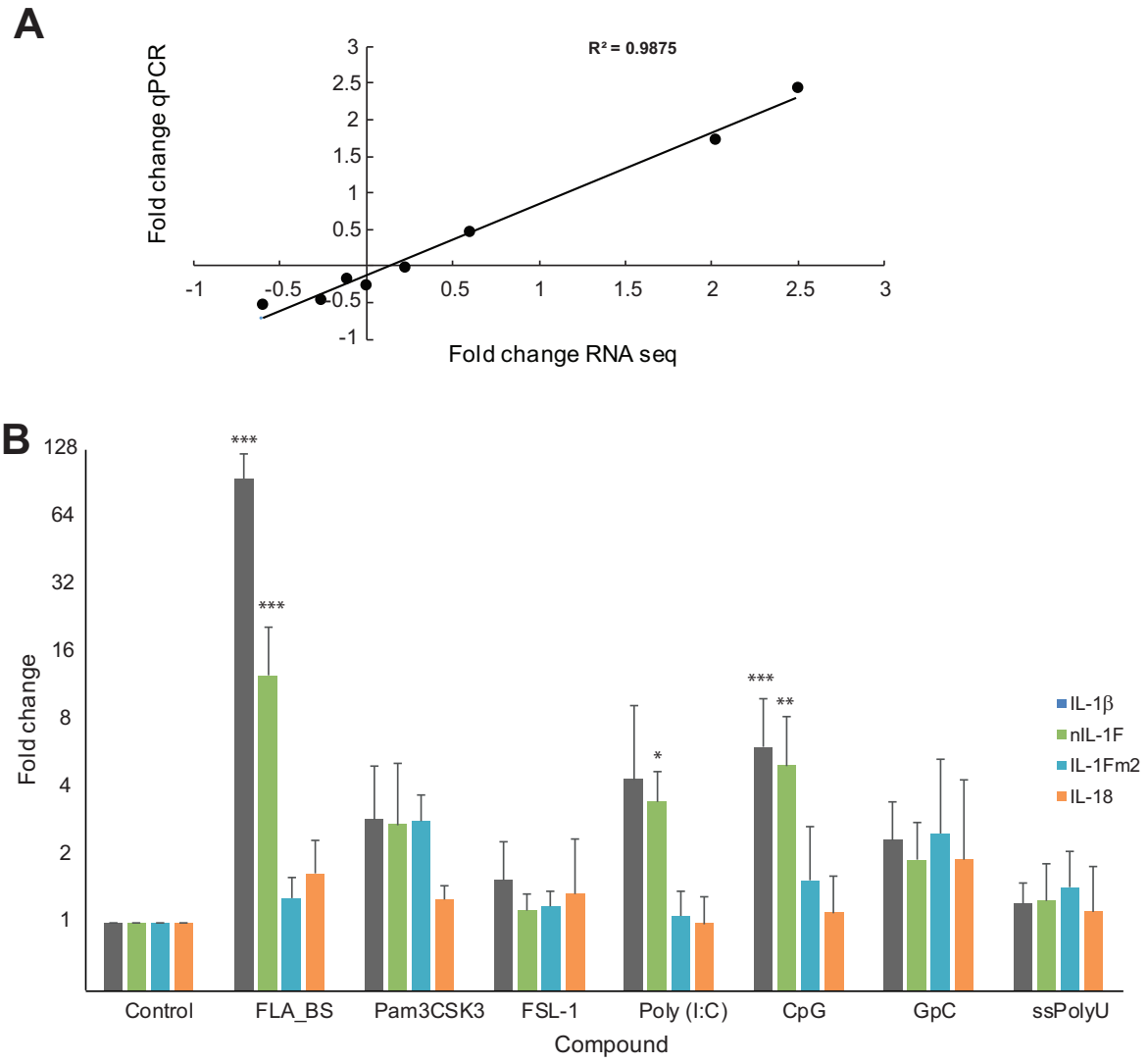
A
R² = 0.9875
Fold change qPCR
Fold change RNA seq
3
2.5
2
1.5
1
0.5
-0.5
-1
-1
-0.5
0.5
1
1.5
2
2.5
3
B
Fold change
128
64
32
16
8
4
2
1
***
***
*
***
**
IL-1β
nIL-1F
IL-1Fm2
IL-18
Control
FLA_BS
Pam3CSK3
FSL-1
Poly (I:C)
CpG
GpC
ssPolyU
Compound

Figure 6

Figure 7

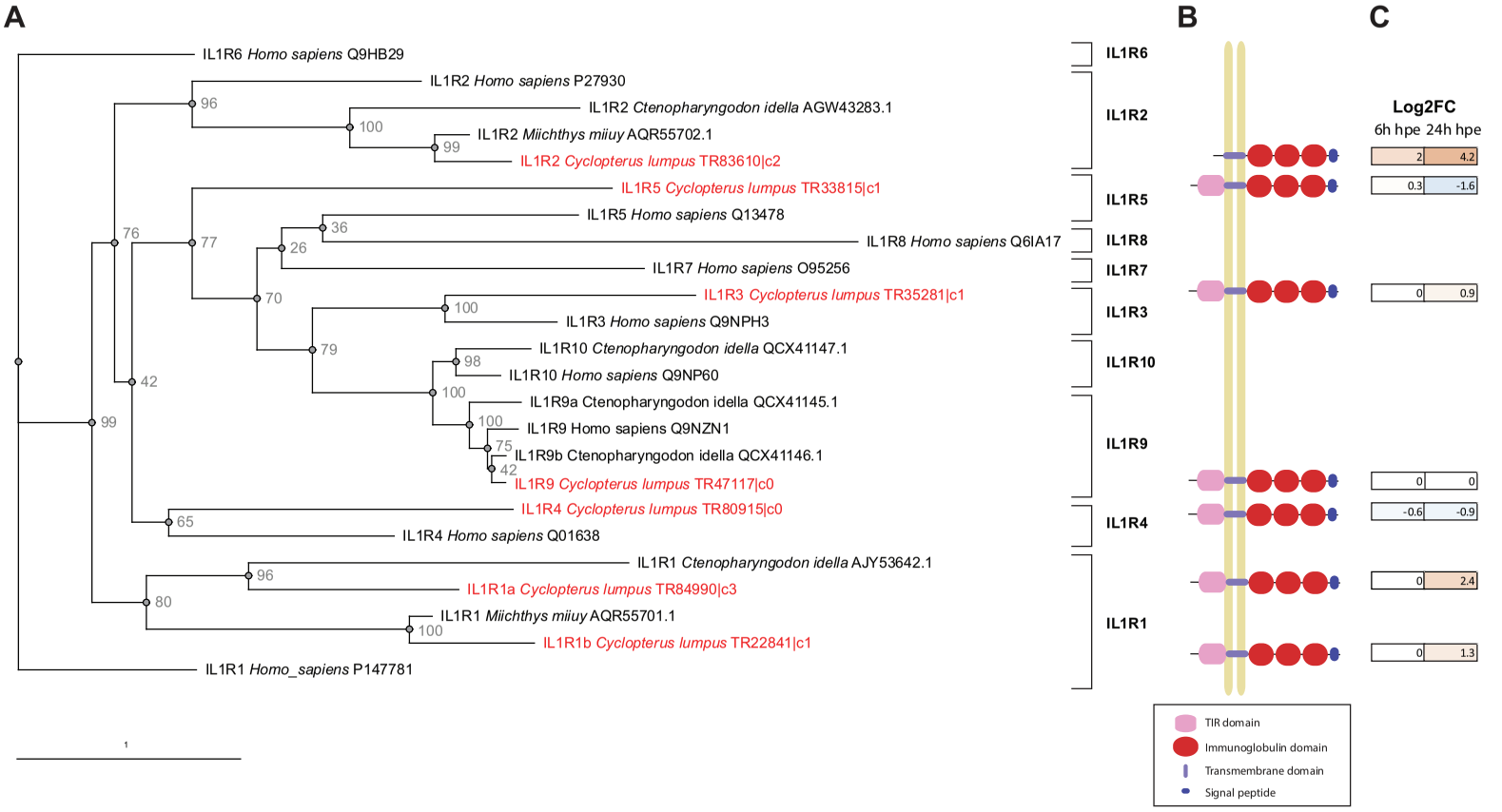
A
B
C
IL1R6 Homo sapiens Q9HB29
IL1R2 Homo sapiens P27930
IL1R2 Ctenopharyngodon idella AGW43283.1
IL1R2 Miichthys miiuy AQR55702.1
IL1R2 Cyclopterus lumpus TR83610|c2
IL1R5 Cyclopterus lumpus TR33815|c1
IL1R5 Homo sapiens Q13478
IL1R8 Homo sapiens Q6IA17
IL1R7 Homo sapiens O95256
IL1R3 Cyclopterus lumpus TR35281|c1
IL1R3 Homo sapiens Q9NPH3
IL1R10 Ctenopharyngodon idella QCX41147.1
IL1R10 Homo sapiens Q9NP60
IL1R9a Ctenopharyngodon idella QCX41145.1
IL1R9 Homo sapiens Q9NZN1
IL1R9b Ctenopharyngodon idella QCX41146.1
IL1R9 Cyclopterus lumpus TR47117|c0
IL1R4 Cyclopterus lumpus TR80915|c0
IL1R4 Homo sapiens Q01638
IL1R1 Ctenopharyngodon idella AJY53642.1
IL1R1a Cyclopterus lumpus TR84990|c3
IL1R1 Miichthys miiuy AQR55701.1
IL1R1b Cyclopterus lumpus TR22841|c1
IL1R1 Homo_sapiens P147781
96
100
99
76
77
36
26
70
100
79
98
42
100
99
100
75
42
65
96
80
100
1
IL1R6
IL1R2
IL1R5
IL1R8
IL1R7
IL1R3
IL1R10
IL1R9
IL1R4
IL1R1
Log2FC
6h hpe 24h hpe
2
4.2
0.3
-1.6
0
0.9
0
0
-0.6
-0.9
0
2.4
0
1.3
TIR domain
Immunoglobulin domain
Transmembrane domain
Signal peptide

Species
Subfamily
Order
Series
Superorder
Subcohort
Cohort
Infraclass
Class
Superclass
Infraphylum
Subphylum
Taxonomic level
Callorhinchus milii
Anguilla anguilla
Scleropages formosus
Clupea harengus
Danio rerio
Cyprinus carpio
Carassius auratus
Carassius carassius
Pygocentrus nattereri
Astyanax mexicanus
Coregonus maraena
Salmo salar
Oncorhynchus mykiss
Gadus morhua
Scophthalmus maximus
Paralichthys olivaceus
Astatotilapia burtoni
Oreochromis niloticus
Fundulus heteroclitus
Nothobranchius furzeri
Takifugu rubripes
Takifugu nigroviridis
Gasterosteus aculeatus
Cyclopterus lumpus
Latimeria chalumnae
Homo sapiens
Cyprininae
Salmoninae
Clupeiformes
Cypriniformes
Characiformes
Salmoniformes
Pleuronecti-formes
Cichliformes
Cyprinodonti-formes
Tetraodonti-formes
Perciformes
Otophysi
Protacanthopterygii
Paracanthopterygii
Acanthopterygii
Neoteleostei
Euteleostomorpha
EOO: Elopomorpha, Otomorpha and Osteoglossomorpha
Teleostei
Actinopterygii
Sarcopterygii
Osteichthyes
Chondrichthyes
Gnathostomata
Vertebrata

Figure 8

Supplementary material Paper I

Transcriptome-wide mapping of signaling pathways and early immune responses in lumpfish leukocytes upon *in vitro* bacterial exposure

Håvard Ø. Eggestøl[1], Harald S. Lunde[1], Anita Rønneseth[1], David Fredman[2], Kjell Petersen[2], Charitra K. Mishra[2], Tomasz Furmanek[2], Duncan J. Colquhoun[1,3], Heidrun I. Wergeland[1] and Gyri T. Haugland[1]*.

[1]Department of Biology, University of Bergen, Bergen, Norway
[2]Computational Biology Unit, Department of Informatics, University of Bergen, Bergen, Norway
[3]Norwegian Veterinary Institute, Oslo, Norway
* Gyri.Haugland@bio.uib.no

Supplementary materials:

Supplemental Table 1. Overview of the most significantly regulated genes at 6 and 24 hpe (sorted by adjpval) *

Most significantly regulated genes at 24 hpe						
gene_id	**logFC_24h**	**adjpval_24h**	**Annotations**	**Full record name**	**Species**	**E-value**
TR41627	6.90	9.11E-11	TLR5	Toll-like_receptor_5	*Homo sapiens*	6E-92
TR13890	6.73	1.16E-10	IL8	Interleukin-8-like	*Serola dumerili*	6E-21
TR87025	5.27	1.16E-10	Uncharacterized	PREDICTED: uncharacterized protein LOC108879818	*Lates calcarifer*	5E-73
TR41114	6.52	1.16E-10	C1QL3	Complement_C1q-like_protein_3	*Mus musculus*	2E-12
TR41155	4.19	1.16E-10	NFAT5	Nuclear_factor_of_activated_T-cells_5	*Mus musculus*	8E-23
TR53083	-5.90	1.16E-10	MRC1	Macrophage_mannose_receptor_1	*Mus musculus*	0
TR70021	-5.18	1.30E-10	SIAE	Sialate_O-acetylesterase	*Mus musculus*	1E-19
TR22616	4.01	1.74E-10	HS74L	Heat_shock_70_kDa_protein_4L	*Homo sapiens*	5E-170
TR81788	4.50	2.43E-10	DDX24	ATP-dependent_R._helicase_DDX24	*Pongo*	4E-41
TR52303	3.06	2.53E-10	IL12R-B2	Interleukin-12 receptor subunit beta-2-like	*Notothenia coriiceps*	3E-141
TR69283	5.17	2.56E-10	Hypothetical	hypothetical protein Z043_122910	*Scleropages formosus*	9E-05
TR79163	7.34	2.67E-10	TRFE	Serotransferrin	*Oryzias latipes*	0
TR8937	3.43	2.67E-10	CEP192	PREDICTED: centrosomal protein of 192 kDa	*Larimichtys crocea*	0E+00
TR71746	4.12	2.67E-10	NFAT5	Nuclear_factor_of_activated_T-cells_5	*Homo sapiens*	3E-58
TR70589	4.88	2.67E-10	PTGES	Prostaglandin_E_synthase	*Equus caballus*	4E-28
TR37961	4.42	2.67E-10	TAF4B	Transcription_initiation_factor_TFIID_subunit_4B	*Mus musculus*	6E-19
TR81776	8.77	2.83E-10	CC chemokine 20	C-C motif chemokine 20 precursor	*Anoplopoma fimbria*	8E-45
TR14360	8.27	2.83E-10	IL1B	Interleukin-1_beta	*Oncorhynchus mykiss*	9E-73
TR8934	3.21	2.83E-10	MAST3	Microtubule-associated_serine/threonine-protein_kinase_3	*Xenopus laevis*	4E-107
TR65236	3.68	2.83E-10	TIMP2	Metalloproteinase_inhibitor_2	*Cavia porcellus*	7E-109
Most significantly regulated genes at 6 hpe						
gene_id	**logFC_6h**	**adjpval_6h**	**Annotations**	**Full record name**	**Specie**	**E-value**
TR31519	4.31	8.49E-10	NR4A1	Nuclear_receptor_subfamily_4_group_A_member_1	*Xenopus laevis*	6E-52
TR13890	6.39	9.31E-10	IL8	Interleukin-8-like	*Serola dumerili*	6E-21
TR87025	5	1E-09	Uncharacterized	PREDICTED: uncharacterized protein LOC108879818	*Lates calcarifer*	5E-73
TR41627	4.28	2.90E-09	TLR5	Toll-like_receptor_5	*Homo sapiens*	6E-92
TR52303	2.66	2.90E-09	IL12R-B2	Interleukin-12 receptor subunit beta-2-like	*Notothenia coriiceps*	3E-141
TR69283	4.27	2.90E-09	Hypothetical protein	hypothetical protein Z043_122910	*Scleropages formosus*	9E-05
TR81776	6.17	2.90E-09	CC chemokine 20	C-C motif chemokine 20 precursor	*Anoplopoma fimbria*	8E-45
TR28159	3.15	2.90E-09	PTGIS	Prostacyclin_synthase	*Bos taurus*	3E-30
TR86119	4.40	3.17E-09	TNIP2	TNFAIP3-interacting_protein_2	*Mus musculus*	2E-31
TR19609	3.24	4.21E-09	IKBA	NF-kappa-B_inhibitor_alpha	*Gallus gallus*	6E-57
TR49945	5.26	7.93E-09	GL.	Glutamine_synthetase,_mitochondrial	*Squalus acanthias*	6E-22
TR87414	5.19	7.93E-09	GL.	Glutamine_synthetase	*Canis lupus*	2E-147
TR80474	2.48	7.93E-09	SIK2	Serine/threonine-protein_kinase_SIK2	*Mus musculus*	5E-143
TR59888	2.70	7.93E-09	unnamed protein	Unnamed protein product	*Tetraodon nigroviridis*	1.4E-01
TR129039	3.61	7.93E-09	HSP 90-beta-3	Putative heat shock protein HSP 90-beta-3	*Tupaia chinensis*	4E-05
TR1049	1.83	7.93E-09	DDX41	Probable_ATP-dependent_R._helicase_DDX41	*Mus musculus*	0

TR59631	2.61	7.93E-09	FOS	Proto-oncogene_c-Fos	*Takifugu rubripes*	4E-100
TR81788	3.26	7.93E-09	DDX24	ATP-dependent_R._helicase_DDX24	*Pongo*	4E-41
TR14360	6.69	7.93E-09	IL1B	Interleukin-1_beta	*Oncorhynchus mykiss*	9E-73
TR8934	2.65	7.93E-09	MAST3	Microtubule-associated_serine/threonine-protein_kinase_3	*Xenopus laevis*	4E-107

* Positive logFC values= upregulated transcripts, negative logFC values=down-regulated transcripts

Supplemental Table 2. Overview of the 50 most up-regulated genes at 24 hpe (sorted by logFC)

50 most upregulated genes at 24 hpe (sorted by logFC)						
gene_id	**logFC_24h**	**adjpval_24h**	**Annotations**	**Full record name**	**Specie**	**E-value**
TR26702|c0_g1	9.50	1.97E-06	N42L1	NEDD4-binding_protein_2-like_1	*Mus musculus*	3E-07
TR78231|c0_g1	9.07	1.21E-04	GDF15	Growth/differentiation_factor_15	*Mus musculus*	2E-24
TR81776|c4_g4	8.77	2.83E-10	CC chemokine 20	C-C motif chemokine 20 precursor	*Anoplopoma fimbria*	8E-45
TR74252|c0_g1	8.68	1.11E-07	CFAH	Complement_factor_H	*Homo sapiens*	2E-34
TR45367|c1_g1	8.35	1.85E-07	HPT	Haptoglobin	*Sus scrofa*	3E-40
TR14360|c3_g2	8.27	2.83E-10	IL1B	Interleukin-1_beta	*Oncorhynchus mykiss*	9E-73
TR30315|c0_g1	8.05	3.91E-07	CO8A	Complement_component_C8_alpha_chain	*Oryctolagus cuniculus*	1E-157
TR23708|c0_g1	8.03	1.17E-07	NMES1	Normal_mucosa_of_esophagus-specific_gene_1_protein	*Homo sapiens*	2E-23
TR3853|c0_g2	7.83	3.67E-06	BORG1	Cdc42_effector_protein_2	*Homo sapiens*	4E-06
TR27293|c0_g1	7.67	9.05E-07	CO8B	Complement_component_C8_beta_chain	*Paralichthys olivaceus*	0
TR80849|c0_g2	7.59	2.06E-08	SAA1	Serum_amyloid_A-1_protein	*Mus musculus*	3E-11
TR76870|c0_g2	7.53	7.24E-07	EPGN	Epigen	*Gallus gallus*	1E-09
TR67971|c1_g1	7.49	3.57E-06	LPP	Lipoma-preferred_partner_homolog	*Gallus gallus*	1E-28
TR82903|c2_g2	7.42	6.94E-06	PHOS	Phosducin	*Bos taurus*	1E-65
TR79163|c0_g5	7.34	2.67E-10	TRFE	Serotransferrin	*Orizias latipes*	0
TR80347|c0_g1	7.17	2.83E-10	HEMO	Hemopexin_{ECO:0000250|UniProtKB:P20058}	*Danio rerio*	9E-46
TR45367|c1_g2	7.14	4.55E-05	HPT	Haptoglobin	*Rattus norwegicus*	1E-19
TR11634|c0_g2	7.10	4.82E-06	GAB	Alpha-N-acetylgalactosaminidase	*Gallus gallus*	3E-35
TR87818|c0_g1	7.10	4.16E-10	IL6	Interleukin-6	*Paralichthys olivaceus*	7E-70
TR42629|c0_g1	7.07	5.14E-06	INHBB	Inhibin_beta_B_chain	*Gallus gallus*	1E-77
TR13042|c4_g6	7.04	8.57E-09	DPYD	Dihydropyrimidine_dehydrogenase_[.DP(+)]	*Danio rerio*	5E-38
TR14183|c0_g1	6.91	4.16E-10	RET7	Retinoid-binding_protein_7	*Mus musculus*	5E-54
TR41627|c0_g1	6.90	9.11E-11	TLR5	Toll-like_receptor_5	*Homo sapiens*	6E-92
TR13890|c0_g3	6.73	1.16E-10	IL8	interleukin-8-like	*Serola dumerili*	6E-21
TR70589|c2_g2	6.70	1.97E-04	PTGES	Prostaglandin_E_synthase	*Equus ferus*	1E-22
TR76899|c0_g1	6.63	6.22E-06	IL17F	Interleukin-17F	*Rattus norwegicus*	1E-11
TR28096|c4_g11	6.57	9.52E-06	GRM4	Metabotropic_glutamate_receptor_4	*Rattus norwegicus*	7E-63
TR41114|c0_g2	6.52	1.16E-10	C1QL3	Complement_C1q-like_protein_3	*Mus musculus*	2E-12
TR41089|c3_g7	6.52	4.31E-06	MORC2	MORC_family_CW-type_zinc_finger_protein_2	*Homo sapiens*	2E-27
TR32785|c0_g2	6.42	6.87E-07	A2GL	Leucine-rich_alpha-2-glycoprotein	*Homo sapiens*	7E-46
TR13469|c0_g1	6.33	1.47E-05	MA7D2	MAP7_domain-containing_protein_2	*Pongo sp.*	5E-08
TR47931|c1_g1	6.30	2.65E-07	MOT4	Monocarboxylate_transporter_4	*Gallus gallus*	2E-149
TR31477|c0_g1	6.28	7.76E-06	NDF4	Neurogenic_differentiation_factor_4	*Homo sapiens*	7E-68

TR74574|c0_g2	6.25	2.64E-05	RGS5	Regulator_of_G-protein_signaling_5	*Rattus norwegicus*	1E-26
TR8953|c5_g4	6.22	6.56E-08	CO5	Complement_C5	*Homo sapiens*	0
TR48860|c0_g1	6.12	3.43E-04	EMAL6	Echinoderm_microtubule-associated_protein-like_6	*Homo sapiens*	1E-98
TR45357|c0_g2	6.08	2.31E-09	TGM2	Protein-glutamine_gamma-glutamyltransferase_2	*Pagrus major*	4E-153
TR38005|c0_g2	6.07	2.99E-07	HME2A	Homeobox_protein_engrailed-2-A	*Xenopus laevis*	5E-61
TR64331|c3_g1	6	4.16E-10	DPYD	Dihydropyrimidine_dehydrogenase_[.DP(+)]	*Danio rerio*	2E-49
TR81910|c0_g1	5.89	7.57E-09	CHSP1	Calcium-regulated_heat_stable_protein_1	*Rattus norwegicus*	2E-19
TR45395|c0_g1	5.85	3.36E-05	SPIC	Transcription_factor_Spi-C	*Bos taurus*	1E-34
TR78110|c0_g1	5.83	9.67E-05	CFAB	Complement_factor_B	*Bos taurus*	3E-63
TR57748|c0_g1	5.81	1.28E-05	KC.3	Potassium_voltage-gated_channel_subfamily_A_member_3	*Mus musculus*	0
TR71513|c0_g2	5.80	7.24E-05	S6A17	Sodium-dependent_neutral_amino_acid_transporter_SLC6A17	*Mus musculus*	1E-65
TR42615|c0_g1	5.63	3.76E-05	TRI55	Tripartite_motif-containing_protein_55	*Rattus norwegicus*	2E-37
TR10806|c0_g1	5.58	2.38E-05	GRAM3	GRAM_domain-containing_protein_3	*Rattus norwegicus*	5E-10
TR145009|c0_g1	5.55	8.80E-05	SIA4B	CMP-N-acetylneuraminate-beta-galactosamide-alpha-2,3-sialyltransferase_2	*Homo sapiens*	3E-118
TR78132|c0_g1	5.51	8.84E-05	FABP7	Fatty_acid-binding_protein,_brain	*Mus musculus*	9E-08
TR23250|c0_g1	5.50	2.12E-05	FXYD6	FXYD_domain-containing_ion_transport_regulator_6	*Mus musculus*	6E-22

Supplemental Table 3. Overview of the 50 most down-regulated genes at 24 hpe (sorted by logFC)

50 most downregulated genes at 24 hpe (sorted by logFC)						
gene_id	**logFC_24h**	**adjpval_24h**	**Annotations**	**Full record name**	**Specie**	**E-value**
TR41171|c0_g1	-7.56	2.02E-06	LRC3B	Leucine-rich_repeat-containing_protein_3B	*Homo sapiens*	9E-65
TR70719|c4_g4	-7.46	4.49E-07	NSMA2	Sphingomyelin_phosphodiesterase_3	*Mus musculus*	3E-85
TR45504|c0_g2	-7.30	1.59E-07	S43A3	Solute_carrier_family_43_member_3	*Homo sapiens*	2E-72
TR51281|c0_g3	-7.26	1.44E-06	TGM2	Protein-glutamine_gamma-glutamyltransferase_2	*Gallus gallus*	8E-80
TR53083|c0_g1	-7.17	5.90E-06	MRC1	Macrophage_mannose_receptor_1	*Mus musculus*	2E-39
TR15942|c0_g2	-7.09	5.77E-07	DMBT1	Deleted_in_malignant_brain_tumors_1_protein	*Homo sapiens*	1E-73
TR80906|c0_g1	-7	1.21E-05	IL17F	Interleukin-17F	*Rattus norwegicus*	4E-11
TR31532|c0_g1	-6.74	1.13E-05	KCJ12	ATP-sensitive_inward_rectifier_potassium_channel_12	*Gallus gallus*	0
TR68049|c0_g1	-6.56	9.71E-05	CNKR2	Connector_enhancer_of_kinase_suppressor_of_ras_2	*Homo sapiens*	0
TR3259|c0_g1	-6.53	3.10E-06	TNR3	Tumor_necrosis_factor_receptor_superfamily_member_3	*Homo sapiens*	8E-09
TR53083|c0_g2	-6.45	2.87E-05	MRC1	Macrophage_mannose_receptor_1	*Mus musculus*	1E-39
TR65297|c3_g1	-6.44	1.44E-06	TMM88	Transmembrane_protein_88	*Mus musculus*	2E-12
TR69288|c0_g1	-6.36	9.32E-07	TNR11	Tumor_necrosis_factor_receptor_superfamily_member_11A	*Mus musculus*	9E-13
TR28894|c2_g1	-6.28	5.44E-06	COR2A	Coronin-2A	*Homo sapiens*	0
TR2247|c0_g1	-6.23	2.19E-06	RLBP1	Retinaldehyde-binding_protein_1	*Bos taurus*	2E-158
TR144820|c0_g2	-6.10	2.97E-05	PRDM1	PR_domain_zinc_finger_protein_1	*Mus musculus*	2E-26
TR6306|c0_g2	-6.03	1.49E-03	EVA1A	Protein_eva-1_homolog_A	*Danio rerio*	5E-37
TR87113|c1_g2	-6.01	9.36E-04	CEBPD	CCAAT/enhancer-binding_protein_delta	*Homo sapiens*	2E-56
TR53083|c1_g5	-5.90	1.16E-10	MRC1	Macrophage_mannose_receptor_1	*Mus musculus*	0
TR80012|c0_g1	-5.87	5.45E-08	S12A4	Solute_carrier_family_12_member_4	*Homo sapiens*	0
TR49079|c0_g3	-5.75	3.21E-06	MITF	Microphthalmia-associated_transcription_factor	*Homo sapiens*	1E-67
TR65368|c1_g21	-5.73	6.74E-05	ANKR1	Ankyrin_repeat_domain-containing_protein_1	*Gallus gallus*	4E-49
TR26688|c3_g1	-5.72	1.34E-02	ENOG	Gamma-enolase	*Rattus norwegicus*	2E-133
TR40542|c0_g1	-5.68	7.31E-07	HECA2	HEPACAM_family_member_2	*Homo sapiens*	1E-06
TR37184|c1_g3	-5.62	2.73E-04	FDXA1	Ferredoxin-fold_anticodon-binding_domain-containing_protein_1_homolog	*Mus musculus*	2E-27
TR8782|c0_g1	-5.56	3.30E-05	EPD2	Ependymin-2	*Carassius auratus*	3E-22
TR68285|c0_g1	-5.50	5.35E-05	DTBP1	Dysbindin	*Gallus gallus*	6E-31
TR880|c0_g2	-5.48	2.73E-05	MAP6	Microtubule-associated_protein_6_homolog	*Gallus gallus*	1E-31
TR71817|c0_g1	-5.44	2.54E-05	TGFA1	Transforming_growth_factor-beta_receptor-associated_protein_1	*Mus musculus*	1E-123
TR101|c0_g1	-5.41	1.04E-06	VAT1	Synaptic_vesicle_membrane_protein_VAT-1_homolog	*Danio rerio*	0
TR34008|c0_g1	-5.33	2.52E-07	SEM4G	Semaphorin-4G	*Homo sapiens*	0
TR44282|c0_g1	-5.32	3.20E-06	PHEX	Metalloendopeptidase_homolog_PEX	*Mus musculus*	0

TR43339|c0_g1	-5.31	1.36E-05	NFIL3	Nuclear_factor_interleukin-3-regulated_protein	*Rattus norwegicus*	2E-17
TR62246|c0_g1	-5.25	2.81E-05	JIP1	C-Jun-amino-terminal_kinase-interacting_protein_1	*Homo sapiens*	2E-141
TR14442|c0_g1	-5.21	6.43E-05	TLR13	Toll-like_receptor_13	*Mus musculus*	3E-66
TR54313|c0_g2	-5.19	5.12E-06	FABPL	Fatty_acid-binding_protein,_liver	*Ginglymostoma cirratum*	2E-14
TR5820|c0_g1	-5.14	1.30E-04	SREC	Scavenger_receptor_class_F_member_1	*Homo sapiens*	9E-37
TR85479|c0_g2	-5.14	7.80E-05	S29A1	Equilibrative_nucleoside_transporter_1	*Rattus norwegicus*	3E-42
TR78540|c0_g2	-5.11	9.48E-05	PERF	Perforin-1	*Rattus norwegicus*	8E-129
TR9527|c0_g1	-4.99	3.57E-06	NUAK1	NUAK_family_SNF1-like_kinase_1	*Homo sapiens*	0
TR65997|c0_g1	-4.98	1.54E-05	EFNB2	Ephrin-B2a	*Danio rerio*	5E-40
TR156627|c0_g3	-4.96	8.03E-03	CBP	CREB-binding_protein	*Rattus norwegicus*	1E-08
TR40644|c0_g2	-4.95	1.74E-04	RGS5	Regulator_of_G-protein_signaling_5	*Rattus norwegicus*	7E-55
TR38943|c0_g1	-4.93	3.66E-04	FGF4	Fibroblast_growth_factor_4	*Gallus gallus*	6E-09
TR6306|c0_g5	-4.90	4.04E-05	EVA1A	Protein_eva-1_homolog_A	*Danio rerio*	4E-37
TR25290|c0_g4	-4.90	1.61E-04	KCNH6	Potassium_voltage-gated_channel_subfamily_H_member_6	*Rattus norwegicus*	2E-83
TR12896|c0_g2	-4.85	1.08E-03	AMPN	Aminopeptidase_N_{ECO:0000312|EMBL:ACZ95799.1}	*Gallus gallus*	4E-141
TR1713|c0_g2	-4.84	2.41E-05	APOA4	Apolipoprotein_A-IV	*Papio anubis*	2E-28
TR56616|c0_g1	-4.72	2.88E-04	TGM2	Protein-glutamine_gamma-glutamyltransferase_2	*Homo sapiens*	3E-145

Supplemental Table 4. Overview of the 50 most up-regulated genes at 6 hpe (sorted by logFC)

50 most upregulated genes at 6 hpe (sorted by logFC)						
gene_id	**logFC_6h**	**adjpval_6h**	**Annotations**	**Full record name**	**Specie**	**E-value**
TR76899|c0_g1	9.37	7.35E-06	IL17F	Interleukin-17F	*Rattus norwegicus*	1E-11
TR26702|c0_g1	9.05	8.57E-06	N42L1	NEDD4-binding_protein_2-like_1	*Mus musculus*	3E-07
TR20674|c0_g2	7.73	4.87E-06	HYAS1	Hyaluronan_synthase_1	*Xenopus laevis*	0
TR45366|c0_g1	7.13	2.38E-05	ZN648	Zinc_finger_protein_648	*Homo sapiens*	7E-112
TR78231|c0_g1	6.87	1.18E-03	GDF15	Growth/differentiation_factor_15	*Mus musculus*	2E-24
TR32785|c0_g2	6.74	7.21E-05	A2GL	Leucine-rich_alpha-2-glycoprotein	*Homo sapiens*	7E-46
TR14360|c3_g2	6.69	7.93E-09	IL1B	Interleukin-1_beta	*Oncorhynchus mykiss*	9E-73
TR87818|c0_g1	6.51	1.62E-07	IL6	Interleukin-6	*Paralichthys olivaceus*	7E-70
TR13890|c0_g3	6.39	9.31E-10	IL8	interleukin-8-like	*Serola dumerili*	6E-21
TR81776|c4_g4	6.17	2.90E-09	CC chemokine 20	C-C motif chemokine 20 precursor	*Anoplopoma fimbria*	8E-45
TR76870|c0_g2	5.85	4.53E-07	EPGN	Epigen	*Gallus gallus*	1E-09
TR45395|c0_g1	5.60	4.71E-04	SPIC	Transcription_factor_Spi-C	*Bos taurus*	1E-34
TR19933|c0_g1	5.47	1.69E-08	GL.	Glutamine_synthetase	*Acomys cahirinus*	4E-109
TR67971|c1_g1	5.46	5.24E-05	LPP	Lipoma-preferred_partner_homolog	*Gallus gallus*	1E-28
TR74252|c0_g1	5.40	9.82E-06	CFAH	Complement_factor_H	*Homo sapiens*	2E-34
TR49945|c0_g1	5.26	7.93E-09	GL.	Glutamine_synthetase,_mitochondrial	*Squalus acanthias*	6E-22
TR87414|c0_g1	5.19	7.93E-09	GL.	Glutamine_synthetase	*Canis familiaris*	2E-147
TR44307|c0_g2	5.17	2.60E-04	VAX2B	Ventral_anterior_homeobox_2b	*Xenopus laevis*	5E-63
TR27410|c1_g1	5.15	8.04E-07	NOXO1	.DPH_oxidase_organizer_1	*Mus musculus*	4E-59
TR81910|c0_g1	5.13	1.67E-06	CHSP1	Calcium-regulated_heat_stable_protein_1	*Rattus norwegicus*	2E-19
TR66238|c0_g2	5.08	1.50E-04	CN159	UPF0317_protein_C14orf159_homolog,_mitochondrial	*Mus musculus*	2E-15
TR87025|c0_g2	5	1E-09	Uncharacterized protein	PREDICTED: uncharacterized protein LOC108879818	*Lates calcarifer*	5E-73
TR68048|c0_g1	5	2.42E-04	GRAM3	GRAM_domain-containing_protein_3	*Rattus norwegicus*	2E-10
TR14183|c0_g1	4.94	6.67E-08	RET7	Retinoid-binding_protein_7	*Mus musculus*	5E-54
TR11634|c0_g2	4.91	4E-06	.GAB	Alpha-N-acetylgalactosaminidase	*Gallus gallus*	3E-35
TR61339|c0_g1	4.85	6.62E-04	ISL2A	Insulin_gene_enhancer_protein_isl-2a	*Danio rerio*	0
TR80347|c0_g1	4.70	1.70E-07	HEMO	Hemopexin_{ECO:0000250|UniProtKB:P20058}	*Danio rerio*	9E-46
TR34004|c3_g1	4.50	7.93E-09	TNIP2	TNFAIP3-interacting_protein_2	*Mus musculus*	5E-20
TR78134|c0_g1	4.46	2.34E-03	SSR2	Somatostatin_receptor_type_2	*Sus scrofa*	3E-118
TR44039|c0_g1	4.41	4.89E-03	ETV6	Transcription_factor_ETV6	*Homo sapiens*	5E-20
TR86119|c0_g1	4.40	3.17E-09	TNIP2	TNFAIP3-interacting_protein_2	*Mus musculus*	2E-31
TR69814|c0_g2	4.38	2.80E-08	TNFA	Tumor_necrosis_factor	*Sparus auratus*	3E-114
TR45367|c1_g2	4.35	3.78E-03	HPT	Haptoglobin	*Rattus norwegicus*	1E-19
TR31519|c0_g1	4.31	8.49E-10	NR4A1	Nuclear_receptor_subfamily_4_group_A_member_1	*Xenopus laevis*	6E-52

TR45033|c0_g1	4.30	2.83E-03	SSR2	Somatostatin_receptor_type_2	*Homo sapiens*	1E-62
TR27348|c0_g2	4.30	2.48E-02	IKBA	NF-kappa-B_inhibitor_alpha	*Sus scrofa*	5E-06
TR41627|c0_g1	4.28	2.90E-09	TLR5	Toll-like_receptor_5	*Homo sapiens*	6E-92
TR69283|c1_g1	4.27	2.90E-09	Hypothetical protein	hypothetical protein Z043_122910	*Scleropages formosus*	9E-05
TR57748|c0_g1	4.24	4.95E-04	KC.3	Potassium_voltage-gated_channel_subfamily_A_member_3	*Mus musculus*	0
TR31477|c0_g1	4.20	6.99E-04	NDF4	Neurogenic_differentiation_factor_4	*Homo sapiens*	7E-68
TR45357|c0_g2	4.18	3.24E-07	TGM2	Protein-glutamine_gamma-glutamyltransferase_2	*Pagrus major*	4E-153
TR57132|c0_g1	4.17	9.26E-03	LORF2	LINE-1_retrotransposable_element_ORF2_protein	*Homo sapiens*	3E-20
TR80347|c0_g2	4.12	1.69E-03	HEMO	Hemopexin_{ECO:0000250|UniProtKB:P20058}	*Danio rerio*	3E-14
TR80849|c0_g2	4.11	1.47E-03	SAA1	Serum_amyloid_A-1_protein	*Mus musculus*	3E-11
TR23312|c0_g1	4.10	1.10E-08	ADTRP	Androgen-dependent_TFPI-regulating_protein	*Homo sapiens*	4E-06
TR69281|c3_g2	4.08	4.79E-03	MTSS1	Metastasis_suppressor_protein_1	*Homo sapiens*	2E-31
TR64314|c0_g1	4.05	5.05E-05	S12A2	Solute_carrier_family_12_member_2	*Mus musculus*	1E-06
TR61516|c0_g2	3.95	3.33E-03	BIRC6	Baculoviral_IAP_repeat-containing_protein_6	*Homo sapiens*	4E-125
TR45367|c1_g1	3.94	4.97E-04	HPT	Haptoglobin	*Sus scrofa*	3E-40
TR41618|c1_g3	3.94	1.11E-04	PDK2	[Pyruvate_dehydrogenase_(acetyl-transferring)]_kinase_isozyme_2,_mitochondrial	*Rattus norwegicus*	7E-09

Supplemental Table 5. Overview of the 50 most down-regulated genes at 6 hpe (sorted by logFC)

50 most downregulated genes at 6 hpe (sorted by logFC)						
gene_id	**logFC_6h**	**adjpval_6h**	**Annotations**	**Full record name**	**Specie**	**E-value**
TR145793|c0_g6	-6.30	2.63E-02	ZFX	Zinc_finger_X-chromosomal_protein	*Mus musculus*	9E-117
TR53083|c0_g2	-5.29	1.61E-03	MRC1	Macrophage_mannose_receptor_1	*Mus musculus*	1E-39
TR55536|c0_g2	-4.63	2.16E-02	CCR6	C-C_chemokine_receptor_type_6	*Homo sapiens*	2E-76
TR40542|c0_g1	-4.24	7.23E-04	HECA2	HEPACAM_family_member_2	*Homo sapiens*	1E-06
TR145793|c0_g1	-4.23	4.14E-02	ZFX	Zinc_finger_X-chromosomal_protein	*Mus musculus*	1E-116
TR85757|c0_g4	-3.68	6.06E-02	ZBT37	Zinc_finger_and_BTB_domain-containing_protein_37	*Homo sapiens*	2E-79
TR62246|c0_g1	-3.61	1.49E-03	JIP1	C-Jun-amino-terminal_kinase-interacting_protein_1	*Homo sapiens*	2E-141
TR150022|c0_g1	-3.56	4.70E-03	LPAR4	Lysophosphatidic_acid_receptor_4	*Mus musculus*	5E-17
TR53083|c0_g1	-3.52	1.60E-03	MRC1	Macrophage_mannose_receptor_1	*Mus musculus*	2E-39
TR71817|c0_g1	-3.48	2.46E-03	TGFA1	Transforming_growth_factor-beta_receptor-associated_protein_1	*Mus musculus*	1E-123
TR40529|c0_g3	-3.26	1.98E-02	JDP2	Jun_dimerization_protein_2	*Rattus norwegicus*	6E-57
TR57429|c0_g9	-3.24	9.04E-03	ABI3	ABI_gene_family_member_3	*Homo sapiens*	5E-10
TR16539|c0_g2	-3.17	5.35E-02	TSN8	Tetraspanin-8	*Bos taurus*	2E-07
TR36086|c0_g2	-3.08	3E-02	CXCR5	C-X-C_chemokine_receptor_type_5	*Rattus norwegicus*	1E-36
TR67966|c4_g1	-3.04	1.09E-01	UB2G2	Ubiquitin-conjugating_enzyme_E2_G2	*Pongo sp.*	8E-10
TR33782|c1_g4	-3.04	3.81E-06	MMP14	Matrix_metalloproteinase-14	*Mus musculus*	5E-138
TR67966|c4_g4	-3.02	6.91E-02	UB2G2	Ubiquitin-conjugating_enzyme_E2_G2	*Pongo sp.*	7E-10
TR633|c0_g3	-3.02	1.51E-01	ADAT2	tR.-specific_adenosine_deaminase_2	*Danio rerio*	1E-71
TR44789|c0_g1	-3	1.69E-01	KAD2	Adenylate_kinase_2,_mitochondrial_{ECO:0000255|HAMAP-Rule:MF_03168}	*Salmo salar*	2E-15
TR34008|c0_g1	-2.93	3.81E-06	SEM4G	Semaphorin-4G	*Homo sapiens*	0
TR69449|c4_g10	-2.92	1.96E-02	RTXE	Probable_R.-directed_D._polymerase_from_transposon_X-element	*Drosophila melongaster*	2E-13
TR70501|c4_g2	-2.91	7.79E-03	ABI2	Abl_interactor_2	*Mus musculus*	2E-101
TR65297|c3_g1	-2.88	5.13E-04	TMM88	Transmembrane_protein_88	*Mus musculus*	2E-12
TR25793|c0_g1	-2.85	2.12E-02	FHOD3	FH1/FH2_domain-containing_protein_3	*Mus musculus*	8E-22
TR2196|c0_g2	-2.83	3.60E-02	WDR18	WD_repeat-containing_protein_18	*Danio rerio*	1E-76
TR35910|c0_g2	-2.77	1.18E-01	ADA1D	Alpha-1D_adrenergic_receptor	*Sus scrofa*	5E-36
TR49070|c0_g1	-2.75	5.86E-05	SPTB2	Spectrin_beta_chain,_non-erythrocytic_1	*Mus musculus*	3E-13
TR84473|c0_g1	-2.74	1.25E-02	TLR2	Toll-like_receptor_2	*Cricetulus griseus*	3E-15
TR87042|c0_g6	-2.73	1.65E-01	ADCK1	Uncharacterized_aarF_domain-containing_protein_kinase_1	*Homo sapiens*	8E-09
TR27448|c0_g3	-2.72	3.35E-01	SC6A8	Sodium-_and_chloride-dependent_creatine_transporter_1	*Rattus norwegicus*	0
TR15942|c0_g2	-2.70	4.75E-06	DMBT1	Deleted_in_malignant_brain_tumors_1_protein	*Homo sapiens*	1E-73
TR25104|c0_g5	-2.68	1.95E-01	FND3A	Fibronectin_type-III_domain-containing_protein_3A	*Homo sapiens*	3E-13
TR85479|c0_g2	-2.66	4.34E-03	S29A1	Equilibrative_nucleoside_transporter_1	*Rattus norwegicus*	3E-42
TR84456|c0_g3	-2.64	1.85E-01	PSPC1	Paraspeckle_component_1	*Danio rerio*	2E-134

TR65271|c0_g1	-2.63	1.26E-02	VINC	Vinculin	*Xenopus laevis*	5E-15
TR60099|c0_g2	-2.63	1.16E-01	TRIM3	Tripartite_motif-containing_protein_3	*Mus musculus*	2E-94
TR24328|c0_g1	-2.61	2.38E-03	TM158	Transmembrane_protein_158	*Mus musculus*	7E-63
TR85510|c0_g3	-2.60	7.17E-03	F264	6-phosphofructo-2-kinase/fructose-2,6-bisphosphatase_4	*Mus musculus*	6E-40
TR74312|c1_g7	-2.58	3.17E-03	PI42A	Phosphatidylinositol_5-phosphate_4-kinase_type-2_alpha	*Gallus gallus*	6E-111
TR43358|c0_g1	-2.55	5.16E-03	I22R2	Interleukin-22_receptor_subunit_alpha-2	*Mus musculus*	2E-22
TR65255|c0_g11	-2.48	3.49E-03	LORF2	LINE-1_retrotransposable_element_ORF2_protein	*Mus musculus*	2E-46
TR25130|c0_g2	-2.46	1.92E-02	AQP8	Aquaporin-8	*Homo sapiens*	2E-17
TR22880|c0_g3	-2.46	1.95E-01	MED23	Mediator_of_R._polymerase_II_transcription_subunit_23	*Danio rerio*	0
TR41097|c0_g1	-2.45	2.94E-03	MAGI1	Membrane-associated_guanylate_kinase,_WW_and_PDZ_domain-containing_protein_1	*Rattus norwegicus*	6E-44
TR65980|c0_g1	-2.42	2.11E-04	FAT3	Protocadherin_Fat_3	*Rattus norwegicus*	0
TR8375|c0_g1	-2.41	9.46E-05	P2RX5	P2X_purinoceptor_5	*Rattus norwegicus*	2E-82
TR57480|c0_g1	-2.40	2.56E-05	SPTN5	Spectrin_beta_chain,_non-erythrocytic_5	*Homo sapiens*	4E-20
TR26681|c0_g5	-2.38	1.47E-01	SOS1	Son_of_sevenless_homolog_1	*Homo sapiens*	3E-158
TR28080|c0_g1	-2.38	2.15E-03	SVEP1	Sushi,_von_Willebrand_factor_type_A,_EGF_and_pentraxin_domain-containing_protein_1	*Homo sapiens*	0
TR40831|c1_g1	-2.36	1.58E-01	CEGT	Ceramide_glucosyltransferase	*Mus musculus*	3E-69
TR59866|c0_g1	-2.36	4.71E-08	P5CS	Delta-1-pyrroline-5-carboxylate_synthase	*Pongo sp.*	1E-165

Supplemental Table 6. Overview of verified lumpfish genes in the complement cascade

			Top BLAST hit			
Gene-ID	**Name**	**KEGG orthology ID**	**Description**	**E-value**	**Species**	**Accession number**
Complement components						
TR16469|c0_g4	C1R	K01330	complement component C1q receptor	0	*Monopterus albus*	XP_020479096
TR40321|c0_g2	C1R/1S	K01331	Ca2+-dep.complex C1R/C1S subunit	5.14E-152	*Perca flavescens*	ABU63968
TR74292|c0_g1	C1S	K01331	complement component 1s	2.38E-162	*Oplegnathus fasciatus*	AIZ96980
TR74819|c0_g1	C2	K01332	complement component 2	1.20E-143	*Oplegnathus fasciatus*	AIN76765
TR104686|c0_g1 TR63519|c0_g1	C3 C3	K03990 K03990	PRED: complement C3-like PRED: complement C3-like	7E-54 8E-57	*Lates calcarifer* *Lates calcarifer*	XP_018528015 XP_018528013
TR56223|c0_g1 TR1140|c0_g2 TR78116|c0_g1	C3 C3 C3	K03990 K03990 K03990	complement C3-like complement C3-like complement C3-like	2.16E-165 2E-144 0	*Acanthochromis polyacanthus* *Oryzias latipes* *Stegastes partitus*	XP_022077167 XP_020555289 XP_008298001
TR77762|c0_g1	C3	K03990	PRED: complement component C3	6E-46	*Paralichthys olivaceus*	XP_019939804
TR88215|c0_g1	C3	K03990	complement component C3	8E-47	*Acanthochromis polyacanthus*	XP_022064368
TR64828|c1_g1	C4	K03989	complement component 4	0	*Oplegnathus fasciatus*	AIN76766
TR8953|c5_g4	C5	K03994	PRED: complement C5	0	*Lates calcarifer*	XP_018549132
TR49109|c2_g3 TR67474|c0_g1 TR62911|c0_g1	C5AR1 C5AR1 C5AR1	K04010 K04010 K04010	C3a anaphylatoxin chemotactic receptor C3a anaphylatoxin chemotactic receptor C3a anaphylatoxin chemotactic receptor	3.36E-156 1.77E-131 0	*Larimichthys crocea* *Seriola dumerili* *Seriola dumerili*	XP_010733778 XP_022617678 XP_022616734
TR48847|c0_g1 TR48847|c0_g2 TR70869|c1_g1 TR70745|c3_g1	C5AR1 C5AR1 C5AR1 C5AR1	K04010 K04010 K04010 K04010	chemokine-like receptor 1 chemokine-like receptor 1 chemokine-like receptor 1 chemokine-like receptor 1	0 0 0 7.7E-170 0	*Notothenia coriiceps* *Notothenia coriiceps* *Acanthochromis polyacanthus* *Acanthochromis polyacanthus*	XP_010785059 XP_010785059 XP_022065692 XP_022065692
TR121251|c0_g1 TR43399|c0_g1	C6 C6	K03995 K03995	complement component C6 isoform X1 complement component C6-like protein	2.08E-30 3.4E-155	*Labrus bergylta* *Siniperca chuatsi*	XP_020491684 AKA66307
TR15677|c0_g1 TR69965|c1_g1	C6 C6	K03995 K03995	complement component C6 complement component C6	2.18E-44 1.16E-94	*Kryptolebias marmoratus* *Notothenia coriiceps*	XP_017259971 XP_010771775
TR77069|c0_g1	C7	K03996	complement component C7	1.8E-100	*Oplegnathus fasciatus*	AFZ93893
TR40591|c0_g1	C7	K03996	PRED: complement component C7 X2	2.13E-31	*Larimichthys crocea*	XP_019120079
TR62647|c0_g1	C7	K03996	complement component C7-2	3.59E-67	*Miichthys miiuy*	AKM12676
TR37853|c0_g1 TR94503|c0_g1	C7 C7	K03996 K03996	PRED: complement component C7-like PRED: complement component C7-like	5.71E-124 5.71E-124	*Notothenia coriiceps* *Notothenia coriiceps*	XP_010792065 XP_010792065
TR122188|c0_g1 TR53398|c0_g1	C7 C7	K03996 K03996	complement component C7-like complement component C7-like	9.5E-57 4.1E-153	*Monopterus albus* *Monopterus albus*	XP_020479067 XP_020479067

TR126963|c0_g1	C7	K03996	complement component C7-like	1.17E-41	*Seriola dumerili*	XP_022600176
TR30315|c0_g1	C8A	K03997	complement component 8 alpha	0	*Siniperca chuatsi*	AKA66305
TR27293|c0_g1	C8B	K03998	complement component 8 beta	0	*Oplegnathus fasciatus*	AFZ93889
TR122188|c0_g1 TR53398|c0_g1 TR126963|c0_g1	C9 C9 C9	K04000 K04000 K04000	complement component 9 complement component 9 complement component 9	3.3E-06 1.01E-57 2.22E-60	*Oryzias latipes* *Paralichthys olivaceus*	XP_004074560 BAA86878 BAA86878
TR78110|c0_g1	CFB	K01335	PRED: complement factor B-like	0	*Lates calcarifer*	XP_018547243
TR5891|c0_g1	CFD	K01334	PRED: complement factor D-like	1.54E-162	*Lates calcarifer*	XP_018541031
TR62909|c0_g1 TR74252|c0_g1	CFH CFH	K04004 K04004	PRED: complement factor H-like PRED: complement factor H-like	0 6e-122	*Hippocampus comes* *Lates calcarifer*	XP_019740144 XP_01852636
TR84448|c0_g1	CFI	K01333	complement factor I	0	*Labrus bergylta*	XP_020514187
TR62930|c0_g1	CFP	K15412	properdin	0	*Acanthochromis polyacanthus*	XP_022073264
TR63188|c0_g1	CLU	K17252	clusterin	1.08E-168	*Monopterus albus*	XP_020459633
TR13054|c1_g2 TR64830|c2_g2	CR3 CR3	K06461 K06461	Integrin alpha-M (ITAM) Integrin alpha-M (ITAM)	0 0	*Dicentrarchus labrax* *Dicentrarchus labrax*	CBN81367 CBN81367
TR100|c0_g1 TR15999|c3_g3	ITGB2 ITGB2	K06464 K06464	integrin beta-2-like integrin beta-2-like	6.70 6.70	*Hippocampus comes* *Hippocampus comes*	XP_019731231 XP_019731231
TR13103|c3_g7	ITGB2	K06464	integrin beta-2-like	0	*Monopterus albus*	XP_020462274
TR1125|c1_g2	MASP1	K03992	Mannan-binding lectin serine protease 1	0	*Larimichthys crocea*	KKF27967

Supplemental Table 7. Overview of the species included in the phylogenetic analyses

Species	Authorities	Common name	Teleost order (Nelson et al 2016)	Teleost order (Betancur-R et al.2013)	Family[1]
Danio rerio	Hamilton, 1822	zebrafish	*Cypriniformes*	*Cypriniformes*	*Cyprinidae*
Takifugu rubripes	Temminck & Schlegel, 1850	fugu	*Tetraodontiformes*	*Tetraodontiformes*	*Tetraodontidae*
Gasterosteus aculeatus	Linnaeus, 1758	stickleback	*Gasterosteiformes*	*Perciformes*	*Gasterosteidae*
Oryzias latipes	Temminck & Schlegel, 1850	medaka	*Beloniformes*	*Beloniformes*	*Adrianichthyidae*
Gadus morhua	Linnaeus, 1758	cod	*Gadiformes*	*Gadiformes*	*Gadidae*
Cyclopterus lumpus	Linnaeus, 1758	lumpfish	*Scorpaniformes*	*Perciformes*	*Cyclopteridae*
Miichthys miiuy	Basilewsky, 1855	croaker	*Perciformes*	*Percomorpharia* *	*Sciaenidae*
Ictalurus punctatus	Rafinesque, 1818	catfish	*Siluriformes*	*Siluriformes*	*Ictaluridae*
Plecoglossus altivelis altivelis	Temminck & Schlegel, 1846	ayu sweetfish	*Osmeriformes*	*Osmeriformes*	*Plecoglossidae*
Oncorhynchus mykiss	Walbaum, 1792	rainbow trout	*Salmoniformes*	*Salmoniformes*	*Salmonidae*
Coregonus maraena	Bloch, 1779	mareana whitefish	*Salmoniformes*	*Salmoniformes*	*Salmonidae*
Sparus aurata	Linnaeus, 1758	gilthead seabream	*Perciformes*	*Spariformes*	*Sparidae*
Scophthalmus maximus	Linnaeus, 1758	turbot	*Pleuronectiformes*	*Pleuronectiformes*	*Scophtalmidae*
Paralichthys olivaceus	Temminck & Schlegel, 1846	bastard halibut	*Pleuronectiformes*	*Pleuronectiformes*	*Paralichthyidae*
Oplegnathus fasciatus	Temminck & Schlegel, 1844	barred knifejaw	*Perciformes*	*Percomorpharia* *	*Oplegnathidae*
Cirrhinus mrigala	Hamilton, 1822	mrigal carp	*Cypriniformes*	*Cypriniformes*	*Cyprinidae*
Carassius auratus	Linnaeus, 1758	goldfish	*Cypriniformes*	*Cypriniformes*	*Cyprinidae*
Ctenopharyngodon idella	Valenciennes, 1844	grass carp	*Cypriniformes*	*Cypriniformes*	*Cyprinidae*
Cyprinus carpio	*Linnaeus, 1758*	common carp	*Cypriniformes*	*Cypriniformes*	*Cyprinidae*
Megalobrama amblycephala	Yih, 1955	wuchang bream	*Cypriniformes*	*Cypriniformes*	*Cyprinidae*
Salmo salar	Linnaeus, 1758	Atlantic salmon	*Salmoniformes*	*Salmoniformes*	*Salmonidae*
Larimichthys crocea	Richardson, 1846	large yellow croaker	*Perciformes*	*Percomorpharia* *	*Sciaenidae*
Epinephelus coioides	Hamilton, 1822	orange-spotted grouper	*Perciformes*	*Perciformes*	*Serranidae*
Carassius gibelio	Bloch, 1782	prussian carp	*Cypriniformes*	*Cypriniformes*	*Cyprinidae*
Gobiocypris rarus	Ye & Fu, 1983	N.A.	*Cypriniformes*	*Cypriniformes*	*Cyprinidae*
Squaliobarbus curriculus	b	barbel chub	*Cypriniformes*	*Cypriniformes*	*Cyprinidae*
Cynoglossus semilaevis	Günther, 1873	tounge sole	*Pleuronectiformes*	*Pleuronectiformes*	*Cynoglossidae*
Fundulus heteroclitus	Linnaeus, 1766	mummichug	*Cyprinodontiformes*	*Cyprinodontiformes*	*Fundulidae*
Trematomus bernacchii	Boulenger, 1902	emerald rockcod	*Perciformes*	*Perciformes*	*Nototheniidae*
Chionodraco hamatus	Lönnberg, 1905	crocodile icefishes	*Perciformes*	*Perciformes*	*Channichthyidae*

Nothobranchius furzeri	Jubb, 1971	turquoise killifish	*Cyprinodontiformes*	Not examined	*Notobranchiidae*
Nothobranchius rachovii	Ahl, 1926	bluefin notho	*Cyprinodontiformes*	Not examined	*Notobranchiidae*
Nothobranchius kadleci	Richard, 2010	N.A.	*Cyprinodontiformes*	Not examined	*Notobranchiidae*
Labeo rohita	Hamilton, 1822	roho labeo	*Cypriniformes*	*Cypriniformes*	*Cyprinidae*
Tachysurus fulvidraco	Richardson, 1846	yellow catfish	*Siluriformes*	*Siluriformes*	*Bagridae*
Tetraodon nigroviridis	Marion de Procé, 1822	spotted green pufferfish	*Tetraodontiformes*	*Tetraodontiformes*	*Tetraodontidae*
Gymnocypris przewalskii	Kessler, 1876	N.A.	*Cypriniformes*	*Cypriniformes*	*Cyprinidae*
Scleropages formosus	Müller & Schlegel, 1840	asian arowana	*Osteoglossiformes*	*Osteoglossiformes*	*Osteoglossidae*
Siniperca chuatsi	Basilewsky, 1855	mandarin fish	*Perciformes*	*Percomorpharia* *	*Perchichtyidae*
Seriola lalandi	Valenciennes,1833	yellowtail amberjack	*Perciformes*	*Carangiformes*	*Carangidae*
Lates calcarifer	Bloh, 1790	barramundi	*Perciformes*	*Carangimorpharia**	*Latidae*
Catla catla	Hamilton, 1822	catla	*Cypriniformes*	*Cypriniformes*	*Cyprinidae*
Clarias batrachus	Linnaeus, 1758	philippine catfish	*Siluriformes*	*Siluriformes*	*Clariidae*
Oreochromis niloticus	Linnaeus, 1758	nile tilapia	*Perciformes*	*Cichliformes*	*Cichlidae*
Labrus bergylta	Ascanius, 1767	ballan wrasse	*Perciformes*	*Labriformes*	*Labridae*
Stegastes partitus	Poey, 1868	bicolor damselfish	*Perciformes*	*Ovalentariae**	*Pomacentridae*
Maylandia zebra	Boulenger, 1899	zebra mbuna	*Perciformes*	*Cichliformes*	*Cichlidae*
Callorhinchus milii	Bory de Saint-Vincet, 1823	ghost shark	*Chimaeriformes*	Not examined	*Callorhichidae*

* incertae sedis. N.A. = non applicable

References:

Nelson, J. S., Grande, T. C. & Wilson, M. V. H. *Fishes of the world, 5th Edition.* (2016).
Betancur, R. R. *et al*. The tree of life and a new classification of bony fishes. *PLoS Curr* doi:10.1371/current.tol.53ba26640df0ccaee75bb165c8c26288 (2013)

Supplemental Table 8: Accession numbers of genes in the phylogenetic analyses of TLRs

Abbrevation	Species	Acc. No.
TLR1		
TLR1	*Coregonus maraena*	CEF90214.1
TLR1	*Ctenopharyngodon idella*	ACT68332.1
TLR1	*Cyprinus carpio*	BAU98379.1
TLR1	*Epinephelus coioides*	AEB32452.1
TLR1	*Gymnocypris przewalskii*	ANQ46688.1
TLR1	*Homo sapiens*	Q15399
TLR1	*Larimichthys crocea*	AHB51065.1
TLR1	*Megalobrama amblycephala*	APT35500.1
TLR1	*Miichthys miiuy*	AKJ66261.1
TLR1	*Mus musculus*	Q9EPQ1
TLR1	*Oncorhynchus mykiss*	ACV92063.1
TLR1	*Oryzias latipes*	XP_011478513.1
TLR1	*Paralichthys olivaceus*	AFW04264.1
TLR1	*Tachysurus fulvidraco*	ANA09008.1
TLR1	*Takifugu rubripes*	AAW69368.1
TLR1	*Tetraodon nigroviridis*	ABO15772.1
TLR2		
TLR2	*Carassius gibelio*	AGR53440.1
TLR2	*Chionodraco hamatus*	ACT64127.1
TLR2	*Cirrhinus mrigala*	AHI59129.1
TLR2	*Ctenopharyngodon idella*	ACT68333.1
TLR2	*Cyprinus carpio*	BAU98381.1
TLR2	*Epinephelus coioides*	AEB32453.1
TLR2	*Homo sapiens*	O60603
TLR2	*Ictalurus punctatus*	ABD17347.1
TLR2	*Labeo rohita*	ADQ74644.1
TLR2	*Larimichthys crocea*	AJP16420.1
TLR2	*Latescalcarifer*	XP_18558738.1
TLR2	*Latimeria chalumnae*	ENSLACT00000017309

TLR2	*Lepisosteus oculatus*	ENSLOCT00000021874
TLR2	*Megalobrama amblycephala*	APT35501.1
TLR2	*Mus musculus*	Q9QUN7
TLR2	*Oncorhynchus mykiss*	CCK73195.1
TLR2	*Oplegnathus fasciatus*	AFZ81806.1
TLR2	*Oryzias latipes*	XP_004079640.2
TLR2	*Paralichthys olivaceus*	BAD01044.1
TLR2	*Scophthalmus maximus*	AMQ35498.1
TLR2	*Tachysurus fulvidraco*	ANA09009.1
TLR2	*Trematomus bernacchii*	ACT64128.1
TLR2.1	*Larimichthys crocea*	KKF28982.1
TLR2.2	*Larimichthys crocea*	KKF15865.1
TLR2a	*Cyprinus carpio*	ACP20793.2
TLR2b-P	*Oncorhynchus mykiss*	NP_001117891.1
TLR2c	*Cyprinus carpio*	BAU98380.1
TLR2-P	*Danio rerio*	NP_00997977.1
TLR3		
TLR3	*Carassius auratus*	ABC86865.1
TLR3	*Carassius gibelio*	AGR53439.1
TLR3	*Ctenopharyngodon idella*	ABI64155.1
TLR3	*Cyprinus carpio*	ABL11473.1
TLR3	*Danio rerio*	AAT37633.1
TLR3	*Gadus morhua*	ENSGMOP00000000792
TLR3	*Epinephelus coioides*	ADZ76423.1
TLR3	*Gobiocypris rarus*	ABL11471.1
TLR3	*Homo sapiens*	O15455
TLR3	*Ictalurus punctatus*	AEI59664.1
TLR3	*Megalobrama amblycephala*	ABI83673.1
TLR3	*Miichthys miiuy*	ALJ55565.1
TLR3	*Mus musculus*	Q99MB1
TLR3	*Oncorhynchus mykiss*	AAX68425.1
TLR3	*Oryzias latipes*	XP_011475331.1
TLR3	*Paralichthys olivaceus*	BAM11216.1

TLR3	*Salmo salar*	AKE14222.1
TLR3	*Scophthalmus maximus*	AHW76803.1
TLR3	*Squaliobarbus curriculus*	ALO75529.1
TLR3	*Takifugu rubripes*	AAW69373.1
TLR3.2	*Cyprinus carpio*	AHE74142.1
TLR3.2	*Larimichthys crocea*	ADR01099.1
TLR3b	*Paralichthys olivaceus*	BAD01047.1
TLR3-P	*Ictalurus punctatus*	NP_001186997.1
TLR3-P	*Larimichthys crocea*	NP_001290242.1
TLR4		
TLR4	*Cyprinus carpio*	BAU98382.1
TLR4	*Homo sapiens*	O00206
TLR4	*Labeo rohita*	AOM81178.1
TLR4	*Mus musculus*	Q9QUK6
TLR4.1	*Ctenopharyngodon idella*	AEQ64877.1
TLR4.2	*Ctenopharyngodon idella*	AEQ64878.1
TLR4.3	*Ctenopharyngodon idella*	AEQ64879.1
TLR4.4	*Ctenopharyngodon idella*	AEQ64880.1
TLR4a	*Megalobrama amblycephala*	ALB39038.1
TLR4a-P	*Danio rerio*	NP_001315534.1
TLR4b	*Danio rerio*	AAH68358.1
TLR4b	*Megalobrama amblycephala*	AMH41158.1
TLR4ba	*Cyprinus carpio*	AHH85806.1
TLR4ba	*Danio rerio*	NP_001124523.1
TLR4bb	*Cyprinus carpio*	AHH85807.1
TLR4bb-P	*Danio rerio*	NP_00997978.2
TLR4c	*Megalobrama amblycephala*	AKP20514.1
TLR5		
TLR5	*Homo sapiens*	O60602
TLR5	*Mus musculus*	Q9JLF7
TLR5a	*Ctenopharyngodon idella*	AIO11757.1
TLR5b	*Ctenopharyngodon idella*	AIO11758.1
TLR5M	*Carassius auratus*	AQX43081.1

TLR5M	*Cirrhinus mrigala*	AHI59128.1
TLR5M	*Coregonus maraena*	CEF90216.1
TLR5M	*Cyprinus carpio*	BAU98383.1
TLR5M	*Ictalurus punctatus*	AEI59669.1
TLR5M	*Megalobrama amblycephala*	APT35502.1
TLR5M	*Miichthys miiuy*	ALJ55566.1
TLR5M	*Oplegnathus fasciatus*	AQT26515.1
TLR5M	*Oryzias latipes*	XP_011490072.1
TLR5M	*Paralichthys olivaceus*	BAJ16367.1
TLR5M	*Plecoglossus altivelis altivelis*	BAI68384.1
TLR5M	*Scophthalmus maximus*	AMQ35502.1
TLR5M-P	*Danio rerio*	NP_001124067.2
TLR5M-P	*Oncorhynchus mykiss*	NP_001118216.1
TLR5S	*Miichthys miiuy*	ALJ55567.1
TLR5S	*Paralichthys olivaceus*	AEN71826.1
TLR5S	*Scophthalmus maximus*	ANS71058.1
TLR5S	*Sparus aurata*	CCP37739.1
TLR5S	*Takifugu rubripes*	AAW69378.1
TLR5S-P	*Ictalurus punctatus*	NP_001187158.1
TLR5S-P	*Oncorhynchus mykiss*	NP_001117680.1
TLR6		
TLR6	*Homo sapiens*	Q9Y2C9
TLR6	*Mus musculus*	Q9EPW9
TLR7		
TLR7	*Cyprinus carpio*	BAJ19518.1
TLR7	*Homo sapiens*	Q9NYK1
TLR7	*Gadus morhua*	ENSGMOP00000001755
TLR7	*Ictalurus punctatus*	AEI59670.1
TLR7	*Larimichthys crocea*	AGO28200.1
TLR7	*Megalobrama amblycephala*	APT35503.1
TLR7	*Miichthys miiuy*	ALJ55568.1
TLR7	*Mus musculus*	P58681
TLR7	*Oncorhynchus mykiss*	ACV41797.1

TLR7	*Oryzias latipes*	XP_0011488154.1
TLR7	*Salmo salar*	CCX35457.1
TLR7	*Scophthalmus maximus*	AMQ35499.1
TLR8		
TLR8	*Homo sapiens*	Q9NR97
TLR8	*Mus musculus*	P58682
TLR8	*Takifugu rubripes*	AAW69376.1
TLR8	*Gadus morhua*	ENSGMOP00000001741
TLR8	*Larimichthys crocea*	AGO28201.1
TLR8	*Miichthys miiuy*	ALJ55569.1
TLR8	*Paralichthys olivaceus*	AOS00680.1
TLR8	*Scophthalmus maximus*	AQU15238.1
TLR8a	*Cyprinus carpio*	BAU98387.1
TLR8a	*Megalobrama amblycephala*	APT35504.1
TLR8a1	*Oncorhynchus mykiss*	ACV41799.1
TLR8a1	*Coregonus maraena*	CEF90219.1
TLR8a1	*Salmo salar*	NP_001155165.1
TLR8a2	*Oncorhynchus mykiss*	ACV41798.1
TLR8a2	*Salmo salar*	CCX35458.1
TLR8b	*Cyprinus carpio*	BAU98386.1
TLR8b2	*Coregonus maraena*	CEF90223.1
TLR9		
TLR9	*Chionodraco hamatus*	ACT64129.1
TLR9	*Coregonus maraena*	CEF90220.1
TLR9	*Ctenopharyngodon idella*	ADB96920.1
TLR9	*Cynoglossus semilaevis*	ACL68661.1
TLR9	*Fundulus heteroclitus*	JAR68992.1
TLR9	*Gadus morhua*	ENSGMOP00000012030
TLR9	*Homo sapiens*	Q9EQU3
TLR9	*Megalobrama amblycephala*	APT35506.1
TLR9	*Miichthys miiuy*	ALJ55570.1
TLR9	*Mus musculus*	Q9NR96
TLR9	*Paralichthys olivaceus*	BAE80691.1

TLR9	*Scophthalmus maximus*	AQU15239.1
TLR9	*Takifugu rubripes*	AAW69377.1
TLR9	*Trematomus bernacchii*	ACT64130.1
TLR9a	*Epinephelus coioides*	ACV04893.1
TLR9a	*Larimichthys crocea*	ACF60624.1
TLR9a	*Sparus aurata*	AAW81697.1
TLR9b	*Epinephelus coioides*	ACV04894.1
TLR9b	*Sparus aurata*	AAW81696.1
TLR9P	*Larimichthys crocea*	ACF60625.1
TLR9-P	*Danio rerio*	NP_001124066.1
TLR9-P	*Oncorhynchus mykiss*	NP_001123463.1
TLR9-P	*Salmo salar*	NP_001117125.1
TLR10, TLR11, TLR12		
TLR10	*Homo sapiens*	Q9BXR5
TLR11	*Mus musculus*	Q6R5P0
TLR12	*Mus musculus*	Q6QNU9
TLR13		
TLR13	*Mus musculus*	Q6R5N8
TLR13	*Miichthys miiuy*	ALJ55571.1
TLR13	*Salmo salar*	NP_001133860.1
TLR13	*Oryzias latipes*	XP_004078275.1
TLR13a	*Larimichthys crocea*	KKF19122.1
TLR13b	*Larimichthys crocea*	KKF22613.1
TLR13-P	*Larimichthys crocea*	NP_001290325.1
TLR13-P	*Oreochromis niloticus*	NP_001298246.1
TLR14		
TLR14	*Miichthys miiuy*	ALJ55572.1
TLR14	*Paralichthys olivaceus*	BAJ78226.1
TLR18		
TLR18	*Danio rerio*	AAI63840.1
TLR18	*Ictalurus punctatus*	AEI59674.1
TLR18	*Ctenopharyngodon idella*	AIB55030.1
TLR18	*Megalobrama amblycephala*	APT35507.1

TLR18	*Gadus morhua*	ENSGMOP00000004019
TLR18	*Salmo salar*	CDK60413.1
TLR18a	*Cyprinus carpio*	BAU98389.1
TLR18b	*Cyprinus carpio*	BAU98388.1
TLR19		
TLR19	*Megalobrama amblycephala*	APT35508.1
TLR19	*Cyprinus carpio*	BAU98390.1
TLR20		
TLR20	*Cyprinus carpio*	AHH85805.1
TLR20	*Ctenopharyngodon idella*	AHN49762.1
TLR20	*Megalobrama amblycephala*	APT35509.1
TLR20.2	*Danio rerio*	NP_001170914.2
TLR20a	*Ictalurus punctatus*	NP_001187159.1
TLR21		
TLR21	*Epinephelus coioides*	ADM34974.2
TLR21	*Gadus morhua*	AFK76484.1
TLR21	*Paralichthys olivaceus*	AFW04263.1
TLR21	*Ctenopharyngodon idella*	AGM21642.1
TLR21	*Clarias batrachus*	AGM39445.1
TLR21	*Oplegnathus fasciatus*	AIT52504.1
TLR21	*Miichthys miiuy*	ALJ55573.1
TLR21	*Scophthalmus maximus*	AMQ35500.1
TLR21	*Larimichthys crocea*	AOZ21302.1
TLR21	*Cyprinus carpio*	BAU98391.1
TLR21	*Danio rerio*	CAQ13807.1
TLR21	*Ictalurus punctatus*	NP_001186994.1
TLR21/13	*Seriola lalandi*	ALI16363.1
TLR21-P	*Takifugu rubripes*	NP_001027751.1
TLR22	*Carassius auratus*	AQX43082.1
TLR22	*Catla catla*	AGW43269.2
TLR22	*Ctenopharyngodon idella*	ADX97523.2
TLR22	*Epinephelus coioides*	AGA84053.1
TLR22	*Labeo rohita*	AHV90682.1

TLR22	*Lates calcarifer*	AOV82293.1
TLR22	*Miichthys miiuy*	ALJ55574.1
TLR22	*Scophthalmus maximus*	AIC75881.1
TLR22	*Seriola lalandi*	AKN10669.1
TLR22	*Siniperca chuatsi*	AFC95889.1
TLR22	*Sparus aurata*	CDK37745.1
TLR22	*Takifugu rubripes*	AAW69372.1
TLR22		
TLR22a	*Cyprinus carpio*	BAU98393.1
TLR22a	*Danio rerio*	NP_001122147.2
TLR22a	*Salmo salar*	CAJ80696.1
TLR22a2	*Salmo salar*	CAR62394.1
TLR22a-P	*Oncorhynchus mykiss*	NP_001117884.1
TLR22b	*Cyprinus carpio*	BAU98395.1
TLR22b	*Danio rerio*	AAI63527.1
TLR22b	*Gadus morhua*	AFK76486.1
TLR22c	*Cyprinus carpio*	BAU98394.1
TLR22d	*Gadus morhua*	AFK76488.1
TLR22g	*Gadus morhua*	AFK76491.1
TLR22i	*Gadus morhua*	AFK76493.1
TLR22l	*Gadus morhua*	AFK76496.1
TLR22-P	*Scleropages formosus*	KPP60030.1
TLR23	*Miichthys miiuy*	ALJ55575.1
TLR23a	*Gadus morhua*	AFK76497.1
TLR23b	*Gadus morhua*	AFK76498.1
TLR23-TLR26		
TLR	*Nothobranchius furzeri*	SBP54052.1
TLR	*Nothobranchius kadleci*	SBP83130.1
TLR	*Nothobranchius rachovii*	SBR74107.1
TLR25	*Ictalurus punctatus*	AEI59680.1
TLR25a	*Cyprinus carpio*	BAU98397.1
TLR25b	*Cyprinus carpio*	BAU98396.1
TLR1_25	*Oryzias latipes*	XP_004083162.1

TLR26	*Ictalurus punctatus*	AEI59681.1
TLR27		
TLR27	*Callorhinchus milii*	XP_007893881.1
TLR27	*Latimeria chalumnae*	ENSLACP00000017183
TLR27	*Lepisosteus oculatus*	ENSLOCP00000021836
TLR28		
TLR2.2	*Epinephelus coioides*	AIS23533.1
TLR2.2	*Maylandia zebra*	XP_14266344.1
TLR2.2	*Oreochromis niloticus*	XP_019215654.1
TLR2.2	*Oryzias latipes*	XP_004078522.1
TLR2.2	*Stegastes partitus*	XP_008295222.1
TLR2.2	*Labrus bergylta*	XP_020495322.1
TLR2.2	*Lates calcarifer*	XP_018558738.
TLR28	*Miichthys miiuy*	AKN63433.1

Supplementary Methods for Assembly and Annotation:

We have used Trinity v2.0.6 (https://github.com/trinityrnaseq/trinityrnaseq/wiki) installed on our Linux server (CentOS release 6.9). Transcripts were assembled using all the raw reads (n=13) with additional trinity parameters, defined for library type (RF), trimmomatic quality trimming and reads normalization, resulted assembly fasta file. Assembly was subjected for removal of vector contamination using blastn. Thereafter, reference preparation, abundance estimation, generation of expression value matrices, generic contaminants removal from matrices and detection of differentially expressed genes were performed. To add functional annotations, as recommended by Trinity, we used Trinotate v2.0.2 https://trinotate.github.io/ and TransDecoder v2.0.1 (https://github.com/TransDecoder/TransDecoder/wiki). The steps performed during assembly and annotations are available in Supplementary Figure 1 given below. All the commands used for Trinity, contaminants removal, Trinotate and TransDecoder are available in Supplementary Methods for Bioinformatic scripts.

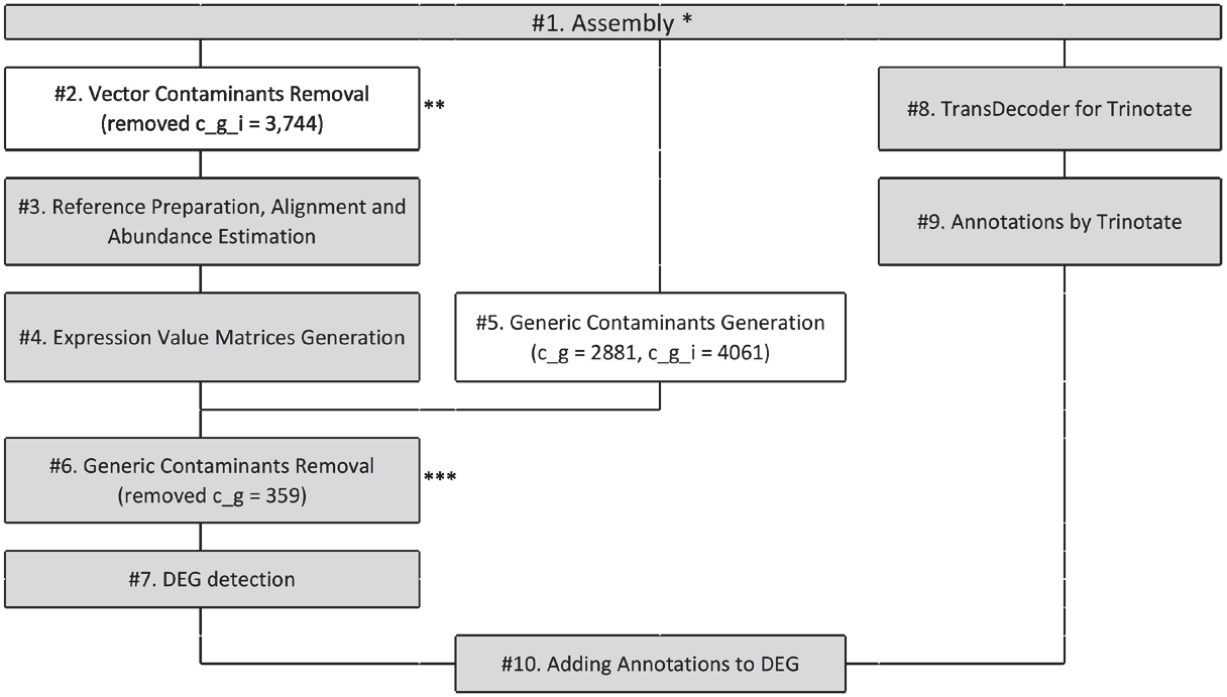

*, Raw reads .fastq.gz were trimmed during assembly with additional trinity parameters defined for trimmomatic quality trimming and resulted trimmed .fastq.gz.P.qtrim.gz files. These files were submitted to array express and available as .fastq.gz files

**, Assembly after vector contaminants removal submitted to Array Express and available as Cyclopterus_lumpus_assembly_post_trinity_Cleaned.fasta

***, Expression value matrices after removing generic contaminants submitted to Array Express as differential_expression_table.txt

c_g_i, contig_gene_isoform generated by trinity

Supplementary Figure 1. Steps performed during de novo assembly and annotations.

Supplementary Methods for Bioinformatic scripts

1. Assembly
##############
$ /trinityrnaseq-2.0.6/Trinity --seqType fq --left all_left --right all_right --output trinity_out_dir --SS_lib_type RF --trimmomatic --normalize_reads --max_memory 200G --CPU 60

2. Vector contaminants removal
##############################

1) Vector genomes seq in fasta were downloaded form NCBI:

gi|9630635|ref|NC_001915.1| Infectious pancreatic necrosis virus segment A, complete sequence

gi|9630638|ref|NC_001916.1| Infectious pancreatic necrosis virus segment B, complete sequence

gi|336122587|ref|NC_015633.1| Vibrio anguillarum 775 chromosome I, complete sequence

gi|336125405|ref|NC_015637.1| Vibrio anguillarum 775 chromosome II, complete sequence

2) All_Vector.fsa file was generated using txt editor combining vector genomes

$ /ncbi-blast-2.2.31+/bin/makeblastdb -in Vector_Genome_fa/All_Vector.fsa -parse_seqids -dbtype nucl -out nt

$ /ncbi-blast-2.2.31+/bin/blastn -task megablast -db nt -perc_identity 90 -max_target_seqs 1 -outfmt "7 qacc qstart qend sacc sstart send sstrand" -query Trinity.fasta -out result_.out -num_threads 4

3) good_ids.txt was generated by filtering vector ids from trinity.fasta ids using linux commands and assembly was cleaned using following commands:

$ perl -ne 'if(/^>(\S+)/){$c=$i{$1}}$c?print:chomp;$i{$_}=1 if @ARGV' good_ids.txt Trinity.fasta > Trinity_Cleaned.fasta

Note: After removing vector contamination, assembly was renamed as Trinity_Cleaned.fasta

Trinity Assembly_Stat

$ /trinityrnaseq-2.0.6/util/TrinityStats.pl Trinity_Cleaned.fasta

3. Reference Preparation, Alignment and Abundance Estimation (n=13)
##

Ref Preparation:

$ /trinityrnaseq-2.0.6/util/align_and_estimate_abundance.pl --transcripts Trinity_Cleaned.fasta --est_method RSEM --aln_method bowtie --trinity_mode --prep_reference --SS_lib_type RF --output_prefix --debug --thread_count 20

Abundance Estimation: individual run for each sample using bowtie and RSEM (below is example for first sample only)

$ /trinityrnaseq-2.0.6/util/align_and_estimate_abundance.pl --transcripts Trinity_Cleaned.fasta --seqType fq --left 1-Haugland_ATCACG_L008_R1_001.fastq.gz.PwU.qtrim.fq --right 1-Haugland_ATCACG_L008_R2_001.fastq.gz.PwU.qtrim.fq --est_method RSEM --aln_method bowtie --trinity_mode --SS_lib_type RF --output_dir Sample_1_out --output_prefix Sample_1_ --debug --thread_count 5

Detailed Assessment of Read Content of the Assembly

$ cd Sample_1_out

$ /trinityrnaseq-2.0.6/util/bowtie_PE_separate_then_join.pl --seqType fq --left 1-Haugland_ATCACG_L008_R1_001.fastq.gz.PwU.qtrim.fq --right 1-Haugland_ATCACG_L008_R2_001.fastq.gz.PwU.qtrim.fq --target Trinity_Cleaned.fasta --aligner bowtie --SS_lib_type RF --retain_intermediate_files -- -p 4 --all --best --strata -m 300 > bowtie_PE_separate_then_join.out

$ /trinityrnaseq-2.0.6/util/SAM_nameSorted_to_uniq_count_stats.pl bowtie_out/bowtie_out.nameSorted.bam > SAM_nameSorted_to_uniq_count_stats.out

4. Expression Value Matrices Generation
#####################################

$ /trinityrnaseq-2.0.6/util/abundance_estimates_to_matrix.pl --est_method RSEM --cross_sample_fpkm_norm TMM --out_prefix Trinity_genes Sample_1_.genes.results Sample_2_.genes.results Sample_3_.genes.results Sample_4_.genes.results Sample_5_.genes.results Sample_6_.genes.results Sample_7_.genes.results Sample_8_.genes.results Sample_9_.genes.results Sample_10_.genes.results Sample_11_.genes.results Sample_12_.genes.results Sample_13_.genes.results > genes_abundance_estimates_to_matrix.pl.out

5. Generic Contaminants Generation
##################################

generating and removing generic contaminants contigs by blasting against NT for clearly non-eukaryote sequences
1) the contigs of the assembly was split into 20 blast jobs, example commandline

$ blastn -query lumpfish_unclean00.fa -db nt -num_threads 4 -outfmt '6 qseqid sseqid evalue staxids sskingdoms' 2> lumpfish_unclean00.fa_blast_results.log | gzip -c > lumpfish_unclean00.fa_blast_results.txt.gz

2) the blast results were parsed to compute an Alien Index [**Gladyshev et al, 2008**], a corrected log ratio between the E-value for the best Eukaryote and best non-Eukaryote blast hits of each contig. We used an Alien Index >= 45, corresponding to an E-value >= 20 orders of magnitude difference between the best non-metazoan hit to the best metazoan hit, to identify 4061 non-Eukaryote contigs most likely being contaminant. These were removed from the transcript set and not used in subsequent analysis.

$ for FN in `ls lumpfish_*blast_results.txt.gz`; do alienIndex -c 4 -e 2 -m Eukaryota -i <(zcat $FN) > ai_output.${FN}.txt; done

$ cat ai_output* | perl -lane 'print if $F[3] > 45' | cut -f1 > trId_isBacterial.txt

6. Generic Contaminants Removal
################################
Note: generic contaminants were removed from expression matrices before DEG detection. This was done as part of the R-script provided below using geneId_isContaminant.txt. Ids in trId_isBacterial.txt file were in c_g_i (contig_gene_isoform) format and only isoform ids (_i) were removed to generate geneId_isContaminant.txt file. geneId_isContaminant.txt file contained only gene Ids (c_g).

7. DEG detection (p-value 0.1)
############################

The differential expression analysis was performed in R using the limma-voom method in the limma package [Ritchie et al 2015] based on the RSEM read count estimates per gene (Trinity_genes.counts.matrix). see R-script provided.

8. TransDecoder for Trinotate
############################

$ TransDecoder.LongOrfs -t /export/kjempetujafs/service/projects/2015-06_Haugland_transcriptome/WD_Charitra/TransDecoder_out_dir/Trinity_Cleaned_perl.fasta

$ ncbi-blast-2.2.31+/bin/blastp -query Trinity_Cleaned_perl.fasta.transdecoder_dir/longest_orfs.pep -db uniprot_sprot.trinotate.pep -max_target_seqs 1 -outfmt 6 -evalue 1e-5 -num_threads 30 > blastp.outfmt6

$ hmmer-3.1b2-linux-intel-x86_64/binaries/hmmscan --cpu 30 --domtblout pfam.domtblout Pfam-A.hmm longest_orfs.pep & tail -f nohup.out

$ TransDecoder-2.0.1/TransDecoder.Predict -t Trinity_Cleaned.fasta --retain_pfam_hits pfam.domtblout --retain_blastp_hits blastp.outfmt6

9. Annotations by Trinotate
#########################
Trinotate: https://trinotate.github.io

Capturing BLAST Homologies

$ ncbi-blast-2.2.31+/blastx -query Trinity_Cleaned_perl.fasta -db uniprot_uniref90.trinotate.pep -num_threads 8 -max_target_seqs 1 -outfmt 6 > uniref90.blastx.outfmt6

$ ncbi-blast-2.2.31+/blastp -query Trinity_Cleaned_perl.fasta.transdecoder.pep -db uniprot_uniref90.trinotate.pep -num_threads 8 -max_target_seqs 1 -outfmt 6 > uniref90.blastp.outfmt6

Running HMMER

$ hmmer-3.1b2-linux-intel-x86_64/binaries/hmmscan --cpu 8 --domtblout TrinotatePFAM.out Pfam-A.hmm Trinity_Cleaned.fasta.transdecoder.pep > pfam.log

Running signalP to predict signal peptides

$ signalp-4.1/signalp -f short -n signalp.out Trinity_Cleaned.fasta.transdecoder.pep

Running tmHMM to predict transmembrane regions

$ tmhmm-2.0c/bin/tmhmm --short < Trinity_Cleaned.fasta.transdecoder.pep > tmhmm.out

Running RNAMMER

$ perl /Trinotate-2.0.2/util/rnammer_support/RnammerTranscriptome.pl --transcriptome Trinity_Cleaned.fasta --path_to_rnammer rnammer-1.2.src/rnammer

Loading Above Results into a Trinotate SQLite Database

$ Trinotate /Trinotate-2.0.2/Trinotate.sqlite init --gene_trans_map Trinity.fasta.gene_trans_map --transcript_fasta Trinity_Cleaned.fasta --transdecoder_pep Trinity_Cleaned.fasta.transdecoder.pep

$ Trinotate /Trinotate-2.0.2/Trinotate.sqlite LOAD_swissprot_blastp blastp.outfmt6

$ Trinotate /Trinotate-2.0.2/Trinotate.sqlite LOAD_swissprot_blastx blastx.outfmt6

$ Trinotate /Trinotate-2.0.2/Trinotate.sqlite LOAD_pfam TrinotatePFAM.out

$ Trinotate /Trinotate-2.0.2/Trinotate.sqlite LOAD_tmhmm tmhmm.out

$ Trinotate /Trinotate-2.0.2/Trinotate.sqlite LOAD_signalp signalp.out

$ Trinotate /Trinotate-2.0.2/Trinotate.sqlite report > trinotate_annotation_report.xls

10. Adding Annotations to DEG
##############################
Annotations in .xls file were added to DEG table using simple text/excel editor.

R-script
##########

```{r config}

library(limma)

library(edgeR)

library(dplyr)

library(ggplot2)


#library(DESeq2)


#setwd("")

```


Load RSEM read count estimates per gene


```{r loadData, echo="FALSE"}

x = read.delim("../Trinity_genes.counts.matrix")


names(x) = c('gene_id',

        'ctrl_6h_r1','ctrl_6h_r2','ctrl_6h_r3',

        'treat_6h_r1','treat_6h_r2','treat_6h_r3',
```

```
        'ctrl_24h_r1','ctrl_24h_r2','ctrl_24h_r3',
        'treat_24h_r1','treat_24h_r2','treat_24h_r3',
        'ipnv_24h_r1')
row.names(x)=x$gene_id
```

2016-04 Remove contaminants (detected by BLAST analysis)

```{r rmContaminants}
isContaminant=read.table("..geneId_isContaminant.txt")
isContaminant = as.character(isContaminant$V1)
x = x[!x$gene_id %in% isContaminant,]
```

```{r, echo=FALSE}
x=x[,-1] #strip gene_id column
```

Remove genes that are not appreciably expressed (min 10 reads)

```{r dropLowAbundant}
keep=rowSums(x>10) >= 3 #at least 10 reads in at least 3 samples
table(keep) #keep 34280 genes/221k
x = x[keep,]
```

Set up experimental design matrix

```{r designMatrix}
treatment <- factor(c('ctrl_6h','ctrl_6h','ctrl_6h','treat_6h','treat_6h','treat_6h',
                      'ctrl_24h','ctrl_24h','ctrl_24h','treat_24h','treat_24h','treat_24h',
                      'inpv'), levels=c('ctrl_6h','treat_6h','ctrl_24h','treat_24h','inpv')) #ctrl_mo experimental design
sample_pool <- factor(c(1,2,3,1,2,3,1,2,3,1,2,3,3), levels=c(1,2,3))

design <- model.matrix(~0 + treatment + sample_pool)
data.frame(Sample=colnames(x),treatment,sample_pool)

rownames(design) <- colnames(x)
```

limma-voom analysis

```{r limma_scale_counts}
y <- DGEList(counts=x,group=treatment)
y <- calcNormFactors(y)
v <- voom(y,design,plot=TRUE)
plotMDS(v,top=50,labels=treatment,
      col=ifelse(treatment=="treat_6h","blue","red"),gene.selection="common")
fit <- lmFit(v,design)
fit <- eBayes(fit)

```

Examine the different contrasts (treatment vs control at each time-point)

```{r limmaDEResults}
cont.matrix <- makeContrasts(TvsC_6h=treatmenttreat_6h-treatmentctrl_6h,
                      TvsC_24h=treatmenttreat_24h-treatmentctrl_24h,
                      INPVvsC=treatmentinpv-treatmentctrl_24h,
#                       TvsT=treatmenttreat_24h-treatmenttreat_6h,
```

```
#                       CvsC=treatmentctrl_24h-Intercept,
                      levels=design)
#cont.matrix
#row.names(cont.matrix) = c("(Intercept)","sample_pool2","sample_pool3",
#                      "treatmenttreat_6h","treatmentctrl_24h","treatmenttreat_24h",
#                      "treatmentinpv") #fix for (Intercept) vs Intercept

fit2 <- contrasts.fit(fit, contrast=cont.matrix)
fit2 <- eBayes(fit2)

#fit2 <- contrasts.fit(fit, contrast=c(-1,0,0,1,0,0,0)) #treat vs ctrl 6h
#fit2 <- eBayes(fit2)
top_TvsC_6h = topTable(fit2, coef="TvsC_6h", number = Inf, adjust="BH")
sum(top_TvsC_6h$adj.P.Val<0.05)
sum(top_TvsC_6h$adj.P.Val<0001)
#head(top_TvsC_6h)
#x['TR31519|c0_g1',]
#x['TR35037|c0_g2',]

top_TvsC_24h = topTable(fit2, coef="TvsC_24h", number = Inf, adjust="BH")
```

```
sum(top_TvsC_24h$adj.P.Val<0.05)

sum(top_TvsC_24h$adj.P.Val<0001)


#fit2 <- contrasts.fit(fit, contrast=c(0,0,0,0,-1,0,1)) #INPV vs ctrl 24h

#fit2 <- eBayes(fit2)

top_VcsC = topTable(fit2, coef="INPVvsC", number= Inf, adjust="BH")


#fit2 <- contrasts.fit(fit, contrast=c(0,0,0,-1,0,1,0)) #treat 24h vs treat_6h

#fit2 <- eBayes(fit2)

#topTable(fit2, coef="TvsT", adjust="BH")


#fit2 <- contrasts.fit(fit, contrast=c(-1,0,0,0,1,0,0)) #ctrl 24h vs ctrl_6h

#fit2 <- eBayes(fit2)

#topTable(fit2, coef="CvsC", adjust="BH")

###
```

Merge 6h and 24h results for QC and plots

merge the DE contrast tables for export

```{r mergeTimepoints}
top_6_24 = merge(top_TvsC_6h, top_TvsC_24h,by="row.names",all.x=TRUE)
names(top_6_24) = c('geneID',
                    'logFC_6h',
                    'avgExpr_6h',
                    't_6h',
                    'pval_6h',
                    'adjpval_6h',
                    'b_6h',
                    'logFC_24h',
                    'avgExpr_24h',
                    't_24h',
                    'pval_24h',
                    'adjpval_24h',
                    'b_24h')
```

QC: Examine the concordance of the two timepoints

```{r rankPlot}
```

```
rank_6h = top_TvsC_6h %>% mutate(rank = rank(adj.P.Val)) %>% select(rank)

rank_24h = top_TvsC_24h %>% mutate(rank = rank(adj.P.Val)) %>% select(rank)

rank_6_24 = merge(rank_6h, rank_24h, by="row.names",all.x=TRUE)


cor(rank_6_24$rank.x,rank_6_24$rank.y, method="spearman") #spearman corr 0.90


ggplot(rank_6_24, aes(x=rank.x,y=rank.y)) + geom_point(aes(alpha=0.1)) +

  labs(title="Concordance of gene DE P-value rank at 6 and 24 hrs",

       x="P-value rank 6 hrs",

       y="P-value rank 24 hrs") +

       theme(legend.position = "none")


#top 100

ggplot(rank_6_24, aes(x=rank.x,y=rank.y)) + geom_point(aes(alpha=0.1)) +

  labs(title="Concordance of gene DE P-value rank at 6 and 24 hrs",

       x="P-value rank 6 hrs",

       y="P-value rank 24 hrs") +

       theme(legend.position = "none") +

       xlim(0, 100) +

       ylim(0,100)
```

```

Conclusion: The genes that are differentially regulated at 6 hrs are also diff regulated at 24 hrs

Now, diagnostic exploration of of p-values - se DESeq manual for background

```{r pvaldist}
plot_pval_diag = function(padj){
  orderInPlot = order(padj)
  showInPlot = (padj[orderInPlot] <= 0.01)
  alpha = 0.01
  plot(seq(along=which(showInPlot)), padj[orderInPlot][showInPlot], pch=".", xlab = expression(rank(p[i])), ylab=expression(p[i]))
  abline(a=0, b=alpha/length(padj), col="red3", lwd=2)
}
plot_pval_diag(top_6_24$adjpval_6h)
plot_pval_diag(top_6_24$adjpval_24h)

plot_pval_cutoff_comp = function(padj){
  padj.log <- -log10(padj)
```
```

```
  orderInPlot = order(padj.log)
  plot(padj.log[orderInPlot], type="l")
  sigline <- c(.05, .01, 5, 1,05, 01)
  sigline <- -log10(sigline)
  sigcolors <- c("red", "blue", "green", "yellow","pink","purple")
  sapply(1:length(sigline), function(x){abline(h=sigline[padj.log], col=sigcolors[padj.log])})
}
plot_pval_cutoff_comp(top_6_24$adjpval_6h)
plot_pval_cutoff_comp(top_6_24$adjpval_24h)

plot_pval_histograms = function(pval){
  hist(top_6_24$adjpval_6h, breaks=5000, ylim = c(0,100))
  hist(top_6_24$adjpval_6h, breaks=2000, xlim = c(0,0.1))
  hist(top_6_24$adjpval_6h, breaks=1000000, xlim = c(0,0.01))
  hist(top_6_24$adjpval_6h, breaks=1000000, xlim = c(0,02))
  hist(top_6_24$adjpval_6h, breaks=1000000, xlim = c(0,005))
  hist(top_6_24$adjpval_6h, breaks=1000000, xlim = c(0,0005))
}

#  ggplot(top_6_24, aes(adjpval_2h)) + geom_histogram(bins=5000) + ylim(0,100)
```

```
#  ggplot(top_6_24, aes(adjpval_6h)) + geom_histogram(bins=2000) + xlim(0,0.1)
#  ggplot(top_6_24, aes(adjpval_6h)) + geom_histogram(bins=2000) + xlim(0,0.01)
#  ggplot(top_6_24, aes(adjpval_6h)) + geom_histogram(bins=2000) + xlim(0,02)
#  ggplot(top_6_24, aes(adjpval_6h)) + geom_histogram(bins=2000) + xlim(0,002)
#  ggplot(top_6_24, aes(adjpval_6h)) + geom_histogram(bins=2000) + xlim(0,0002)

plot_pval_histograms(top_6_24$adjpval_6h)
plot_pval_histograms(top_6_24$adjpval_24h)
```

Volcano plot

```{r volcanoPlot, eval=FALSE, echo=FALSE}
res <- top_6_24 %>% dplyr::select(geneID, logFC_6h,pval_6h, adjpval_6h)
names(res) = c("geneID","log2FoldChange", "pvalue", "padj")

# Make a basic volcano plot
with(res, plot(log2FoldChange, -log10(pvalue), pch=20, main="Volcano plot", xlim=c(-2.5,2)))
```

```
# Add colored points: red if padj<0.05, orange of log2FC>1, green if both)
with(subset(res, padj<001 ), points(log2FoldChange, -log10(pvalue), pch=20, col="red"))
with(subset(res, abs(log2FoldChange)>1), points(log2FoldChange, -log10(pvalue), pch=20, col="orange"))
with(subset(res, padj<001 & abs(log2FoldChange)>1), points(log2FoldChange, -log10(pvalue), pch=20, col="green"))
# Label points with the textxy function from the calibrate plot
library(calibrate)
with(subset(res, padj<001 & abs(log2FoldChange)>1), textxy(log2FoldChange, -log10(pvalue), labs=geneID, cex=.8))

#volcano plot
#scattering the M values (log2 ratio) on the x axis against the p value (-log10 the p value).
ggplot(top_6_24, aes(x=logFC_6h, y = -log10(adjpval_6h))) + geom_point(aes(alpha=0.1))
detach("package:calibrate", unload=TRUE) #calibrate select conflicts with dplyr
```

Export DE Tables

```{r exportDETables}
top_6_24_out = top_6_24 %>% select(geneID,logFC_6h,avgExpr_6h,adjpval_6h,logFC_24h,avgExpr_24h,adjpval_24h) %>% arrange(adjpval_24h)
write.table(top_6_24_out, file="differential_expression_table.txt", quote=FALSE, sep = "\t")
```

```
#down 6h

downreg_6 = top_6_24 %>% filter(adjpval_6h < 1e-5 & logFC_6h < 0) %>%select(geneID,logFC_6h,avgExpr_6h,adjpval_6h) %>%
arrange(adjpval_6h)

write.table(downreg_6, file="differential_expression_down_6h.txt",

        quote=FALSE, sep = "\t", row.names = FALSE)


upreg_6 = top_6_24 %>% filter(adjpval_6h < 1e-5 & logFC_6h > 0) %>%select(geneID,logFC_6h,avgExpr_6h,adjpval_6h) %>% arrange(adjpval_6h)

write.table(upreg_6, file="differential_expression_up_6h.txt",

        quote=FALSE, sep = "\t", row.names = FALSE)


downreg_24 = top_6_24 %>% filter(adjpval_24h < 1e-5 & logFC_24h < 0) %>%select(geneID,logFC_24h,avgExpr_24h,adjpval_24h) %>%
arrange(adjpval_24h)

write.table(downreg_24, file="differential_expression_down_24h.txt",

        quote=FALSE, sep = "\t", row.names = FALSE)


upreg_24 = top_6_24 %>% filter(adjpval_24h < 1e-5 & logFC_24h > 0) %>%select(geneID,logFC_24h,avgExpr_24h,adjpval_24h) %>%
arrange(adjpval_24h)

write.table(upreg_24, file="differential_expression_up_24h.txt",

        quote=FALSE, sep = "\t", row.names = FALSE)


# write labels file for Trinity GO analysis (label\tgeneid)
```

```
# because row.names (geneIds) can not be repeated, we do 6h and 24h separately
labels_6h = rbind(
data.frame('label' = rep("down_6",nrow(downreg_6)), 'geneID' = downreg_6$geneID),
data.frame('label' = rep("up_6",nrow(upreg_6)), 'geneID' = upreg_6$geneID))
write.table(labels_6h, file="differential_expression_labels_for_go_6h.txt",
        quote=FALSE, sep = "\t", row.names = FALSE, col.names = FALSE)

labels_24h = rbind(
data.frame('label' = rep("down_24",nrow(downreg_24)), 'geneID' = downreg_24$geneID),
data.frame('label' = rep("up_24",nrow(upreg_24)), 'geneID' = upreg_24$geneID)
)
write.table(labels_24h, file="differential_expression_labels_for_go_24h.txt",
        quote=FALSE, sep = "\t", row.names = FALSE, col.names = FALSE)
```

Running the Go overrep code through trinity

```{r gooverrep, engine="bash", eval=FALSE}
```

/trinity/Analysis/DifferentialExpression/run_GOseq.pl --genes_single_factor=differential_expression_labels_6h.txt --GO_assignments=go_annotations.txt --lengths=gene_length.txt > go_overrep_6h.txt

/trinity/Analysis/DifferentialExpression/run_GOseq.pl --genes_single_factor=differential_expression_labels_24h.txt --GO_assignments=go_annotations.txt --lengths=gene_length.txt > go_overrep_24h.txt

```

DESeq2 plots for QA

```{r DESeq2Plots}
countData = round(x)
colData = data.frame(sample_pool,treatment)
row.names(colData) = colnames(countData)
library(DESeq2)
dds <- DESeqDataSetFromMatrix(countData = countData,
                              colData = colData,
                              design = ~ sample_pool + treatment)
dds <- DESeq(dds)

rld <- rlog(dds)
```
```

```
vsd <- varianceStabilizingTransformation(dds)

rlogMat <- assay(rld)

vstMat <- assay(vsd)
```

```{r gene_heatmap_1-30}
library("RColorBrewer")

library("gplots")

select <- order(rowMeans(counts(dds,normalized=TRUE)),decreasing=TRUE)[1:30]

hmcol <- colorRampPalette(brewer.pal(9, "GnBu"))(100)

heatmap.2(assay(vsd)[select,], col = hmcol,

        Rowv = FALSE, Colv = FALSE, scale="none",

        dendrogram="none", trace="none", margin=c(10, 6))

```

```{r gene_heatmap_1-100}
library("RColorBrewer")

library("gplots")
```

```
select <- order(rowMeans(counts(dds,normalized=TRUE)),decreasing=TRUE)[1:100]
hmcol <- colorRampPalette(brewer.pal(9, "GnBu"))(100)

heatmap.2(assay(vsd)[select,], col = hmcol,
        Rowv = FALSE, Colv = FALSE, scale="none",
        dendrogram="none", trace="none", margin=c(10, 6))
```

```{r gene_heatmap_genefilter_rowVars_1-30}
library("RColorBrewer")
library("gplots")
select <- order(genefilter::rowVars(counts(dds,normalized=TRUE)),decreasing=TRUE)[1:30]
hmcol <- colorRampPalette(brewer.pal(9, "GnBu"))(100)

heatmap.2(assay(vsd)[select,], col = hmcol,
        Rowv = FALSE, Colv = FALSE, scale="none",
        dendrogram="none", trace="none", margin=c(10, 6))
```

```{r gene_heatmap_genefilter_rowVars_1-100}

library("RColorBrewer")

library("gplots")

select <- order(genefilter::rowVars(counts(dds,normalized=TRUE)),decreasing=TRUE)[1:100]

hmcol <- colorRampPalette(brewer.pal(9, "GnBu"))(100)


heatmap.2(assay(vsd)[select,], col = hmcol,

        Rowv = FALSE, Colv = FALSE, scale="none",

        dendrogram="none", trace="none", margin=c(10, 6))


```

```{r sample_heatmap}

library(ggplot2)


distsRL <- dist(t(assay(rld)))

mat <- as.matrix(distsRL)

rownames(mat) <- colnames(mat) <- with(colData(dds),

                                paste(sample_pool, treatment, sep=" : "))

hc <- hclust(distsRL)
```

```
heatmap.2(mat, Rowv=as.dendrogram(hc),
          symm=TRUE, trace="none",
          col = rev(hmcol), margin=c(13, 13))

#plotPCA(rld, intgroup=c("treatment", "sample_pool"))

data <- plotPCA(rld, intgroup=c("treatment", "sample_pool"), returnData=TRUE)
percentVar <- round(100 * attr(data, "percentVar"))
ggplot(data, aes(PC1, PC2, color=sample_pool, shape=treatment)) +
  geom_point(size=3) +
  xlab(paste0("PC1: ",percentVar[1],"% variance")) +
  ylab(paste0("PC2: ",percentVar[2],"% variance"))
```

Supplementary Results of Trinity RSEM

Table 1. Read count matrix from RSEM output

								Genes expressed		
Sample			**proper_pairs**	**total aligned**	improper_ pairs	left_only	right_only	**≥ 2 FPKM**	**≥ 1 FPKM**	Total
Control-1	**1**	count	24,189,368	29,980,237	3,976,458	1,137,983	676,428	39,506	66,391	221,659
		pct	80.68	--	13.26	3.8	2.26	--	--	--
	2	count	27,178,664	32,937,998	4,168,232	956,390	634,712	36,077	65,219	221,659
		pct	82.51	--	12.65	2.9	1.93	--	--	--
	3	count	28,659,252	37,114,067	6,626,260	1,097,874	730,681	36,250	66,468	221,659
		pct	77.22	--	17.85	2.96	1.97	--	--	--
Treated-1	**4**	count	24,899,860	31,065,905	4,472,704	1,028,504	664,837	36,935	65,105	221,659
		pct	80.15	--	14.4	3.31	2.14	--	--	--
	5	count	21,999,490	27,276,150	3,793,870	886,000	596,790	37,203	63,440	221,659
		pct	80.65	--	13.91	3.25	2.19	--	--	--
	6	count	24,627,776	30,329,773	4,052,902	985,884	663,211	37,970	66,678	221,659
		pct	81.2	--	13.36	3.25	2.19	--	--	--
Control-2	**7**	count	26,683,856	33,281,629	4,862,120	1,062,160	673,493	36,291	62,730	221,659
		pct	80.18	--	14.61	3.19	2.02	--	--	--
	8	count	23,200,556	29,769,028	4,832,936	1,025,958	709,578	38,483	64,273	221,659
		pct	77.94	--	16.23	3.45	2.38	--	--	--
	9	count	26,758,676	32,816,055	4,297,730	1,060,466	699,183	36,797	63,158	221,659
		pct	81.54	--	13.1	3.23	2.13	--	--	--
Treated-2	**10**	count	25,713,468	31,888,148	4,358,192	1,117,602	698,886	35,393	60,377	221,659
		pct	80.64	--	13.67	3.5	2.19	--	--	--
	11	count	23,517,108	29,484,868	4,255,492	1,038,233	674,035	37,826	64,233	221,659
		pct	79.76	--	14.43	3.52	2.29	--	--	--
	12	count	22,513,278	27,487,774	3,394,564	949,623	630,309	39,037	67,158	221,659
		pct	81.9	--	12.35	3.45	2.29	--	--	--
Treated-3	**13**	count	20,204,506	26,674,188	4,519,114	1,212,334	738,234	39,580	65,727	221,659
		pct	75.75	--	16.94	4.54	2.77	--	--	--

Note: Vector contaminated seq were removed before RSEM output.

################################
Counts of transcripts, etc.
################################
Total trinity 'genes': 221659
Total trinity transcripts: 346430
Percent GC: 46.65

##
Stats based on ALL transcript contigs:
##

Contig N10: 6782
Contig N20: 4988
Contig N30: 3947
Contig N40: 3144
Contig N50: 2502

Median contig length: 585
Average contig: 1250.14
Total assembled bases: 433087424

###
Stats based on ONLY LONGEST ISOFORM per 'GENE':
###

Contig N10: 5514
Contig N20: 3647
Contig N30: 2446
Contig N40: 1608
Contig N50: 1071

Median contig length: 401
Average contig: 735.04
Total assembled bases: 162928446

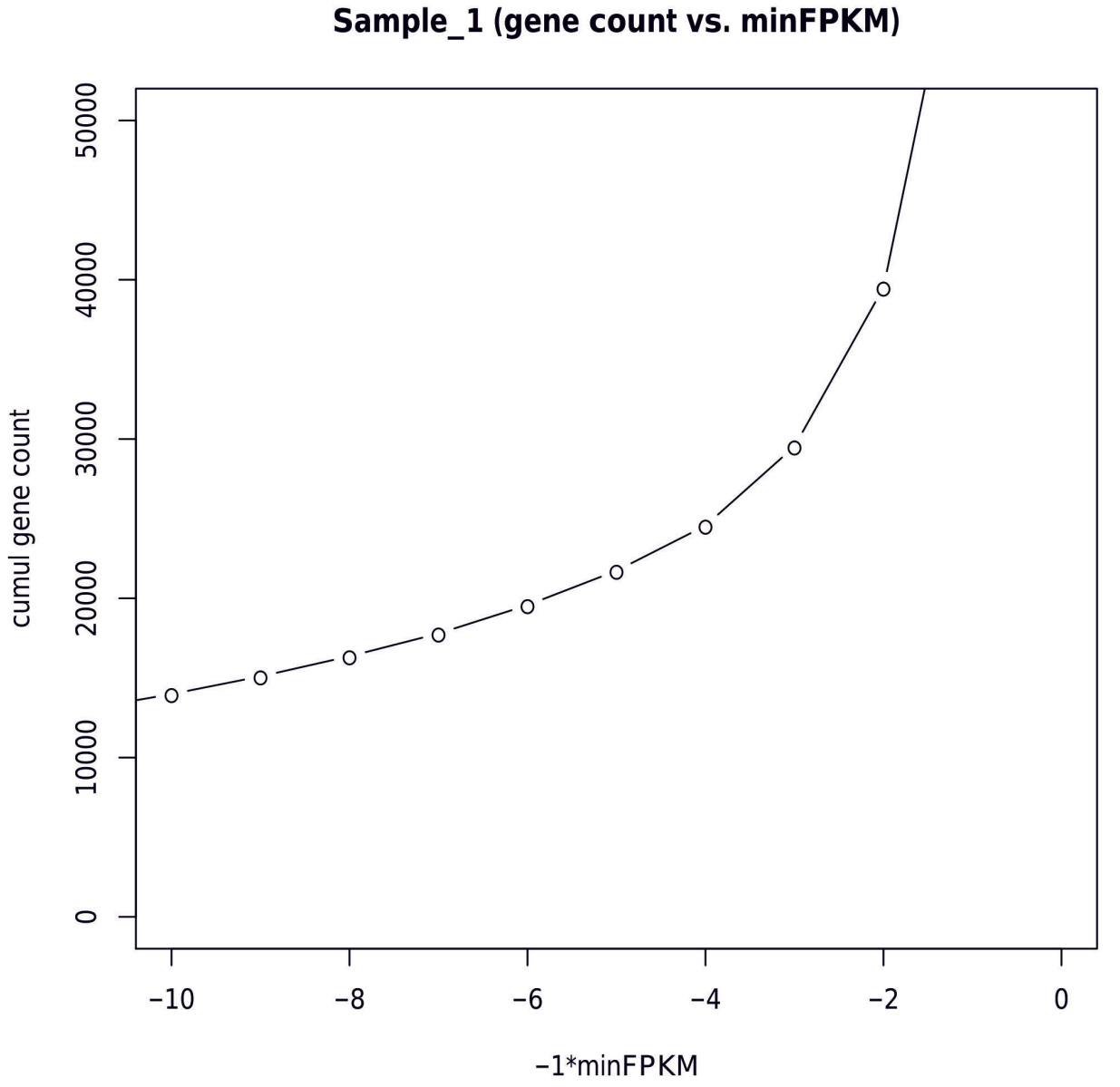
Sample_1 (gene count vs. minFPKM)
cumul gene count
0
10000
20000
30000
40000
50000
−10
−8
−6
−4
−2
0
−1*minFPKM

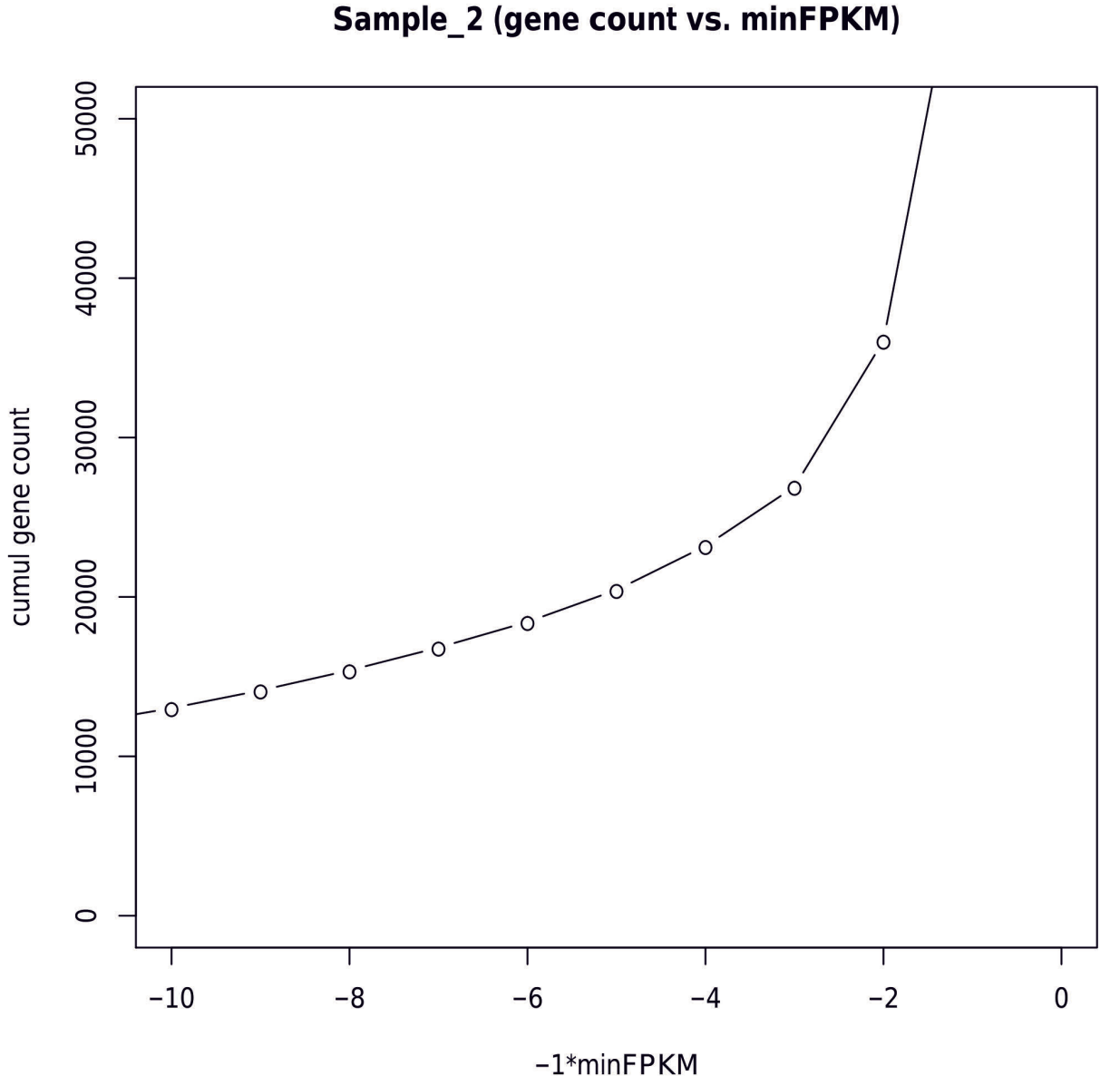
Sample_2 (gene count vs. minFPKM)
cumul gene count
0
10000
20000
30000
40000
50000
−10
−8
−6
−4
−2
0
−1*minFPKM

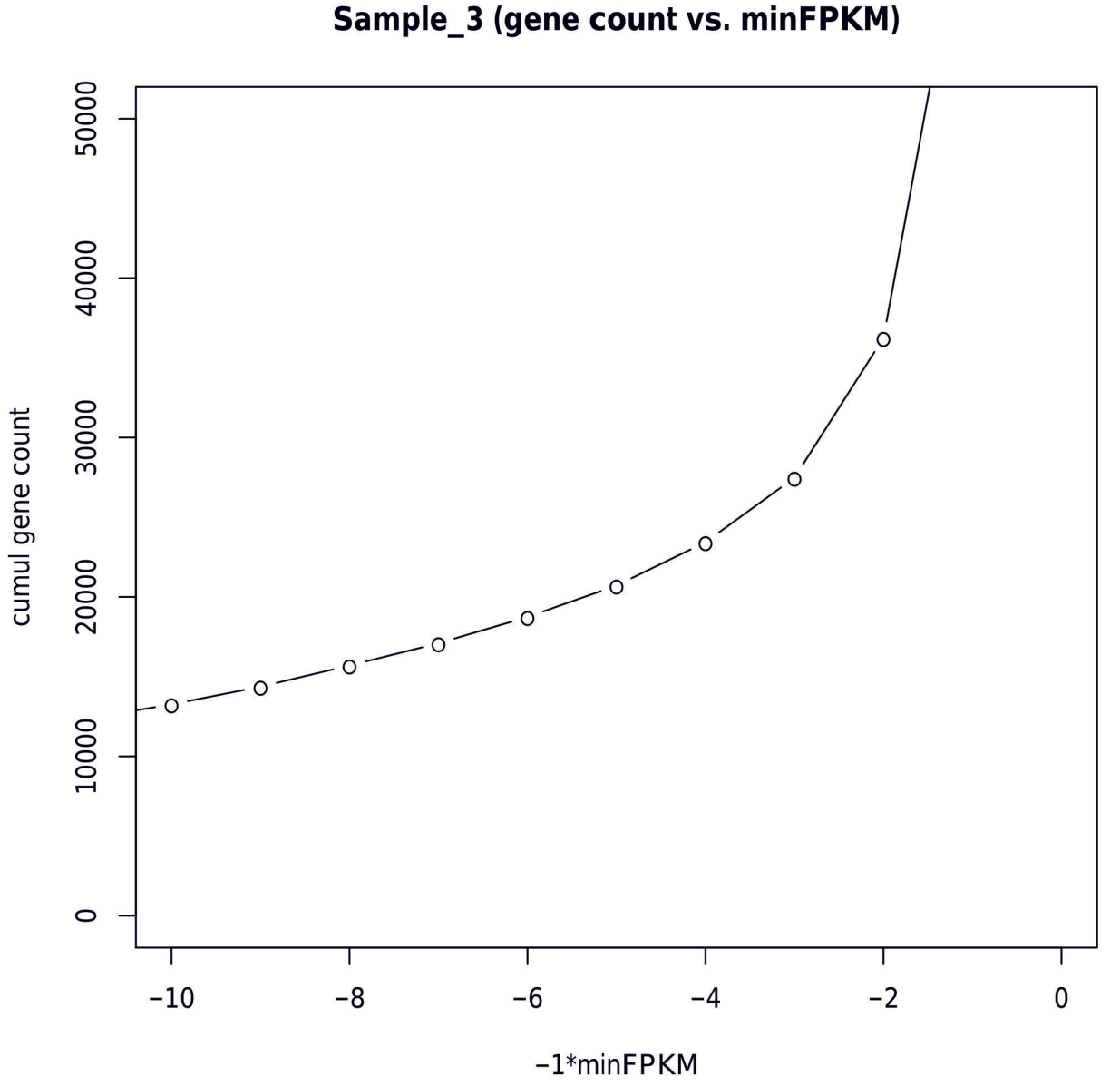
Sample_3 (gene count vs. minFPKM)
cumul gene count
0
10000
20000
30000
40000
50000
−10
−8
−6
−4
−2
0
−1*minFPKM

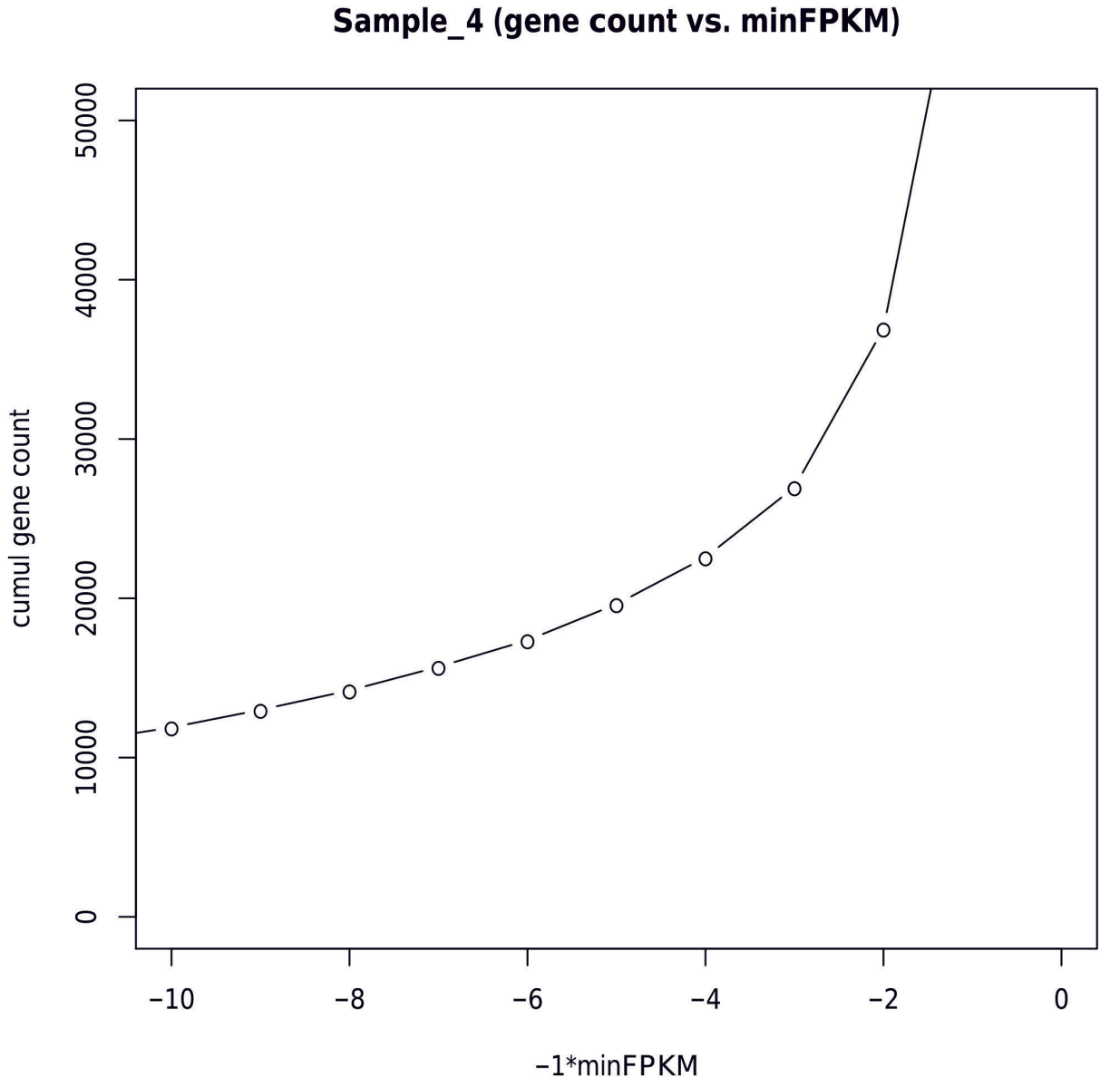
Sample_4 (gene count vs. minFPKM)
cumul gene count
0
10000
20000
30000
40000
50000
−10
−8
−6
−4
−2
0
−1*minFPKM

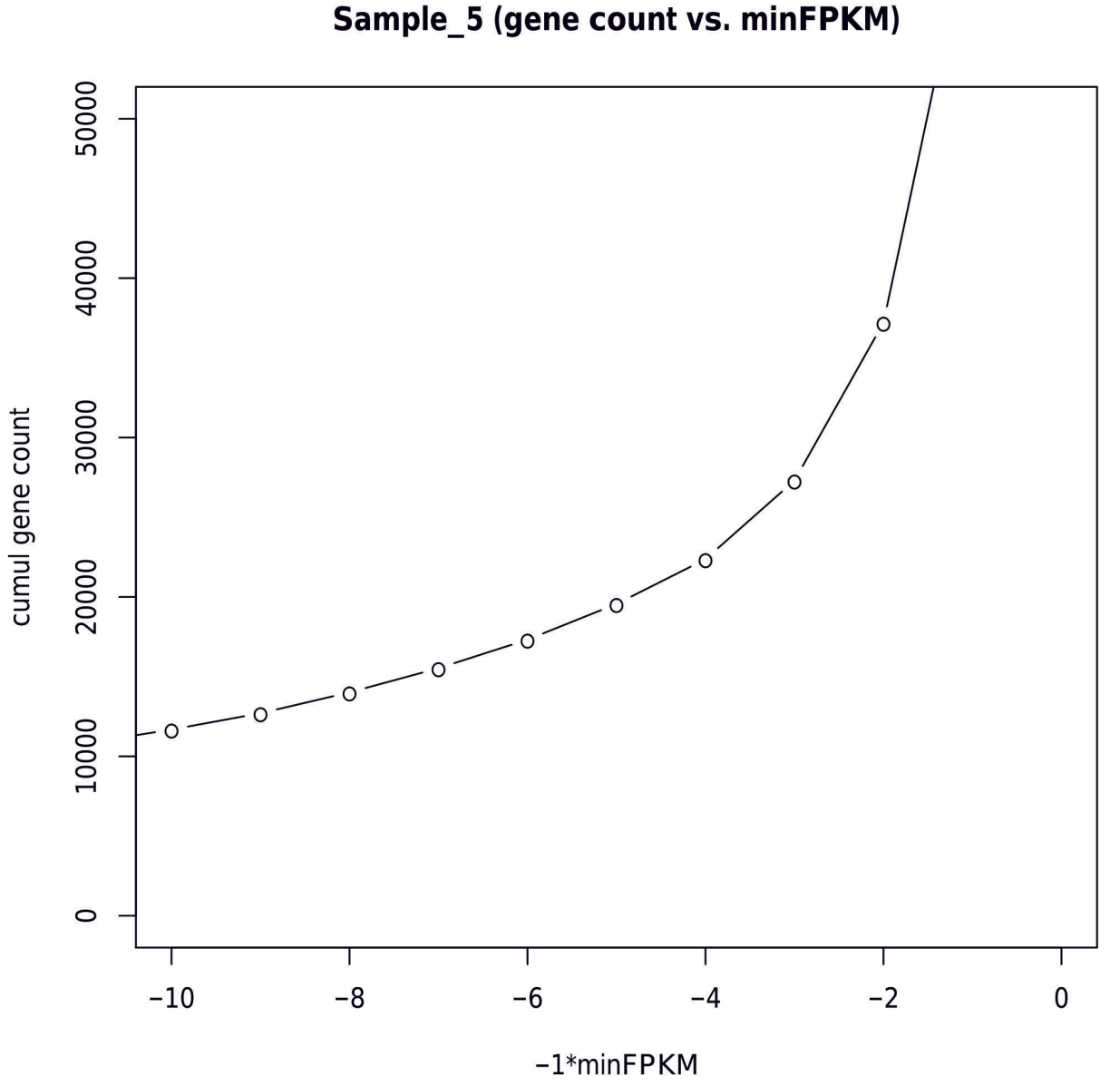
Sample_5 (gene count vs. minFPKM)
cumul gene count
0
10000
20000
30000
40000
50000
−10
−8
−6
−4
−2
0
−1*minFPKM

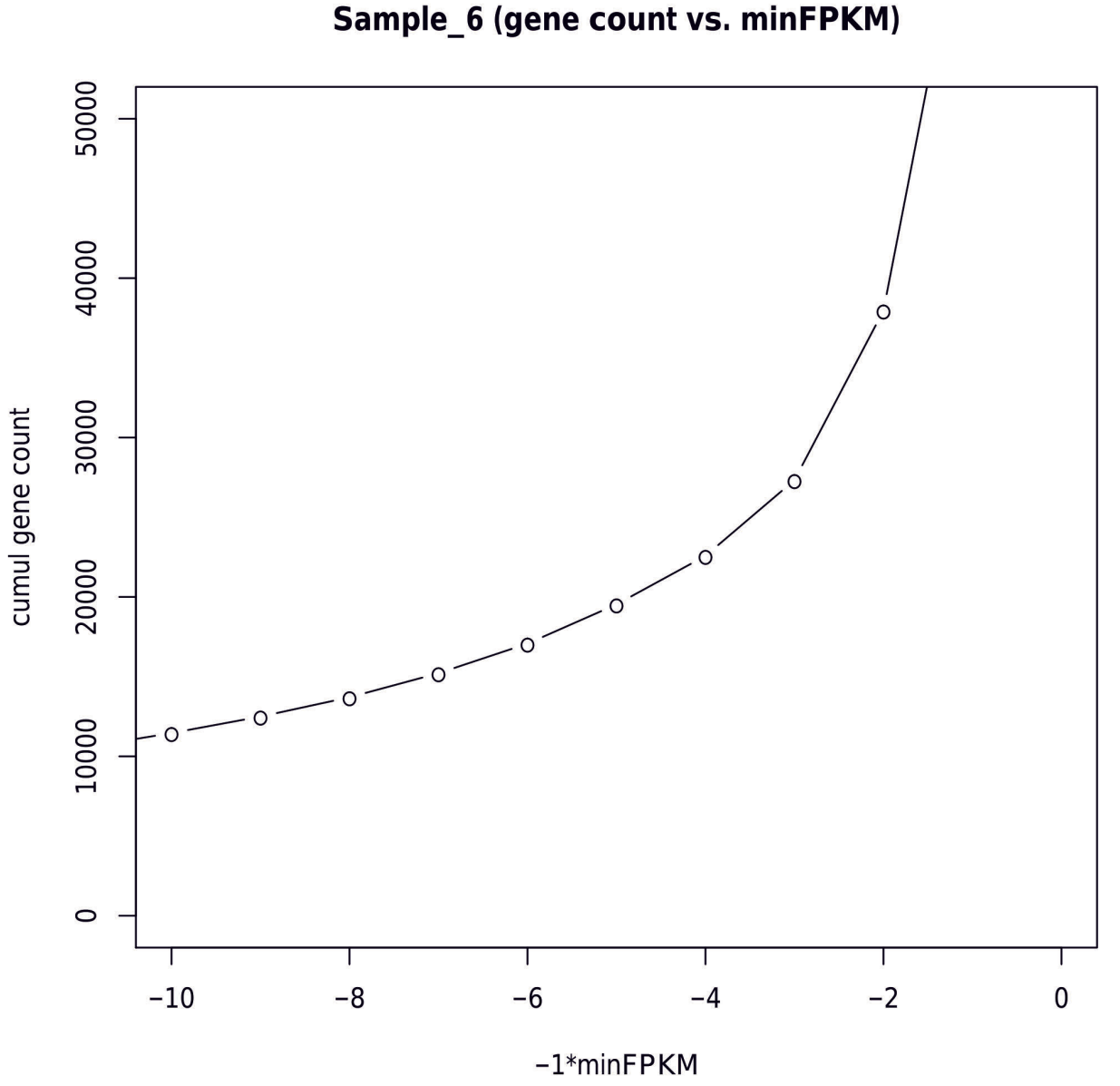
Sample_6 (gene count vs. minFPKM)
cumul gene count
0
10000
20000
30000
40000
50000
−10
−8
−6
−4
−2
0
−1*minFPKM

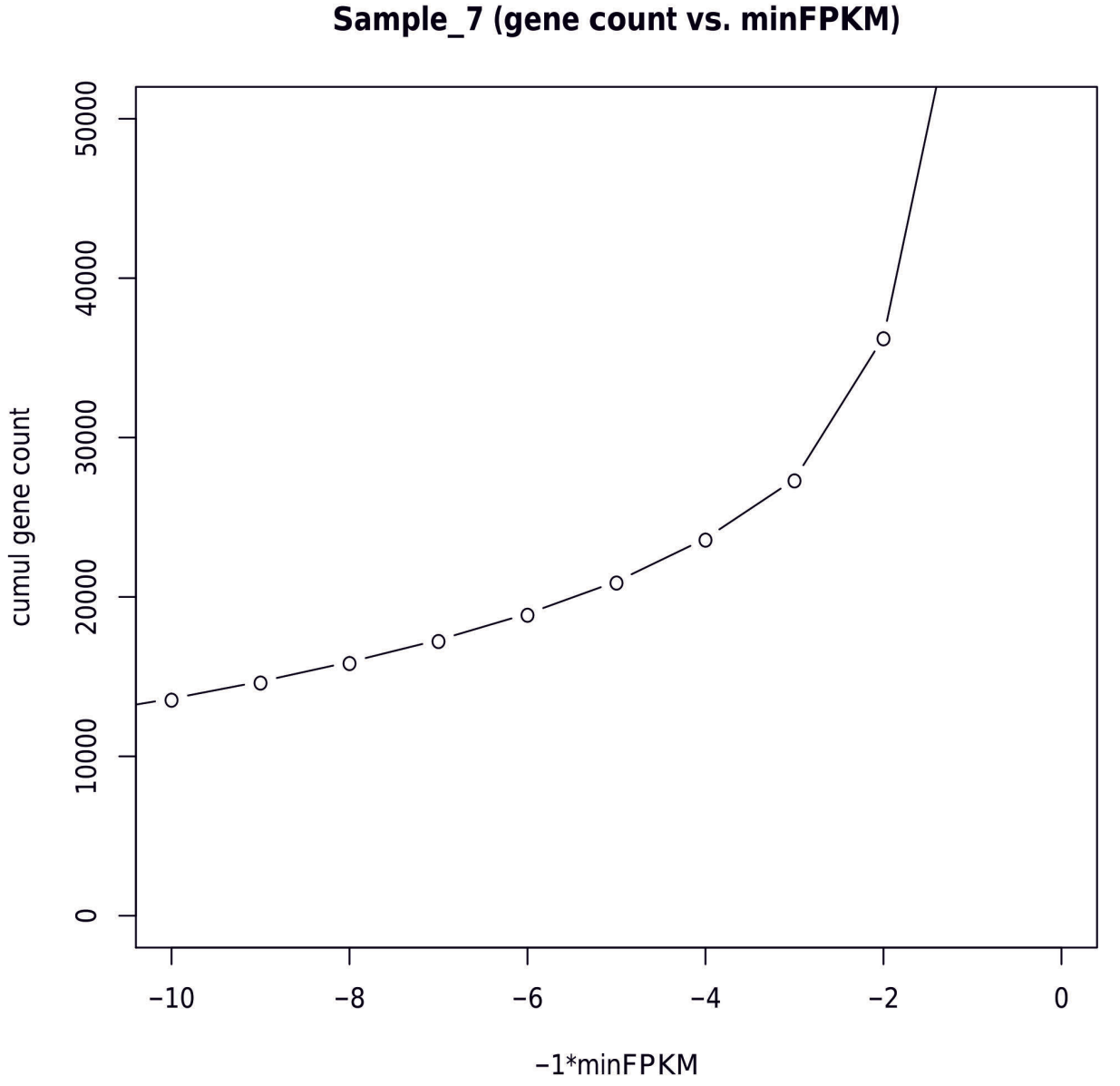
Sample_7 (gene count vs. minFPKM)
cumul gene count
0
10000
20000
30000
40000
50000
−10
−8
−6
−4
−2
0
−1*minFPKM

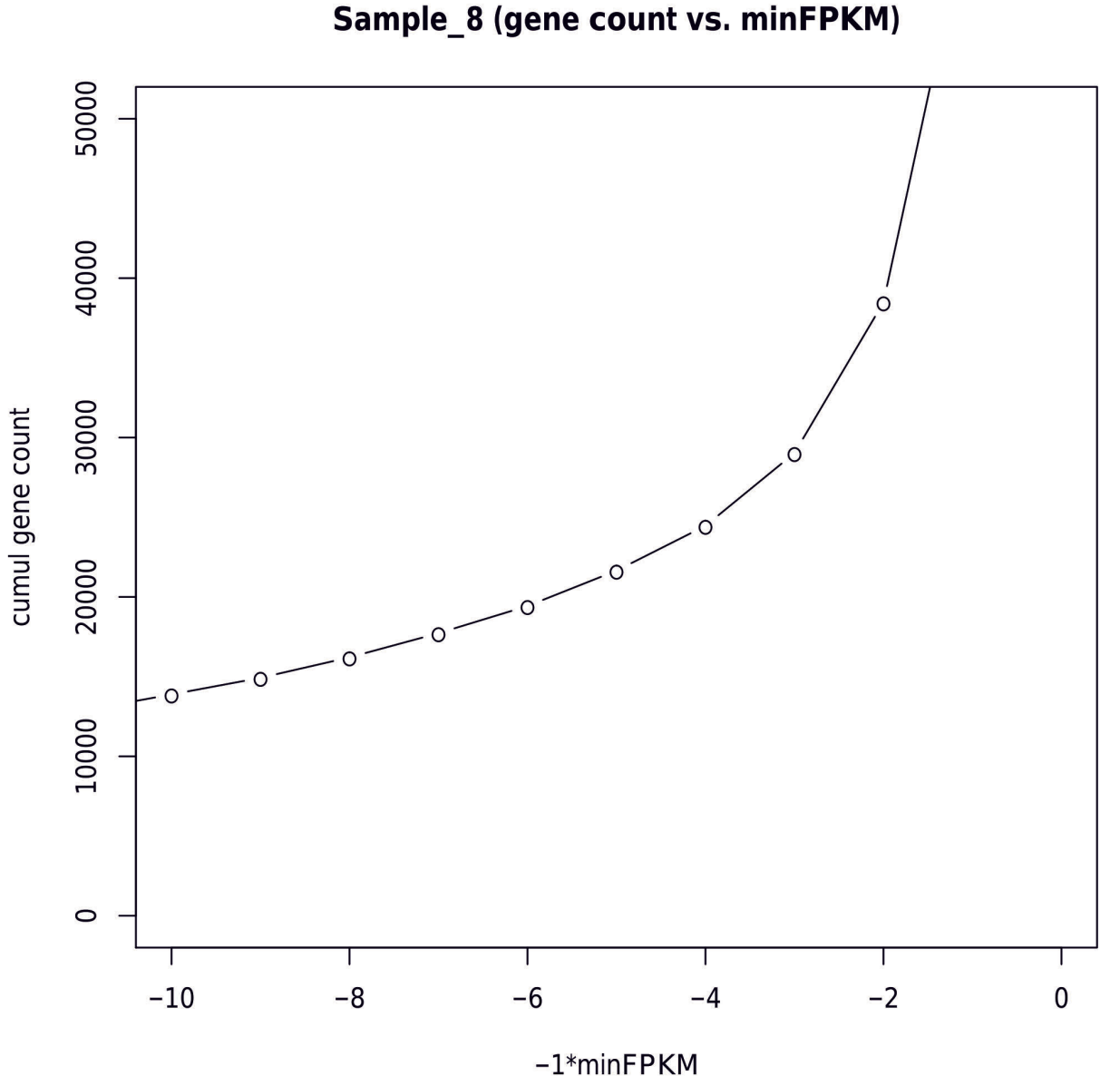
Sample_8 (gene count vs. minFPKM)
cumul gene count
0
10000
20000
30000
40000
50000
−10
−8
−6
−4
−2
0
−1*minFPKM

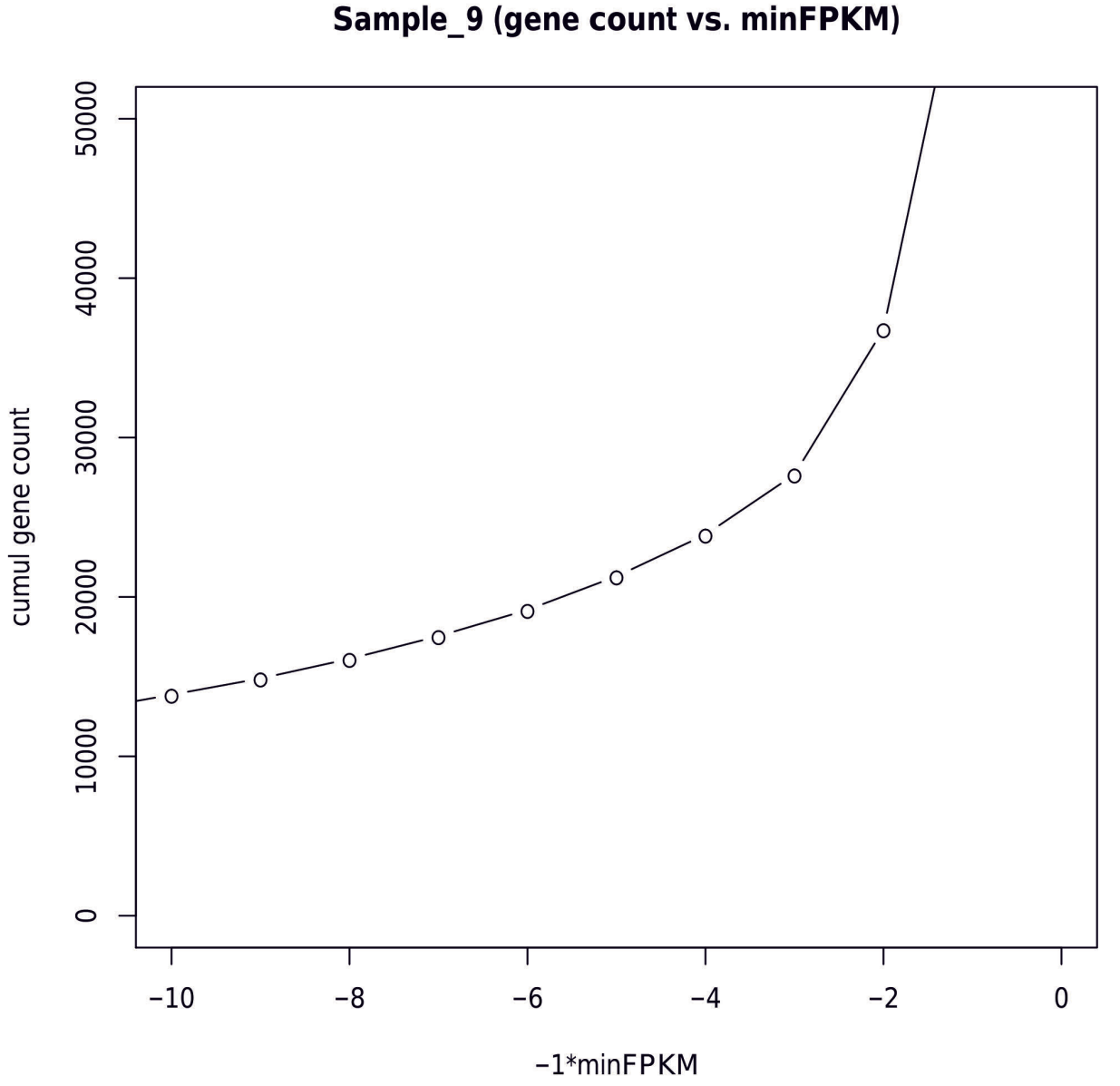
Sample_9 (gene count vs. minFPKM)
cumul gene count
0
10000
20000
30000
40000
50000
−10
−8
−6
−4
−2
0
−1*minFPKM

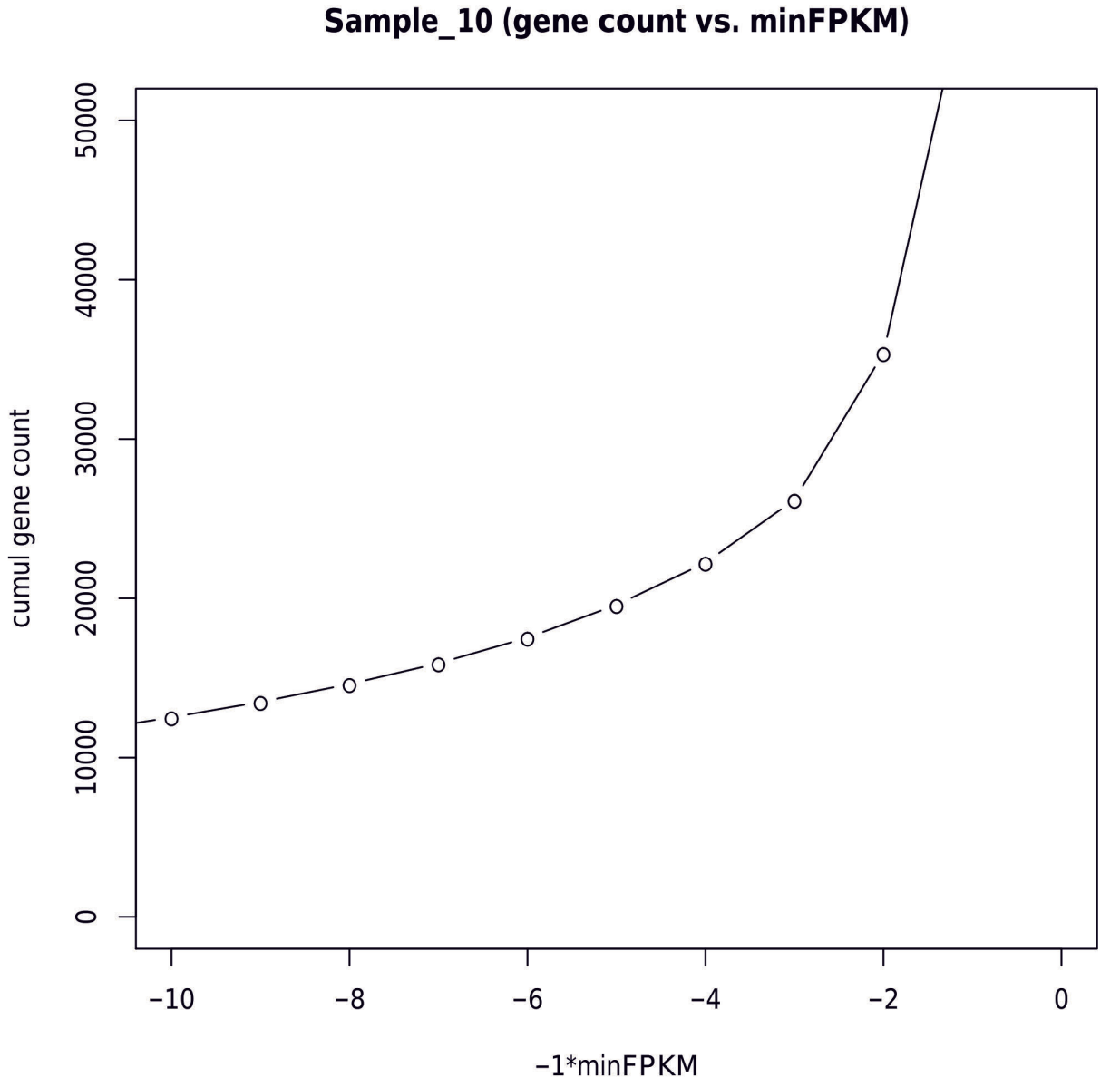
Sample_10 (gene count vs. minFPKM)
cumul gene count
0
10000
20000
30000
40000
50000
−10
−8
−6
−4
−2
0
−1*minFPKM

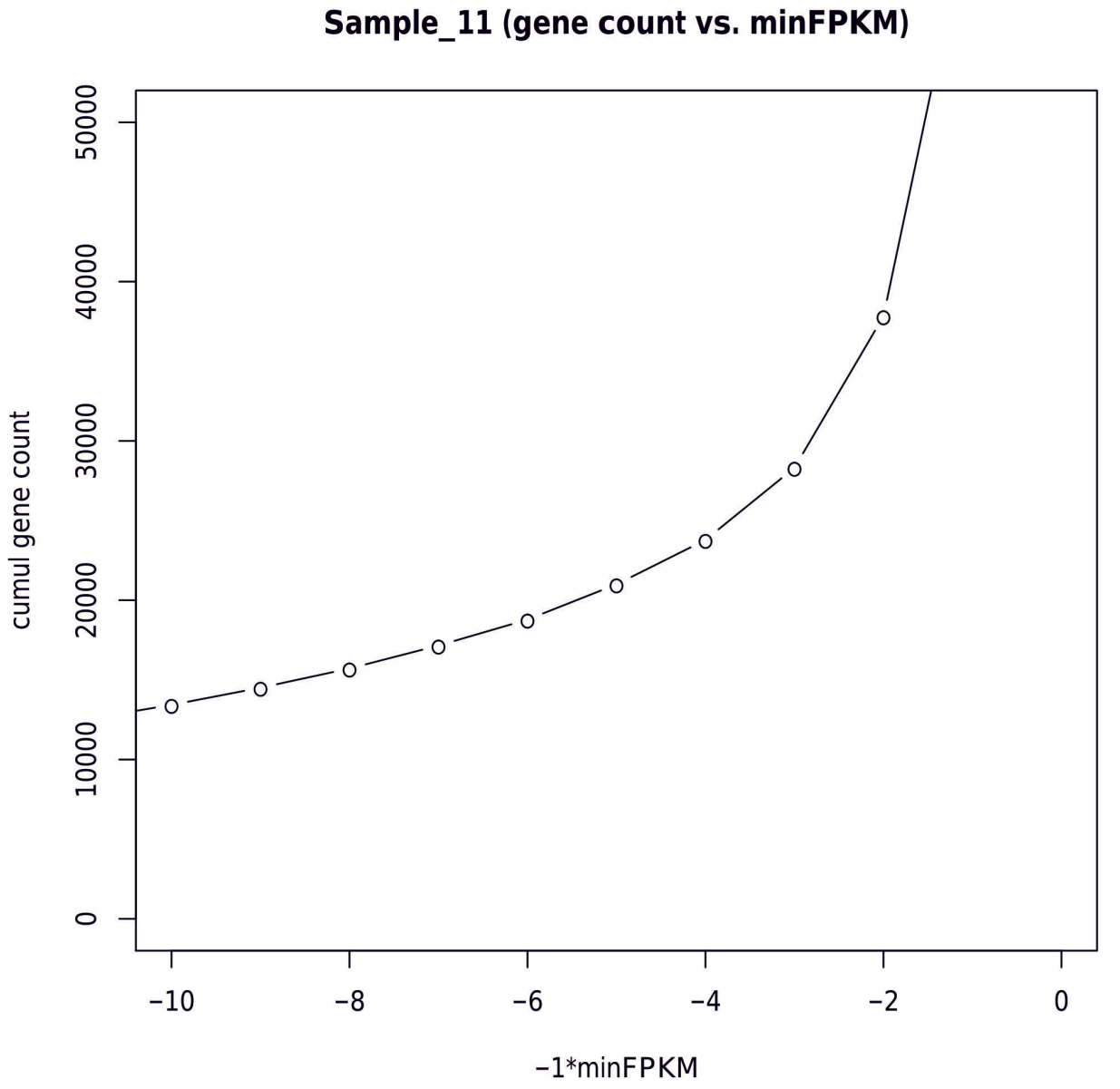
Sample_11 (gene count vs. minFPKM)
cumul gene count
0
10000
20000
30000
40000
50000
−10
−8
−6
−4
−2
0
−1*minFPKM

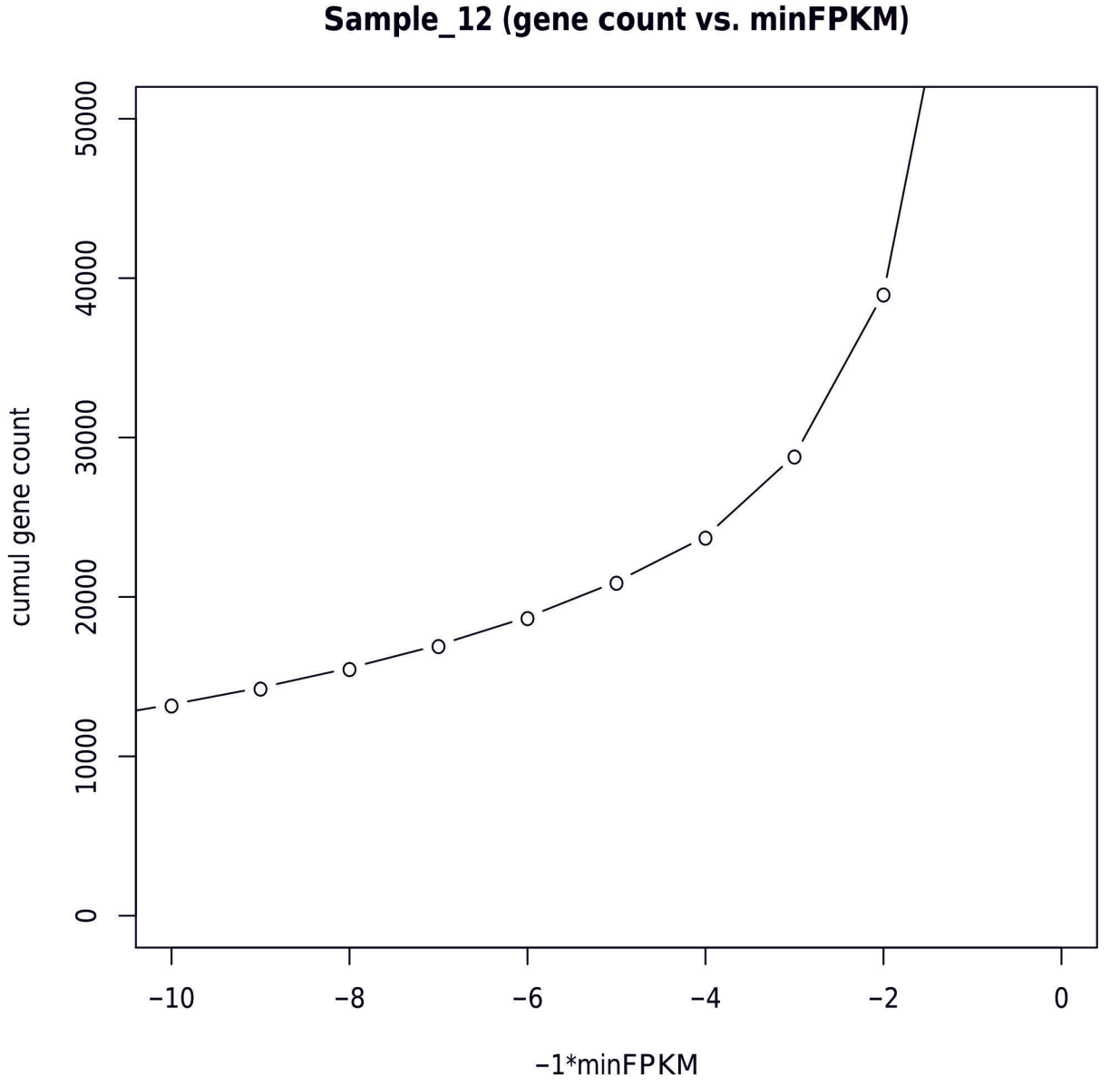
Sample_12 (gene count vs. minFPKM)
cumul gene count
0
10000
20000
30000
40000
50000
−10
−8
−6
−4
−2
0
−1*minFPKM

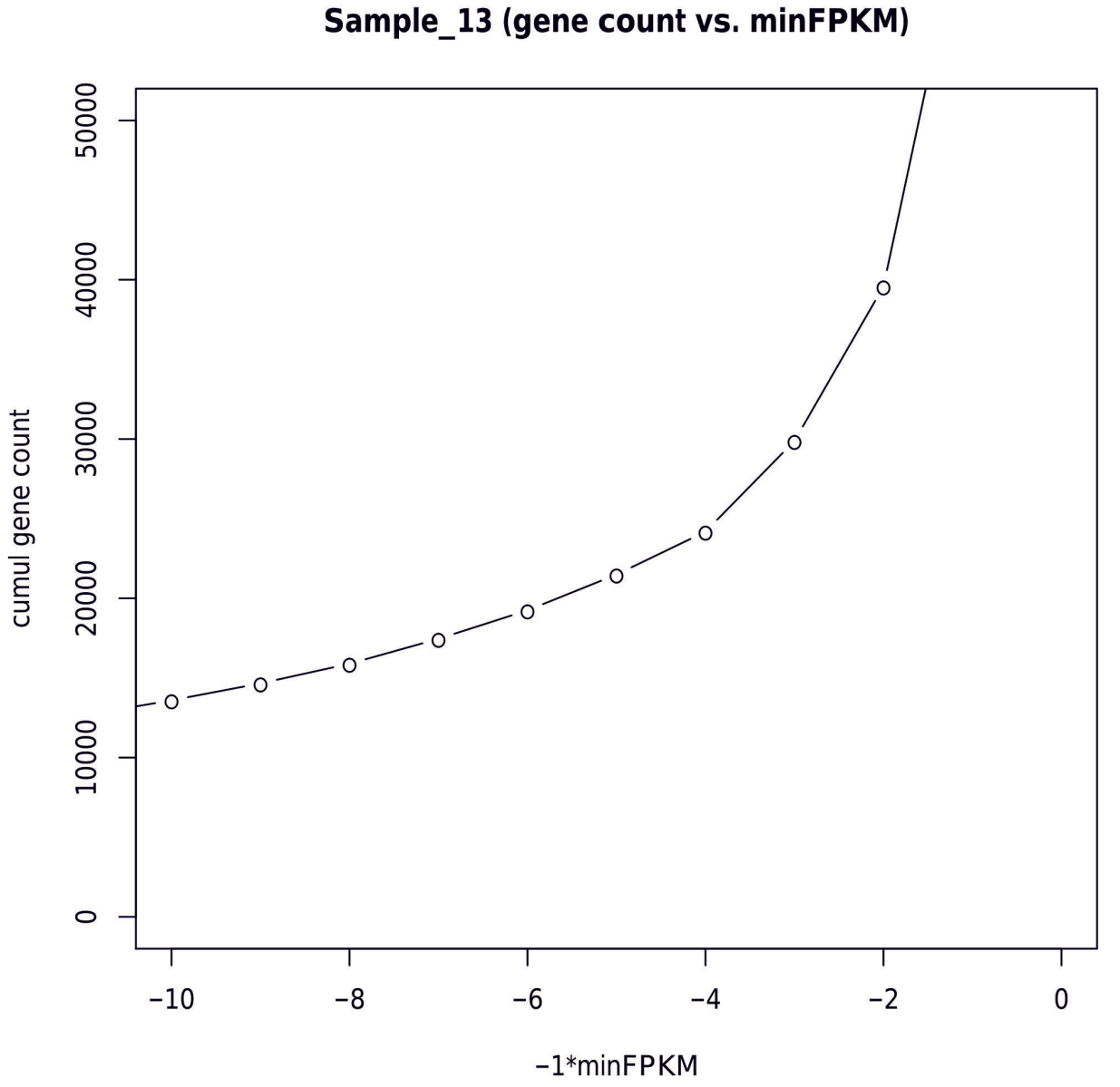
Sample_13 (gene count vs. minFPKM)
cumul gene count
0
10000
20000
30000
40000
50000
−10
−8
−6
−4
−2
0
−1*minFPKM

Supplementary material Paper II

Supplementary Fig. S1

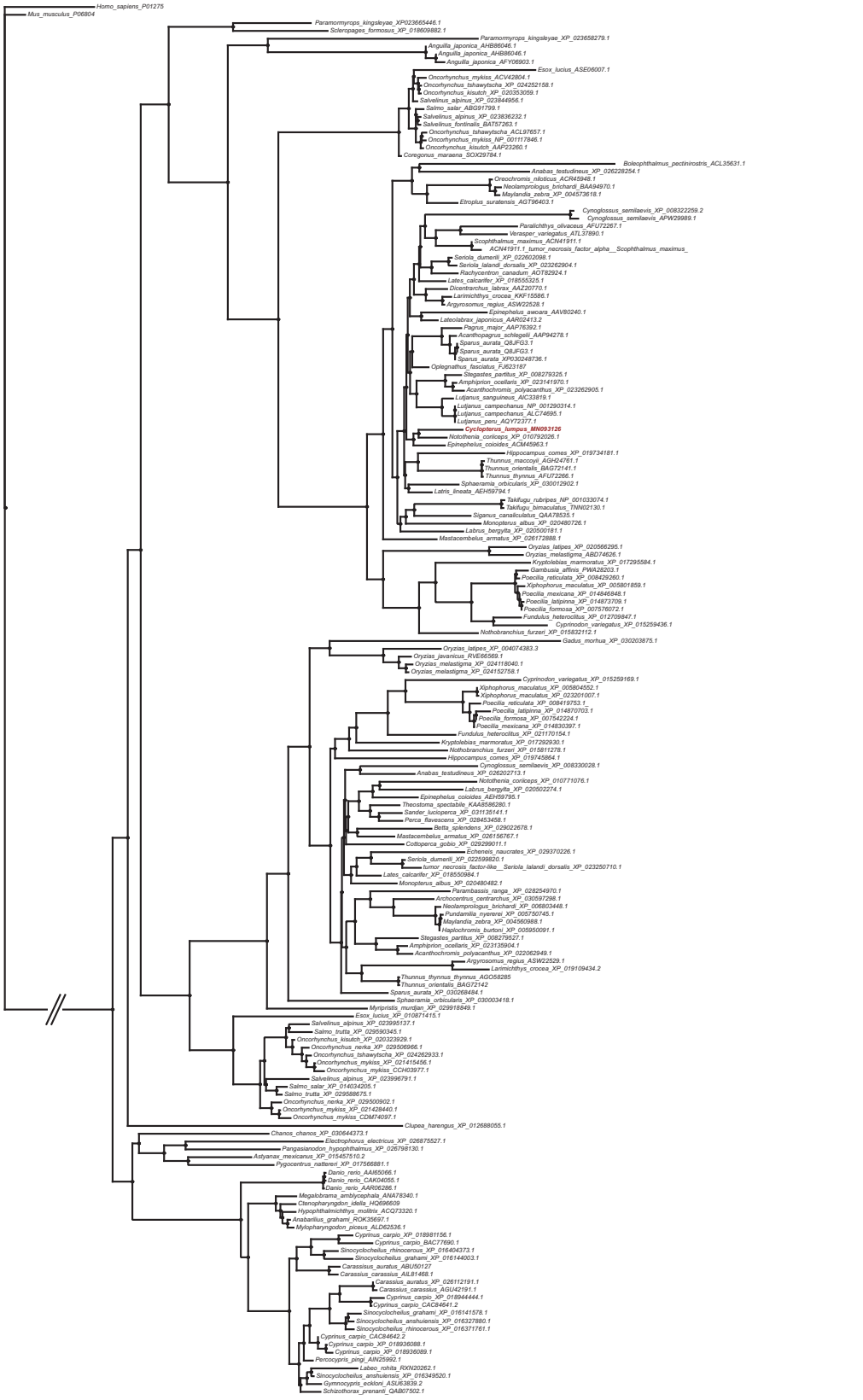

Supplementary Fig. S2

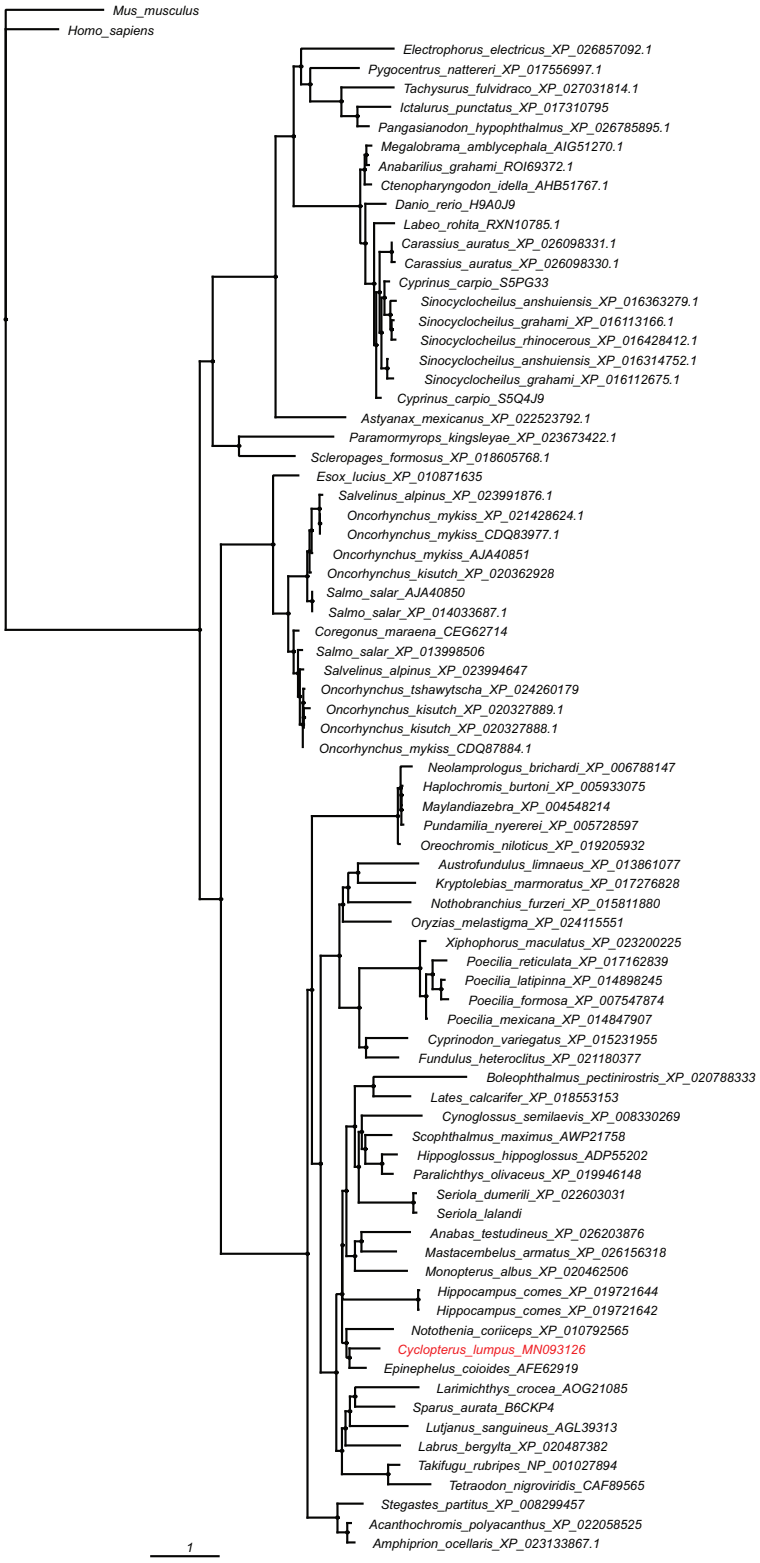

Supplementary material Paper III

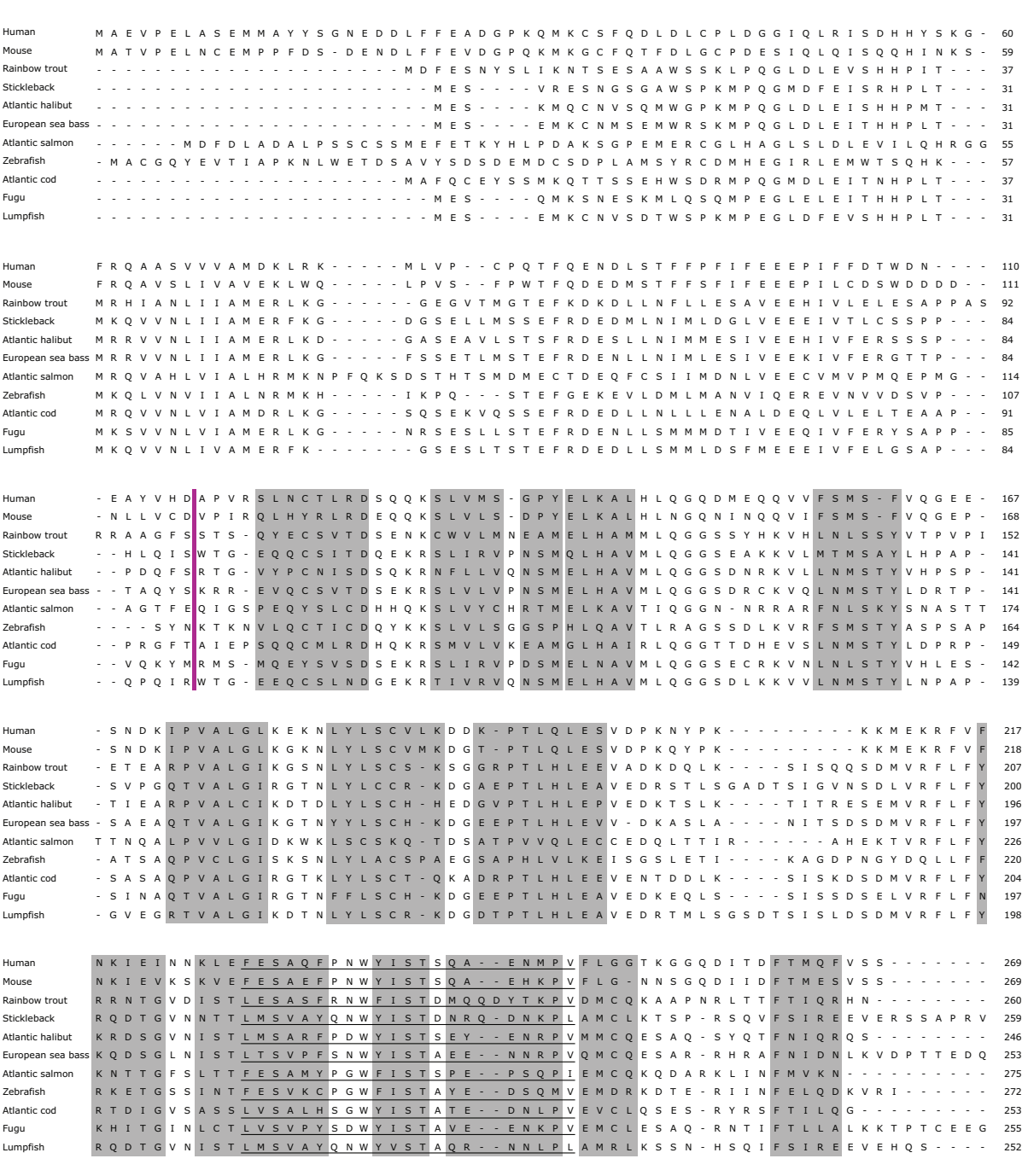

SUPPLEMENTAL FIGURE 1_IL1β

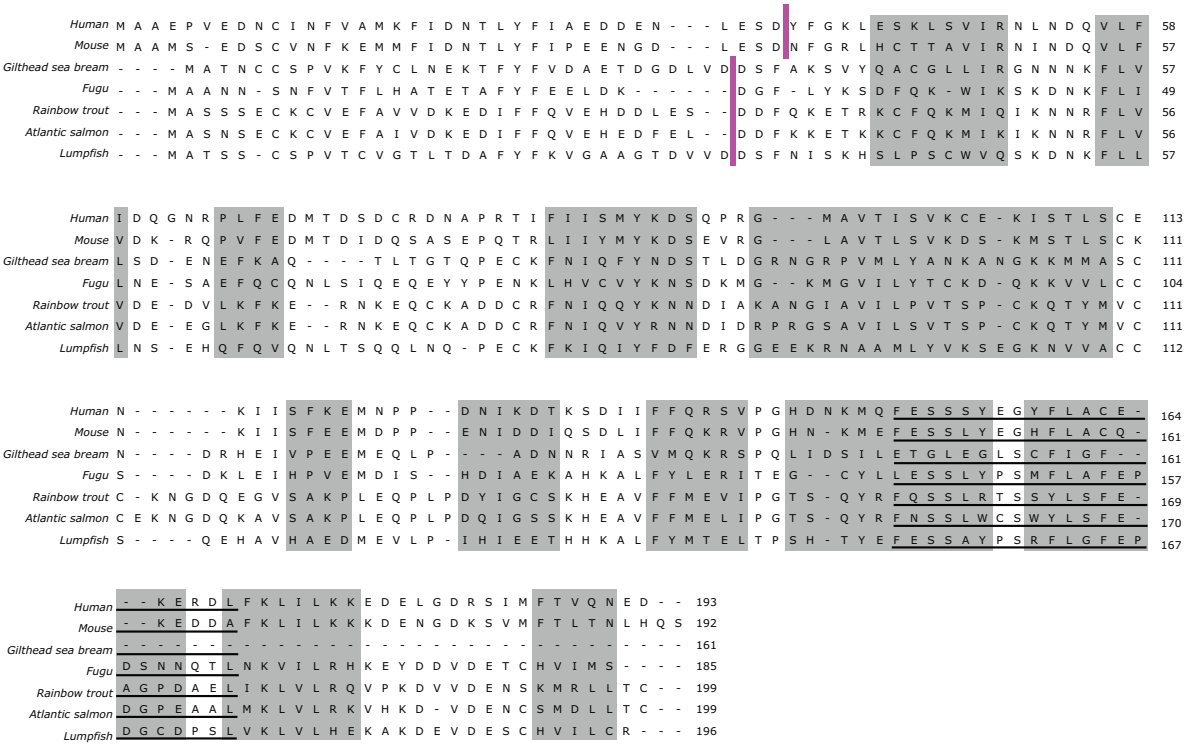

Supplemental Figure 2

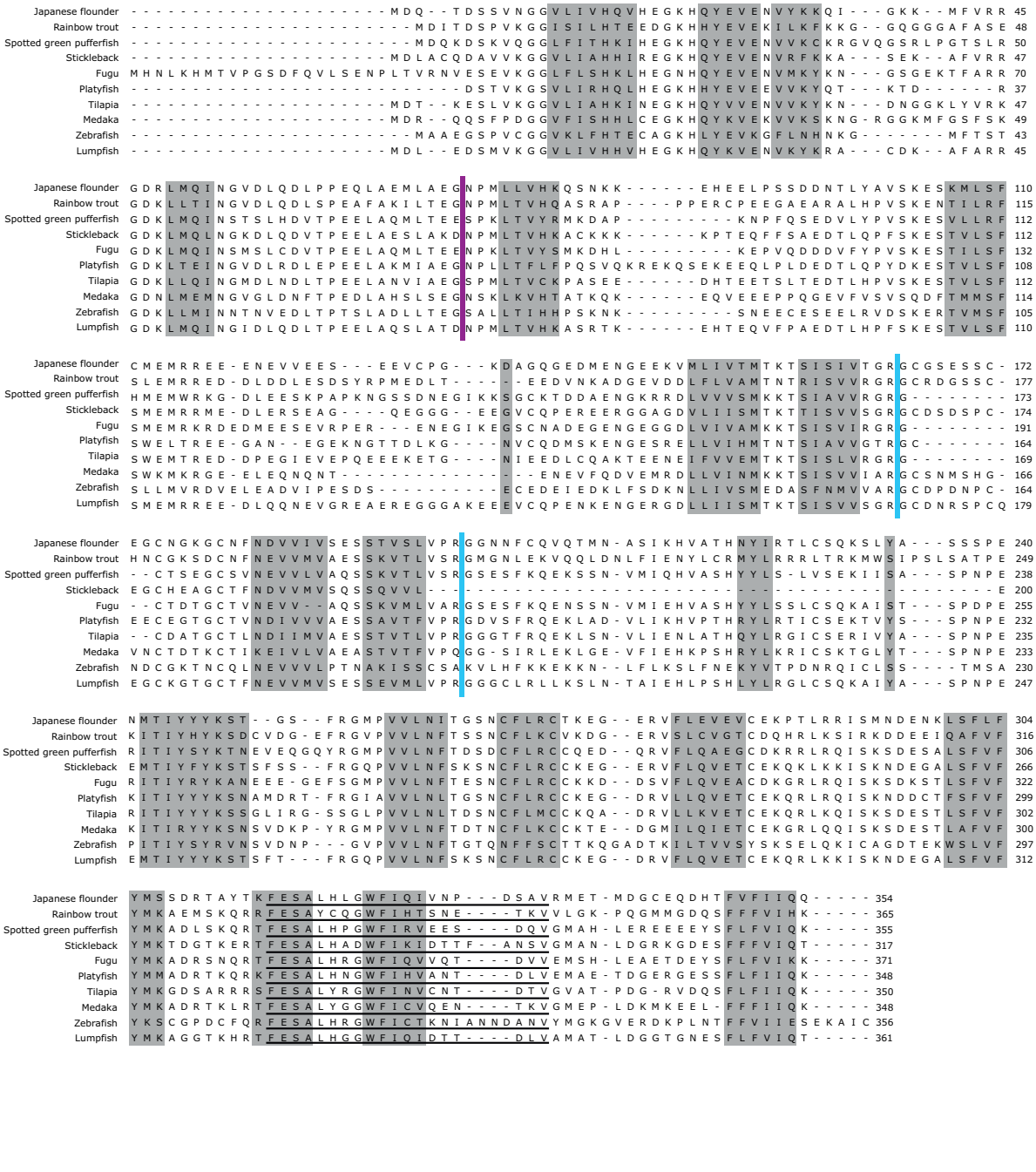

SUPPLEMENTAL FIGURE 3_nIL-1F

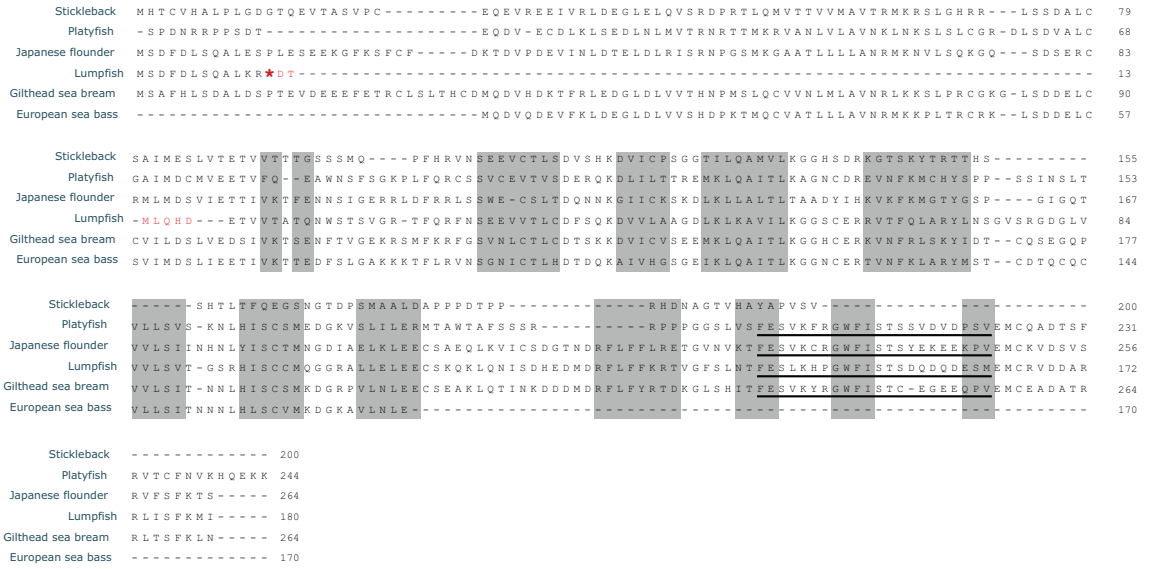

SUPPLEMENTAL FIGURE 4_IL-1Fm2 alignment

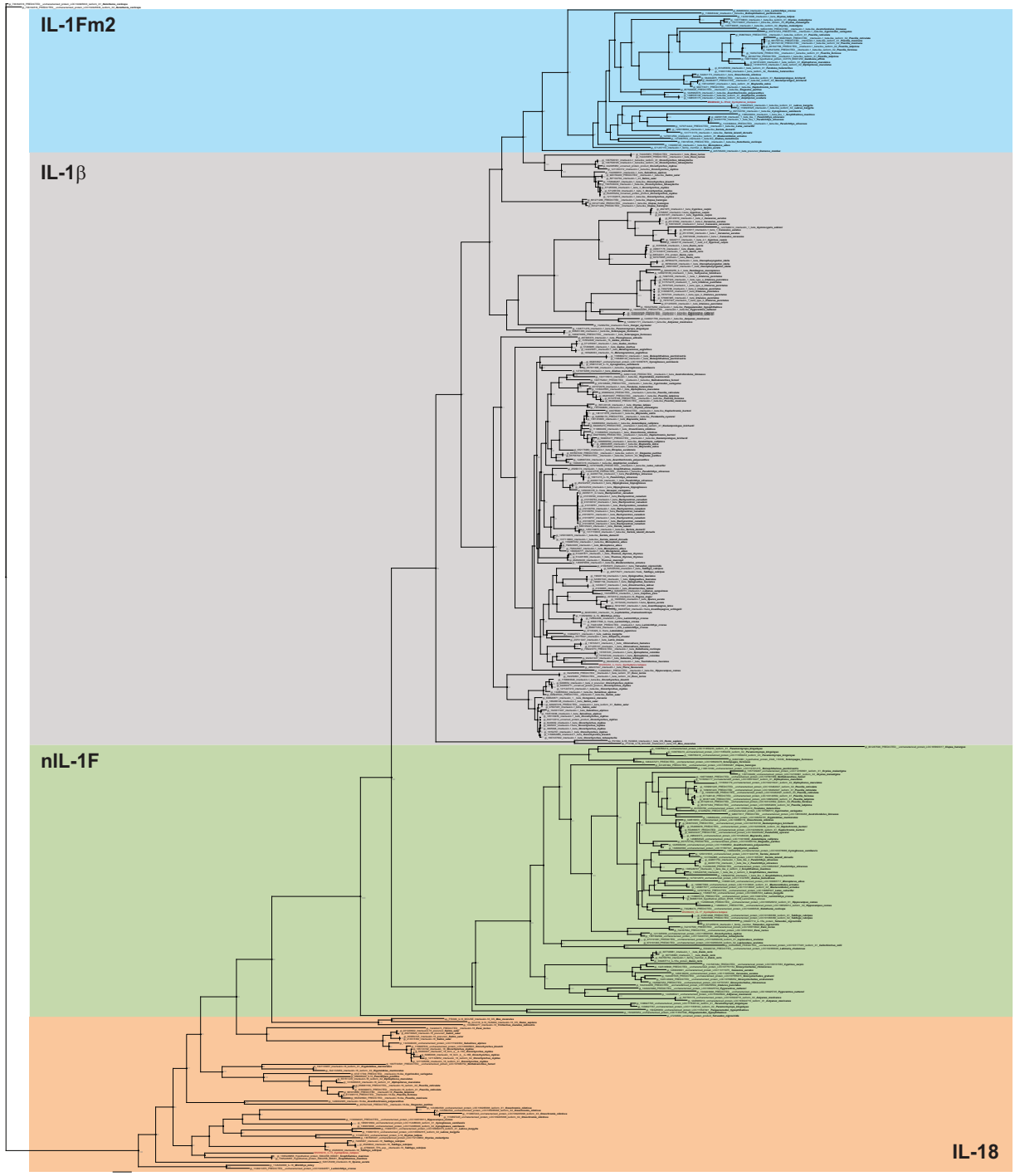

Supplemental Figure 5

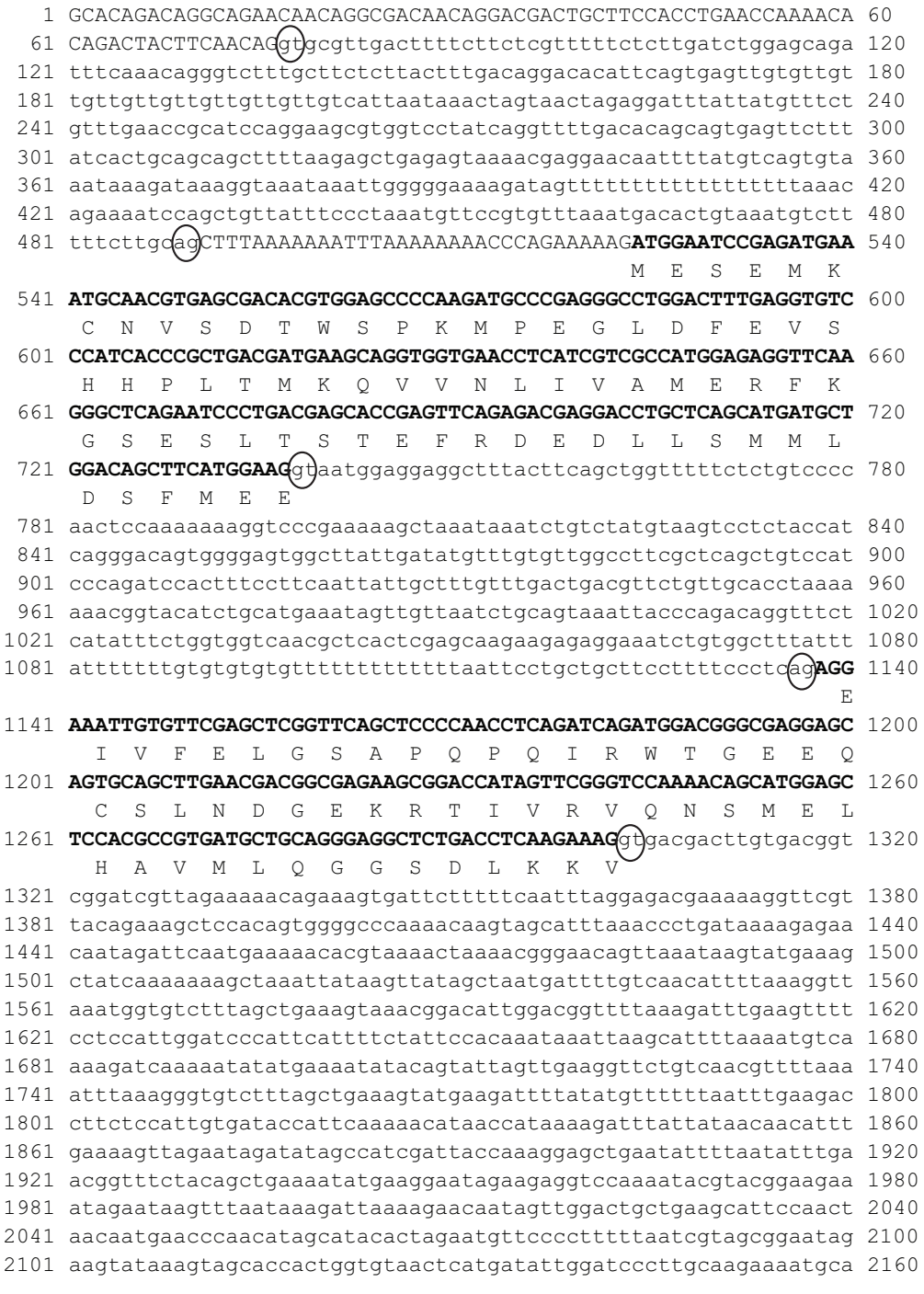

```
2161 cttaaagtatcggcgtgtcagttttcaatcaaaatgaacctccgtcctctcttcgctcct 2220
2221 cagTTGTCCTGAACATGTCGACGTACTTGAACCCGGCACCCGGCGTGGAGGGCAGAACGG 2280
        V  L  N  M  S  T  Y  L  N  P  A  P  G  V  E  G  R  T  V
2281 TGGCTCTGGGCATCAAGGACACAAATCTCTACCTGTCTTGCCGCAAGGATGGCGACACGC 2340
      A  L  G  I  K  D  T  N  L  Y  L  S  C  R  K  D  G  D  T  P
2341 CAACTCTGCACCTGGAGgtaaacgtcacgactcggtacaggatactgtcaccgcgttcgt 2400
      T  L  H  L  E
2401 cgcggcactatgtgaaagggcaacgcagggacccttacgcagtggttgggcctgacctt 2460
2461 tacccccccttttcccaccctcagGCCGTGGAGGACAGAACCATGTTGAGCGGATCGGA 2520
                              A  V  E  D  R  T  M  L  S  G  S  D
2521 CACGAGCATCAGCTTGGACAGCGACATGGTGCGATTCCTCTTCTACAGACAGGACACCGG 2580
      T  S  I  S  L  D  S  D  M  V  R  F  L  F  Y  R  Q  D  T  G
2581 GGTGAACATCAGCACCCTCATGTCCGTCGCCTACCAGAACTGGTACGTCAGCACTGCGCA 2640
      V  N  I  S  T  L  M  S  V  A  Y  Q  N  W  Y  V  S  T  A  Q
2641 GCGCAACAACCTGCCGTTGGCGATGCGCCTGAAGTCCTCCAATCACTCCCAGATCTTCAG 2700
      R  N  N  L  P  L  A  M  R  L  K  S  S  N  H  S  Q  I  F  S
2701 CATCCGAGAGGAGGTCGAACATCAGAGTTAAAAAGCCTGCCGGAGACACCCGCAGTGGGA 2760
      I  R  E  E  V  E  H  Q  S  *
2761 TGTGGACGTGCTTCCTCAGAGTTTGACCCTCTGAGGAAGCACGTTTCTTTGGGTGTATAC 2820
2821 TGCACTTTTTATTGATTCAAGAATGCAACAAAGACGCTACGGCTGTCTGGTAACAAGTTG 2880
2881 CGAGTGTTACAGAGCTTCTTATTCACCGTCTGTACCAAGTACAGGCAGTGAAATGCTTTT 2940
2941 GTGTATTGACTTACGTCAACTTTTTACCAGAAGATGGCATCATCGTGCTTCTCTGGAGAA 3000
3001 CACCCCTGTGTATTTATTGTGCCGAATGACACGCATGTTGATGCTTTTTATCTATTCATG 3060
3061 TATTTATATATTTATGCGACGGTTTAATAATAATTTATGTATTTATTTGGACATCTGCGT 3120
3121 ACTAACAATTATTTAAATGATGTGCAGCAACATATTTAATAAAGCCTTGTAACTTATTTG 3180
3181 GATTTGTGTTTTACATTTGTTCACTCAAGACGTTGACTCAGGGAAATGATAAAGAACCTC 3240
3241 TCAGTAGATTTTAGCTGCAGCCCATTTTTAGAGACAGTAATACTTCAGATTTTGAGCTGA 3300
3301 AGTATAAAGTATAAATACTATTTCCACAACACACGGAGGATCAAAAATGGCAGTTTAGTT 3360
3361 TTGACTTAGTCCTACTTGTACTTGTACTTTCGACTTTATACTGTATTTACGATTCAGAGG 3420
3421 CAAATTATTATTGGATTTGATTTTAATAATTTAATCCAAATCTAAAAAGTAACTAATTGA 3480
3481 ATAAATTATGATCAACAAATACATCTGGATGTATTTTTTATGGATTAAGATCAAACTTTA 3540
3541 TTGATCCCCATGGGGAGAAATTCACAAGCGGTAT                           3574
```

```
   1 CTTTGAAAAGCCAGGCAGAAAAGCAGGTGCAGTTTTTCCAAAAATTTACGAAACACTCGG 60
  61 AGACCGTAACGCTTGCATCATAACAGACTGAAGCTGACCCTGCAGGgtaagttaaaaatg 120
 121 ctgcctgacctggtgcaaagtgtgtttgcgtttgtcaacaaactaaagctgttcgaggcg 180
 181 catattcaaaagggagatttaacacattttcatactctgctaaaagccagtgagcaagtc 240
 241 accagcgccgccctgaaaagaaaagagacagatatgcaacactggttgcaaacctgcaca 300
 301 aagctttgtgacccggttctgtgatctacaactgaaaagaccacagattatgttcctcgt 360
 361 cgacccatttaatgcggagacagactgtttgaaagccccgctcgtcacagatgaggctgc 420
 421 ggctgagttggagatgatcgacctttgtgaggaggatcaactgaaagctgttttaaggga 480
 481 agggaccgttgagttctggaaaagtgtgccaattgaaaaataccccaacatcaaacgagc 540
 541 tgcgcttaagatactgtccatgtttgggtcaacgtacgtctgcgagtctgtgttttctac 600
 601 cctgaaacaaacaaatcaaagcatcgatctgttctgactgacactcatttgaaagaattg 660
 661 cttagagtggcaacaacagaatacaagccagatttgaagaggattgttcaagataaggaa 720
 721 tgccagaagtctcactaagcagcatagtaagagaaagatgttattgaaaattattctatt 780
 781 attgtttgtttgaactgagagtgtgtgtgtgtgtgagacagtgcacacaatgttaactgt 840
 841 tgaaaattactgatattatcatgttggtgtggttattttcattagatctggctgagcaga 900
 901 ggtctgtgtatgcgtgcatacatgattaaaagatgatgttcttgtgtacccatgtgtatg 960
 961 atgtggctctttgcagtaacgcagaaaaaaaagtggctcttagtctctgactagttggcc 1020
1021 acccctgccctatcctaacgtcttgacacacagtacattaacaacatatattataaaaaa 1080
1081 acatgttgtggttatgtccgacccacctgaatgtggaattccttcatcacctcagacagc 1140
1141 aaggggtcctgttcgacatcaagttggcagccggtggcgagccagatcatatctccagtc 1200
1201 cagtggccccccagtgctgagtgagaggctccaggcctggctcctgtagcaccagctggc 1260
1261 ttcactcacctggacagtcgcatgagattgatgtaaaaaccttccattcaccacactctc 1320
1321 aacttcacgcccatgctccgctacctgacagtacgtcttcatgtccacccgtccattcag 1380
1381 gatgaacggctgcaggtgggacgtaggcctccggggtgacggctcctcctttcctcgcct 1440
1441 ggcgaatcatagccaggcgtttgtggaggctccgctcattgtagaactgcctcaggtagg 1500
1501 cttggccatccatcttgatgccgtgctccacgtgggagtaacggcccaccaggctctcca 1560
1561 cgtcgcccacgtcaaactgctttaactgcaggagaaacaacgaggacctgatgcgcttgt 1620
1621 gctggaggccgacagctatatctacagttatggtctgcatgcagcttcacactgtcacta 1680
1681 gacctggaggtgcttcctcatgacccatgtcacacggctggcaccttgctgcagggcaat 1740
1741 tgagacgacatgagcgctggtcagacctccaccaactaccattactctctgccctgcctc 1800
1801 acacactacacacacgtctacacacacaaacagcacttgtaaaggaaaattgtgcgacga 1860
1861 ggacgggggatcaaatcaaaaacctcaggtgaaagcaacgttttattgattattctgcaa 1920
1921 aaaacaaaaaaacactagtaaatgggcattgagtctgaaaaagaaggcctaaatattgtt 1980
1981 tccctgcagagtttttctgtattattgtgatgtgacataatgctcagaggaaagctgact 2040
2041 taccttgagtgggaaaagtgtctttctgtttttgccgagcggttggcagctggtgcatga 2100
2101 ggtgcactgtgtgttgcaagcgctcctctgggtagctctctgcaatgcttttcacccatg 2160
2161 aagggatgtttgccatctgggcacgggtcggacctgtcgccataacgacctggcgggctt 2220
2221 ttagggacgatgccctcttgaaggtggacttgaaaatacctcaccctcttcctttcggtc 2280
2281 actctcttggcttcacactcagccctgtcctccaccacgggggcgatgtgctccactgtt 2340
2341 cccttcagcagcactttgtccaagttgtatctctccacctgtatgttcagattcactagc 2400
2401 tcagaaaatagaaacgctcagatcccggtgctcatgctgcttaatggataacatgttcac 2460
2461 gtatttttttccatctactgtaagtgaagacacaaatatttaacaaacgagtctaagattt 2520
2521 tctttttaaaggtgcaatgtacgggattaagagcattgataaagcagcaaaccccttcag 2580
2581 cactgttagcaccattagctgttgccgccagctcgccagtcgacatgttgagaggtgttg 2640
2641 aaaggcaatagaattgctcccaatctcatataaagcacctttaaagtgacacgtttcatt 2700
2701 ggagtattgtataatgcaagcttgtgattatatatttctatctgttctttcttcgatttc 2760
2761 agatttcagaacacacacccacaaatatatgctgcgtctaacctgatctttaaagaaatc 2820
2821 cacacttagattggttcctggcagactgaaggataaactcttcttgagtgttgtagtgac 2880
2881 gttgaggcgtttcctctctttcctgccgagcctcatgtcattgaaaaatgcgttttcgtc 2940
2941 cagaatgtaaacctggtctgggagactgtgaagctctgcagagcgatccgactttaaaac 3000
3001 aaagtcctgcagggctttctgacaaagaaaaacacacacacacacctgcttctttacatc 3060
3061 ctgtaaaagcaccttcctggcttctacttcaggggaagttggttgtgcttctaccttatt 3120
3121 gagagggtctgtgtgcaccagtgtgtgtgagcgcagatgagggatgttcagagctgtgaa 3180
```

3181 ctggctctcccacagagttgtccactctccataagaatccaccacacggagactcaacgg 3240
3241 gggaagtggaccctctctgacatcgttgacttgtctggtcgctccttcagtgtcgagcct 3300
3301 gcaactaatcacagagagcaaaacacattgaactgggagtccgtttgattgtggtgcgtc 3360
3361 acatttatgtcaaaatgaagaagtgggaacagtgacaaaggatcagccatttattgtgtg 3420
3421 ccttctttgtgatgcaaccgggttcaataacatttttaattgaatgaatgaagtctgaat 3480
3481 atcaagctgatagcaaactcattcctgctgggaaaatcaaccggacaggatcgacaggcc 3540
3541 gaagtcaaaagtaagtcaggagagaagctgatgaaaaaatattgtgatttactcaattca 3600
3601 aatgatttctcaaaataatgagatagttgtacttgttcataatttgtgtgactagttcag 3660
3661 aatttaaattatgactaggtaaatcaaactgatttaactgaattttaagtatgaattatg 3720
3721 agaaatgaaaaagaagcgatgacttactagataaagatataacaaaacaattgacttact 3780
3781 gactggtaatgcaaaaattccccatttatgtcattatgtggcaacttgtgatttttttttt 3840
3841 catcatcgattaatctgctaattattttctcaaagagttgatttctgaatagttggggac 3900
3901 atttttttgttttttacagaacacgggtgaaaatatccttcagaatcttcccaaattaa 3960
3961 catcttcaaaatatctaattttgttcgaccaacagtctaaaaccccaacataaagagttt 4020
4021 agtattgcataagagccaagagattagaacattctcacaatttagaaactggatcgttgc 4080
4081 aatgtttgaccaataataagtcaaaactctcaacttatgtaaatatgtagtatatgattt 4140
4141 agtgagtgaaacccagctcatggtaccagctgcgactcttctcttcttcctgccaccgca 4200
4201 gcttttgttgtttgatgtttctgggtttgtctgaggccccgaagggtccgaggaggaaga 4260
4261 ggaggaggaggaggaggagagggctaagtcatgtccgaggtctgagtgtggatcagggtc 4320
4321 agggttggatagcaagctggcgagggtcaaggcatgagggccacccccctattattaacac 4380
4381 atcgagtatccccatctgaaacacacgcagacacaatacagacagggcagtgctgttgta 4440
4441 gttgtgatggttacttgtactttcaaagccagacagttccttaaaatatcacatgtgagt 4500
4501 caatctgaggctatggcggtttgacttctcagatgaccgttttttcgagtgttcagttca 4560
4561 gcattcatgaaatgaactctatgaattattactaaagattaaaacgacacatttcaaaca 4620
4621 acacctcgtagcaaagctgtgtgtgattggttgaaataatgaaagtgcctcaaactttat 4680
4681 catccaactgtaaaaccaagtgaaatgcactgcagaggtcaacggtactcgacaccttca 4740
4741 gctgctacgataatgaaactgttctgggcccatgcagcacatcgtatacagtttatgatc 4800
4801 agtgcctcacaatacctgcttgagtttggatcgtcaccgcgtgccgcctctgagacggtg 4860
4861 gaaatgtgcggcactgggcggtggcagacctcaaggttttgcgacagtggcgtgtgcttc 4920
4921 ccatgtaactcaatccacctcagagccgacagatttagctggactggaaatagcttcagt 4980
4981 gtgtgtttgtttgtgtgtgcgtgtgtgtgtgtgtgtgtgagtgtgagtgtgcctgtttaa 5040
5041 atattagcacagctcatcccagtattaaaactactttacttaattaaaaaaaattagaat 5100
5101 tagaggaaatattcctacttcttaagctaaataaatgtaaaaggccctttggatcagctg 5160
5161 gaaaatgaatcatcaccgagctgaaaaagggccatttctcttcatggttcccacagaacg 5220
5221 tgatgcattaatatagattaaactaaccaacagcaaataaaggagttgaaaacatcttca 5280
5281 gccgtaaaatgcgacacacacattaatgcaaaagagatatcgtacataatagtaaaacac 5340
5341 agacagggaacagttgacctcataatgagtacttgacagtttaactacatgttgctgata 5400
5401 atacttacacacttgtactgaagtaaggtttagaatgtaggacttttgttttggggtat 5460
5461 tttcagtgtggtattagtacgagtagtaatataaaaattttagacagagaacatttaata 5520
5521 aaatcaaagtaaaaaggtaaaacatgaaggctatgtaaacatttgttgtttactatattc 5580
5581 acctttaataaaataccagcctgacatcatgtgaagccaaaaagtaacaaaatggctat 5640
5641 tttagtttgtgaagagccgttaatgattgcttcctttcaattaggacattgttgaaccac 5700
5701 acatcgtatacattgaaatccactacagttactgtcacataggaagtcatgccttcccct 5760
5761 agttcctatgtttaatgtgagatcaaccataatttcctcttatttctgtttcctgtaata 5820
5821 actttataggtattactaaaaatcaagaagtgaacatccagtaatagaacaaaagaagtg 5880
5881 ttttctatttgacatgcagtacagtatagaatgagcgtgagagtcagataacatcacttg 5940
5941 gcttctagcttttctcagtgagacctttgctggtgctacagaatgatcacaggtggacca 6000
6001 ggtaccgaaacagatgaactctctcctcaacttctgttttatactaaaaagatcaataaa 6060
6061 aaataatacattcgagtctccgatttcattgtaccaatcttcattcacttcctcttctga 6120
6121 catcagGTTCCACATCCATCAGTGTCAGTGGCCTCTCAGTCCTACTTCCCCCTCTGTTCAT 6180
6181 GCAAAGCGGAAGCACAGACGCACTGGGGGCTTTTAAATGCCAGCGCGTTCCCTGGGGACG 6240
6241 GCTTCAGTCTTTTGCTTTACCAGCAACGGACACCGGCAGCACC**ATGGATCTGGAG**Ggtgggg 6300
M D L E

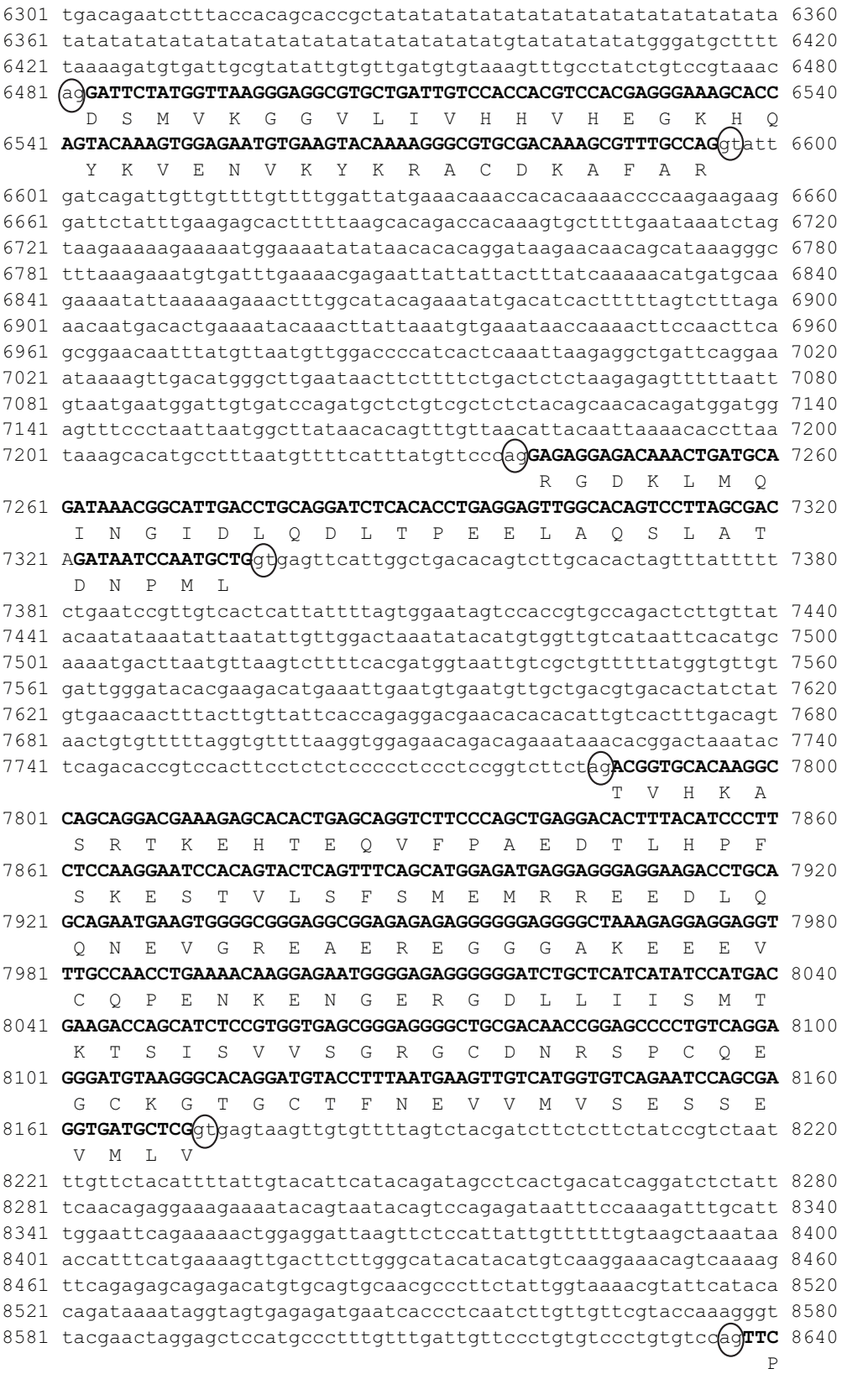

8641 **CAAGAGGAGGTGGATGTTTACGTCTGCTAAAGTCATTGAACACTGCAATCGAACATTTGC** 8700
R G G G C L R L L K S L N T A I E H L P
8701 **CGTCTCATCTATACCTCAGAGGTCTCTGCTCACAGAAGGCTATA**T**ATGCTTCACCGAACC** 8760
S H L Y L R G L C S Q K A I Y A S P N P
8761 **CAG**gtttgttattcagagcagcagattcatttacggtcatcacaaatgttgttttggatt 8820
E
8821 tctgttttcaattgattagtgaaatcacttgtttgttttcatttctttcgtgtccag**AGG** 8880
E
8881 **AGATGACCATTTACTACTACAAGTCAACCAGTTTCACCTTCAGAGGACAGCCCGTGGTCC** 8940
M T I Y Y Y K S T S F T F R G Q P V V L
8941 **TGAACTTTAGCAAGTCCAACTGCTTCCTCCGGTGCTGCAAGGAAGGGGACAGGGTGTTCC** 9000
N F S K S N C F L R C C K E G D R V F L
9001 **TACAAGTGGAG**gtaataactgctactgcgtgagttcatgtacacatagttagatttaaca 9060
Q V E
9061 tgcatcgacctgacttttgctctaaagtgaccaacaggttgacacttttggctttcctg 9120
9121 aaatttaaaaccaaactgttacatggactaccatttggcagctgaaaaggctcatgaata 9180
9181 cttggacacagacaacatcacttgaatgactcaatctcgtcgactaactgaagtgaaaat 9240
9241 aatctttgtttggctgagcggcaatactcacaaacatgggcacatgctacggctagcatc 9300
9301 catttagcgggtcaaagatcagcagcacttgtttggatgcagtttctctcatgagtatct 9360
9361 gttgaaagagcggcacaagataaagagggaagtagttactgtcagaaacaaaggaagagt 9420
9421 ccttttctcttatgtttgcattctttaaggtcacagaatgtcgtgaaaacggtcctcgtc 9480
9481 ccatttaatgtactgcacaacagcatgtgtctctctatcaggcgatatccatggtttatt 9540
9541 actatttaggttcggacaagtgcatttggtgaagaattaggatctacatatcatttaaaa 9600
9601 cccaaagtgtaggattgggaacttgatctgggatttcagctacttgtcagaaatgactcg 9660
9661 ctccaacctctgaaaaatatataatgtcattaagtgttaagtggcaagtctccagtcatg 9720
9721 ctctgtgtggctgtacgtaagcacagcgctggttttagctaattgctcacataatgcttg 9780
9781 cttgttaatgtttgcaggtataatgtttactcaccatcttgctgatgatacttacagtgc 9840
9841 atacttttactgaagtaaggttttgaatgtaggacattgctaatatttgttaataagcac 9900
9901 taaacacaaagttatgcggaggctgatgggaatgtcatgagttattatgcaggtattcgg 9960
9961 tcaccgcctttctgccaggatgttaaagagccacctgtcctcttcatgacggatgtccac 10020
10021 atctttgttgttgctgcag**ACTTGCGAGAAGCAGAGGTTGAAGAAGATCTCCAAGAACGA** 10080
T C E K Q R L K K I S K N D
10081 **CGAGGGCGCCCTCTCCTTCGTCTTCTACATGAAGGCCGGGGGGACCAAACATCGGACGTT** 10140
E G A L S F V F Y M K A G G T K H R T F
10141 **TGAGTCAGCGCTGCACGGCGGCTGGTTCATCCAAATAGACACCACCGATTTAGTGGCCAT** 10200
E S A L H G G W F I Q I D T T D L V A M
10201 **GGCAACCCTGGATGGAGGGACGGGGAACGAATCGTTCCTCTTCGTCATTCAGACTTAAAA** 10258
A T L D G G T G N E S F L F V I Q T*
10261 GTTTACCATTCAAATTCACGTGCCGGAAAGACAAACATGAGAGGAGTTCTTTAGTTTGAC 10320
10321 CCACCTGGGCCTGTGACAGAAAAAACACGTCACTGTGTCAAATTCTGTTATTGCAGAAGT 10380
10381 GTGTAGATATGTATCATACAACTAGATCTAATTAAAAAATGTTTTGTGTGCGTGTAAGCA 10440
10441 TGTAATCTATTTTGTTGTTTATGGTGACCTTTCAAACTGATTGTTG 10486

Supplemental Figure 8

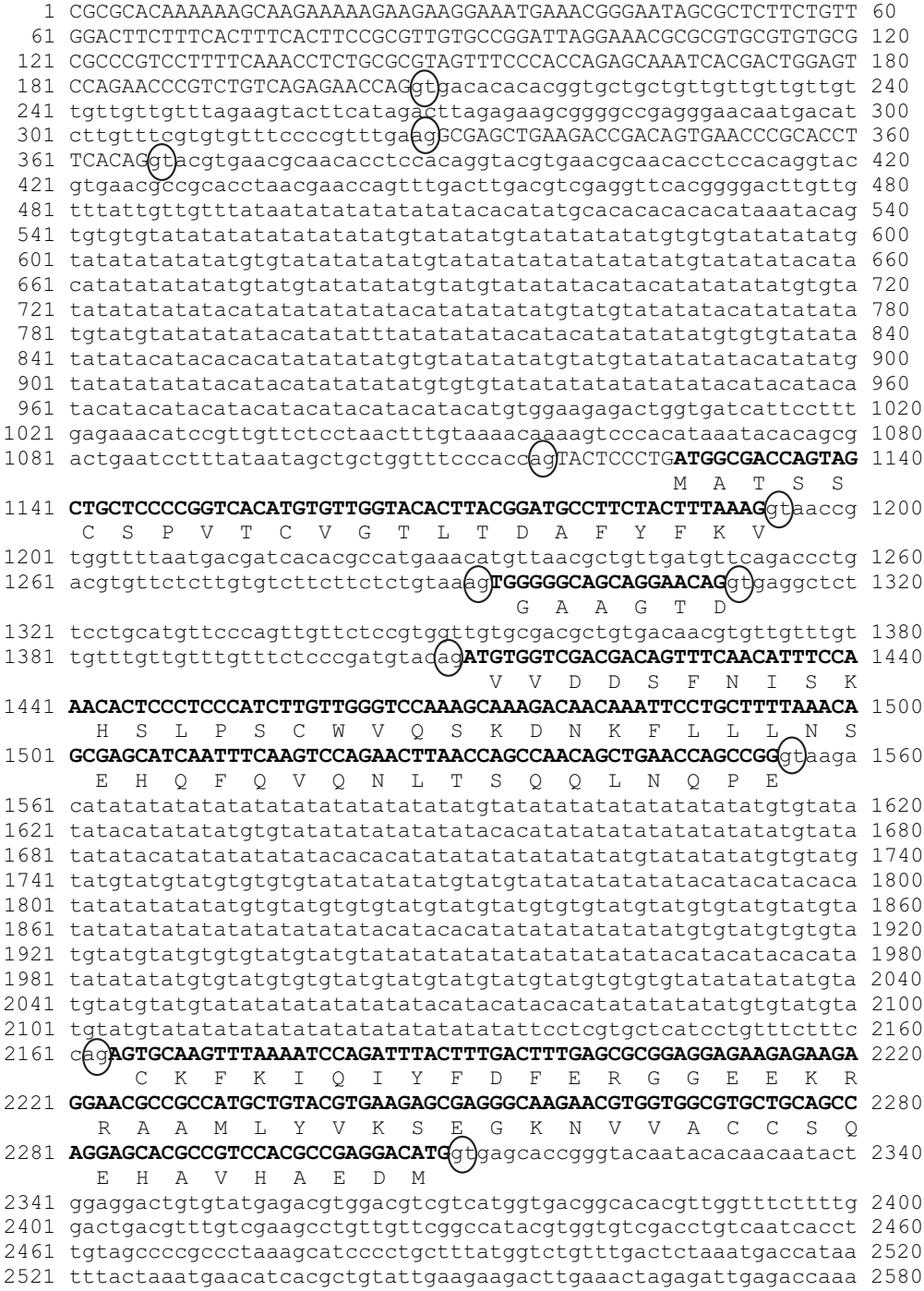

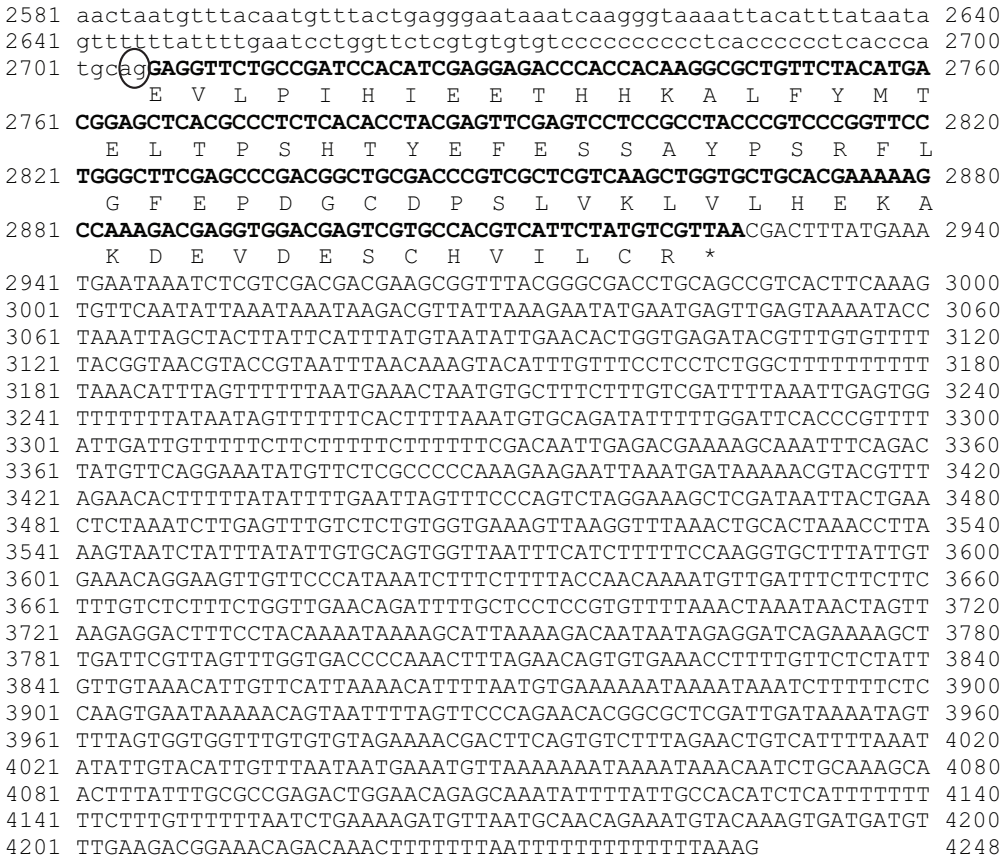

Supplemental Figure 7

```
   1 GTGTGTGTGTGTGGGTGTGCGTGTGTGTGTGTGTGtgtgtgtgtgagcgtgtgagcat  60
  61 gtgtgtgtgtgtgtgtgagcgtgtgtgtgtgtgtgtgagcgtgtgtgtgtgtgtgtgt 120
 121 gtgtgtgtgagggtgtgtgtgtgtgtgagcgtgtgtgtgtgtgtgtgagcgtgtgtgagc 180
 181 gtgtgtgtgtgtgtgtgtgtgtgtgtgtgtgtgtgtgtgtgtgagcgtgtgtgtgtgt 240
 241 gtgtgtgagcgtgtgagtgtgtgtgtgtgtgtgtgtgagcgtgtgtgtgtgtgtgtgt 300
 301 gtgtgtgtgtgtgtgtgagcgtgtgtgtgtgtgtgtgagcgtgtgtgtgtgtgtgtgagcgt 360
 361 gtgtgtgtgtgtgagcgtgtgtgtgtgtgagcgtgtgtgtgtgtgtgtgtgtgtgtgt 420
 421 gtgagcgtgtgtgtgtgtgtgtgtgagcgtgtgagCGGGTGTGCGTGCGTGTGTGTGAGC 480
 481 GTGTGTGTGTTTGTAGCCACAACCTACTACCAGGAAGCAGAGAAGCAAAGAAAAGAGTCG 540
 541 CTCAGTGAACTTCTCTCAACACACGATGAGCGACTTTGATCTGTCTCAAGCGTTAAAGAG 600
 601 gtgagttgttcatataactataattatatacttatttatacaattatataattatataac 660
 661 tatatcattaaataattatatttaaaacaggagacacattttaatgacgtgaaactgaat 720
 721 acttagaaagatactttgtagctgaacgtctcactttatactacatctcagaggtacttt 780
 781 atagaggtactttataccacatctaagaggtactttatactacatctaagaggtacttta 840
 841 tactacatctcagaggtactttatactacatctaagaggtactttataccacatctcaga 900
 901 ggtactttatactacatctaagaggtacttcataccacatctcagaggtactttatacta 960
 961 catctaagaggtactttataccacatctaagaggtactttatactacatctaagaggtac 1020
1021 tttataccacatctcagaggtactttataccacatctaagaggtactttatagaggtact 1080
1081 ttataccacatctaagaggtactttatactacatctcagaggtactttataccacatctc 1140
1141 agaggtactttataccacatctcagaggtactttataccacatctaagaggtactttata 1200
1201 ccacatctaagaggtactttataccacatctaacaggtactttataccacatctaagagg 1260
1261 tactttataccacatctcagaggtactttataccacatctaagaggtactttataccaca 1320
1321 tctcagaggtactttatactacatctaagaggtactttataccacatctaagaggtactt 1380
1381 tatagaggtactttataccacatctaagaggtactttatactacatctcagaggtacttt 1440
1441 ataccacatctaagaggtactttatataggtactttataccacatctaagaggtacttta 1500
1501 taccacatctaagaggtactttatactacatctcagaggtactttataccacatctaaga 1560
1561 ggtactttatagaggtactttataccacatctaagaggtactttataccacatctaagag 1620
1621 gtactttatacctacatctcagaggtactttataccacatctaagaggtactttatacca 1680
1681 catccaagaggtactttataccacatctcagaggtactttatactacatctcagaggtac 1740
1741 tttataccacatctcagaggtactttataccacatctaagaggtactttataccacatct 1800
1801 cagaggtactttataccacatctcagaggtactttataccacatctaagaggtactttat 1860
1861 agaggtactttataccacatctaagaggtactttatactacatctcagaggtactttata 1920
1921 ccacatctaagaggtactttatagaggtactttataccacatctaagaggtactttatac 1980
1981 tacatctaacaggtactttataccacatctaagaggtactttatactacatctaacaggt 2040
2041 actttataccacatctaagaggtactttataccacatctaagaggtactttataccacat 2100
2101 ctcagaggtactttatacgacatctcagaggtactttatactacatctcagaggtacttt 2160
2161 atactacatctcagaggtactttatactacatctcagaggtactttataccacatctaag 2220
2221 aggtactttatagaggtactttataccacatctaagaggtactttgtactacatctcaga 2280
2281 ggtactttataccacatctaagaggtactttatagaggtactttataccacatctaagag 2340
2341 gtactttataccacatctaagaggtactttatactacatctcagaggtactttataccac 2400
2401 atctaagaggtactttataccacatctaagaggtactttataccacatctcagaggtact 2460
2461 ttatactacatctcagaggtactttataccacatctcagaggtactttataccacatcta 2520
2521 agaggtactttataccacatctcagaggtactttataccacatctcagaggtactttata 2580
2581 ccacatctaagaggtactttatagaggtactttataccacatctaagaggtactttatac 2640
2641 tacatctcagaggtactttataccacatctaagaggtactttatagaggtactttatacc 2700
2701 acatctaagaggtactttataccacatctaagaggtactttatactacatctcagaggta 2760
2761 ctttataaccacatctaagaggtactttatagaggtactttatactacatctcagaggta 2820
2821 ctttataccacatataagaggtactttatagaggtactttataccacatctaagaggtac 2880
2881 tttatactacatctaacaggtactttatacgacatctcagaggtactttatactacatct 2940
2941 cagaggtactttataccacatctcagaggtactttatactacatctcagaggtactttat 3000
3001 actacatctcagaggtactttataccacatctaagaggtactttataccacatctaagag 3060
3061 gtactttatactacatctcagaggtactttataccacatctaagaggtactttatagagg 3120
3121 tactttataccacatctaagaggtactttatactacatctcagaggtactttataccaca 3180
3181 tctaagaggtactttatactacatctaacaggtactttataccacatctaagaggtactt 3240
```

3241 tataccacatctaagaggtactttataccacatctcagaggtactttatactacatctca 3300
3301 gaggtactttatactacatctcagaggtactttataccacatctcagaggtactttatac 3360
3361 cacatctaagaggtactttataccacatctaagaggtactttataccacatctcagaggt 3420
3421 actttatacgacatctcagaggtactttataccacatctcagaggtactttatactacat 3480
3481 ctcagaggtactttatactacatctcagaggtactttataccacatctaagaggtacttt 3540
3541 atagaggtactttataccacatctaagaggtactttatactacatctcagaggtacttta 3600
3601 taccacatctaagaggtactttatactacatctaacaggtactttataccacatctaaga 3660
3661 ggtactttataccacatctaagaggtactttataccacatctcagaggtactttatacta 3720
3721 catctcagaggtactttatactacatctcagaggtactttataccacatctcagaggtac 3780
3781 tttataccacatctaagaggtactttataccacatctaagaggtactttataccacatct 3840
3841 cagaggtactttataccacatctaagaggtactttatactacatctcagaggtactttat 3900
3901 accacatctcagaggtactttataccacatctcagaggtactttataccacatctaagag 3960
3961 gtactttataccacatctaagaggtactttataccacatctaacaggtactttataccac 4020
4021 atctaagaggtactttataccacatctcagaggtactttataccacatctaagaggtact 4080
4081 ttataccacatctcagaggtactttatactacatctaagaggtactttataccacatcta 4140
4141 agaggtactttatagaggtactttataccacatctaagaggtactttatactacatctca 4200
4201 gaggtactttatactacatctaacaggtactttataccacatctaagaggtactttatat 4260
4261 aggtactttataccacatctaagaggtactttataccacatctaagaggtactttatact 4320
4321 acatctcagaggtactttataccacatctaagaggtactttatagaggtactttatacca 4380
4381 catctaagaggtactttataccacatctaagaggtactttataccacatctcaagaggta 4440
4441 ctttataccacatctaagaggtactttataccacatctaagaggtactttataccacatc 4500
4501 tcagaggtactttatactacatctcagaggtactttataccacatctcagaggtacttta 4560
4561 taccacatctaagaggtactttatagaggtactttataccacatctaagaggtactttat 4620
4621 accacatctaagaggtactttataccacatctcagaggtactttataccacatctaagag 4680
4681 gtactttatagaggtactttataccacatctaagaggtactttataccacatctaagagg 4740
4741 tactttatactacatctcagaggtactttataccacatctaagaggtactttatagaggt 4800
4801 actttatactacatctcagaggtactttataccacatctaagaggtactttatagaggta 4860
4861 ctttataccacatctaagaggtactttatactacatctaacaggtactttatacgacatc 4920
4921 tcagaggtactttatactacatctcagaggtactttataccacatctcagaggtacttta 4980
4981 tactacatctcagaggtactttatactacatctcagaggtactttataccacatctaaga 5040
5041 ggtactttataccacatctaagaggtactttatactacatctcagaggtactttatacca 5100
5101 catctaagaggtactttatagaggtactttataccacatctaagaggtactttatactac 5160
5161 atctcagaggtactttataccacatctaagaggtactttatactacatctaacaggtact 5220
5221 ttataccacatctaagaggtactttataccacatctaagaggtactttataccacatctc 5280
5281 agaggtactttatactacatctcagaggtactttatactacatctcagaggtactttata 5340
5341 ccacatctcagaggtactttataccacatctaagaggtactttataccacatctaagagg 5400
5401 tactttataccacatctcagaggtactttatacgacatctcagaggtactttataccaca 5460
5461 tctcagaggtactttatactacatctcagaggtactttataccacatctcagaggtacat 5520
5521 atagtactttaaacagtactacatatcagaggtacatgtagtactttattcagtactcca 5580
5581 tatcagaggtacatatagtactttatacagtactacatctcagaggtacatatagtactt 5640
5701 tatacagtactacattcatgtatttgttttaaatccatatgttgtgtatttcagATGAGA 5760
5761 CACG**ATGCTTCAACATGACG**gtgagaatctgaaagatataattcacttaattcacttcct 5820
M L Q H D E
5821 ctccagtattttcactctcatattcaacagtttcacactcatgtactctttcagatgtgt 5880
5881 gtgagaagagaatgtgtgtgtgtgtgtgtgtgtgtgtgtgtgtgtgtgagaagagaatgt 5940
5941 gtgtgtgtgtgtgtgagaagagaatgtgtgtgtgtgtgtgtgtgtgtgtgtgtgtgtgtg 6000
6001 agaagagaatgtgtgtgtgtgtgtgtgtgtgtgtgagaagagaatgtgtgtgtgtgtgtg 6060
6061 tgtgtgtgtgtgtgtgtgtgtgtgtgtgtgtgagaagagaatgtgtgtgtgtgtgaga 6120
6121 agagaatgtgtgtgtgtgtgtgtgagaagagaatgtgtgtgtgtgtgtgtgtgtgt 6180
6181 gtgtgtgagaagagaatgtgtccgtcccttcatctctccgtccctccatccctccatctc 6240
6241 atcatctctccatctcatcatctctccgttttccatctctccatcccttcatctctccgt 6300
6301 ctctccatccctccatctcatcatctctccgtctctccatctcatcatctctccatctca 6360
6361 tcatctctccgtctctccatctcttcatctctccgtctctccatctctccgtctctccat 6420

```
6421 ctcatcatctctccgtctctccatctcatcatctctccgtctctccatctctccatccct 6480
6481 tcatcgctccgtctctccatctctccgtcccttcatctctctgtccctccatccctccat 6540
6541 ctcatcatctctccgtccctccatccctccatctcatcatctctccatctcaccatctct 6600
6601 ccgtccctccatccctccatctcatcatctctccatctcatcatctctccgtctctccat 6660
6661 ctcatcatctctccatctcatcatctctccgtctctccatctcatcatctctccatctct 6720
6721 ccatcccttcatctctccgtctctccatctctccgtcccttcatctctctgtccctccat 6780
6781 ccctccatctcatcatctctccgtccctccatccctccatctcatcatctctccatctca 6840
6841 tcatctctccgtttttccatctctccatcccttcatctctccgtctctccatccctccat 6900
6901 ctcatcatctctccgtctctccatctcatcatctctccatctcatcatctctccgtctct 6960
6961 ccatctcatcatctctccgtctctccatctctccatcccttcatctctccgtctctccat 7020
7021 ctctccatcccttcatctctctgtccctccatccctccatctcatcatctctccgtccct 7080
7081 ccatccctccatctcatcatctctccatcccttcatctctccgtctctccatctctccgt 7140
7141 cccttcatctctccgtccctccatccctccacag|AAACCGTCGTCACGGCGACACAGAAC 7200
                                        T  V  V  T  A  T  Q  N
7201 TGGTCCACGAGCGTGGGGAGGACGTTTCAGCGTTTCAACAGCGAAGAAGTCGTCACTCTG 7260
     W  S  T  S  V  G  R  T  F  Q  R  F  N  S  E  E  V  V  T  L
7261 TGCGACTTCTCCCAGAAGGACGTGGTCCTGGCTGCAGGAGACCTGAAGCTGAAGGCCGTC 7320
     C  D  F  S  Q  K  D  V  V  L  A  A  G  D  L  K  L  K  A  V
7321 ATCCTGAAGGGAGGAAGCTGTGAGCGCAGAG|gtaccgcggaccgggcgagaagtacttca 7380
     I  L  K  G  G  S  C  E  R  R  V
7381 ccgagtactttcagggtgtacctgtacttgtacttgtagatttgatactttgtacccggt 7440
7441 agtatacaaagtatctcaaattggctctaaatgtatgacctttaacatcaaaatactctc 7500
7501 atgtgaatctattagtcataacaacgtaaacatataatattctataataataaaacacag 7560
7561 tattacattaattgaagtacatttcactaatattactacttttacttttactgtacatttt 7620
7621 gaatgcaggactggttgtgagaaacaataatgaaataatgaacttcccctctcttcttct 7680
7681 ccccgtcag|TGACCTTCCAACTGGCGAGGTACCTGAACTCCGGCGTCTCCCGTGGCGACG 7740
                T  F  Q  L  A  R  Y  L  N  S  G  V  S  R  G  D  G
7741 GCCTGGTGGTGGTGCTGTCCGTCACCGGCAGCCGGCACATCTCCTGCTGCATGCAGGGGG 7800
       L  V  V  V  L  S  V  T  G  S  R  H  I  S  C  C  M  Q  G  G
7801 GGCGGGCGCTGCTGGAGCTGGAG|gtgaagctgctggaggctcctgatggggttatagtgc 7860
       R  A  L  L  E  L  E
7861 attaaaatacaacgctgggactttaatagcatacatttatttatttttatctcgtaattg 7920
7921 taacttttatctcttgattattatcgttaaacgaataattctgactttaatctcacaatt 7980
7981 ctttttttttacctaataattctgaagttttatcgaataattctaattctaatctaataa 8040
8041 ttataatgttcttctcatcattttgacctctgatataatactttatacttttccttgtaa 8100
8101 agtgtacttttagagtcagatttaactactaattttgacctttttatctaatatttccat 8160
8161 cttttatctcataatgttgacctttaatctaataatttagacttttttatctcttaattca 8220
8221 tacttttatctcttaattattatcgtttaatgaataattcagactttaatctcataattc 8280
8281 tttttttacctaataattctgacgttttatcgaataattctaatctaataattataatg 8340
8341 ttcttctcatcattttgacctctaatataatactttatacttttccttgtaaagttttta 8400
8401 gaatctgatttaactcctaattttgacctttttatctaatatttccatcttttatctcata 8460
8461 atgttgacctttaatctaataatgtagacttcttatctcataattcatacttatccttat 8520
8521 acattttacttgttatcatgaatctgaaacaactaatgtgtaatagttgactttaaatca 8580
8581 tgattaacttttaatatattattatttcgccccccctccttttttgttttttactgttaaa 8640
8641 actctactttcattgtcgtggcag|GAATGCAGCAAACAAAAGCTGCAGAACATCAGCGAC 8700
                              E  C  S  K  Q  K  L  Q  N  I  S  D
8701 CACGAGGACATGGACCGCTTCCTGTTCTTCAAGAGGACCGTGGGCTTCTCCCTGAACACC 8760
     H  E  D  M  D  R  F  L  F  F  K  R  T  V  G  F  S  L  N  T
8761 TTCGAGTCCCTGAAGCACCCCGGATGGTTCATCAGCACCTCGGACCAGGACCAGGACGAG 8820
     F  E  S  L  K  H  P  G  W  F  I  S  T  S  D  Q  D  Q  D  E
8821 TCCATGGAGATGTGCAGGGTGGACGACGCACGCCGCCTCATCTCCTTCAAGATGATCTAA 8880
     S  M  E  M  C  R  V  D  D  A  R  R  L  I  S  F  K  M  I  *
8881 AAACACACTTTAGTGCAGCTTGAAGGTTTCCATTATGATGCTGAGCTGTTCCCTGCCTCG 8940
8941 CCACCAGATGGCGCCGTTGTCTGTTAATGATGGAGCAAGAATCCATTAAAAATGTGTTGT 9000
```

```
9001 TGTTTTTTTTTACTCACTGATGTTTTCTCCTTTGAAAGAGAAAGTTGTAACAGGATATTC 9060
9061 CTCAAAAAGTTTTTCGTTTATTATTCTGAATAAAGTTGTATTTTTAGAACCAGGCTTGAA 9120
9121 AGTGTACTATACGTATAATTAACACAAATTTTATTGTGTTTTATTGTTATTTATTTTAGG 9180
9181 TGTGTTTATGTAAGTATTTTGTGTTTCCACGAAGAATAAGAATGGCATGTTAATCCTTGT 9240
9241 TTTTACAAATTATAGTTGTAACAAATTCTCACACCGATGCAAATTATGTTATAACTATTA 9300
9301 AAATGACTCTCTAAAAAAA                                          9319
```

Supplemental Figure 9

Supplemental Table 1. Ct-values of RPS20 in selected tissues and leukocytes.

Sample	Individual	Replicate	CT value
HKL (non-stimulated)	1	1	24.75
	1	2	24.70
	1	3	24.70
	2	1	25.15
	2	2	25.06
	2	3	25.06
	3	1	23.19
	3	2	23.16
HKL (stimulated with CpG)	1	1	23.94
	1	2	23.84
	1	3	23.86
	2	1	24.88
	2	2	24.89
	2	3	24.87
	3	1	23.30
	3	2	23.33
	3	3	23.33
Skin mucus	1	1	26.71
	1	2	26.86
	1	3	26.75
	2	1	26.50
	2	2	26.54
	2	3	26.32
	3	1	26.50
	3	2	26.64
	3	3	26.40
Head kidney	1	1	25.19
	1	2	25.40
	1	3	25.36
	2	1	25.50
	2	2	25.73
	2	3	25.75
	3	1	26.16
	3	2	26.19
	3	3	26.12
Brain	1	1	26.83
	1	2	27.01
	1	3	26.98
	2	1	26.95
	2	2	27.09
	2	3	26.99
	3	1	26.42
	3	2	26.44
	3	3	26.38

Supplemental Table 2. NFκB signaling pathway components identified in lumpfish, including DEG values upon bacterial exposure.

Box name	Pathway name	Kegg annotation	Annotation	Log2 fold change 6h	Log2fold change 24h
IL1β	Interleukin 1 beta	K04519	IL1B	6.7	8.3
IL-8	Interleukin-8	K10030	IL-8	6.4	6.7
TNFα	Tumor necrosis factor superfamily. member 2	K03156	TNFA	4.4	4.9
COX2	Prostaglandin-endoperoxide synthase 2	K11987	PGH2	2.2	4.5
IL1R	Interleukin-1 receptor type 2	K04387	IL1R2	2.1	4.2
LBP/BPI	Lipopolysaccharide-binding protein	K05399	BPI	1.2	3.7
TNFAIP3a	Tumor necrosis factor. alpha-induced protein 3	K11859	T.P3	2.9	3.5
NFκβ2	Nuclear factor NF-kappa-B light polypeptide gene enhancer in B-cells 2	K04469	NFKB2	3.2	3.4
IL1R1	Interleukin 1 receptor type 1	K04387	IL1R1	0.0	2.4
BIRC2_3	Baculoviral IAP repeat-containing protein 2/3	K16060	BIR	1.3	2.1
BIRC2_3	Baculoviral IAP repeat-containing protein 2/3	K16060	PIAP	1.2	2.0
NIK	Mitogen-activated protein kinase kinase kinase 14	K04466	M3K14	1.2	1.9
CD40	Tumor necrosis factor receptor superfamily member 5	K03160	CD40	2.1	1.7
CCL4	C-C motif chemokine 4	K12964	CCL4	1.6	1.7
NFκBIα	NF-kappa-B inhibitor alpha	K04734	IKBA	2.6	1.5
IL1R	Interleukin 1 receptor type 1	K04386	IL1R2	0.0	1.3
TRAF3	TNF receptor-associated factor 3	K03174	TRAF3	0.8	1.2
IKKα	Inhibitor of nuclear factor kappa-B kinase subunit alpha	K04467	IKKA	0.0	1.2
RIP1	Receptor-interacting serine/threonine-protein kinase 1	K02861	RIPK1	0.0	1.2
IRAK1&4	Interleukin-1 receptor-associated kinase 1	K04733	IRAK4	0.4	1.1
Syk	Spleen tyrosine kinase	K05855	KSYK	-0.7	1.1
TAB	TAK1-binding protein 1	K04403	TAB1	0.0	1.0
IL1R	Interleukin 1 receptor type 1	K04386	IL1RAcP	0.0	0.9
ERC1	ELKS/RAB6-interacting/CAST family member 1	K16072	RB6I2	0.3	0.8
RELA	Transcription factor p65	K04735	REL	0.5	0.8
CFLAR	CASP8 and FADD-like apoptosis regulator	K04724	CFLAR	0.4	0.8

RELA	Transcription factor p65	K04735	TF65	0.6	0.7
TRIM25	Tripartite motif-containing protein 25	K10652	TRIM8	0.0	0.7
BCL10	B-cell CLL/lymphoma 10	K07368	BCL10	0.0	0.6
CK2	Casein kinase II subunit beta	K03115	CSK2B	0.3	0.6
RELB	Transcription factor RelB	K09253	RELB	0.9	0.5
TRADD	Tumor necrosis factor receptor type 1-associated DEATH domain protein	K03171	TRADD	0.0	0.5
PLCγ1	Phosphatidylinositol phospholipase C. gamma-1	K01116	PLCG1	0.0	0.5
TAB	TAK1-binding protein 3	K12793	TAB3	0.0	0.5
Lyn	Tyrosine-protein kinase Lyn	K05854	LYN	-0.6	0.3
PLCγ2	Phosphatidylinositol phospholipase C. gamma-2	K05859	PLCG2	0.0	0.3
TNFAIP3b	Tumor necrosis factor. alpha-induced protein 3	K11859	ZRAN1	0.0	0.3
CK2	Casein kinase II subunit alpha	K03097	CSK21	0.0	0.3
CK2	Casein kinase II subunit alpha	K03097	CSK22	0.0	0.2
NEMO	Inhibitor of nuclear factor kappa-B kinase subunit gamma	K07210	SPS2	0.0	0.0
MALT1	Mucosa-associated lymphoid tissue lymphoma translocation protein 1	K07369	MALT1	-0.4	0.0
ATM	Serine-protein kinase ATM	K04728	ATM	0.0	0.0
BCL2	Apoptosis regulator Bcl-2	K02161	BCL2	0.0	0.0
BCR	Immunoglobulin heavy chain	K06856	HVM63	0.0	0.0
BIRC4	E3 ubiquitin-protein ligase XIAP	K04725	XIAP	2.4	0.0
CXCL12	C-X-C motif chemokine 12	K10031	SDF1	0.0	0.0
IL1R	Interleukin 1 receptor type 1	K04386	IL1RAcP	0.0	0.0
NEMO	Inhibitor of nuclear factor kappa-B kinase subunit gamma	K07210	OPTN	-0.4	0.0
NFκB	Nuclear factor NF-kappa-B p105 subunit	K02580	NFKB1	0.0	0.0
NFκB2	Nuclear factor NF-kappa-B light polypeptide gene enhancer in B-cells 2	K04469	DHE3	0.6	0.0
TAB	TAK1-binding protein 2	K04404	TAB2	0.0	0.0
TAK1	Mitogen-activated protein kinase kinase kinase 7	K04427	M3K7	-0.3	0.0
TCR	T-cell receptor beta chain V region	K10785	TVB4	0.0	0.0
TNFSF14	Tumor necrosis factor receptor superfamily member 14	K05477	TNF14	0.1	0.0
TNFβ	Tumor necrosis factor superfamily. member 2	K03156	TNFB	0.0	0.0
TRAF5	TNF receptor-associated factor 5	K09849	TRAF5	0.0	0.0

TRIM25	Tripartite motif-containing protein 25	K10652	STXA	0.0	0.0
TRAF6	TNF receptor-associated factor 6	K03175	TRAF6	0.0	0.0
BCR	Immunoglobulin heavy chain	K06856	HV02	0.0	0.0
UBE2I	Ubiquitin-conjugating enzyme E2 I	K10577	UBC9	-0.2	0.0
BCR	Immunoglobulin heavy chain	K06856	HV303	-0.1	-0.1
ERC1	ELKS/RAB6-interacting/CAST family member 1	K16072	ERC2	0.2	-0.1
TRAF2	TNF receptor-associated factor 2	K03173	TRAF2	-0.3	-0.2
BCL2L1	Bcl-2-like 1 (apoptosis regulator Bcl-X)	K04570	B2CL1	-0.3	-0.2
TRIM25	Tripartite motif-containing protein 25	K10652	TRI25	-1.0	-0.3
TRIM25	Tripartite motif-containing protein 25	K10652	TRI16	-0.3	-0.6
IL8	Interleukin 8-like	K10030	IL8like	1.4	-0.6
NFκB2	Nuclear factor NF-kappa-B light polypeptide gene enhancer in B-cells 2	K04469	FA35A	0.4	-0.6
TCR	T-cell receptor alpha chain V region	K10784	TVA3	0.0	-0.6
PKCβ	classical protein kinase C beta type	K19662	KPCB	0.0	-0.7
TCR	T-cell receptor beta chain V region	K10785	TRBC2	0.0	-0.7
LBP/BPI	Lipopolysaccharide-binding protein	K05399	LBP	0.0	-0.8
TIRAP	Toll-interleukin 1 receptor (TIR) domain-containing adaptor protein	K05403	TIRAP	-1.2	-0.9
TNFSF13B	Tumor necrosis factor receptor superfamily member 13B	K05476	TN13B	0.0	-0.9
TRIM25	Tripartite motif-containing protein 25	K10652	TRI29	-0.8	-1.0
PIDD	Leucine-rich repeats and death domain-containing protein	K10130	PIDD1	-0.4	-1.1
TNF-R1	Tumor necrosis factor receptor superfamily member 1A	K03158	TNR1A	-2.5	-1.1
PKCθ	Novel protein kinase C theta type	K18052	KPCT	0.0	-1.2
Lck	Lymphocyte cell-specific protein tyrosine kinase	K05856	BLK	1.0	-1.3
TRIM25	Tripartite motif-containing protein 25	K10652	TRI39	0.3	-1.3
ZAP	Tyrosine-protein kinase ZAP70	K07360	ZAP70	0.0	-1.5
Zap	Bruton agammaglobulinemia tyrosine kinase	K07370	BTK	0.0	-1.5
Lck	Lymphocyte cell-specific protein tyrosine kinase	K05856	LCK	0.0	-1.6
CARD10	Caspase recruitment domain-containing protein 11	K07367	CAR11	0.0	-1.7
TNFAIP3c	Tumor necrosis factor. alpha-induced protein 3	K11859	OTU7A	0.0	-2.6
TNFR3	Lymphotoxin beta receptor TNFR superfamily member 3	K03159	TNFR3	-2.3	-4.3

CD40	Tumor necrosis factor receptor superfamily member 5	K03160	CD40	0.0	-5.0
TNFRSF11A	Tumor necrosis factor receptor superfamily member 11A	K05147	TNR11	0.0	-6.4

Supplemental Table 3. MAPK signaling pathway components identified in lumpfish, including DEG values upon bacterial exposure.

Box name	Pathway name	Kegg identifier	Annotation	LogFC 6hpe	LogFC 24hpe
IL1β	Interleukin 1 beta	K04519	IL1B	6.7	8.3
TNFα	Tumor necrosis factor	K03156	TNFA	4.4	4.9
IL1R	Interleukin 2 receptor	K04387	IL1R2	2.1	4.2
BDNF	Brain-derived neurotrophic factor	K04355	BDNF	0.0	4.2
NFAT4	Nuclear factor of activated T-cells. cytoplasmic 3	K17333	NFAT5	2.2	4.1
SRF	Serum response factor	K04378	NA	0.0	3.5
MKP	Dual specificity MAP kinase phosphatase	K04459	DUS1	2.0	2.9
FLNA	Filamin	K04437	FLNB	0.0	2.8
MKP	Dual specificity MAP kinase phosphatase	K04459	DUS2	3.6	2.6
IL1R	Interleukin 1 receptor	K04386	IL1R1	0.0	2.4
HSP72	Heat shock 70kDa protein 1/2/6/8	K03283	HSP71	0.9	2.4
G12	Guanine nucleotide-binding protein subunit alpha-12	K04347	GBG12	0.7	2.3
NFκB	Nuclear factor of kappa light polypeptide gene enhancer in B-cells 2	K04469	NFKB2	0.9	2.3
RasGRP	RAS guanyl-releasing protein 1. 2. 3 and 4	K04350	GRP4	1.7	2.3
CACN	Voltage-dependent calcium channel beta-4	K04865	CACB4	2.9	2.2
RAC. CDC42	RAS-related C3 botulinum toxin substrate 3	K04393	RHOU	0.0	2.1
MAPK1/3	Mitogen-activated protein kinase 1/3	K04371	MK15	-0.1	1.9
MAP3K14	Mitogen-activated protein kinase kinase kinase 14	K04466	M3K14	1.2	1.9
AKT	RAC serine/threonine-protein kinase	K04456	AKT3	0.0	1.6
FGF	Fibroblast growth factor	K04358	FG17	0.0	1.6
RPS6KA5	Ribosomal protein S6 kinase alpha-5	K04445	KS6A4	0.3	1.4
MKP	Dual specificity MAP kinase phosphatase	K04459	DUS6	0.0	1.4
JUND	Transcription factor jun-D	K04449	JUND	2.7	1.3
IL1R	Interleukin 1 receptor	K04386	IL1R2	0.0	1.3
PAK1&2	p21-activated kinase 1&2	K04409	ZN282	0.0	1.3
MKP	Dual specificity MAP kinase phosphatase	K04459	DUS8	0.0	1.2
CPLA2	cytosolic phospholipase A2	K16342	PA24F	0.0	1.2

PAK1&2	p21-activated kinase 1&2	K04409	ZN423	0.0	1.2
IKKA	Inhibitor of nuclear factor kappa-B kinase subunit alpha	K04467	IKKA	0.0	1.2
NR4A1	Nuclear receptor subfamily 4 group A member 1	K04465	NR4A1	3.3	1.2
JUN	Transcription factor AP-1	K04448	JUN	1.6	1.2
FGF	Fibroblast growth factor	K04358	FGF7	0.0	1.2
PTPRR	Receptor-type tyrosine-protein phosphatase R	K04458	PTPRR	0.0	1.2
PTPRR	Dual specificity phosphatase 3	K18019	PTN7	-0.9	1.2
GADD45	Growth arrest and DNA-damage-inducible protein	K04402	GA45G	1.6	1.1
MAPKAPK2.3&4	Mitogen-activated protein kinase.activated protein kinase 2 and 3	K04443	MAPK2	0.4	1.1
TAB1	TAK1-binding protein 1	K04403	TAB1	0.0	1.0
MKP	Dual specificity MAP kinase phosphatase	K04459	DUS16	0.5	1.0
CASP	Caspase	K02187	CASP3	0.0	1.0
MAP3K2	Mitogen-activated protein kinase kinase kinase 2	K04421	NA	0.0	1.0
IL1R1	Interleukin 1 receptor	K04386	IL1RAcP	0.0	0.9
MAP3K13	Mitogen-activated protein kinase kinase kinase 13	K04422	M3K13	1.0	0.9
TNFSF6	Tumor necrosis factor ligand superfamily member 6	K04389	TNFL6	0.0	0.9
MNK1/2	MAP kinase interacting serine/threonine kinase	K04372	MKNK2	1.3	0.9
p38	p38 MAP kinase	K04441	MK14B	0.0	0.9
PAK1&2	p21-activated kinase 1&2	K04409	ZN226	0.0	0.9
CACN	Voltage-dependent calcium channel N type alpha - 1C	K04850	CAC1C	0.0	0.8
MNK1/2	MAP kinase interacting serine/threonine kinase	K04372	MOB3C	0.7	0.8
NFκβ	Transcription factor p65	K04735	REL	0.5	0.8
RAP1	RAS-related protein Rap-1A	K04353	RAP2B	-0.7	0.8
STK3&4	Serine/threonine kinase 3	K04412	STK26	0.0	0.8
RAS	GTPase Kras	K07827	RASH	0.0	0.8
DAXX	Death-associated protein 6	K02308	DAXX	0.0	0.8
NFκβ	Nuclear factor kappa beta	K09253	RELB	1.0	0.8
RAP1	RAS-related protein Rap-1B	K07836	RAP2B	1.0	0.8
ARRB	Beta-arrestin	K04439	ARR1	0.0	0.7
STK3&4	Serine/threonine kinase 3	K04412	STK24	0.0	0.7

MAPKAPK2.3&4	Mitogen-activated protein kinase.activated protein kinase 4	K04444	MAPK3	0.0	0.7
NFκβ	Transcription factor p65	K04735	TF65	0.6	0.7
GADD45	Growth arrest and DNA-damage-inducible protein	K04402	GA45A	1.3	0.7
RAC. CDC42	Cell division control protein 42	K04393	CDC42	0.0	0.7
MAP3K2	Mitogen-activated protein kinase kinase kinase 2	K04421	CRYD	-1.0	0.7
P53	Tumor protein p53	K04451	P53	0.4	0.7
PPM1B	Protein phosphatase 1B	K04461	NA	0.0	0.7
ELK-1	ETS domain-containing protein ELK1	K04375	ELK1	0.0	0.6
AKT	RAC serine/threonine-protein kinase	K04456	MAST3	0.3	0.6
NF1	Neurofibromin	K08052	NF1	0.0	0.6
PPP3c	Serine/threonine-protein phosphatase 2B catalytic subunit	K04348	PP2BB	0.0	0.5
JNK	Mitogen-activated protein kinase 8/9/10	K04440	MK09	0.0	0.5
MAP2K5	Mitogen-activated protein kinase kinase 5	K04463	MP2K5	-0.7	0.5
MAP2K1	Mitogen-activated protein kinase kinase 1	K04368	MP2K1	1.4	0.5
NFAT4	Nuclear factor of activated T-cells. cytoplasmic 3	K17333	NFAC3	0.0	0.5
PPP3C	Serine/threonine-protein phosphatase 2B regulatory subunit	K06268	CHP1	-0.4	0.5
STK3&4	Serine/threonine kinase 3	K04411	STK24	0.0	0.5
RafB	B-Raf proto-oncogene serine/threonine-protein kinase	K04365	BRAF	0.0	0.5
NFATC2	Nuclear factor of activated T-cells. cytoplasmic 1	K04446	NFAT5	0.0	0.5
PP1A	Protein phosphatase 1A	K04457	PPM1A	0.0	0.4
MAPKAPK5	Mitogen-activated protein kinase.activated protein kinase 5	K04442	MAPK5	0.0	0.4
NLK	Nemo like kinase	K04468	NLK2	0.0	0.4
AKT	RAC serine/threonine-protein kinase	K04456	AKT2	0.0	0.4
EVI1	Ecotropic virus integration site 1 protein	K04462	ZN236	0.0	0.3
STK3&4	Serine/threonine kinase 3	K04412	STK3	0.0	0.3
ELK-4	ETS domain-containing protein ELK4	K04376	ELK3	0.0	0.3
PPP3c	Serine/threonine-protein phosphatase 2B catalytic subunit	K04348	PP2BC	0.0	0.3
PAK1&2	p21-activated kinase 1&2	K04409	ZN250	0.0	0.3
PAK1&2	p21-activated kinase 1&2	K04409	ZN271	0.0	0.3

JUND	Transcription factor jun-D	K04449	JUN	0.6	0.2
PAK1&2	p21-activated kinase 1&2	K04410	PAK2	-0.2	0.2
RPS6KA	Ribosomal protein S6 kinase alpha-1/2/3/6	K04373	KS6A3	0.0	0.2
AKT	RAC serine/threonine-protein kinase	K04456	AKT1	-0.3	0.2
MAP4K3	Mitogen-activated protein kinase kinase kinase kinase 3	K04406	M4K3	0.1	0.2
TAO	Thousand and one amino acid protein kinase	K04429	TAOK1	0.0	0.2
HSP72	Heat shock 70kDa protein 1/2/6/8	K03283	HSP7C	0.9	0.1
p38	p38 MAP kinase	K04441	MK14A	-0.3	0.1
MAP4K4	Mitogen-activated protein kinase kinase kinase kinase 4	K04407	MINK1	0.0	0.1
PAK1&2	p21-activated kinase 1&2	K04410	NA	0.0	0.1
PKA	Protein kinase A	K04345	KAPCA	0.2	0.1
MAX	Max protein	K04453	MAX	0.0	0.1
IKKA	Inhibitor of nuclear factor kappa-B kinase subunit alpha	K07210	SPS2	0.0	0.0
IL1R	Interleukin 1 receptor	K04386	IL1RAcP	0.0	0.0
PAK1&2	p21-activated kinase 1&2	K04409	PAK1	0.0	0.0
PAK1&2	p21-activated kinase 1&2	K04409	ZG57	-0.2	0.0
MAPK1/3	Mitogen-activated protein kinase 1/3	K04371	MK01	0.0	0.0
RPS6KA5	Ribosomal protein S6 kinase alpha-5	K04445	KS6A5	0.0	0.0
MAPK7	Mitogen-activated protein kinase 7	K04464	MK07	0.0	0.0
TAO	Thousand and one amino acid protein kinase	K04429	TAOK2	0.8	0.0
ARRB	Beta-arrestin	K04439	ARRB1	0.1	0.0
CACN	Voltage-dependent calcium channel N type alpha - 1H	K04855	CAC1H	0.0	0.0
CACN	Voltage-dependent calcium channel T type alpha - 1I	K04856	PPR29	0.0	0.0
CACN	Voltage-dependent calcium channel L tyoe alpha - 1S	K04857	CAC1S	0.0	0.0
CACN	Voltage-dependent calcium channel alpha-2/delta-2	K04859	CA2D2	0.0	0.0
CACN	Voltage-dependent calcium channel alpha-2/delta-4	K04861	NA	0.0	0.0
CACN	Voltage-dependent calcium channel gamma-7	K04872	CCG7	0.0	0.0
CPLA2	cytosolic phospholipase A2	K16342	JMJD7	0.0	0.0

CREB	Cyclic AMP-dependent transcription factor ATF-4	K04374	ATF4	0.1	0.0
CREBP1	Cyclic AMP-dependent transcription factor ATF-2	K04450	ATF2	0.0	0.0
CREBP1	Cyclic AMP-dependent transcription factor ATF-2	K04450	ATF7	0.0	0.0
CRK II	Proto-oncogene C-crk	K04438	CRKL	0.0	0.0
ELK-4	ETS domain-containing protein ELK4	K04376	ELK4	0.0	0.0
ELK-4	ETS domain-containing protein ELK4	K04376	FURIN	0.0	0.0
FGF	Fibroblast growth factor	K04358	FGF19	0.0	0.0
FGF	Fibroblast gowth factor 1	K18496	NFI1L	0.0	0.0
FGFR1	Fibroblast growth factor receptor 2	K05093	PTK7	0.0	0.0
FOS	Proto-oncogene protein c-fos	K04379	FOS	2.6	0.0
GRB2	Growth factor receptor-binding protein 2	K04364	GRB2	-0.4	0.0
HSP72	Heat shock 70kDa protein 1/2/6/8	K03283	GIN1	0.0	0.0
HSP72	Heat shock 70kDa protein 1/2/6/8	K03283	HSP70	0.0	0.0
IKKA	Inhibitor of nuclear factor kappa-B kinase subunit alpha	K07210	OPTN	-0.4	0.0
IL1R1	Interleukin 1 receptor	K04386	IL1R1	0.0	0.0
JIP3	Mitogen-activated protein kinase 8 interacting protein 3	K04436	JIP3	0.0	0.0
MAP2K2	Mitogen-activated protein kinase kinase 2	K04369	MP2K2	-0.4	0.0
MAP2K7	Mitogen-activated protein kinase kinase 4	K04431	MP2K7	-0.3	0.0
MAP3K11	Mitogen-activated protein kinase kinase kinase 11	K04419	M3K11	0.0	0.0
MAP3K11	Mitogen-activated protein kinase kinase kinase 11	K04419	M3KL4	0.0	0.0
MAP3K2	Mitogen-activated protein kinase kinase kinase 2	K04420	M3K19	0.0	0.0
MAP3K7	Mitogen-activated protein kinase kinase kinase 7	K04427	M3K7	-0.3	0.0
MAP3K8	Mitogen-activated protein kinase kinase kinase 8	K04415	M3K8	0.7	0.0
MAP4K1	Mitogen-activated protein kinase kinase kinase kinase 1	K04408	M4K5	0.0	0.0
MAP4K2	Mitogen-activated protein kinase kinase kinase kinase 2	K04414	M4K5	0.0	0.0
MAP4K2	Mitogen-activated protein kinase kinase kinase kinase 2	K04414	RBM41	-0.5	0.0
MAP4K3	Mitogen-activated protein kinase kinase kinase kinase 3	K04406	M4K5	-0.3	0.0
MAPK1/3	Mitogen-activated protein kinase 1/3	K04371	MK03	-0.6	0.0
MAPK1/3	Mitogen-activated protein kinase 1/3	K04371	MK06	0.0	0.0

MAX	Max protein	K04453	NA	0.0	0.0
MKP	Dual specificity MAP kinase phosphatase	K04459	DUS5	0.9	0.0
MKP	Dual specificity protein phosphatases	K20216	S17A5	0.8	0.0
MOS	Proto-oncogene serine/threonine-protein kinase mos	K04367	MOS	0.0	0.0
MYC	Myc proto-oncogene protein	K04377	MYC2	0.0	0.0
NFκβ	Nuclear factor of kappa light polypeptide gene enhancer in B-cells 2	K04469	DHE3	0.6	0.0
NFκβ	Nuclear factor kappa beta	K02580	NFKB1	0.0	0.0
p120GAF	RAS GTPase-activating protein 1	K04352	RASA1	-0.6	0.0
p38	p38 MAP kinase	K04441	MK11	0.3	0.0
p38	p38 MAP kinase	K04441	SELO	0.0	0.0
PAK1&2	p21-activated kinase 1&2	K04409	ZN208	0.0	0.0
PAK1&2	p21-activated kinase 1&2	K04409	ZN234	0.0	0.0
PAK1&2	p21-activated kinase 1&2	K04409	ZN521	0.0	0.0
PAK1&2	p21-activated kinase 1&2	K04409	ZN574	0.0	0.0
PAK1&2	p21-activated kinase 1&2	K04409	ZN793	0.0	0.0
PKA	Protein kinase A	K04345	PRKX	0.0	0.0
PPM1B	Protein phosphatase 1B	K04461	PPM1B	0.0	0.0
PPP5C	Serine/threonine-protein phosphatase 5	K04460	PPP5	-0.5	0.0
RPS6KA	Ribosomal protein S6 kinase alpha-1/2/3/6	K04373	KS6A6	0.4	0.0
RPS6KA	Ribosomal protein S6 kinase alpha-1/2/3/6	K04373	KS6AA	-0.5	0.0
SOS	Son of sevenless	K03099	RGPS1	0.0	0.0
SOS	Son of sevenless	K03099	SOS1	0.0	0.0
STK3&4	Serine/threonine kinase 3	K04411	OXSR1	0.0	0.0
STK3&4	Serine/threonine kinase 3	K04411	STK4	0.0	0.0
STK3&4	Serine/threonine kinase 3	K04412	OXSR1	-1.7	0.0
STK3&4	Serine/threonine kinase 3	K04412	STK25	0.0	0.0
TAB2	TAK1-binding protein 2	K04404	TAB2	0.0	0.0
TAO	Thousand and one amino acid protein kinase	K04429	NA	0.0	0.0
TGFBR	TGF-beta receptor type-2	K04674	TGFR1	0.0	0.0

TNF	Tumor necrosis factor	K03156	TNFB	0.0	0.0
PPP3C	Serine/threonine-protein phosphatase 2B catalytic subunit	K04348	PP2BA	0.0	0.0
TGFBR	TGF-beta receptor type-2	K04388	TGFR2	0.0	0.0
PAK1&2	p21-activated kinase 1&2	K04409	ZN273	0.0	0.0
TRAF6	TNF receptor-associated factor 6	K03175	TRAF6	0.0	0.0
CRK II	Proto-oncogene C-crk	K04438	CRK	0.0	0.0
PAK1&2	p21-activated kinase 1&2	K04409	ZN665	0.0	0.0
ESCIT	Evolutionarily conserved signaling indermediate in Toll pathway	K04405	ECSIT	0.0	0.0
HSP72	Heat shock 70kDa protein 1/2/6/8	K03283	HSP7E	0.4	0.0
RAC. CDC42	RAS-related C3 botulinum toxin substrate 1	K04392	RAC1	0.0	0.0
PPP3C	Serine/threonine-protein phosphatase 2B regulatory subunit	K06268	CANB1	0.3	0.0
PAK1&2	p21-activated kinase 1&2	K04409	ZN433	0.0	0.0
MYC	Myc proto-oncogene protein	K04377	MYC	0.0	0.0
PAK1&2	p21-activated kinase 1&2	K04409	Z658B	0.0	-0.1
PAK1&2	p21-activated kinase 1&2	K04409	ZN160	0.0	-0.1
PAK1&2	p21-activated kinase 1&2	K04409	ZN835	-0.9	-0.1
PAK1&2	p21-activated kinase 1&2	K04409	ZSCA2	0.0	-0.1
AKT	RAC serine/threonine-protein kinase	K04456	AKT2A	0.0	-0.1
JIP3	Mitogen-activated protein kinase 8 interacting protein 3	K04436	JIP4	0.0	-0.1
MAP4K4	Mitogen-activated protein kinase kinase kinase kinase 4	K04407	M4K4	-0.1	-0.1
PAK1&2	p21-activated kinase 1&2	K04409	ZN724	-0.1	-0.1
PKC	Classical protein kinase C	K02677	KPCA	-0.2	-0.2
MAP4K2	Mitogen-activated protein kinase kinase kinase kinase 2	K04414	RBM4	0.0	-0.2
CPLA2	cytosolic phospholipase A2	K16342	PA24A	-1.2	-0.2
MAP4K4	Mitogen-activated protein kinase kinase kinase kinase 4	K04407	TNIK	-0.2	-0.3
PAK1&2	p21-activated kinase 1&2	K04409	ZN235	0.0	-0.3
RAC. CDC42	RAS-related C3 botulinum toxin substrate 2	K04392	RAC2	0.3	-0.3
MAP2K4	Mitogen-activated protein kinase kinase 4	K04430	MP2K4	0.0	-0.3

RAC. CDC42	Ras-related C3 botulinum toxin substrate 1	K07861	RAC1	0.0	-0.4
TGFB	Transforming growth factor beta-1	K13375	TGFB1	0.7	-0.4
RAPGEF2	Rap guanine nucleotide exchange factor 2	K08018	RPGF2	0.3	-0.4
MAP4K2	Mitogen-activated protein kinase kinase kinase kinase 2	K04414	RBM4B	0.0	-0.5
MAP4K4	Mitogen-activated protein kinase kinase kinase kinase 4	K04407	NA	1.0	-0.5
PAK1&2	p21-activated kinase 1&2	K04409	ZN652	-0.1	-0.5
PAK1&2	p21-activated kinase 1&2	K04409	ZNF91	0.0	-0.5
PKA	Protein kinase A	K04345	KAPCB	0.0	-0.5
PPM1B	Protein phosphatase 1B	K04461	PPM1G	0.0	-0.5
PDGFR	Platelet-derived growth factor receptor beta	K05089	PGFRB	-0.6	-0.5
NFATC2	Nuclear factor of activated T-cells. cytoplasmic 1	K04446	NFAC1	0.0	-0.5
RPS6KA	Ribosomal protein S6 kinase alpha-1/2/3/6	K04373	ST32C	0.0	-0.5
GADD45	Growth arrest and DNA-damage-inducible protein	K04402	GA45B	-0.4	-0.5
NFκβ	Nuclear factor of K light polypeptide gene enhancer in B-cells 2	K04469	FA35A	0.4	-0.6
AKT	RAC serine/threonine-protein kinase	K04456	NA	0.0	-0.6
p38	p38 MAP kinase	K04441	MK13	-0.6	-0.6
MKP	Dual specificity MAP kinase phosphatase	K04459	DUS7	-1.0	-0.6
PKC	Classical protein kinase C beta type	K19662	KPCB	0.0	-0.7
JNK	Mitogen-activated protein kinase 8/9/10	K04440	MK08	0.0	-0.7
RasGRP	RAS guanyl-releasing protein 1. 2. 3 and 4	K04350	GRP1	0.0	-0.7
PAK1&2	p21-activated kinase 1&2	K04409	ZBT11	0.0	-0.8
ZAK	Sterile alpha motif and leucine zipper containing kinase AZK	K04424	MLTK	0.0	-0.8
CACN	Voltage-dependent calcium channel N type alpha - 1D	K04851	CAC1D	0.0	-0.8
PAK1&2	p21-activated kinase 1&2	K04409	ZBT24	0.0	-0.8
CDC25B	M-phase inducer phosphatase 2	K05866	MPIP2	0.0	-0.8
TAO	Thousand and one amino acid protein kinase	K04429	TAOK3	0.0	-0.8
PAK1&2	p21-activated kinase 1&2	K04409	XFIN	0.0	-0.9
RPS6KA5	Ribosomal protein S6 kinase alpha-5	K04445	SG494	0.0	-0.9
STMN1	Stathmin	K04381	STMN1	0.0	-0.9

RASGRF	Ras-specific guanine nucleotide-releasing factor 2	K12326	RGRF2	0.2	-0.9
RAS	RAS-related protein R-Ras2	K07830	RRAS	0.0	-1.0
MAP3K4	Mitogen-activated protein kinase kinase kinase 4	K04428	M3K4	0.0	-1.0
MKP	Dual specificity MAP kinase phosphatase	K04459	DUS4	0.0	-1.0
CACN	Voltage-dependent calcium channel alpha-2/delta-4	K04861	CA2D4	-1.6	-1.0
TRAF2	TNF receptor-associated factor 2	K03173	TRAF2	-0.8	-1.1
MAP3K2	Mitogen-activated protein kinase kinase kinase 2	K04420	M3K2	-0.5	-1.1
MAP3K2	Mitogen-activated protein kinase kinase kinase 2	K04421	M3K3	-0.5	-1.1
TNFR	Tumor necrosis factor receptor	K03158	TNR1A	-2.5	-1.1
SRF	Serum response factor	K04378	SRF	1.1	-1.2
MEF2C	MADS-box transcription enhancer factor 2C	K04454	MEF2C	-0.5	-1.2
FGFR1	Fibroblast growth factor receptor 2	K05094	FGRL1	-2.4	-1.2
TNFR	Tumor necrosis factor receptor	K03158	NA	-0.8	-1.3
CACN	Voltage-dependent calcium channel alpha-2/delta-3	K04860	CA2D3	0.0	-1.4
TNFSF6	Tumor necrosis factor ligand superfamily member 6	K04389	NA	0.0	-1.5
FLNA	Filamin	K04437	FLNC	0.0	-1.6
p38	p38 MAP kinase	K04441	MK12	0.0	-1.6
RPS6KA5	Ribosomal protein S6 kinase alpha-5	K04445	ST32A	0.0	-1.7
PTPRR	Dual specificity phosphatase 3	K17614	DUS27	0.0	-1.7
RASGRP	RAS guanyl-releasing protein 2	K12361	GRP2	-0.6	-1.8
MAP3K5	Mitogen-activated protein kinase kinase kinase 5	K04426	M3K5	-0.1	-1.8
MAP2K6	Mitogen-activated protein kinase kinase 6	K04433	MP2K6	0.0	-1.9
NTRK	Neurotrophic tyrosine kinase receptor	K04360	DDR2	-1.0	-2.0
JIP1&2	Mitogen-activated protein kinase 8 interacting protein 1	K04434	JIP1	-1.8	-2.2
FLNA	Filamin	K04437	FL.	0.0	-2.2
CACN	Voltage-dependent calcium channel N type alpha - 1B	K04849	CAC1B	0.0	-2.2
NFκβ	Transcription factor p65	K04735	NA	0.0	-2.2
GRB2	Growth factor receptor-binding protein 2	K04364	GRAP	0.0	-2.5
RAP1	RAS-related protein Rap-1A	K04353	RAP1B	0.0	-2.5

RAS	RAS-related protein R-Ras2	K07830	RRAS2	0.0	-2.6
RASA2	RAS GTPase-activating protein 2	K08053	RASA2	0.0	-2.6
PDGF	Platelet-derived growth factor subunit B	K04359	PDGFB	-5.0	-3.0
MAP3K12	Mitogen-activated protein kinase kinase kinase 12	K04423	M3K12	0.0	-3.9
TGFB	Transforming growth factor beta-3	K13377	TGFB3	-3.2	-4.1
MAPK1/3	Mitogen-activated protein kinase 1/3	K04371	MK04	-1.9	-5.2

Suplemental Table 4. Sequences included in the phylogenetic tree

GI number	Full name	Specie
IL-18		
gi|1007733581	PREDICTED: uncharacterized protein LOC107380752	*Nothobranchius furzeri*
gi|1039366873	PREDICTED: interleukin-18 isoform X1	*Poecilia reticulata*
gi|1041133957	interleukin-18 isoform X1	*Kryptolebias marmoratus*
gi|1041133959	interleukin-18 isoform X2	*Kryptolebias marmoratus*
gi|1108913370	PREDICTED: uncharacterized protein LOC104940571	*Larimichthys crocea*
gi|1110897243	uncharacterized protein LOC109205098 isoform X3	*Oreochromis niloticus*
gi|1110897245	uncharacterized protein LOC109205098 isoform X4	*Oreochromis niloticus*
gi|1130004025	PREDICTED: uncharacterized protein LOC109510913	*Hippocampus comes*
gi|1148294668	IL-18	*Miichthys miiuy*
gi|1158907633	uncharacterized protein LOC109905603	*Oncorhynchus kisutch*
gi|1168915311	uncharacterized protein LOC109992315 isoform X1	*Labrus bergylta*
gi|1168915313	uncharacterized protein LOC109992315 isoform X2	*Labrus bergylta*
gi|1211326050	interleukin 18 isoform X1	*Oncorhynchus mykiss*
gi|1211326052	interleukin 18 isoform X2	*Oncorhynchus mykiss*
gi|1229002985	interleukin-18-like	*Acanthochromis polyacanthus*
gi|1316063835	interleukin-18 isoform X1	*Xiphophorus maculatus*
gi|1334664277	interleukin-18	*Trichechus manatus latirostris*
gi|1343040406	uncharacterized protein LOC111949364	*Salvelinus alpinus*
gi|1389919994	uncharacterized protein LOC112486949 isoform X1	*Cynoglossus semilaevis*
gi|1389919996	uncharacterized protein LOC112486949 isoform X2	*Cynoglossus semilaevis*
gi|1395226856	Hypothetical protein SMAX5B 8461	*Scophthalmus maximus*
gi|1395226857	Hypothetical protein SMAX5B 8461	*Scophthalmus maximus*
gi|1434964500	uncharacterized protein LOC109205098 isoform X1	*Oreochromis niloticus*
gi|1434964502	uncharacterized protein LOC109205098 isoform X2	*Oreochromis niloticus*
gi|185133182	interleukin 18	*Oncorhynchus mykiss*
gi|209736822	Interleukin-18 precursor	*Salmo salar*
gi|213515160	Interleukin-18	*Salmo salar*

gi|221220822	Interleukin-18 precursor	*Salmo salar*
gi|303664145	Interleukin-18 precursor	*Salmo salar*
gi|45260639	interleukin-18	*Takifugu rubripes*
gi|45260642	interleukin-18	*Takifugu rubripes*
gi|50080007	interleukin 18 form a, IL-18A	*Oncorhynchus mykiss*
gi|50080008	interleukin 18 form b, IL-18B	*Oncorhynchus mykiss*
gi|529125499	interleukin-18	*Sparus aurata*
gi|551511472	interleukin-18 isoform X2	*Xiphophorus maculatus*
gi|617495115	PREDICTED: interleukin-18-like	*Poecilia formosa*
gi|657547446	PREDICTED: interleukin-18-like	*Stegastes partitus*
gi|658881169	PREDICTED: interleukin-18 isoform X2	*Poecilia reticulata*
gi|74095937	interleukin-18	*Takifugu rubripes*
gi|742249475	PREDICTED: interleukin-18	*Esox lucius*
gi|958906940	IL18	*Poeciliopsis prolifica*
gi|961974860	PREDICTED: interleukin-18	*Poecilia latipinna*
gi|962020624	PREDICTED: interleukin-18-like	*Poecilia mexicana*
gi|974117749	PREDICTED: interleukin-18-like	*Cyprinodon variegatus*
P70380	IL18 MOUSE Interleukin-18	*Mus musculus*
Q14116	IL18 HUMAN Interleukin-18	*Homo sapiens*
TBA	IL18	*Cyclopterus lumpus*
IL-1b		
gi|1049222026	PREDICTED: interleukin-1 beta-like	*Pygocentrus nattereri*
gi|1049222285	PREDICTED: interleukin-1 beta-like	*Pygocentrus nattereri*
gi|1049222287	PREDICTED: interleukin-1 beta-like	*Pygocentrus nattereri*
gi|1083270956	PREDICTED: interleukin-1 beta	*Scleropages formosus*
gi|1158862069	interleukin-1 beta	*Oncorhynchus kisutch*
gi|1158883640	interleukin-1 beta-like	*Oncorhynchus kisutch*
gi|1158946287	interleukin-1 beta-like	*Oncorhynchus kisutch*
gi|12049717	interleukin 1 beta 43467	*Cyprinus carpio*
gi|12049719	interleukin 1 beta 43498	*Cyprinus carpio*

gi|1211247410	interleukin-1 beta-like	*Oncorhynchus mykiss*
gi|1211332815	interleukin-1 beta-like	*Oncorhynchus mykiss*
gi|1211353172	interleukin-1 beta-like	*Oncorhynchus mykiss*
gi|1237948414	interleukin 1 beta	*Gymnocypris eckloni*
gi|1249021769	interleukin-1 beta-like	*Astyanax mexicanus*
gi|1249021771	interleukin-1 beta-like	*Astyanax mexicanus*
gi|1338771276	interleukin-1 beta-like	*Paramormyrops kingsleyae*
gi|1342968161	interleukin-1 beta	*Salvelinus alpinus*
gi|1343017407	interleukin-1 beta	*Salvelinus alpinus*
gi|1348556044	interleukin-1 beta-like	*Salvelinus alpinus*
gi|1367437602	interleukin-1 beta	*Oncorhynchus tshawytscha*
gi|1367506101	interleukin-1 beta-like isoform X1	*Oncorhynchus tshawytscha*
gi|1367506105	interleukin-1 beta-like isoform X2	*Oncorhynchus tshawytscha*
gi|1367536039	interleukin-1 beta-like	*Oncorhynchus tshawytscha*
gi|144225831	interleukin-1 beta	*Melanogrammus aeglefinus*
gi|1450278189	interleukin 1 beta	*Tachysurus fulvidraco*
gi|1503276292	interleukin-1 beta-like	*Pangasianodon hypophthalmus*
gi|152962704	interleukin-1beta	*Conger myriaster*
gi|157652606	interleukin 1b	*Gadus morhua*
gi|164510038	interleukin-1 beta	*Salvelinus alpinus*
gi|165929363	interleukin 1b	*Melanogrammus aeglefinus*
gi|18152761	interleukin-1 beta	*Oncorhynchus mykiss*
gi|185133434	interleukin-1 beta	*Oncorhynchus mykiss*
gi|186288128	interleukin-1 beta	*Salmo salar*
gi|25137090	interleukin-1 beta-1	*Carassius auratus*
gi|25137092	interleukin-1 beta-2	*Carassius auratus*
gi|2821975	interleukin-1 beta	*Cyprinus carpio*
gi|307075895	interlukin-1 beta	*Danio rerio*
gi|317414915	interleukin 1 beta	*Danio rerio*
gi|317574215	interleukin 1 beta	*Ictalurus punctatus*

gi|318098733	interleukin-1 beta	*Ictalurus punctatus*
gi|33356628	interleukin 1 beta	*Danio rerio*
gi|3805826	interleukin-1 beta	*Oncorhynchus mykiss*
gi|3805831	interleukin-1-beta	*Oncorhynchus mykiss*
gi|38143017	interleukin-1 beta 1	*Carassius auratus*
gi|38143019	interleukin-1 beta 2	*Carassius auratus*
gi|387864279	interleukin-1 beta	*Ctenopharyngodon idella*
gi|387864328	interleukin-1 beta	*Ctenopharyngodon idella*
gi|390483256	IL-1 beta	*Hemibagrus macropterus*
gi|393010847	interleukin-1 beta	*Ctenopharyngodon idella*
gi|431831911	interleukin-1 beta	*Cyprinus carpio*
gi|47607481	interleukin-1 beta	*Salmo salar*
gi|487395370	Interleukin-1 beta	*Plecoglossus altivelis*
gi|498917176	interleukin-1 beta	*Danio rerio*
gi|507104794	interleukin-1 b3	*Salmo salar*
gi|536720426	interleukin-1 beta-1	*Carassius carassius*
gi|536720431	interleukin-1 beta-2	*Carassius carassius*
gi|5708097	interleukin-1-beta	*Cyprinus carpio*
gi|571255055	interleukin-1 beta	*Ictalurus punctatus*
gi|571255097	interleukin-1 beta	*Gadus morhua*
gi|571255099	Interleukin-1 beta 3	*Oncorhynchus mykiss*
gi|571255109	Interleukin-1 beta 3	*Oncorhynchus mykiss*
gi|57283085	interleukin 1 beta	*Gadus morhua*
gi|576887285	Interleukin-1 beta	*Ictalurus punctatus*
gi|642003711	unnamed protein product	*Oncorhynchus mykiss*
gi|642055264	unnamed protein product	*Oncorhynchus mykiss*
gi|642085950	unnamed protein product	*Oncorhynchus mykiss*
gi|642112014	unnamed protein product	*Oncorhynchus mykiss*
gi|6468654	interleukin-1 beta 2 precursor	*Oncorhynchus mykiss*
gi|68534031	Il1b protein	*Danio rerio*

gi|698320871	interleukin 1 beta	*Coregonus maraena*
gi|74027236	interleukin 1 beta 1	*Ictalurus punctatus*
gi|74027238	interleukin 1 beta 2	*Ictalurus punctatus*
gi|742245874	PREDICTED: interleukin-1 beta	*Esox lucius*
gi|742245876	PREDICTED: interleukin-1 beta	*Esox lucius*
gi|742250859	PREDICTED: interleukin-1 beta isoform X1	*Esox lucius*
gi|742250861	PREDICTED: interleukin-1 beta isoform X2	*Esox lucius*
gi|78707325	interleukin 1 beta type a	*Ictalurus punctatus*
gi|78707327	interleukin 1 beta type b	*Ictalurus punctatus*
gi|78707329	interleukin 1 beta type a	*Ictalurus punctatus*
gi|78707331	interleukin 1 beta type b	*Ictalurus punctatus*
gi|8249932	interleukin-1 beta	*Oncorhynchus mykiss*
gi|831271282	PREDICTED: interleukin-1 beta-like	*Clupea harengus*
gi|831271284	PREDICTED: interleukin-1 beta-like	*Clupea harengus*
gi|831271286	PREDICTED: interleukin-1 beta-like	*Clupea harengus*
gi|929156400	PREDICTED: interleukin-1 beta-like	*Salmo salar*
gi|929245524	PREDICTED: interleukin-1 beta-like	*Salmo salar*
gi|929297216	PREDICTED: interleukin-1 beta isoform X1	*Salmo salar*
gi|938051386	interleukin-1 beta-like	*Scleropages formosus*
P01584	IL1B HUMAN Interleukin-1 beta	*Homo sapiens*
P10749	IL1B MOUSE Interleukin-1 beta	*Mus musculus*
TBA	Interleukin 1 beta	*Cyclopterus lumpus*
IL-1Fm2		
gi|1025472254	PREDICTED: interleukin-1 beta-like isoform X1	*Poecilia formosa*
gi|1025472256	PREDICTED: interleukin-1 beta-like isoform X2	*Poecilia formosa*
gi|1079714444	PREDICTED: interleukin-1 beta-like	*Lates calcarifer*
gi|1143368044	PREDICTED: interleukin-1 beta-like	*Paralichthys olivaceus*
gi|1168937023	interleukin-1 beta-like isoform X1	*Labrus bergylta*
gi|1168937025	interleukin-1 beta-like isoform X2	*Labrus bergylta*
gi|1169063128	interleukin-1 beta-like	*Monopterus albus*

gi|1188083442	interleukin-1 beta-like	*Boleophthalmus pectinirostris*
gi|1199311892	interleukin-1 beta isoform X2	*Fundulus heteroclitus*
gi|1228982676	interleukin-1 beta-like	*Acanthochromis polyacanthus*
gi|1250169094	interleukin-1 beta-like	*Seriola dumerili*
gi|1308535136	interleukin-1 beta-like isoform X1	*Amphiprion ocellaris*
gi|1308535175	interleukin-1 beta-like isoform X2	*Amphiprion ocellaris*
gi|1316107519	interleukin-1 beta isoform X2	*Xiphophorus maculatus*
gi|1317113170	interleukin-1 beta-like	*Seriola lalandi dorsalis*
gi|1343910006	interleukin-1 beta	*Oryzias latipes*
gi|1357736833	interleukin-1 beta-like isoform X1	*Oryzias melastigma*
gi|1357736835	interleukin-1 beta-like isoform X2	*Oryzias melastigma*
gi|1357736837	interleukin-1 beta-like isoform X3	*Oryzias melastigma*
gi|1381445067	interleukin-1 beta isoform X1	*Maylandia zebra*
gi|1387734041	hypothetical protein CCH79 1250	*Gambusia affinis*
gi|1395229004	Interleukin 1 beta-like 1	*Scophthalmus maximus*
gi|1470014534	interleukin-1 beta-like isoform X1	*Mastacembelus armatus*
gi|1472967553	interleukin-1 beta-like	*Anabas testudineus*
gi|225706200	Interleukin-1 beta precursor	*Osmerus mordax*
gi|422001748	interleukin 1 beta-like 1	*Paralichthys olivaceus*
gi|422001750	interleukin 1 beta-like 1	*Paralichthys olivaceus*
gi|542241173	interleukin-1 beta	*Oreochromis niloticus*
gi|571257110	interleukin-1 family member 2	*Sparus aurata*
gi|584004675	PREDICTED: interleukin-1 beta-like isoform X1	*Neolamprologus brichardi*
gi|584004677	PREDICTED: interleukin-1 beta-like isoform X2	*Neolamprologus brichardi*
gi|657588828	PREDICTED: interleukin-1 beta-like	*Stegastes partitus*
gi|657793760	interleukin-1 beta-like	*Cynoglossus semilaevis*
gi|658876923	PREDICTED: interleukin-1 beta-like isoform X1	*Poecilia reticulata*
gi|658876925	PREDICTED: interleukin-1 beta-like isoform X2	*Poecilia reticulata*
gi|736195106	PREDICTED: interleukin-1 beta-like	*Notothenia coriiceps*
gi|808860934	Interleukin-1 beta	*Larimichthys crocea*

gi|831485658	interleukin-1 beta isoform X1	*Fundulus heteroclitus*
gi|928043369	PREDICTED: interleukin-1 beta-like	*Austrofundulus limnaeus*
gi|930773371	PREDICTED: interleukin-1 beta-like	*Haplochromis burtoni*
gi|941812403	interleukin-1 beta isoform X1	*Xiphophorus maculatus*
gi|961793134	PREDICTED: interleukin-1 beta-like isoform X1	*Poecilia mexicana*
gi|961793136	PREDICTED: interleukin-1 beta-like isoform X2	*Poecilia mexicana*
gi|961847762	PREDICTED: interleukin-1 beta-like isoform X1	*Poecilia latipinna*
gi|961847766	PREDICTED: interleukin-1 beta-like isoform X2	*Poecilia latipinna*
gi|974107253	PREDICTED: interleukin-1 beta-like	*Cyprinodon variegatus*
TBA	Interleukin 1 family member 2	*Cyclopterus lumpus*
nIL-1F1		
gi|1007736865	PREDICTED: uncharacterized protein LOC107381689	*Nothobranchius furzeri*
gi|1020401635	PREDICTED: uncharacterized protein LOC107555915	*Sinocyclocheilus grahami*
gi|1025123909	PREDICTED: uncharacterized protein LOC107695052	*Sinocyclocheilus anshuiensis*
gi|1025185898	PREDICTED: uncharacterized protein LOC107751154	*Sinocyclocheilus rhinocerous*
gi|1025387253	PREDICTED: uncharacterized protein LOC107737257	*Sinocyclocheilus rhinocerous*
gi|1039391223	PREDICTED: uncharacterized protein LOC103462027 isoform X1	*Poecilia reticulata*
gi|1039391225	PREDICTED: uncharacterized protein LOC103462027 isoform X2	*Poecilia reticulata*
gi|1039391228	PREDICTED: uncharacterized protein LOC103462027 isoform X3	*Poecilia reticulata*
gi|1042344200	PREDICTED: uncharacterized protein LOC108259564	*Ictalurus punctatus*
gi|1049223988	PREDICTED: uncharacterized protein LOC108425742	*Pygocentrus nattereri*
gi|1049223998	PREDICTED: uncharacterized protein LOC108425745	*Pygocentrus nattereri*
gi|1079739724	PREDICTED: uncharacterized protein LOC108887947	*Lates calcarifer*
gi|1083437271	PREDICTED: uncharacterized protein LOC108920476	*Scleropages formosus*
gi|1101587484	PREDICTED: uncharacterized protein LOC109101583	*Cyprinus carpio*
gi|1109005738	PREDICTED: uncharacterized protein LOC104919762	*Larimichthys crocea*
gi|1129966429	PREDICTED: uncharacterized protein LOC109526012 isoform X1	*Hippocampus comes*
gi|1129966431	PREDICTED: uncharacterized protein LOC109526012 isoform X2	*Hippocampus comes*
gi|1143364395	PREDICTED: uncharacterized protein LOC109624947	*Paralichthys olivaceus*
gi|1168901793	uncharacterized protein LOC109987033	*Labrus bergylta*

gi|1168961425	uncharacterized protein LOC109965717	*Monopterus albus*
gi|1188118180	uncharacterized protein LOC110161215	*Boleophthalmus pectinirostris*
gi|1211305958	uncharacterized protein LOC110500300	*Oncorhynchus mykiss*
gi|1228998298	uncharacterized protein LOC110960892	*Acanthochromis polyacanthus*
gi|1248995010	uncharacterized protein LOC103024716 isoform X1	*Astyanax mexicanus*
gi|1248995021	uncharacterized protein LOC103025024	*Astyanax mexicanus*
gi|1250101633	uncharacterized protein LOC111224736	*Seriola dumerili*
gi|1308390568	uncharacterized protein LOC111567341	*Amphiprion ocellaris*
gi|1316094177	uncharacterized protein LOC102218441 isoform X1	*Xiphophorus maculatus*
gi|1316094179	uncharacterized protein LOC102218441 isoform X2	*Xiphophorus maculatus*
gi|1317092885	uncharacterized protein LOC111651667	*Seriola lalandi dorsalis*
gi|1338766414	uncharacterized protein LOC111850233 isoform X1	*Paramormyrops kingsleyae*
gi|1338766416	uncharacterized protein LOC111850233 isoform X2	*Paramormyrops kingsleyae*
gi|1338766418	uncharacterized protein LOC111850233 isoform X3	*Paramormyrops kingsleyae*
gi|1338827765	uncharacterized protein LOC111838144 isoform X1	*Paramormyrops kingsleyae*
gi|1338827767	uncharacterized protein LOC111838144 isoform X2	*Paramormyrops kingsleyae*
gi|1357729487	uncharacterized protein LOC112160901 isoform X1	*Oryzias melastigma*
gi|1357729489	uncharacterized protein LOC112160901 isoform X2	*Oryzias melastigma*
gi|1367392994	uncharacterized protein LOC112243723	*Oncorhynchus tshawytscha*
gi|1386862434	uncharacterized protein LOC108250161	*Kryptolebias marmoratus*
gi|1389922954	uncharacterized protein LOC103378686	*Cynoglossus semilaevis*
gi|1395229706	Interleukin 1 beta-like 2	*Scophthalmus maximus*
gi|1395229707	Interleukin 1 beta-like 2 isoform 2	*Scophthalmus maximus*
gi|1395229708	Interleukin 1 beta-like 2 isoform 3	*Scophthalmus maximus*
gi|1468850528	uncharacterized protein LOC113019000	*Astatotilapia calliptera*
gi|1469049901	uncharacterized protein LOC113111075	*Carassius auratus*
gi|1469138939	uncharacterized protein LOC113055294	*Carassius auratus*
gi|1469977669	uncharacterized protein LOC113138041 isoform X1	*Mastacembelus armatus*
gi|1469977671	uncharacterized protein LOC113138041 isoform X2	*Mastacembelus armatus*
gi|1473012870	uncharacterized protein LOC113147655	*Anabas testudineus*

gi|1503285850	uncharacterized protein LOC113547441	*Pangasianodon hypophthalmus*
gi|1503285852	uncharacterized protein LOC113547442	*Pangasianodon hypophthalmus*
gi|307746681	interleukin 1 beta	*Danio rerio*
gi|307746683	interleukin 1 beta	*Danio rerio*
gi|339267712	IL-1Ra protein	*Tetraodon nigroviridis*
gi|339267714	IL-1Ra protein	*Danio rerio*
gi|348516653	uncharacterized protein LOC100699119	*Oreochromis niloticus*
gi|410912848	PREDICTED: uncharacterized protein LOC101066360 isoform X1	*Takifugu rubripes*
gi|422001752	interleukin 1 beta-like 2	*Paralichthys olivaceus*
gi|422001754	interleukin 1 beta-like 2	*Paralichthys olivaceus*
gi|47230630	unnamed protein product	*Tetraodon nigroviridis*
gi|498949373	uncharacterized protein LOC101480448	*Maylandia zebra*
gi|548343437	PREDICTED: uncharacterized protein LOC102205482	*Pundamilia nyererei*
gi|554866677	PREDICTED: uncharacterized protein LOC102308236 isoform X1	*Haplochromis burtoni*
gi|554866679	PREDICTED: uncharacterized protein LOC102308236 isoform X2	*Haplochromis burtoni*
gi|556983726	PREDICTED: uncharacterized protein LOC102363048	*Latimeria chalumnae*
gi|571255618	interleukin-1 family member	*Tetraodon nigroviridis*
gi|583970305	PREDICTED: uncharacterized protein LOC102783726	*Neolamprologus brichardi*
gi|594190782	interleukin-1 family member A	*Danio rerio*
gi|597793178	uncharacterized protein LOC103024716 isoform X2	*Astyanax mexicanus*
gi|617426140	PREDICTED: uncharacterized protein LOC103143562 isoform X1	*Poecilia formosa*
gi|617426143	PREDICTED: uncharacterized protein LOC103143562 isoform X2	*Poecilia formosa*
gi|632948885	PREDICTED: uncharacterized protein LOC103177481 isoform X1	*Callorhinchus milii*
gi|657574180	PREDICTED: uncharacterized protein LOC103365194	*Stegastes partitus*
gi|736288474	PREDICTED: uncharacterized protein LOC104963546	*Notothenia coriiceps*
gi|742167560	PREDICTED: uncharacterized protein LOC105019922	*Esox lucius*
gi|742167564	PREDICTED: uncharacterized protein LOC105019922	*Esox lucius*
gi|768935956	PREDICTED: uncharacterized protein LOC101066360 isoform X2	*Takifugu rubripes*
gi|808861535	hypothetical protein EH28 11529	*Larimichthys crocea*
gi|831287494	PREDICTED: uncharacterized protein LOC105893267	*Clupea harengus*

gi|831287596	PREDICTED: uncharacterized protein LOC105893317	*Clupea harengus*
gi|831555769	uncharacterized protein LOC105934419	*Fundulus heteroclitus*
gi|928077817	PREDICTED: uncharacterized protein LOC106536268	*Austrofundulus limnaeus*
gi|938072961	hypothetical protein Z043 110336	*Scleropages formosus*
gi|961871480	PREDICTED: uncharacterized protein LOC106952009 isoform X1	*Poecilia latipinna*
gi|961871484	PREDICTED: uncharacterized protein LOC106952009 isoform X2	*Poecilia latipinna*
gi|973191081	PREDICTED: uncharacterized protein LOC102690436 isoform X1	*Lepisosteus oculatus*
gi|973191083	PREDICTED: uncharacterized protein LOC102690436 isoform X2	*Lepisosteus oculatus*
gi|974059250	PREDICTED: uncharacterized protein LOC107082510	*Cyprinodon variegatus*
TBA	Novel intereleukin 1 family member	*Cyclopterus lumpus*
Other		
gi|736184516	PREDICTED: uncharacterized protein LOC104945633 isoform X1	*Notothenia coriiceps*
gi|736184519	PREDICTED: uncharacterized protein LOC104945633 isoform X2	*Notothenia coriiceps*

Graphic design: Communication Division, UiB / Print: Skipnes Kommunikasjon AS

uib.no

ISBN: 9788230868881 (print)
9788230868607 (PDF)